

# **I C O L D**

**COMMITTEE ON CONCRETE DAMS**

**THE PHYSICAL PROPERTIES OF HARDENED  
CONVENTIONAL CONCRETE IN DAMS**



**January 2009**

AVERTISSEMENT – EXONÉRATION DE RESPONSABILITÉ :

Les informations, analyses et conclusions contenues dans cet ouvrage n'ont pas force de Loi et ne doivent pas être considérées comme un substitut aux réglementations officielles imposées par la Loi. Elles sont uniquement destinées à un public de Professionnels Avertis, seuls aptes à en apprécier et à en déterminer la valeur et la portée et à en appliquer avec précision les recommandations à chaque cas particulier.

Malgré tout le soin apporté à la rédaction de cet ouvrage, compte tenu de l'évolution des techniques et de la science, nous ne pouvons en garantir l'exhaustivité.

Nous déclinons expressément toute responsabilité quant à l'interprétation et l'application éventuelles (y compris les dommages éventuels en résultant ou liés) du contenu de cet ouvrage.

En poursuivant la lecture de cet ouvrage, vous acceptez de façon expresse cette condition.

NOTICE – DISCLAIMER :

The information, analyses and conclusions in this document have no legal force and must not be considered as substituting for legally-enforceable official regulations. They are intended for the use of experienced professionals who are alone equipped to judge their pertinence and applicability and to apply accurately the recommendations to any particular case.

This document has been drafted with the greatest care but, in view of the pace of change in science and technology, we cannot guarantee that it covers all aspects of the topics discussed.

We decline all responsibility whatsoever for how the information herein is interpreted and used and will accept no liability for any loss or damage arising therefrom.

Do not read on unless you accept this disclaimer without reservation.

**COMMITTEE ON CONCRETE DAMS**  
**COMITÉ DES BARRAGES EN BÉTON**  
**(1991-2008)**

*Chairman/Président*

USA/Etats-Unis	J.R. Graham (1992 – 1997)
USA/Etats-Unis/Canada/Canada	R.G. Charlwood (since 1998)

*Vice Chairman/Vice Président*

France/France	J. Launay (since 1998)
---------------	------------------------

*Members/Membres*

Australia/Australie	M. Pegg (to 1996) B. Forbes (since 1997)
Austria/Autriche	H. Huber (1996 - 2000) G. Heigarth (2001) W. Pichler (since 2002)
Brazil/Brésil	F.R. Andriolo (to 2001) J. Marques Filho (since 2002)
Canada/Canada	R.G. Charlwood (1996 - 2006) P. Ko (since 2007)
China/Chine	Shen Conggang (to 1998) Jia Jinsheng (since 1999)
Croatia/Croatie	V. Ukrainczyk (to 2006)
France/France	J. Launay (to 1999) M. Guerinnet (since 2000)
Great Britain/Grande-Bretagne	M.R.H. Dunstan
India/Inde	B.J. Parmar
Iran/Iran	M.E. Omran (to 1997) A.A. Ramazanianpour (1998 – 2006) M. R. Jabarooti (since 2007)
Italy/Italie	P. Bertacchi (to 1995) M. Berra (since 1996)
Japan/Japon	S. Nagataki (to 1997) O. Arai (1998-2002) T. Uesaka (since 2002)
Norway/Norvège	O.J. Berthelsen
Portugal/Portugal	A. Camelo

Russia/Russie	A.D. Osipov (to 2000) G. Kostyrya (since 2000)
South Africa/Afrique du Sud	J. Kroon (to 2004) J. Geringer (since 2005)
Spain/Espagne	J.M. Gaztanaga (to 1999) J. Buil Sanz (since 2000)
Sweden/Suède	J. Alemo (to 2006) T Ekstrom (since 2007)
Switzerland/Suisse	H. Kreuzer (to 2007) M. Conrad (since 2007)
USA/Etats-Unis	V. Zipparro (1999-2000) G. Mass (2001) R.G. Charlwood (since 2002)

## **ACKNOWLEDGEMENTS**

This Bulletin was drafted under the auspices of the ICOLD Committee on Concrete Dams. The Bulletin was initiated under the Committee Chairmanship of J.R. Graham (USA), and completed under the Chairmanship of R.G. Charlwood (USA/Canada).

The lead author of the Bulletin initially was P. Bertacchi (Italy) and since 1996 has been M. Berra (Italy) who has developed and completed the document.

H. Kreuzer (Switzerland) provided a precious assistance in reviewing and editing.

The initial drafting team included P. Bertacchi, M. Berra, G. Ferrara & P. Morabito (Italy), V. Ukrainczyk (Croatia), R. Charlwood (Canada), M. Machado (Portugal), J. Alemo (Sweden) and T. Liu (USA).

The final Bulletin was drafted as follows:

Section 1 - Introduction, was prepared by P. Bertacchi and M. Berra (Italy).

Section 2 – Strength Properties, was initially drafted by V. Ukrainczuk (Croatia) and subsequently redrafted by H. Kreuzer (Switzerland) with inputs regarding sonic measurements from M. Berra (Italy).

Section 3 – Elastic Properties, was initially drafted by R. Charlwood (USA/Canada) and subsequently completed by M. Berra (Italy) with inputs from H. Kreuzer and M. Conrad (Switzerland) and J. Buil Sanz (Spain).

Section 4 – Creep Properties, was drafted by T.C. Liu (USA) and completed with contributions from M. Berra (Italy) and H. Kreuzer ((Switzerland).

Section 5 – Shrinkage, was drafted by M. Berra (Italy).

Section 6 – Thermal Properties, was drafted by P. Morabito (Italy) and completed with contributions of M. Berra (Italy) and H. Kreuzer (Switzerland).

Section 7 – Water Permeability, was initially drafted by J. Alemo (Sweden) and subsequently redrafted by T. Ekstrom (Sweden) with contributions from H. Kreuzer (Switzerland) and M. Berra (Italy).

Section 8 – Frost Resistance, was drafted by M. Berra (Italy) with inputs from H. Kreuzer (Switzerland).

# THE PHYSICAL PROPERTIES OF HARDENED CONVENTIONAL CONCRETE IN DAMS

## Table of contents

Section	Page
Committee on Concrete for Dams	i
Acknowledgements	iii
Table of contents	iv
FOREWORD	vii
1. INTRODUCTION	
1.1 Purpose of the Bulletin	
1.2 Scope	
1.3 Relationship to earlier Bulletins	
1.4 Definitions	
1.5 Content of the Bulletin	
2. STRENGTH PROPERTIES	
2.1 General	
2.2 Concrete testing	
2.3 Compressive strength	
2.4 Tensile strength	
2.4 Shear strength	
2.6 Dynamic strength	
2.7 References	
3. ELASTIC PROPERTIES	
3.1 General	
3.2 Static modulus of elasticity	
3.3 Dynamic modulus of elasticity	
3.4 Poisson's ratio	
3.5 Significance of elastic properties on dam behaviour	
3.6 Use of elastic properties in mathematical models for dam structural analysis	
3.7 References	

#### 4. CREEP PROPERTIES

- 4.1 General
- 4.2 Factors influencing creep
- 4.3 Measurements of creep
- 4.4 Significance of creep properties on dam behaviour
- 4.5 Modelling creep in structural analysis
- 4.6 References

#### 5. SHRINKAGE

- 5.1 General
- 5.2 Types of shrinkage
- 5.3 Causes and mechanism of drying shrinkage
- 5.4 Factors affecting drying shrinkage
- 5.5 Estimation of drying shrinkage
- 5.6 Effect of shrinkage on cracking
- 5.7 Effect of shrinkage on concrete dams
- 5.8 References

#### 6. THERMAL PROPERTIES

- 6.1 General
- 6.2 Temperature rise of young concrete during the hydration of cementitious materials
- 6.3 Thermal conductivity of hardened concrete
- 6.4 Specific heat of hardened concrete
- 6.5 Thermal diffusivity of hardened concrete
- 6.6 Coefficient of thermal expansion of hardened concrete
- 6.7 In situ measurements of concrete temperatures
- 6.8 References

#### 7. WATER PERMEABILITY

- 7.1 Introduction
- 7.2 Factors influencing the concrete water permeability
- 7.3 Tests method for water permeability
- 7.4 Modelling water permeability in saturated concrete
- 7.5 References

## 8. FROST RESISTANCE

8.1 General

8.2 Frost resistance, mechanism and effects

8.3 Factors affecting the frost resistance

8.4 Methods for experimental determination of the concrete frost resistance

8.5 Laboratory diagnostic investigations

8.6 Freezing and thawing on concrete dams

8.7 References



## **FOREWORD**

In 1991, the International Commission on Large Dams (ICOLD) directed that its Technical Committee on Concrete for Dams, then under the Chairmanship of J.R. Graham (USA), and subsequently under the Chairmanship, of R.G. Charlwood (CANADA/USA), to undertake the preparation of a comprehensive report on the physical properties of concrete in dams. A sub-Committee of the ICOLD Committee on Concrete for Dams, chaired initially by P. Bertacchi (Italy) and subsequently M. Berra (Italy), prepared this Bulletin.

The purpose of this Bulletin is to provide a comprehensive treatise on the physical properties of hardened conventional concrete for dams, refreshing the partial information contained in some out-of-date ICOLD Bulletins, giving an account of new approaches and examining also some important properties not included in the previous Bulletins. This document supersedes the ICOLD Bulletins: n° 15 (Frost resistance of concrete - 1960) and n° 26 (Methods of determining effects on shrinkage, creep and temperature on concrete for large dams - 1976).

The main body of this Bulletin addresses the physical properties of the mass concrete used most frequently in design and analyses of concrete dams and appurtenant structures. These include strength, elastic, creep, shrinkage and thermal properties, permeability, and frost resistance.

The scope of the Bulletin is, for each property considered, to show typical behaviour, factors influencing it, methods for experimental determination, and, last but not least, methods to introduce the properties in mathematical models to be utilized both for design and observation.

This Bulletin does not specifically address the properties of hardened concrete of Roller Compacted Concrete (RCC) dams which are partially dealt in the Bulletin n° 75 – Roller Compacted Concrete for Gravity Dams and in Bulletin n° 126 Roller-Compacted Concrete Dams. This specific topic may be the subject of a separate Bulletin at a later date.

During the course of preparation of this Bulletin material was collected and drafted on the topics of the application of fracture mechanics to concrete dams and also on the increasingly important issue of expansion of concrete dams due to chemical reactions. These two topics are proposed to be the subjects of separate new bulletins in the future.

Robin G. Charlwood

Chairman

Committee on Concrete Dams

January 2009

## **1 INTRODUCTION**

<b>1</b>	<b>INTRODUCTION.....</b>	<b>1</b>
<b>1.1</b>	<b>PURPOSE OF THE BULLETIN.....</b>	<b>1</b>
<b>1.2</b>	<b>SCOPE.....</b>	<b>2</b>
<b>1.3</b>	<b>RELATIONSHIP TO EARLIER BULLETINS.....</b>	<b>3</b>
<b>1.4</b>	<b>DEFINITIONS.....</b>	<b>3</b>
<b>1.5</b>	<b>CONTENT OF THE BULLETIN.....</b>	<b>3</b>

### **1.1 PURPOSE OF THE BULLETIN**

The purpose of this Bulletin is to provide a unique, comprehensive and update treatise on the physical properties of hardened conventional concrete for dams, refreshing the partial information contained in some out-of-date ICOLD Bulletins, giving an account of new approaches and examining also some important properties not included in the previous Bulletins.

In particular this new document serves to supersede the following out-of-date ICOLD Bulletins: n° 15 (Frost resistance of concrete - 1960) and n° 26 (Methods of determining effects on shrinkage, creep and temperature on concrete for large dams - 1976).

This Bulletin addresses the physical fundamental properties of the mass concrete material used most frequently in design and analyses of concrete dams and appurtenant structures. These include strength, elastic properties, creep, drying shrinkage and thermal properties, water permeability, and durability.

It is understood that mass concrete material represents the intact concrete inside the mass of the dam and not the more general mass concrete dam that include also structural components and imperfections (Fig. 1.1). In fact, mass concrete material can be thought of as “defect-free” whereas mass concrete structures, such as dams, often have manmade structural components and imperfections as for example construction and contraction joints, interfaces with other materials (e.g. waterstops, injected sealing materials), drains or have cavities like cracks or honey combs. This Bulletin does not intentionally deal with them.

Furthermore this Bulletin does not specifically address the properties of Roller Compacted Concrete (RCC) dams which are partially dealt in the Bulletin n° 75 – Roller Compacted Concrete for Gravity Dams and in the recent Bulletin n° 126 (Roller-Compacted Concrete Dams – State of the art and case histories).

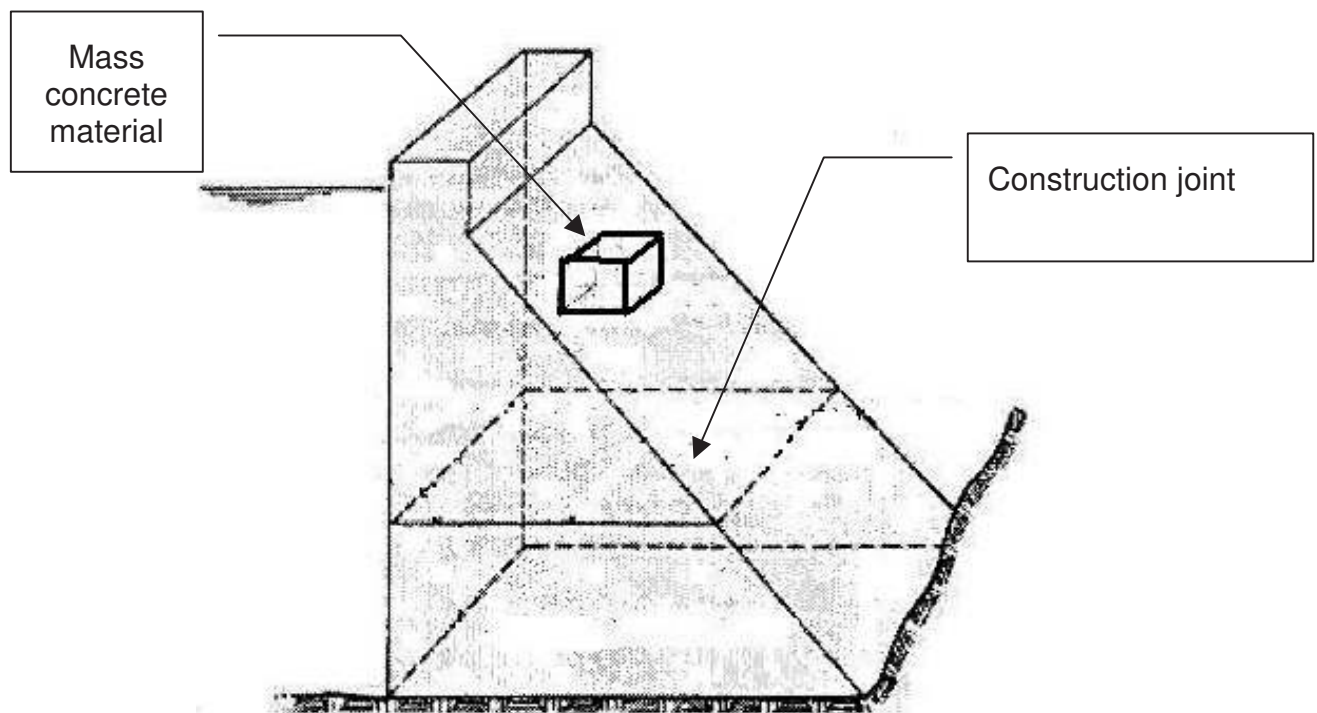


Fig. 1.1 – Mass concrete material in a concrete dam

The properties of fresh concrete are not considered. Chemical reactions and cracking resistance are also intentionally excluded since they are already extensively treated in other recent ICOLD Bulletins (n° 71 - Exposure of dam concrete to special aggressive waters; n° 79 - Alkali-Aggregate Reaction in concrete dams; n° 93 - Ageing of dams and appurtenant works; Bulletin n° 107 - Control and treatment of cracks in concrete dams). The concrete erosion resistance is extensively dealt with in the ACI Report 210 R-93 "Erosion of concrete in hydraulic structures".

The topics of the application of fracture mechanics to concrete dams and also the increasingly important issue of expansion of concrete dams due to chemical reactions, including alkali-aggregate reactions, are proposed to be the subjects of separate new bulletins in the future.

## 1.2 SCOPE

The scope of the Bulletin is, for each property considered, to show typical behaviour, factors influencing it, methods for experimental determination, and, last but not least, methods to introduce the properties in mathematical models to be utilized both for design and back analysis.

### **1.3 RELATIONSHIP TO EARLIER BULLETINS**

There are significant differences in objective and approach between the previous Bulletins and this new one:

Bulletin n° 15 “Frost resistance of concrete” (1960) is really outdated. It contains the results obtained in different laboratories more than 40 years ago. The influence of chemical composition of cement on frost resistance was emphasized; the disruption mechanism due to freezing of the water in the capillaries, the influence of the degree of saturation, of the air content and of the spacing factor were not considered.

Bulletin n° 26 “Methods of determining effects on shrinkage, creep and temperature on concrete for large dams” (1976) was focused mainly at the consequence on the structure, caused by shrinkage, creep and temperature, both from point of view of design and observation of dams. A first part containing these general aspects has been saved, updated and introduced as general considerations; the long list of papers has been omitted and substituted with a more recent one.

### **1.4 DEFINITIONS**

The term “hardened concrete” refers to the properties of the concrete, starting just after initial set of cement. The physical properties of concrete must be addressed in a developing sense, the evolution of a property in fact starts from initial set and depends on age and on curing conditions (temperature, humidity etc.). In some cases an “equivalent age” could be defined to represent the “maturity” of a concrete.

Standard curing conditions are necessary for comparative reference, but don't represent a realistic situation of maturity. When analysing a particular stress situation at a specific age, we must know how the concerned properties have been developed up to that time and in that specific curing condition.

The adjective “conventional” is added to “hardened concrete” just to differentiate from roller compacted concrete that may need a separate treatment in some respects.

### **1.5 CONTENT OF THE BULLETIN**

The physical properties of hardened conventional concrete for dams have been addressed in seven Chapters dealing with all frequently used engineering parameters (strengths, elastic properties, creep, drying shrinkage, thermal properties, water permeability, durability and frost resistance).

The structure of each chapter is generally as follows:

- Definition of the property;
- Typical behaviour, just after construction or during the normal service life of the dam, as reported by the experience acquired;
- Factors influencing the property, such as: components and composition of the concrete, time, ageing related to physical and chemical processes, temperature, humidity, stresses, etc. Expected effects on the property;

- Methods for experimental determination of the property, both in laboratory and in situ;
- Transfer of acquired parameters of the mass concrete material to be utilised in mathematical models, in the design phase, for the total behaviour of the mass concrete dam.

The subject, principal author(s) and content of each Chapter and Appendix are as follows:

### **- Strength properties (Section 2)**

Concrete strength is defined as the maximum stress recorded during the load testing of specimens carried out to failure. The type of loading excites different types of strength: compressive-tensile-shear strengths are of main importance, both for static and dynamic (earthquake) loading.

Typically for dams are strength requirements at high maturity and the rather high scatter of strength values as compared to common civil structures.

New testing techniques taking advantage of knowledge in fracture mechanics could provide most valuable information about post-peak stress-strain behaviour, both under uniaxial and biaxial tensile and compressive stress conditions. However they are not here addressed and could be the subject of another more extensive bulletin in the future.

### **- Elastic Properties (Section 3)**

The stress-strain concrete behaviour is quite complex and it was variously theoretically characterised. However for most of usual applications the classic and simplest constitutive model, based on linear elasticity in an isotropic homogeneous material, can be used. The two parameters of Static Modulus of Elasticity (E) and Poisson's ratio ( $\nu$ ) have been examined with reference to the main factors affecting them and to the proposed correlation with the compressive strength. Dynamic Modulus of Elasticity through non destructive techniques are presented and used both to evaluate the elastic properties and to determine the concrete quality and integrity. Finally the significance of elastic properties on dam behaviour and the use of elastic properties in mathematical models for dam structural analysis are treated.

### **- Creep properties (Section 4)**

Creep is time-dependent deformation due to sustained load. It is generally accepted that concrete creep is a rheological phenomenon associated with the gel-like structure of the cement paste; creep deformation can also be explained partly in terms of viscoelastic deformation of the cement paste and to the gradual transfer of load from cement paste to aggregate. Creep properties are of particular relevance to understand the mechanism leading to the prediction of potential thermal cracking of mass concrete: the most extensive use of creep data is in thermal stress analysis for concrete dams.

### **- Drying Shrinkage (Section 5)**

Volume changes in concrete can be caused by mechanical, physical and chemical processes: in this Chapter only volume changes due to the moisture variations in concrete and the consequent drying shrinkage are dealt with. The effect of drying shrinkage of concrete in large dams is discussed: it reduces rapidly with the thickness and become negligible at a depth of about 0.50 m.

### **- Thermal properties (Section 6)**

Temperature has a very important effect on concrete dams. Two distinct phenomena are considered:

- \* the hydration of the cement which causes an increase of temperature during the hardening phase of concrete;
- \* the environmental variation of temperature under the normal service conditions.

In both cases the analysis of the temperature distribution in the dam and of the consequent induced stresses need data on the conductivity and diffusivity, specific heat and coefficient of thermal expansion.

### **- Water Permeability (Section 7)**

The flow of water or moisture through a concrete dam can affect its general performance and particularly its durability. Permeability and moisture coefficients can be estimated through suitable test methods. Furthermore models describing the mobility of water in a porous material such as concrete have been developed through the years and briefly presented.

### **- Frost resistance (Section 8)**

The deterioration of the concrete in a dam can be ascribed to a series of chemical and physical causes (both internal and external). Freezing and thawing is the most common external physical attack. External exposure conditions and concrete quality are of main importance as they determine the resistance of concrete to freezing and thawing cycles. Main test to evaluate the frost resistance are considered to prevent the phenomenon and specific diagnostic investigations are suggested to identify it in frost affected concrete dams to be repaired.

## 2 STRENGTH PROPERTIES

<b>2 STRENGTH PROPERTIES .....</b>	<b>1</b>
<b>2.1 GENERAL .....</b>	<b>2</b>
<b>2.2 CONCRETE TESTING.....</b>	<b>2</b>
2.2.1 <i>Testing of concrete strength for new dams .....</i>	<i>2</i>
2.2.1.1 <i>Testing in stages .....</i>	<i>2</i>
2.2.1.2 <i>Testing program.....</i>	<i>3</i>
2.2.1.3 <i>Sample Sizes .....</i>	<i>5</i>
2.2.1.4 <i>Wet screening.....</i>	<i>7</i>
2.2.2 <i>Testing of concrete strength in existing dams.....</i>	<i>8</i>
2.2.2.1 <i>General .....</i>	<i>8</i>
2.2.2.2 <i>Semi-destructive or non-destructive methods.....</i>	<i>8</i>
2.2.2.3 <i>Ratio between core diameter and MSA.....</i>	<i>9</i>
2.2.2.4 <i>Length-to-diameter ratio .....</i>	<i>10</i>
2.2.2.5 <i>Core size.....</i>	<i>10</i>
2.2.2.6 <i>Core vs. laboratory strength.....</i>	<i>11</i>
2.2.3 <i>Nominal age of concrete strength .....</i>	<i>12</i>
2.2.4 <i>Test Equipment.....</i>	<i>16</i>
2.2.5 <i>Evaluation of Strength Testing.....</i>	<i>16</i>
2.2.6 <i>Generic Uncertainty in Test Procedures .....</i>	<i>18</i>
<b>2.3 COMPRESSIVE STRENGTH .....</b>	<b>20</b>
2.3.1 <i>Effects of porosity and w/c-ratio on concrete strength .....</i>	<i>20</i>
2.3.2 <i>Effects of maximum size of aggregate (MSA) .....</i>	<i>22</i>
2.3.3 <i>Effects of aggregate properties .....</i>	<i>23</i>
2.3.4 <i>Effects of curing .....</i>	<i>24</i>
2.3.5 <i>Effect of mineral admixtures and blended cements .....</i>	<i>25</i>
2.3.6 <i>Effect of sustained loading.....</i>	<i>26</i>
2.3.7 <i>Multiaxial compressive stress domain in a dam.....</i>	<i>28</i>
<b>2.4 TENSILE STRENGTH.....</b>	<b>29</b>
2.4.1 <i>Tensile loading in the dam .....</i>	<i>29</i>
2.4.2 <i>Type of tensile testing .....</i>	<i>30</i>
2.4.3 <i>Tensile strength ratios.....</i>	<i>31</i>
2.4.4 <i>Size effect .....</i>	<i>32</i>
2.4.5 <i>Tensile strain capacity in dams .....</i>	<i>32</i>
2.4.6 <i>Tensile strength at joints .....</i>	<i>33</i>
2.4.7 <i>Tensile strength criteria.....</i>	<i>34</i>
2.4.8 <i>Use of tensile strength in mathematical models.....</i>	<i>36</i>
2.4.8.1 <i>Linear elastic analysis .....</i>	<i>36</i>
2.4.8.2 <i>Non linear analysis .....</i>	<i>37</i>
<b>2.5 SHEAR STRENGTH .....</b>	<b>39</b>
<b>2.6 DYNAMIC STRENGTH .....</b>	<b>41</b>
2.6.1 <i>Dynamic Compressive Strength.....</i>	<i>42</i>
2.6.2 <i>Dynamic Tensile Strength .....</i>	<i>43</i>
2.6.3 <i>Dynamic Shear Strength.....</i>	<i>45</i>
<b>2.7 REFERENCES.....</b>	<b>46</b>

## **2.1 GENERAL**

Strength is the most commonly considered parameter in structural design of new dams and for monitoring of existing dams.

Types of strength important for dams are compression, several types of tension and shear strength. This corresponds to common loading combinations which give rise to different modes of possible failure. It is then the relevant material strength, which counteracts a specific failure mode to happen.

Factors influencing strength are the concrete constituents, the test conditions, curing, the effects of ageing and size effects.

Concrete strength is tested on small specimens under controlled laboratory conditions; concrete in the dam is exposed to more variables. Correlating the two conditions by sound inductive reasoning based on project-specific data is imperative.

It is perhaps unfortunate that it has become the custom to relate structural safety mainly on compression although no dam ever failed by excessive compressive stresses. However, compressive strength is easy to test and easy to monitor. The use of compression as the predominant strength indicator is also supported by the common assumption that improving compressive strength will improve other concrete parameters as well, both under static and dynamic loading. Such a general assumption may be misleading as, for example, high strength concrete may experience less ultimate strain capacity and thus lead to earlier incipient cracking. This Section will therefore also focus on issues where other than compressive strength criteria are of importance.

Strength is not a deterministic but a random parameter. Standard testing does respect this physical fact; references to test results not in the same manner. This Section therefore tries to emphasize the importance to include scatter (standard deviation, coefficient of variation, confidence limits) as an integral part of reports on concrete strength.

## **2.2 CONCRETE TESTING**

### ***2.2.1 Testing of concrete strength for new dams***

#### *2.2.1.1 Testing in stages*

Testing for new dams is done in stages, coping with the increasing level of desired knowledge about material parameters. Three stages are common for concrete testing during final project phases:

- **STAGE I:** preliminary testing programs to curtail several potential sources of constituents (borrow areas for aggregates, blending for cementitious material). This test stage is intended to set limits for design mixes and will be used as a guide-line for the subsequent test stages.

The approach is for simple tests about main strength parameters with values from the literature for review and comparison.



*ICOLD Bulletin: The Physical Properties of Hardened Conventional Concrete in Dams*  
Section 2 (Strength properties)

- STAGE II: main testing program before construction commences to refine the results of STAGE I with aggregates and cementitious material which are expected to be used for construction
- STAGE III: quality control during construction.  
Testing samples of concrete during construction phase is necessary for controlling the strength results with contract specifications, to be sure that quality of material used in final product (for example, dam body) is comparable with design assumptions and acceptable.  
It is evident that uncertainty levels of any applied conservatism can be reduced drastically if reliable and sufficient test results are available. Thus, pre-construction testing is not only a safety but also an economic issue. It is rarely a benefit to curtail pre-construction programs for economic reasons.

Concrete testing of existing dams will be discussed in Section 2.2.2.

#### *2.2.1.2 Testing program*

The general set-up of test programs comprises the variation of the most significant concrete constituents and may be grouped in several parts:

- Variation of cement content/content of cementitious material
- Variation of type of cementitious material and its blending
- Variation of borrow area
- Variation of aggregate grading and influence of wet-screening
- Investigation about minimum content of cementitious material
- Investigations with different admixtures to investigate required water-cement ratios and workability
- Special testing, as required. Examples are bleeding, Alkali-Aggregate Reaction (AAR), wedge splitting tests, dynamic properties, creep.

Only one component shall be changed at the time and its influence on fresh and hardened concrete properties being tested. The results should allow the following:

- Obtain required strength values to satisfy the result of the static/dynamic stress/stability analysis
- Assess the maximum content of blended material (pozzolans, fly ash etc.)
- Obtain satisfactory workability and permeability
- Assess the benefit of admixtures.

Tab. 2.1 shows an example of a STAGE II test program for hardened concrete properties.

ICOLD Bulletin: The Physical Properties of Hardened Conventional Concrete in Dams  
 Section 2 (Strength properties)

Tab. 2.1 – Example of test Program for hardened concrete properties

Mass Concrete Testing		Summary of Investigations on Hardened Concrete										Comments
Part	Variation of Components	Density	Compressive Strength (days)					Flex. Strength		Permeability	Freezing and Thawing <sup>2)</sup>	
			7	28	90	180	360 <sup>1)</sup>	28	90			
1	Variation of cement content											Constant: aggregate source, grading curve and MSA, air entraining agent, workability (W/C ratio is then a result of acceptable workability). Pre-testing with different admixtures
	150 kg/m <sup>3</sup>	.	.	.	.	.	.	.	.	.	.	
	175 kg/m <sup>3</sup>	.	.	.	.	.	.	.	.	.	.	
	200kg/m <sup>3</sup>	.	.	.	.	.	.	.	.	.	.	
	225kg/m <sup>3</sup>	.	.	.	.	.	.	.	.	.	.	
2a	Variation of cement type (if an option)											
	175 kg/m <sup>3</sup>	.	.	.	.	.	.	.	.	.	.	
	225kg/m <sup>3</sup>	.	.	.	.	.	.	.	.	.	.	
2b	Variation of blending (cement+puzzolans, fly											can replace Part 1 if the use of blended material is preferable from the onset
	120+30=150 kg/m <sup>3</sup>	.	.	.	.	.	.	.	.	.	.	
	100+50=150 kg/m <sup>3</sup>	.	.	.	.	.	.	.	.	.	.	
	160+40=200kg/m <sup>3</sup>	.	.	.	.	.	.	.	.	.	.	
	140+60=200kg/m <sup>3</sup>	.	.	.	.	.	.	.	.	.	.	
3	Variation of borrow area											e.g. quarried aggregates vs. river deposits
	150 kg/m <sup>3</sup>	.	.	.	.	.	.	.	.	.	.	
	225kg/m <sup>3</sup>	.	.	.	.	.	.	.	.	.	.	
4	Minimum content of cementitious material <sup>3)</sup>											
	100+30=130 kg/m <sup>3</sup>	.	.	.	.	.	.	.	.	.	.	
	75+75=150 kg/m <sup>3</sup>	.	.	.	.	.	.	.	.	.	.	
5	Facing concrete: 250kg/m <sup>3</sup> <sup>4)</sup>											
	borrow area 1	.	.	.	.	.	.	.	.	.	.	
	borrow area 2	.	.	.	.	.	.	.	.	.	.	
<p><b>Comments:</b> The table is an example. The scope depends on the variables under discussion. Important is that pre-construction testing is done well ahead of construction to profit from the knowledge of strength development with time and thus prepare a reliable mix design.</p> <p>1) nominal strength for large dams can be extended to the age of 1 year. Therefore this strength value might support to reduce cement content</p> <p>2) as a measure for general durability for facing concrete also at sites without temperatures below zero.</p>												

When setting up test programs any investigator should be flexible enough to scrutinize his/her needs: what is the impact of a particular concrete parameter on costs and safety? - and to define the scope of the program accordingly. It is not reasonable to set up tests for parameters of marginal significance just because they are needed for analysis or it is common practice to test them.

Lets take an example. The modulus of elasticity of concrete,  $E$ , is a value which (a) has a low variability, and (b) is only marginally important for the stress level in a dam. Even in highly stressed arch dams, a change of  $E$  by multiples of its base value will cause a proportionally minor change in stresses. So, why then concentrate on tests to obtain  $E$ ? The literature provides ample values and ways to predict reliable moduli [2.1].

Reliability on structural safety depends on obtaining satisfactory strength in the dam relating it to laboratory test results. It is the relation between these two values, which merits particular attention.

### *2.2.1.3 Sample Sizes*

Typical for dam concrete is the large Maximum Size Aggregate (MSA) with respect to commonly used sample sizes for strength testing. The ensuing bias of strength values has to be given special attention.

Standard test for compressive strength use cylinders, cubes or the broken halves of prism from flexural strength testing. Common cylinder sizes are 150x300mm ( $\Phi=150$  mm and  $h=300$  mm), 300mm cubes and 75x75x300mm prisms.

In Austria samples sizes for compressive strength are 30 cm cubes and for flexural and pure tensile testing 20x20x60cm prisms are used.

Smaller samples sizes than mentioned above would result in unduly influence of the large aggregate sizes on the test result. Tab. 2.2 lists some conversion factors for common sample sizes used for dam concrete testing [2.2] [2.3].

Tab. 2.2 – Conversion Factors for Different Sample Sizes

Reference sample size: 30cm cubes=100%			
Conversion to other sizes		Relative strength	Ref.
Size	Conversion formula for MPa	%	
20cm cubes	$f_{20} = 1.1 f_{30}$	110	ISO 2736 [2.2]
15x30cm (6"x12") cylinders	$f_{15/30} = 0.8 f_{30}$	80	
15x30cm (6"x12") cylinders	$f_{15/30} = 0.98 \cdot (f_{30} - 5.2)$	78 to 83 <sup>1)</sup>	
30x45cm (12"x18") cylinders	$f_{30/45} = 0.91 \cdot (f_{30} - 3.6)$	78 to 82 <sup>1)</sup>	
<div style="border: 1px solid black; padding: 2px; width: fit-content; margin: auto;"> <sup>1)</sup> for a range of 25 to 35 MPa with lower relative strength for the lower absolute compressive strength                 </div>			
Reference sample size: 6"x12" cylinder (15x30cm)=100%			
3"x6" cylinder	$f_{3/6} = 1.06 \cdot f_{6/12}$	106	[2.3]
8"x16" cylinder	$f_{8/16} = 0.96 \cdot f_{6/12}$	96	
12"x24" cylinder	$f_{12/24} = 0.91 \cdot f_{6/12}$	91	
18"x36" cylinder	$f_{18/36} = 0.86 \cdot f_{6/12}$	86	

The commonly required ratio between smaller dimension of the specimen and maximum size aggregate (MSA) in excess of 3 also applies for mass concrete with large size aggregates.

In Switzerland some testing for dam concrete used 40 cm cubes which are then sawed into 8 cubes with size of 20 cm for testing. This is considered as very meaningful. It allows using the full mix and has the advantage to get 8 specimens for the mean strength value of the full mix and the sample-to sample scatter is small. It eliminates the conversion from wet-screened to full mix. However, it is a more cumbersome procedure.

The use of cubes has the advantage that no grinding and capping of the surfaces is necessary and that the scatter in strength values is generally less due to less imperfections in the production of cubes.

Benefits and shortcomings of cylinders vs. cubes are widely discussed in the literature. Cubes are generally used in Continental Europe (except France) and UK. They are easier to test because they need no capping or grinding. Another advantage is that cubes can be tested parallel and perpendicular to the direction of casting to indicate any difference due to casting direction.

On the other hand, cylinders are generally preferred in research because they better represent true strength due to less influence of stress singularities from sample surfaces. Cylinders are the common sample form in the US, France, Canada, Japan, Latin America and Australia.

#### 2.2.1.4 Wet screening

Wet-screening is a common measure to overcome the discrepancy between a mix with full MSA and dimensions of common sample sizes [2.4]. Wet screened concrete needs conversion factors in order to assess the full-mix strength. The US Bureau of Reclamation in its Designation 33 reports conversion factors for wet-screening of the 38 mm to 150 mm sizes which are depending on age. Tab. 2.3 reports a range of compressive strength ratio for two types of concrete, the lower values for blended and the higher values for unblended cement [2.4].

Tab. 2.3 – Compressive strength ratio between full and wet – screened mix [2.4].

Age at testing the wet-screened samples in days	Compressive strength ratio full mix (150 mm)/ wet-screened mix (38 mm)
28	0.7 to 0.8
90	0.65 to 0.75
180	0.65 to 0.77

Results from wet-screened laboratory testing are therefore non-conservative.

Similar results are obtained by Portuguese research with a larger scatter of test results due to comparing full mix cylinders with wet-screened cubes [2.5].

Correlation tests between the strength of wet screened concrete tested at 28 days and test specimens containing the full mass concrete are recommended to be part of a STAGE II testing program (section 2.2.1.1). However, if the site is well equipped for large-scale tests, it may be possible to do it also on site (STAGE III).

## **2.2.2 Testing of concrete strength in existing dams**

### *2.2.2.1 General*

Testing of concrete strength on aged dams during operation may have several objectives. Among those are:

- to evaluate strength gain at ages in excess of sample age in laboratory testing
- to compare laboratory strength with in-situ strength
- to evaluate loss of strength from ageing, or chemical alteration (AAR or sulphate attack), or loss by stress concentrations in certain parts of the dam, demonstrated by unstable cracking or movements.
- to evaluate long-term creep.

Testing is generally either by non-destructive methods or by core drilling. The latter is more commonly used.

Core testing for highly stressed dams is justified. Consider the many differences between laboratory and field conditions: different compaction, different sample size and MSA (Maximum Size of Aggregate), different state of loading (stress free vs. multiaxial), different initial stress implications and different curing. It is therefore not surprising that laboratory strength is different than strength in the completed structure. This has to be accepted. What is essential is to be aware and interpret these differences reasonably.

The extensive French experience is summarized in a comprehensive report by LERM [2.6]. A fine summary of implications with core extraction and testing is also reported in [2.7] by Adam Neville.

### *2.2.2.2 Semi-destructive or non-destructive methods*

There is a whole range of semi-destructive or non-destructive methods of testing concrete strength in situ, e.g. with rebound hammer, measuring the velocity of sonic or ultrasonic pulses through concrete, pull-out tests, break-off tests and penetration tests [2.8].

Non-destructive sonic methods can be used for diagnostic investigations on concrete in existing dams. They are based on the principle that the characteristics of the impulsive sonic signal transmitted across the concrete can be related to the elastic properties and soundness of concrete itself. In practice trains of elastic waves, with frequencies of 5-30 kHz are generated and received by special electro-acoustic transducers located inside or on the surface of the dam. The investigation involves taking sonic logging measurements along boreholes and direct velocity measurements between pairs of adjacent holes or surfaces. By means of tomography techniques it is possible to obtain a detailed map of elastic wave velocities inside the sections of the dam and to evaluate the elastic dynamic characteristics and locally the state of integrity of the concrete. In Italy this technique is widely used and several concrete dams have been checked by means of the sonic tomography [2.9]

It is also possible to obtain a correlation between velocity and concrete strength. But it should be based, for each dam investigated, on traditional destructive compressive tests on samples cored from the structure. In this case a detailed map of concrete strength can be derived (Fig. 2.1).

Q. 65-R. 43

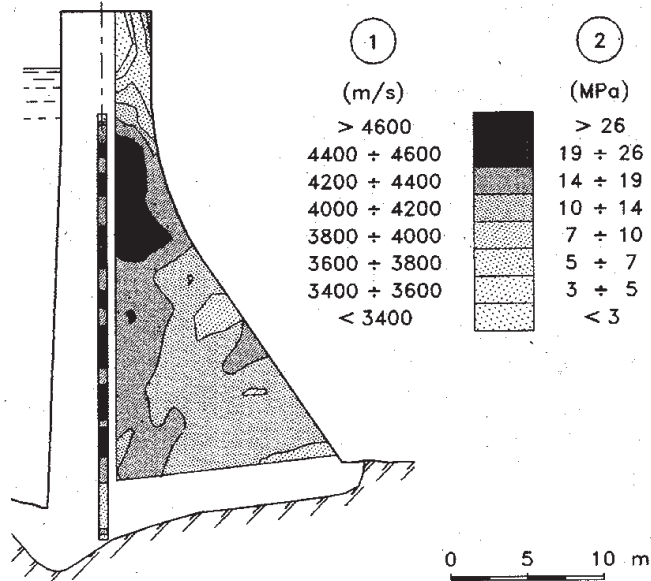


Fig. 2.1 - Sonic tomography of a dam – Map for sonic velocities (1) and for concrete compression strengths (2) [2.9].

### 2.2.2.3 Ratio between core diameter and MSA

Similar to the condition for laboratory test cylinders, the ratio between core diameter and MSA (Maximum Size of Aggregate) should be close to 3 [2.10]. 200 to 300 mm cores are generally used drilled from dam galleries or downstream surfaces, with the 200 mm cores only for smaller MSA, say less than 80 mm. Smaller than 200 mm cores should not be used in any case.

When the desired ratio of 3 is not maintained, the number of samples for calculating a mean strength should be increased.

When core drilling is known to be done it is useful to mark locations between reinforcing bars in the dam galleries already during construction.

#### 2.2.2.4 Length-to-diameter ratio

Strength from cores depends on the length-to-diameter ratio ( $l/d$ ). Standard cylinders have a length-to diameter ratio of 2. However, cores from dams are occasionally difficult to extract with this ratio. Conversion factors have then to applied for assessing the length-to-diameter influence:

Conversion factors as suggested by ASTM and British Standards are (Tab. 2.4):

Tab. 2.4 – Conversion factors suggested by ASTM and British Standards

<b>l/d-ratio</b>	<b>ASTM C42(1990)</b>	<b>BS 1881</b>
2.00	1.00	1.00
1.75	0.98	0.98
1.50	0.96	0.96
1.25	0.93	0.94
1.00	0.87	0.92

Already the comparison of correction factors for low  $l/d$  ratios between these two standards indicate that for  $l/d$ -ratios approaching unity the uncertainty of strength prediction increases rapidly. This is further researched in [2.10]. Thus, it is recommended not to use cylinders with  $l/d < 1.5$ .

#### 2.2.2.5 Core size

Another influence comes from the core size if smaller than 300 mm drillholes are used. This is not recommended for dam concrete although sometimes smaller diameter holes are used because of lack of equipment.

The core diameter has a significant effect on strength. The larger the size of the core, the higher is the compressive strength [2.11]. For example, reducing the diameter from 150 mm to 75 mm would result in a 50% reduction of tested strength (results in [2.11] from a 19 mm MSA concrete). The reason is that the thickness of the surface zone, disturbed from the drilling process, is constant and thus becomes increasingly influential at small core diameters<sup>1</sup>. It is therefore difficult to conclude reasonably on the real strength from small diameter core sampling because of the joint influence of the small core diameter and the heterogeneous concrete structure dominated by the presence or not of coarse aggregates in the core.

---

<sup>1</sup> This finding seems to contradict the inverse relation between diameter of test cylinder and strength as shown in Tab. 2.2. But, unlike molded cylinders, the influence of skin effects (particularly the disturbed bonding by cutting through coarse aggregates) governs the strength reduction with decreasing core diameter.



2.2.2.6 Core vs. laboratory strength

Of interest is to compare laboratory compressive strength with strength from cores. A specimen of the same geometrical characteristics and maturity drilled from a structure has generally a lower strength than laboratory made and cured concrete specimen (10 to 30%). Moreover, the scatter is larger. The above range of 10 to 30% very much depends on quality of drilling, curing and age.

These influences are corroborated by an interesting observation comparing laboratory with field test series from Shasta Dam, USA [2.3] (Fig. 2.2). The two series have different gradients indicating the superposition of two influences, namely (a) the known decreasing rate in gain of strength with increasing age (here demonstrated by the kink at 90 days), and (b) the influence of field-cured cores with less gain at high ages as one would obtain from laboratory test results.

However, there are rare test cases, where the reverse relation, i.e. core strength higher than laboratory strength, is found for dam concrete. It is reported that such reverse relations result from overvibrated concrete, with excessive bleeding of mixing water, which then reduces the w/c ratio leading to higher core strength. Another reason has its origin in the fact that dry cores (not even oven dried) show higher strength than cores from wet concrete due to the influence of pore pressure. Thus, if cores are extracted outside the saturated upstream zone of a dam, 10 to 15% higher strength values might be expected. The difference in dry/wet strength has then to be modified by the influence of a scale effect, i.e. the scale effect is larger in small than in large cores.

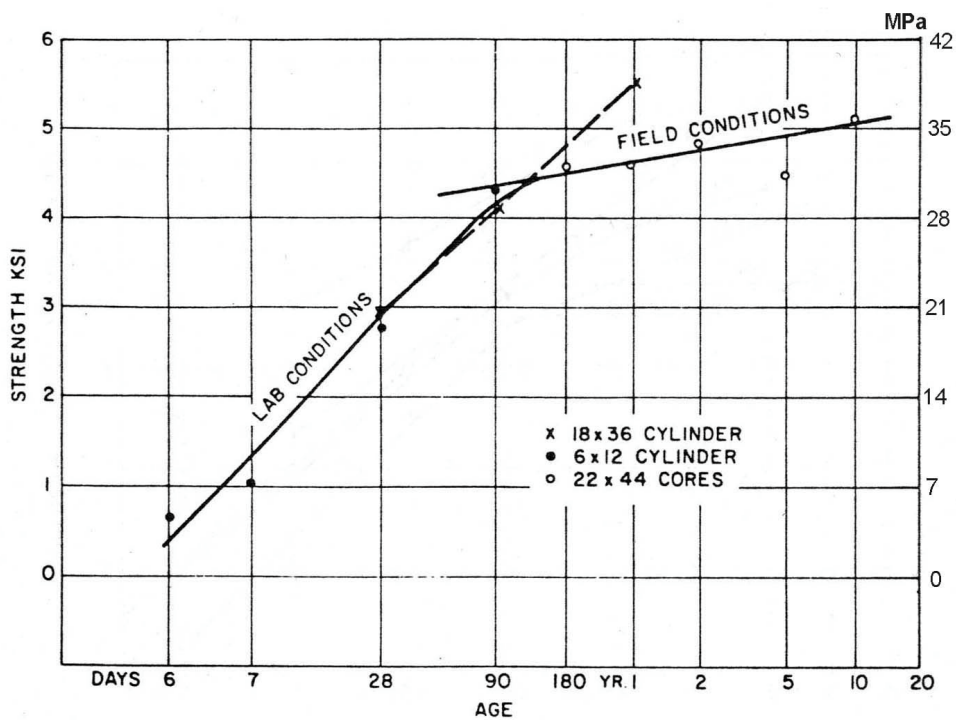


Fig. 2.2 – Development of compressive strength: laboratory vs. field sampling [2.3]

Another factor contributing to the difference between core and laboratory strength is the relief of the multiaxial stress condition after coring. This can be particularly influential in Alkali-Aggregate Reaction (AAR)-damaged concrete, where a damaged matrix can expand and thus reduce core strength.

The above dichotomy leads recommending to core dam concrete as a rule and not only if unsatisfactory laboratory tests are obtained, at least for large, highly stressed dams. Using cored strength values in a back-analysis would provide more reliable safety margins. However, it should be mentioned that checking the compressive strength from drilled dam cores is only successful if drilling is done with much care, if curing is done properly, and if pre-test conditions are representative and realistically interpreted. Otherwise the core strength tends to be unrealistically low.

ASTM C 42 [2.12] and EN 12504 [2.13] can be used as a reference for drilled cores. So can ACI 318, which stipulates that field-cured test cylinders should achieve at least 85% of the strength from laboratory-cured cylinders [2.14]. ACI 318 defines two field curing conditions depending on the expected condition in the structure: one is air drying, the other soaking of the specimens. For dam concrete, soaking is more appropriate for a saturated concrete mass and it should be long enough to eliminate moisture gradients in the sample (curbing the influence of pore water pressure). If the concrete to be tested is assumed to be in a steady-state dry condition then the cores should not be wet-cured. This is important because the difference in compressive core strength between the 2 curing methods can be 20 to 35%, with the air dried being the larger of the two values [2.15].

Other comparative test results for structural concrete (28 days) demonstrate 90% to 76% for core as compared to laboratory strength [2.16]. Percentages depend on stress level: it decreases from close to 100% for low strength (~20 MPa) to 70% for high strength concrete (~60 MPa) [2.17].

### ***2.2.3 Nominal age of concrete strength***

In large hydraulic structures, structural elements are rarely required to withstand substantial stress at early age. Unless unusual circumstances prevail, the Committee recommends an age in excess of 180 days as basis for evaluating the characteristic strength. This last one is defined in the following section 2.2.5.

It is utterly conservative to use 28 or even 90 days for assessing strength safety margins, as occasionally specified for dam concrete. For most dams at least 180 days seem reasonable. ACI 207 reports that design strength is on ages between 90 days and sometimes up to two years [2.18]. In California 1 year is accepted too [2.19].

Accounting for the continued strength development beyond 90 days, especially where pozzolans are applied, the correlation factors at 1 year may range as shown on Tab. 2.5 and Fig. 2.3 from [2.20].

*ICOLD Bulletin: The Physical Properties of Hardened Conventional Concrete in Dams*  
 Section 2 (Strength properties)

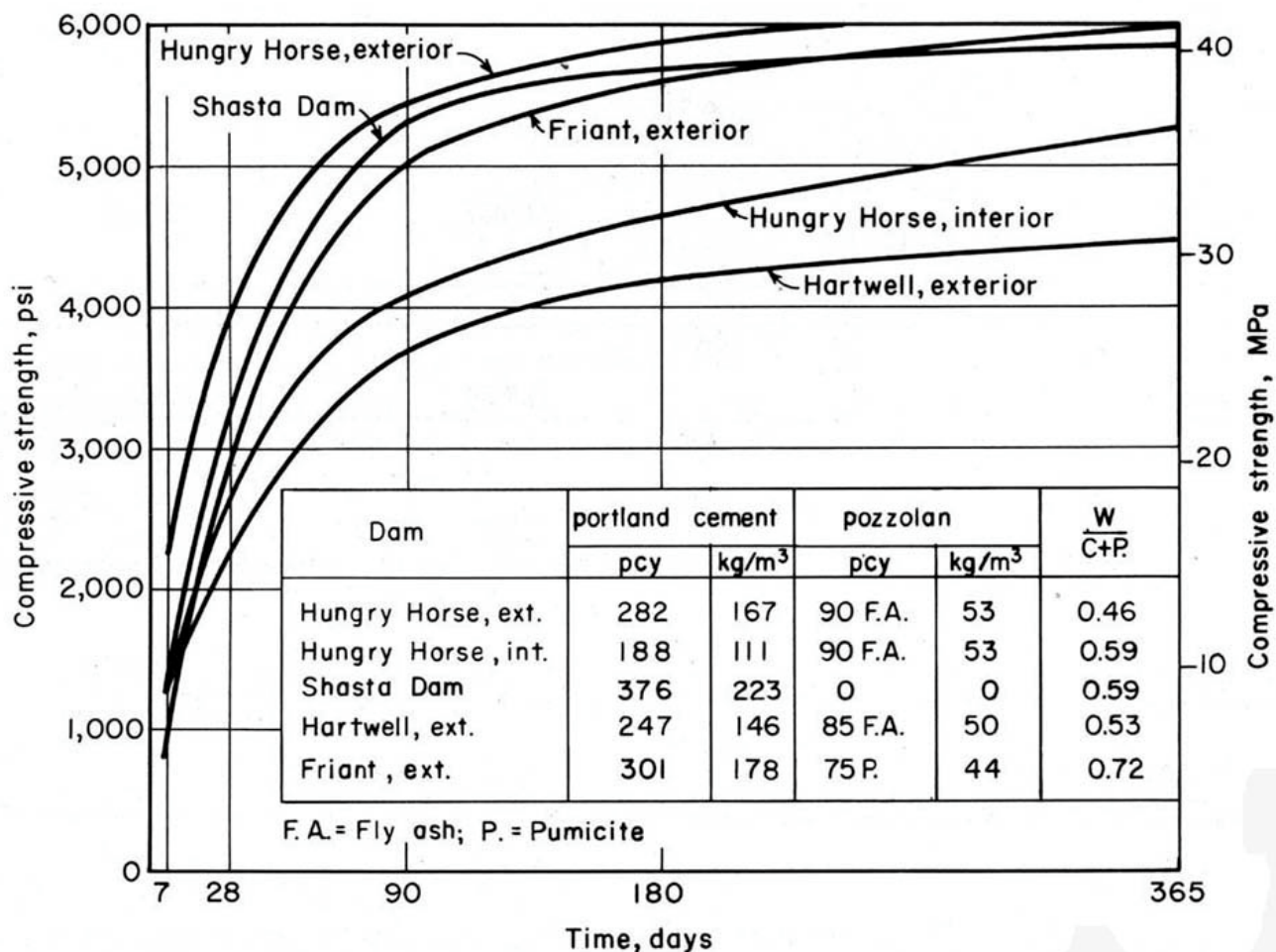
Tab. 2.5 – Gain on Compressive Strength with Age [2.20].

Dam/Country	Year	Blending <sup>1)</sup>			Mean compressive strength [MPa]		Strength ratio 365/90
		OPC	Pozzolan	Quantity	90 days	365 days	
Dworshak/USA	1972	II	fly ash	25%	14.0	21.4	1.53
Glen Canyon/USA	1963	II	Pumicite	34%	33.8	47.0	1.39
Las Portas/Spain	1974		fly ash	22.5-30%	45.0	58.8	1.31
Valparaiso/Spain	1988		fly ash	25-30%	28.6	30.4	1.06
Llauset/Spain			fly ash	25%	31.3	42.3	1.35
Flaming Gorge/USA	1962	II	calc. shale	34%	24.1	32.3	1.34
Puylaurent/France	1995	CEM III	fly ash	40%	24.5	32	1.31
Hoover/USA	1935	IV	none		22.8	29.6	1.30
Libby/USA	1972	II	fly ash	25%	17.0	22.0	1.29
Baserca/Spain			fly ash	25%	29.8	37.6	1.26
Yellowtail/USA	1965	II	fly ash	30%	31.6	38.9	1.23
Katse/Lesotho	1995	II	fly ash	30%	36.2	42.2	1.17
Grand Coulee/USA	1942	II + IV	none		35.6	41.3	1.16
Sambuco/Switzerland	1954	II	none		21.7	24.4	1.12
Morrow Point/USA	1967	II	none		41.1	46.1	1.12
Val Gallina/Italy	1950	IP	pozzolan	33%	47.7	52.7	1.10
Schlegeis/Austria	1971	CEM III			20.5	27	1.32
Grand Dixence/Switzerland	1955	IV	none		26.5	28.9	1.09

**Legend:**

<sup>1)</sup> none..... Ordinary Portland cement (OPC) only, of indicated ASTM or CEM type  
 quantity is % of total cementitious material.

The mean strength values are generally from construction and the mean of a large sample population.



**Gain of compressive strength with age**

Fig. 2.3 – Gain of compressive strength with age [2.20].

Tab. 2.6 shows long-term core strengths from Austrian dams:

Tab. 2.6 – Core strength from Austrian dams [2.21]

Dam	Age of core in years	Core strength ( $\phi$ 200 mm) [MPa]	90 day's cube strength [MPa]
Schlegeis	12	32.0	20.0
Drossen	26	40.3	20.4
Mooser	26	41.1	20.4
Limberg	32	44.5	31.0

From Italian dams, more readily available [2.22] are ratios between 90 and 180 days strength. Some are reported on Tab. 2.7:

Tab. 2.7 – Core strength from Italian dams [2.22]

Dam	Strength 90 days [MPa]	Strength 180 days [MPa]	Strength ratio 180/90
Cignana n.1	15,2	16,2	1,06
Suviana	13,6	14,5	1,06
Goillet	15,7	20,3	1,29
Santa Giustina	44,1	46,6	1,06
Pian Telesio	28,7	30,4	1,06
Campo Moro n.1	37,3	40,8	1,09
Valle di Lei	41,7	44,2	1,06

#### **2.2.4 Test Equipment**

The type of the testing machine (press) may have an effect on the obtained results. These machines are classified as hard (rigid) and soft (less rigid) depending how the head of the machine is following the deformation of the specimen. In a hard machine the head has difficulties to follow rapid deformations; in a soft machine it will follow without delay. The consequence is that in a soft machine the energy stored in the machine is released and acts on the specimen when it starts to fail. This additional energy will cause more extensive crack propagation and indicate failure at lower loads than with a hard machine. In a stress-strain diagram this will result in lower peak stress for a soft as compared to a hard machine.

Loading range of the testing machine shall not exceed 90 % of the maximum range capacity applied during the verification test. Furthermore, in order to improve the reliability of measured values a minimum level of 20% is preferable, as for example set by the Japanese Industrial Standards (JIS). During the test, the compressive load induces lateral tensile strains in both, the steel platens and the concrete specimen, due to Poisson effect. The mismatch between the elastic modules of steel and concrete and the friction between the two, results in lateral restraint forces in the concrete near the platen. The concrete specimen is therefore locally in a triaxial stress state, with the consequent effect on strength. This effect is larger for cubes and smaller for cylinders or prisms.

Most compressive test machines in field laboratories are not free from friction between specimen and platen. This restrains the lateral end-expansion of the specimens and introduces shear stresses, demonstrated by a shear-type failure pattern. This end-effect results in a higher strength than for specimen which are exposed to pure compression (failure pattern  $\approx$  parallel cracks). The effect is more pronounced for specimens with lower l/d-ratios and it is also the reason why cube strength is higher than cylinder strength.

Test machines should therefore be low in frictional resistance between platen and specimen.

#### **2.2.5 Evaluation of Strength Testing**

Strength parameters of a composite material like concrete can never be defined without uncertainty. Strength follows a statistical distribution and is not a deterministic value. The factors contributing to variability are concrete constituents, production, testing and ageing.

The literature of concrete testing has therefore developed a host of theories and methodologies to evaluate scatter of test results and its application for dam concrete. They are not discussed here. The reader is encouraged to consult the numerous publications, among them the Bureau's of Reclamation Concrete Manual [2.4], ACI 214 [2.23], the corresponding ISO Standards 2859 [2.24], 3951 [2.25] and 5479 [2.26], CEB – FIP Model Code [2.27] and reference [2.28].

Some particularities with respect to dam concrete testing are added.

- One is related to the strength gain with age. As mentioned, for dams the characteristic age should be 180 days or, for larger dams (longer construction), one year. This means that one-year strength data should be available when concrete

placement starts. This is not always possible. In order to overcome the impasse, it is often decided to take 28/90 day as characteristic strength or to conservatively extrapolate these early strength data. In most cases, such decisions lead to excessive cement content, which is uneconomic and, as a side effect, contributes to unfavourable thermal conditions. Of course, the obvious remedy is to start early with concrete testing. However, this needs planning, discipline and is often not done because of unknown final concrete constituents.

However the characteristic age have to be always related to the specific dam under examination, taking into account the scale of the structure and the times of construction and service life.

This Bulletin would like to encourage the dam profession to also view the problem from a more pragmatic standpoint. Research, published data from case histories, and preliminary series with similar than the final mix design from the dam in question provide a host of strength-gain values to judge strength gain up to the age of the characteristic strength. Certainly, such a judgement has to be accompanied by assessing the consequences of an anticipated error between assessed and later measured characteristic strength: What, if the required strength is not met? Are the stipulated factors of safety (FS) still acceptable? But: isn't FS=3 just an arbitrary chosen number and FS=2.8 also acceptable? Can a local redistribution of stresses be assumed beneficial in mitigating a lacking safety margin? How much is the gain of strength between one year and the age when the calculated stresses are really occur, e.g. during extreme temperatures, floods or an earthquake?

In many cases the limiting strength is not compression but shear or tension, mostly along local zones, and shear/tensile strength is generally taken as a percentage of compressive strength, not measured per se. This percentage is highly speculative (particularly for dynamic loading) and uncertain in a similar order of magnitude than speculating a particular strength gain between 90 days and one year.

What this all means is that engineering judgement and peer review, based on an increasing data-base, often is a remedy to justify acceptance of uncertainties. This can be beneficial for economy and safety. The shortcut of immediate conservative solutions is not necessarily the only safe way to go.

- Evaluating strength data, the most common design criterion, is based on the following formula [2.23]:

$$f_m = f_c + k \cdot \sigma$$

$f_m$  the mean required strength for which the mix has to be designed

$f_c$  the characteristic strength (specified design strength to meet required safety against stresses)

$k$  a factor derived from the assumed strength distribution which depends on a stipulated proportion of tests (fractile) to fall below the level of  $f_c$ , and on the number of tests carried out.

$\sigma$  standard deviation of strength test series

The k-factor is derived from fractiles of a Normal distribution. Commonly used k values (for high number of tests, generally  $n \geq 30$ ) are reported in Tab. 2.8.

Tab. 2.8 – Examples of k values

Percentage of tests falling outside the limits $\pm k.\sigma$	Percentage of tests falling below $f_c$ (fractile in %)	Chances of tests falling below the lower limit	k
20	10	1 in 10	1.28
10	5	1 in 20	1.65
5	2.5	1 in 40	1.96
2	1	1 in 100	2.33

When comparing laboratory with core strength, the choice of k should be different for both types of tests because of the larger inherent variability of the latter. The procedure have also to be adapted, in the case of concrete strength evaluation from cores of existing structures.

- For statistical evaluation bounded or curtailed distributions (instead of an unbounded Normal distribution) are actually the correct choice because they represent more realistically the physics of statistical scatter. Although most codes still refer to Normal distributions there is a tendency for a change [2.29] as the influence on reliability indices, and thus on safety factors, is considerable [2.30].
- Reporting and archiving of test results is essential. Dams may show signs of distress years and decades after construction. Then, resorting to test documents, fallen into oblivion, should succeed to finding information about test conditions, sources of constituents, details of the mix design, number of samples, the variability of test results and the like.

### **2.2.6 Generic Uncertainty in Test Procedures**

As mentioned previously, in setting up test programs one needs to first assess the impact of a parameter on safety and its costs of testing and then decide if testing is meaningful or if it suffices to rely on published values.

In a similar way goes the decision about the impact of parameters, which are cumbersome to be tested or which are commonly not tested at all although their influence of strength is significant.

An example is the water-cement ratio (w/c ratio). In mass concrete field testing the w/c ratio is, for good reasons, not measured. This is unfortunate, because its share on the standard deviation for compressive strength is considerable (Fig. 2.4) and, were it measured, the scatter of compressive strength could certainly be reduced [2.31].



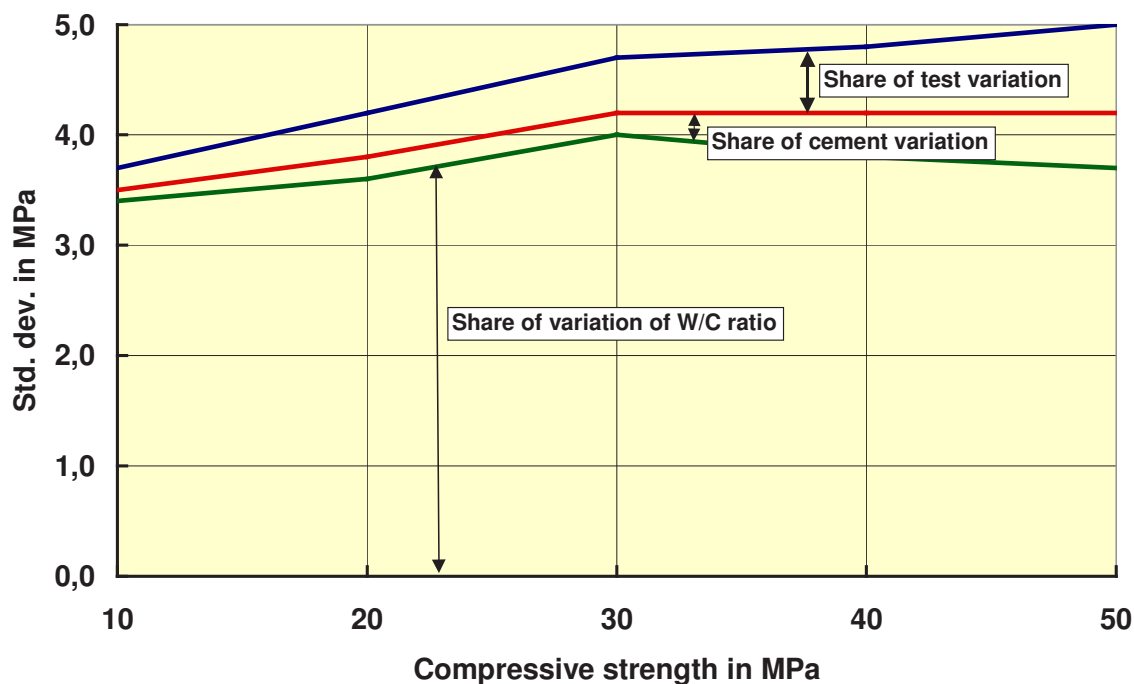


Fig. 2.4 - Shares of standard deviation during testing of compressive strength: above without and below with control of w/c ratio [2.31]

Then, there is the dichotomy of simple tests with high repeatability as against complicated tests with high dependability. The first have their limitations in the declining statistical effectiveness with increasing sample size (Fig. 2.5), the second are delicate to execute and evaluate.

An example is the decision either to assess tensile strength from formulas relating tensile to compressive strength or to rely on the more delicate (pure) tensile strength testing. The latter, if carefully executed more closely approaches reality, however, with the impediment of high scatter if  $n$  is small. Here, the conflict ensues either having to deal with a high uncertainty of the mean value (formula-based assessment) or with a high scatter around a more reliable mean (tensile testing). Certainly, the latter is preferable. It is therefore suggested to incorporate tensile testing in the technical specifications.

What this all means is that the true strength in the dam is a random variable affected by many influencing factors, conditions and testing traditions. Any tested strength value has therefore to be recognized as an interpreted estimate of the unknown true strength.

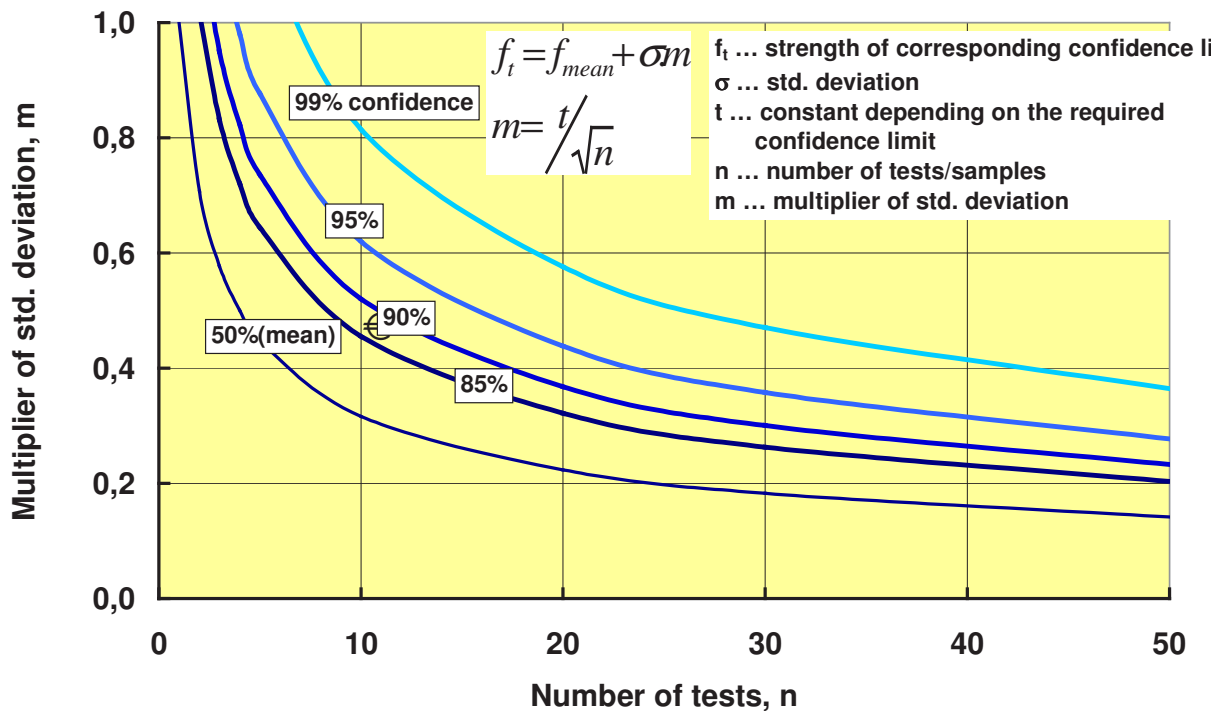


Fig. 2.5 - Reduction of uncertainty with increasing numbers of sampling (inverse proportional to  $\sqrt{n}$ )

## 2.3 COMPRESSIVE STRENGTH

Compressive strength is the predominant property for dam concrete. Concrete dams are designed to carry compressive stresses and to minimize tensile stresses. As discussed in the following, compressive strength is influenced by a wealth of conditions of fresh concrete, its placement and curing.

### 2.3.1 Effects of porosity and w/c-ratio on concrete strength

The strength of ordinary concrete is governed by the porosity of the cement paste, which in turn depends on the water/cement ratio and on the degree of hydration. It is primarily the porosity of the transition zone between the cement paste and the aggregate, which influences strength, because this zone (about 50  $\mu\text{m}$  wide) is the weakest link in the matrix, as cracking initiates within it. Porosity and degree of hydration have a fundamental relation to strength of concrete, but they are not easy to measure. Hence, for practical engineering applications, these parameters are replaced by the free water/cement ratio and the age of concrete when relating them to strength measurement. Typical relations between the water/cement ratios for an age of 28 days, using several theoretical formula and empirical evaluations are shown in Fig. 2.6.

For dam concrete w/c ratios are rarely specified and are predominantly determined experimentally to achieve satisfactory workability. In this context, advantage is taken to reduce the w/c-ratio by the use of water-reducing and plasticizing admixtures. The

ICOLD Bulletin: The Physical Properties of Hardened Conventional Concrete in Dams  
 Section 2 (Strength properties)

curves in Fig. 2.6 can be interpreted in this sense: the range with lower w/c ratios is mainly for concrete in more recent dams where admixtures are more widely used, whereby the higher w/c ratios are typical for older dams where admixtures are limited to an air entraining agent.

One needs to recognise the beneficial effect of water-reducing, plasticizing or superplasticizing agents as a potential means to reduce the water content in the mix. To lower the water content has several advantages. Besides the basic goal of higher strength (at equal content of cementitious material), these are a reduced permeability and thus higher durability (less porosity of the hydrated cement paste), less shrinkage and thus less shrinkage cracking and, if ice is used for cooling, a reduced peak temperature and thus less thermal cracking.

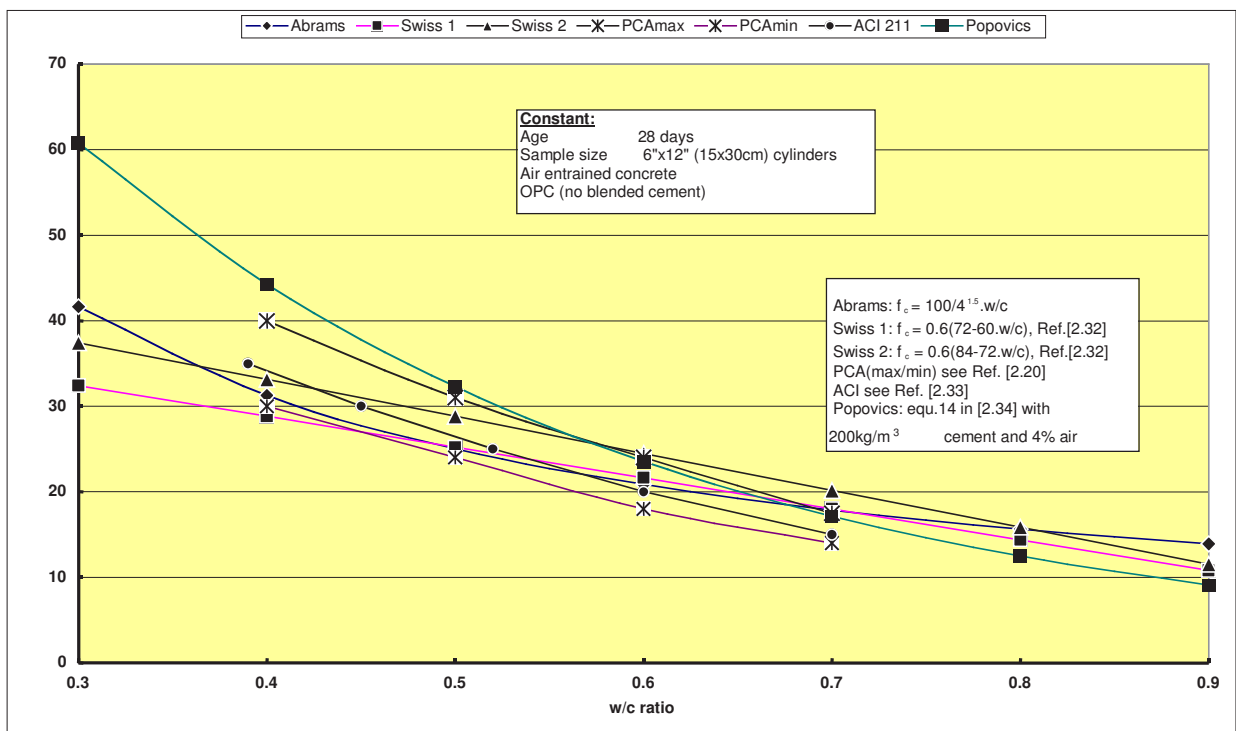


Fig. 2.6 – Compressive Strength vs water/cement ratio.

With respect to the denominator of the w/c-ratio, it is now common practice to use the term "water-cementitious material ratio, (w/cm)", a clumsy term, however appropriate because it makes sure that the denominator also includes all cementitious ingredients such as fly ash, slag, pozzolans, or the like, which participate in strength development together with Ordinary Portland Cement OPC.

French standards use the expression "liant équivalent" and even provide a factored coefficient for "cm" which considers the amount of strength participation of cementitious ingredients (e.g. by means of its pozzolanic activity index) [2.35].

### 2.3.2 Effects of maximum size of aggregate (MSA)

For the main mass of interior concrete a MSA between 120 mm and 150 mm is commonly used (80 mm for older dams). Larger or lower sizes are the exception for large dams.

This rather small range is the result of a long lasting experience balancing to reduce cement content and to achieve a good workability. The larger the aggregate size the less cement is required for a given volume of concrete to produce enough cement paste necessary to cover the aggregate surface.

To achieve the greatest cement efficiency, an optimum maximum size for each compressive strength level has to be obtained with a given MSA and cement content, as shown in Fig. 2.7. The results in [2.36] are from test series for Grand Coulee and Clear Creek dams by the Bureau of Reclamation (USA). For modern dams, however, only the lower third of Fig. 2.7 is applicable because cement content rarely exceeds, say, 250 kg/m<sup>3</sup>. Given the low gradient of the curves in the lower part of Fig. 2.7 and the large scatter band of the Bureau's test series (not shown), the shown relations may differ from dam to dam. Other investigations confirm the low gradients for cement contents below 250 kg/m<sup>3</sup> [2.37].

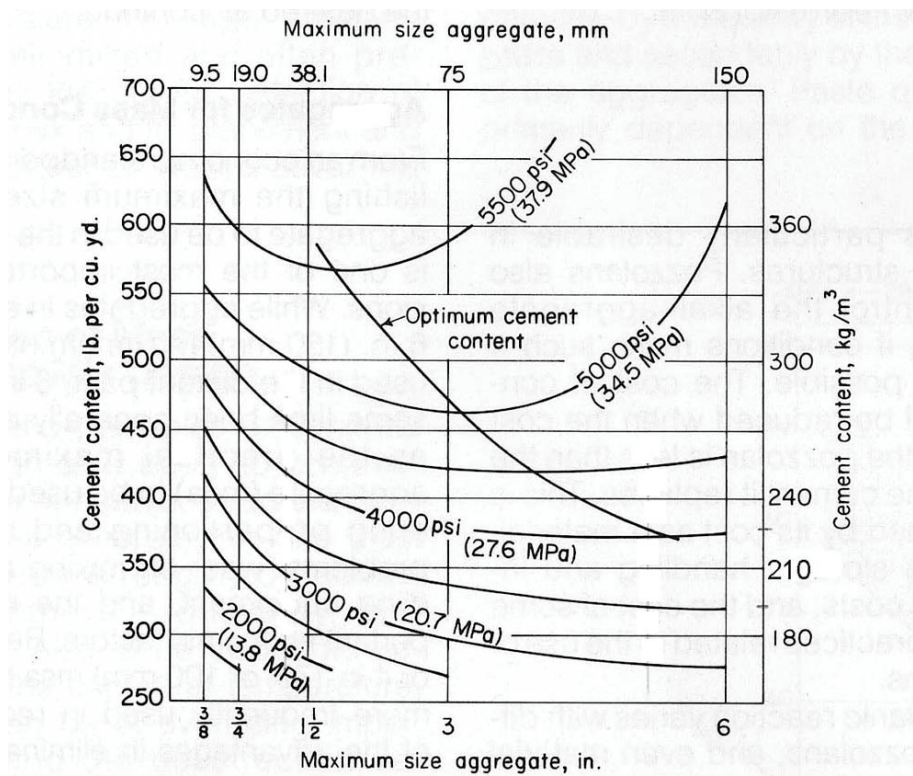


Fig. 2.7 – Effect on Maximum Size Aggregates on Cement Content [2.36]

### 2.3.3 Effects of aggregate properties

Compressive strength is governed by the strength of the aggregates and their water requirement for satisfactory workability. This influence can be large.

Lets take an example: reducing the MSA from 6" to 3" for a 200 kg/m<sup>3</sup> cement content would – according to Fig. 2.7 - reduce the strength by roughly 5 MPa. The difference between, say sandstone and limestone as source of aggregates can be in the same range, even more, as shown in the examples of Fig. 2.8.

Due to the fact that aggregates of marginal qualification are used now more frequently, e.g. for small gravity dams with a low stress level, to know the influence of aggregate quality becomes increasingly important.

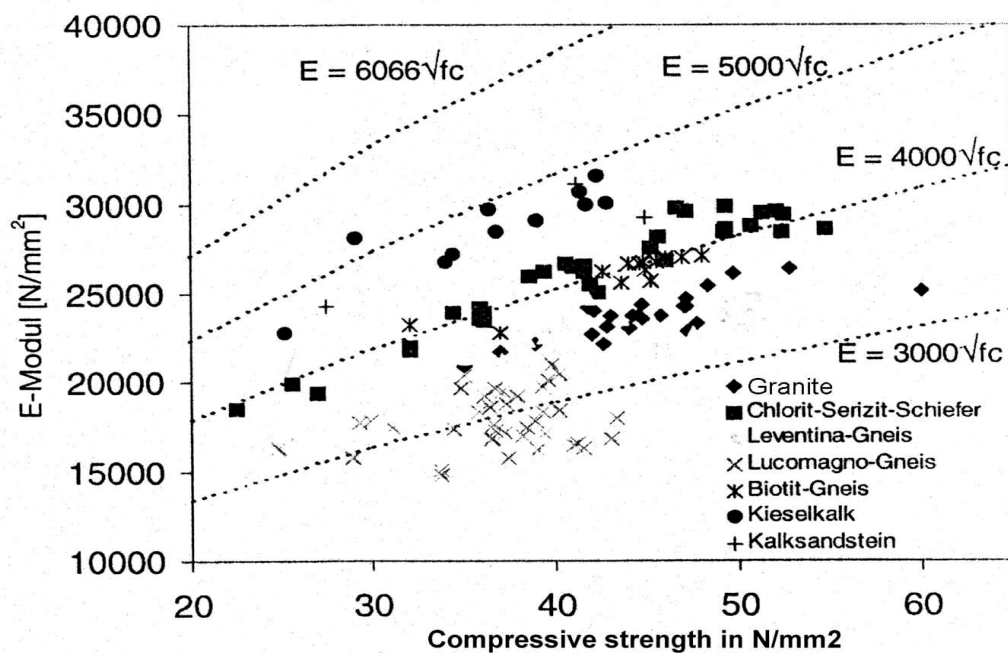


Fig. 2.8 – Compressive strength vs type of aggregates [2.38]

Essential for the acceptance of marginal aggregates is an extensive test program of both the aggregate parameters and then the concrete.

A common detrimental constituent in the aggregates is schist, i.e. rocks with high mica content. Austrian experience is that the content of schist in the sand fraction (0 to 4mm) should be kept low, say less than 5 %. Experiments demonstrated that an increase of schist by 10% in the sand required an increase of 0.05 in the w/c-ratio for equal workability which, in turn, reduced the compressive strength by 12%. Aggregates with 15% content of schist for the concrete of the Kölnbrein dam resulted in an 18% decrease of compressive strength as compared to aggregates free of schist [2.39].

### **2.3.4 Effects of curing**

Here we have to distinguish between curing of test specimens and curing during dam construction.

Curing of test specimens is well defined in standards, e.g. in ACI 308 [2.40] or [2.4]. Given the many factors influencing strength results, strict adherence to curing as stipulated in standardized test methods is mandatory in order not to add another source of uncertainty.

Curing at site is unfortunately often taken less serious than laboratory curing.

It is essential for large dam projects that the contractor provides a fairly uniform product with a specified strength of reasonable scatter as confirmed by periodic testing. However, as soon as the product of this mechanized process leaves the mixer and is placed, its stipulated quality and uniformity is at risk being impaired by deficient curing, which is still labour intensive and therefore prone to lack of care. Dry dam and block surfaces are a common view at construction sites although simple sprinkler devices (such as hoses with holes) are easy to install and to operate. It is a pure matter of discipline and site supervision to overcome this simple problem.

Curing requirements are treated in ICOLD Bulletins n° 47 (Quality Control of Concrete), n° 76 (Conventional Methods in Dam Construction) and a recent Bulletin under publication on "The Specification and Quality Control of Concrete for Dams". This Section therefore only covers some additional aspects to what is said in the above two Bulletins.

Interrupted curing will largely affect the compressive strength development as indicated by the test results of Fig. 2.9 (from [2.4] and [2.41]). Such test would seem to simulate inadequate dam curing, generally caused by intermittent or no moistening of lift and block surfaces.

Reference [2.41] reports of test results on 100x200mm cylinders comparing:

- exposure to environmental conditions (23,0°C+40% RH) for 1 day and fog room curing for 7 days thereafter (23,0°C+95% RH), and
- exposure to environmental conditions throughout (no fog room exposure).

The loss of 28-days compressive strength for 7 types of concrete (with Ordinary Portland Cement and blended cements) between the two curing conditions was between 10% and 40%, the higher loss being for blended (fly ash) concrete.

One may argue now that for dam concrete such a loss of strength is less significant than for structural concrete due to its limited impact on a large mass. However, what counts is that the impact of inadequate curing hits the dam at the joints, its weakest links. A loss of compressive strength also means a loss of shear and tensile strength at lift joints. Lift joints are discontinuities in the concrete mass and they are exposed to high temperature difference, prone to thermal cracking, and occasionally also exposed to uplift. Therefore a loss of strength at this particular location can be particularly detrimental for structural integrity and water tightness.

For the Zillergründl dam in Austria, a curing compound was successfully sprayed on the lift surfaces, immediately after pouring, or after removing the formwork. This also enhances adhesion between lifts.

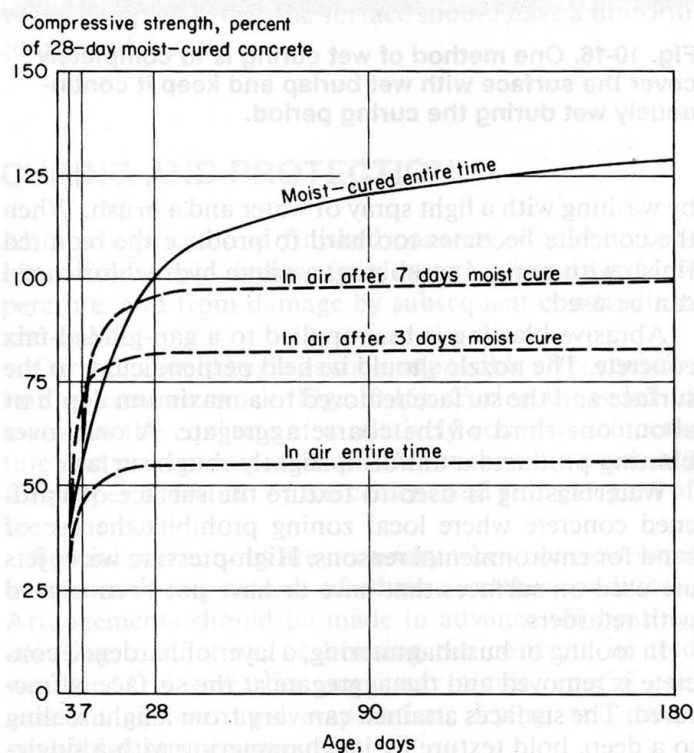


Fig. 2.9 – Compressive strength development for different conditions of curing [2.4]

### 2.3.5 Effect of mineral admixtures and blended cements

Blending of Ordinary Portland Cement (OPC) with pozzolans, fly ash or slag and other mineral admixtures are very common for dam concrete because of their generally economic and performance advantages.

The amount of blending proportions differs largely. It is mainly governed by economic aspects and by the extent to which the blended material is able to contribute to strength development. Tab. 2.9 lists examples of dams with use of blended cement.

Apart from economy, the main benefits from blending is a reduced heat of hydration, improved workability due to the finer gradation, and the reduced risk for Alkali-Aggregate Reaction (AAR). The disadvantage of slower early strength development is not essential for dam concrete, particularly as this strength is recuperated at later ages.

Another advantage comes from the increased paste content when using pozzolans or other fine-grained additions. This increases the capacity for plastic deformation with the advantage of increased tensile strain. This is, however more pronounced if intergrinding the natural pozzolans with Portland cement clinker and not mixing the two compounds at the site.

Tab. 2.9 – Use of blended cements in selective dams

Dam/Country	Type of dam	Concrete volume	Content of cementitious material for interior concrete	Type of blended material	Blending
		10 <sup>3</sup> m <sup>3</sup>	kg/m <sup>3</sup>		%
Zillgraben/Austria	arch	1'400	170	fly ash	33
Katse/Lesotho	arch		180	fly ash	30 to 50
Lumineo/Italy	arch	100	270	pozzolans	25
Cancano II/Italy	gravity	520	240	pozzolans	37
Vajont/Italy	arch	265	250	pozzolans	35
Tagokura/Japan	gravity	1'950	140	fly ash	25
Hitotsuse/Japan	arch	560	215	fly ash	30
Itaipu/Brazil	buttress	12'000	130	fly ash	23
Francisco Morazan/Honduras	arch	1'510	150-180	pozzolans	25
Hungry Horse/USA	arch-gravity	2'350	165	fly ash	55
Monticello/USA	arch-gravity	248	170	calcinated diatom. clay	25
Yellowtail/USA	arch-gravity	1'340	177	fly ash	28
Longyangxia/China	gravity	1'587	160	fly ash	30
Ankang/China	gravity	3'250	130-155	fly ash	30 to 55
Ertan/China	arch-gravity	4'100	174	fly ash	30
Puy-laurent/France	arch	85	250	fly ash	40
Pieve di Cadore/Italy	arch-gravity	377	200	pozzolans	25
Valle di Lei/Switzerland	arch	862	230	pozzolans	35 to 37
Baserca/Spain	arch	238	200	fly ash	25
Llauset/Spain	arch	211	200	fly ash	25
Las Portas/Spain	arch	641	200	fly ash	22.5 to 30
Alcantara/Spain	buttress	950	250	pozzolans	30
Cedillo/Spain	gravity	800	225	pozzolans	30

Blended cements need more testing (a) because of the properties of pozzolans may vary widely and (b) because the quantity of blended materials has to be optimized with respect to strength and durability. Fig. 2.10 [2.42] shows an example of a test series resulting in the choice of 30% fly ash for this particular dam concrete.

Furthermore using blended cements reduces the heat of hydration.

### 2.3.6 Effect of sustained loading

In a standard test, the compressive strength is determined at loading in the range of minutes. As this range of minute increases, lower strengths are recorded than in the case of standard test. If, on the other hand, the load is applied more rapidly, a higher strength is recorded. The well-known Rüschi-diagram in Fig. 2.11 demonstrates this phenomenon impressively [2.43].

Under the low rates of loading, creep occurs. It flattens the stress-strain curve, however only at a degree of loading, which does not exceed 70 to 80 % of the short-term strength. The process of cracking during loading explains this behaviour. The breakdown of concrete consists in the formation of cracks, either their extension with arrest (stable cracking at low stress levels), or their extension without arrest (unstable crack propagation at high stress levels).



ICOLD Bulletin: The Physical Properties of Hardened Conventional Concrete in Dams  
 Section 2 (Strength properties)

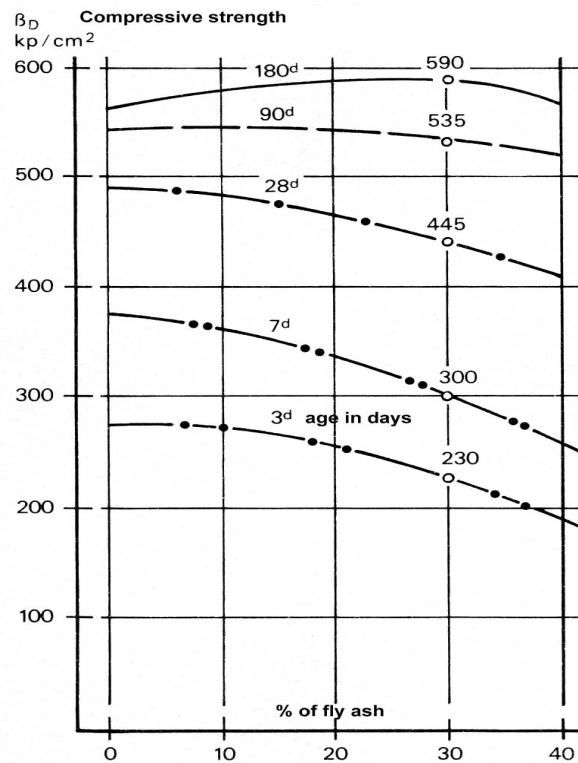


Fig. 2.10 – Trial tests with variable contents of fly ash [2.42]

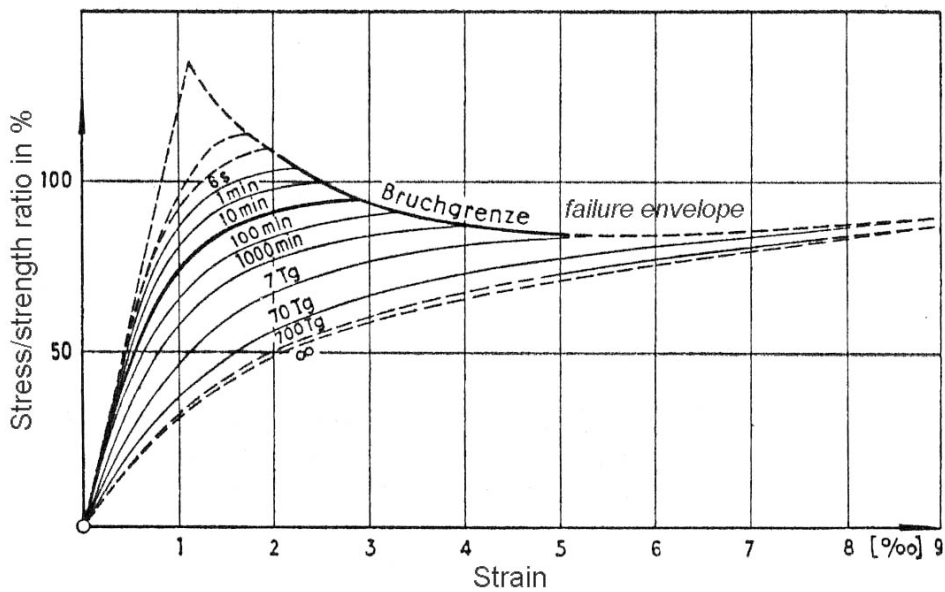


Fig. 2.11 – Influence of sustained loading on strain according to Rüsçh [2.43].

In dams, loading cycles are mainly depending on variation of the reservoir level and on annual temperature cycles. These cycles are extremely slow as compared to common laboratory loading with rates of 0.15 to 0.4 MPa/s. Moreover, they are applied to a structure pre-loaded due to self-weight. For this kind of loading there are little laboratory results available.

Interesting, in this respect, is the observation of increased ultimate tensile strain at loading rates which are common for dams (see Section 2.4).

### 2.3.7 Multiaxial compressive stress domain in a dam

Generally concrete in dams is stressed multiaxially. Because of obvious reasons, it is not common to test dam concrete under biaxial or even triaxial conditions and uniaxial test results are used as strength parameters. This is an acceptable approach as long as biaxial strength envelopes are used for safety evaluations of compressive stress domains in the dam. In other words, the results of uniaxial testing enter as corner point in the chosen strength envelope. Such envelopes exist from the literature; Fig. 2.12 is an example [2.44]. Other examples are given in [2.45] and [2.46]. It would be utterly conservative to use uniaxial compressive strength values alone for safety evaluations.

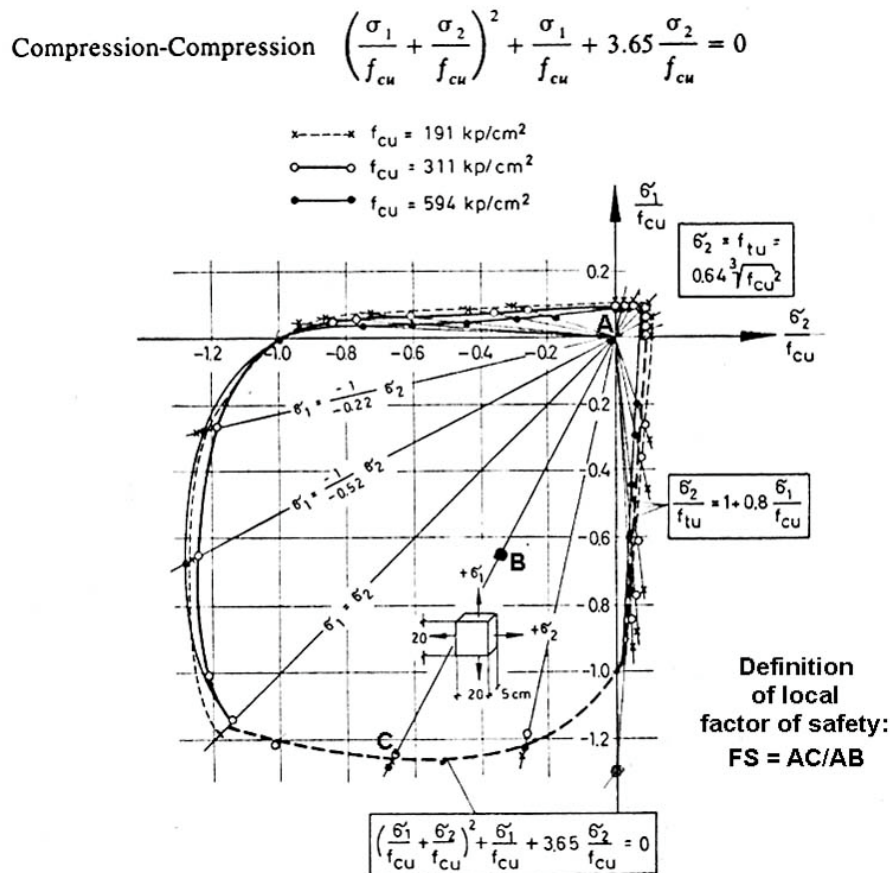


Fig. 2.12 – Example for biaxial strength envelope [2.44]

## 2.4 TENSILE STRENGTH

A critical and important factor in the safety of concrete dams is the tensile strength, both under static and seismic loading. Tensile strength is commonly and basically tested in 3 ways: direct (pure) tension, flexural tension (also termed modulus of rupture) and splitting tension (Brazilian test). Recently a test based on fracture mechanics has been introduced, the wedge splitting test, that provides most valuable information about concrete loading under tensile stress.

In spite of the significance of tension, it is not common to test and evaluate it as consistently as compression. It is common to relate tensile to compressive strength as shown by the example of Fig. 2.13 (from [2.47]).

The following sections try to outline common practices and trends to account for tensile strength.

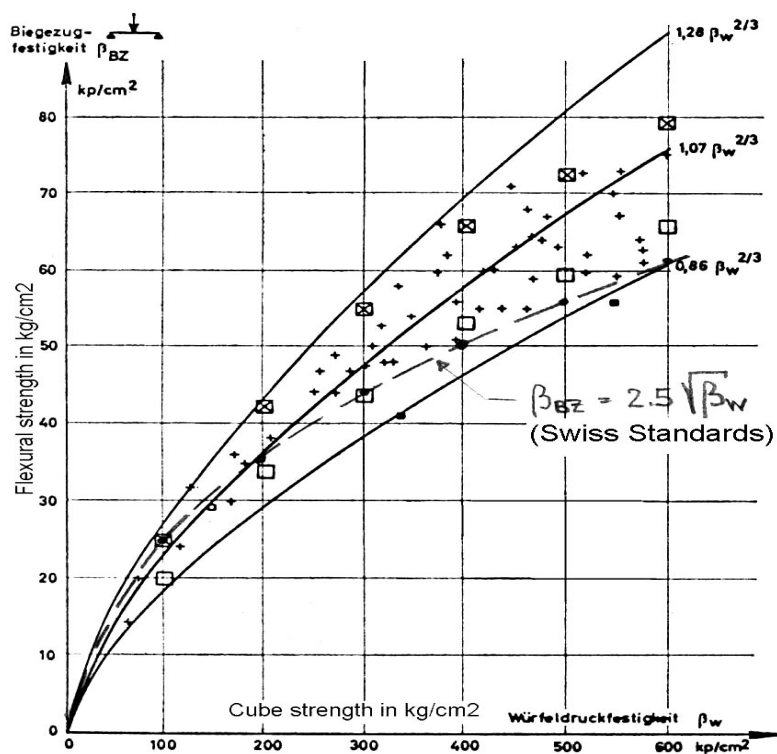


Fig. 2.13 – Compressive vs flexural strength [2.47]<sup>1</sup>

### 2.4.1 Tensile loading in the dam

Which type of tensile strength shall be employed for simulating the real conditions in the dam? Is it direct tension, is it the modulus of rupture, is it splitting strength or is it the result from wedge splitting testing?

The choice should relate to the anticipated mode of failure and is therefore not unique. It has been argued that the modulus of rupture gives values that can be directly used

<sup>1</sup> multiply the coefficients of the  $\beta_{BZ}$ -formulas by 0.464 to obtain coefficients for MPa.

Section 2 (Strength properties)

for matching the results of finite element analysis [2.3]. On the other hand, splitting tests are the easiest to handle and a large number of these simple test would also provide a somewhat more reliable value of this random variable.

However, on a localized level (conditions at the crack tip), it is suggested that typical cracking due to static loading, e.g. at the upstream toes of gravity and arch dams, rather follows the laboratory condition of direct tension.

From the above, a more specific consideration for parts of the dam under tensile stress is warranted and attention should be paid to the following:

- The ability to relate any value of tensile strength to the corresponding mode of cracking in the given part of the dam
- The type of analysis being conducted for which the tensile strength is to be specified (see Section 2.4.8)

**2.4.2 Type of tensile testing**

Notwithstanding the above, tensile testing at site may be restricted to evaluating the flexural strength, preferably on 300x300x900 mm prisms, with splitting test results as a redundant type of test. Such testing needs wet-screening of the large fractions down to a grain size, which allows to respect the ratio between sample size and MSA, see Section 2.2.1. The full mix of the flexural test will exhibit a more elastic strength value (lower modulus of elasticity) because of accounting for aggregate interlock. In order to relate the flexural to the direct tensile strength, the latter should be either taken from the literature or tested in specialised laboratories.

Tab. 2.10 lists some suggestions for tensile strength testing.

Tab. 2.10 - Static tensile strength testing

Symbol	Type of tensile strength	Standard (example)	Sample size of standard test	Sample size recommended for dam concrete	Comments
$f_t$	Direct tension	RILEM CPC 27	variable	-	Only to be tested in specialized laboratories
$f_r$	Flexural strength (modulus of rupture)	ASTM 78 BS 1881 DIN 1048	152x152x508mm 150x150x750mm 150x150x700mm	200x200x600mm or 300x300x900mm	
$f_{sp}$	Splitting strength	ASTM 496 BS 1881 DIN 1048	Variable Variable Cyl. 150x300mm	Drilled core $\phi = 75$ to 100mm	At selective location as dictated by design or monitoring demands

Tensile testing show high scatter as initial stresses might have already impaired the concrete's tensile strength potential even before the external load starts to act. Initial stresses are those from drying shrinkage (causing a tensile stress) and from relaxation due to viscoelastic creep (relieving shrinkage stresses), Fig. 2.14 [2.48]. The

superposition of these effects determine whether or not tensile stresses will result in cracking. They are also the reason for high scatter of tensile in-situ testing.

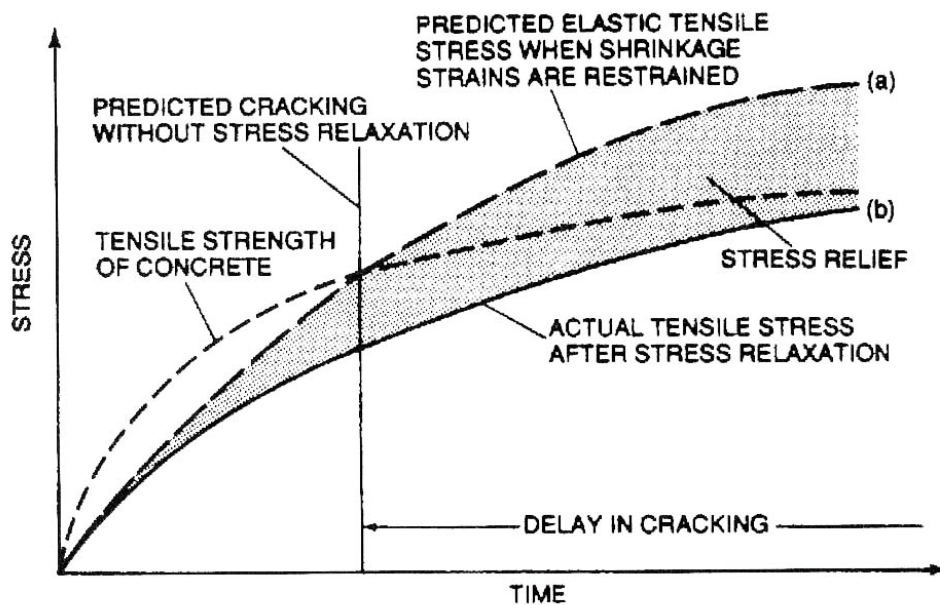


Fig. 2.14 – Influence of shrinkage and creep on tensile strength [2.48]

Among the types of testing tensile strength, the wedge splitting test renders an enhanced level of information as it gives a strain history result (fracture energy, strain softening curve) instead of only a single strength value. It also allows gaining conclusions from observing the broken halves of the specimen. This is of particular interest for judging the consequences of tensile cracking in dams. Post-peak tensile strain not necessarily leads to disintegration of the concrete and thus not to failure. This is beautifully demonstrated by wedge splitting tests and can be a valuable input for nonlinear dynamic analysis (damage parameters).

In view of the above arguments and uncertainties it is recommended that careful thought be given before finally selecting tensile strength criteria.

### 2.4.3 Tensile strength ratios

Similar to what was said for the relation between laboratory and field compressive (core) strength, there are several factors for tension which need to be interpreted wisely before drawing conclusions. J. Raphael reports that large differences in tensile strength between laboratory and field specimens stems from its curing history [2.49]. Drying out between removal (drilling the core) and testing explains the differences of up to 50% lower tensile strength for cores.

A multitude of test series have compared tensile with compressive strength (at the same types of specimen) resulting in conversion factors. Some of these results are given in Tab. 2.11.

Tab. 2.11 - Conversion Tensile to Compressive Strength

No.	Type of strength test	Type of specimens	Conversion to compressive strength $f_c$ after Hellmann [2.46]			Other relations (all in kg/cm <sup>2</sup> )	
			c in $f_t = c \cdot f_c^{2/3}$ [kg/cm <sup>2</sup> ]			Source	Formula
1			min.	average	max.		
1	Flexural: center point load	prisms 10cm high and several lengths	0.86	1.07	1.28	Swiss standard SIA 162	$f_1 = (2.5 \text{ to } 3.0) \cdot \bar{f}_t$
2	Flexural; third-point load	as above	0.76	0.98	1.2	Emosson dam	$f_2 = 2.0 \cdot \bar{f}_t$
		10x10x40cm				A.A.Khan et al. [2.50]	$f_2 = 0.86 \cdot f_c^{2/3}$
		15x15x53cm cyl.				Raphael [2.49]	$f_2 = 0.95 \cdot f_c^{2/3}$
3	Splitting (Brazilian)	6"x12" (15x30cm) cyl.	0.48	0.5	0.7		
4	Pure tension	cyl. 15x30 and 15x25cm; prisms 5x20x20, 9x15x60cm	0.36 <sup>1)</sup>	0.52 <sup>1)</sup>	0.68 <sup>1)</sup>	Raphael [2.49]	$f_4 = 0.7 \cdot f_c^{2/3}$
						Kupfer-Gerstle [2.44]	$f_4 = 0.64 \cdot f_c^{2/3}$
1) somewhat too low because of including tests by Gonnerman and Shuman (1928) Multiplier of c for transformation kg/cm <sup>2</sup> to MPa: 0.464 in 2/3exp.formulas      10kg/cm <sup>2</sup> = 1 MPa $f_c$ is 28 days 20cm cube strength throughout all relations							

#### 2.4.4 Size effect

The size effect is made evident through comparison of geometrically similar structural elements of variable sizes. Results from fracture mechanics indicate that it cannot be discarded when comparing laboratory tensile strength with the one expected in the structure [2.51].

Here it should only be mentioned that the size effect depends on the type of test and on the rate of loading, i.e. it is different for direct, flexural and splitting strength, and also different for static and dynamic loading. It is therefore suggested to use a so-called apparent tensile strength for safety evaluations of tensile zones in the dam [2.52] [2.53].

#### 2.4.5 Tensile strain capacity in dams

It is actually the tensile strain capacity (rather than the tensile stress), which is of interest for the control of cracking in dams. The difference is basic, because only strain (unlike stress) depends on the rate of tensile loading. Research in this field indicates that slow rates of loading, such as they are induced by reservoir or temperature fluctuations, can increase the strain capacity by a factor of 1.1 to 2.1 with respect to laboratory loading rates [2.54].

Interesting in this respect is the observation on Austrian dams, as reported in [2.16], where a much higher tensile strain capacity due to slow cyclic reservoir loading is reported as compared to laboratory test results (Fig. 2.15). This phenomenon defeats the occasionally brought forward argument that a higher content of cementitious material is alleviating cracking. Such argumentation is questionable.

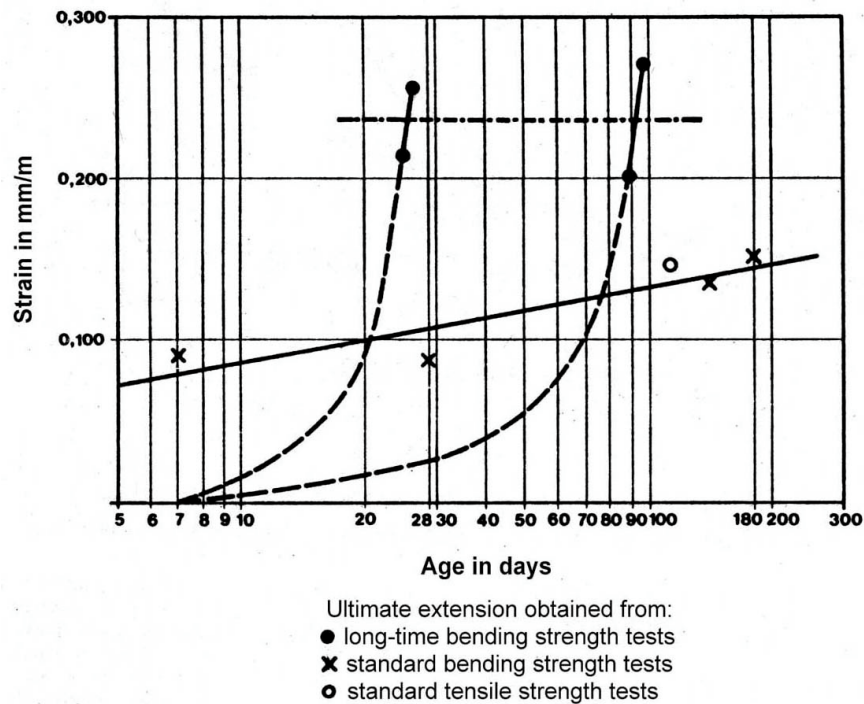


Fig. 2.15 – Tensile strain capacity at slow loading rate [2.16]

#### 2.4.6 Tensile strength at joints

The limiting tensile concrete strength is that which exists at lift joints and across the contact surfaces between the dam and its rock foundation. Even with particular efforts during construction to prepare concrete and foundation contact surfaces for bonding, tensile strengths across bonded lift surfaces and foundation contacts should be expected to be at least 10 to 20 % less than the corresponding intact tensile material strength [2.53].

If tensile stresses are vertical then excess tension may cause opening of lift joints with their reduced tensile strain capacity. Some designers cautiously assume no tensile joint strength at all (zero tension approach) and consider a condition as being safe, if stable cracking is the consequence of tensile stresses. This seems to be a reasonable approach for static loading, however too conservative for transient earthquake and flood loads.

### **2.4.7 Tensile strength criteria**

Similarly to what was said for multiaxial compressive strength considerations, uniaxial tensile strength values can be used to define the corners of a biaxial strength envelope in the tension-compression sectors (Fig. 2.12). However, the scatter of biaxial compression-tension test series is too large as to draw a somewhat reliable biaxial envelope line in this sector and to use it for defining the FS as AC/AB (as in Fig. 2.12). Designers use other safety criteria as soon as tension is involved. Such criteria comprise a no, or better limited, tension analyses. Considering the fact that concrete is an elastic-plastic material, which demonstrates a margin against tensile cracking not considered with a purely elastic model, nonlinear constitutive stress/strain models for high tensile stress loading are more realistically approaching reality.

From phenomenological observations of crack patterns on samples exposed to biaxial loading, idealized failure types can be deduced [2.55] [2.56]. These types depend on the principal stress ratio at the ultimate state of stresses (point at the failure envelope in Fig. 2.16) and can therefore be assessed from Finite Element (FE) - analysis results. They may be termed:

1. cleavage or tensile splitting orthogonal to the tensile stress (case A)
2. transition between 1 and 3 (cases B and C)
3. shear failure or splitting parallel to tensile stress (case D)

From FE-results it may therefore be assessed which type of tensile strength is most appropriate to be introduced in the biaxial failure envelope for a particular part of the dam. Other than locally, cases A and D of Fig. 2.16 are practically inexistant in dams.

There exist also biaxial test results from wedge splitting, which model the conditions in dams more closely than uniaxial wedge splitting results [2.57]. Fig. 2.17 demonstrates how the fracture energy ( $G_f$ ) decreases within the elastic range and that at, the onset of microcracking,  $G_f$  starts to increase again prior to complete material disintegration. This unsteady development ensues from restraints of expansion of the fracture process zone for the descending  $G_f$  branch and from aggregate interlock for the rising branch. The relevance for dam concrete is a fringe resistance of a cracked concrete mass for post-peak loading.



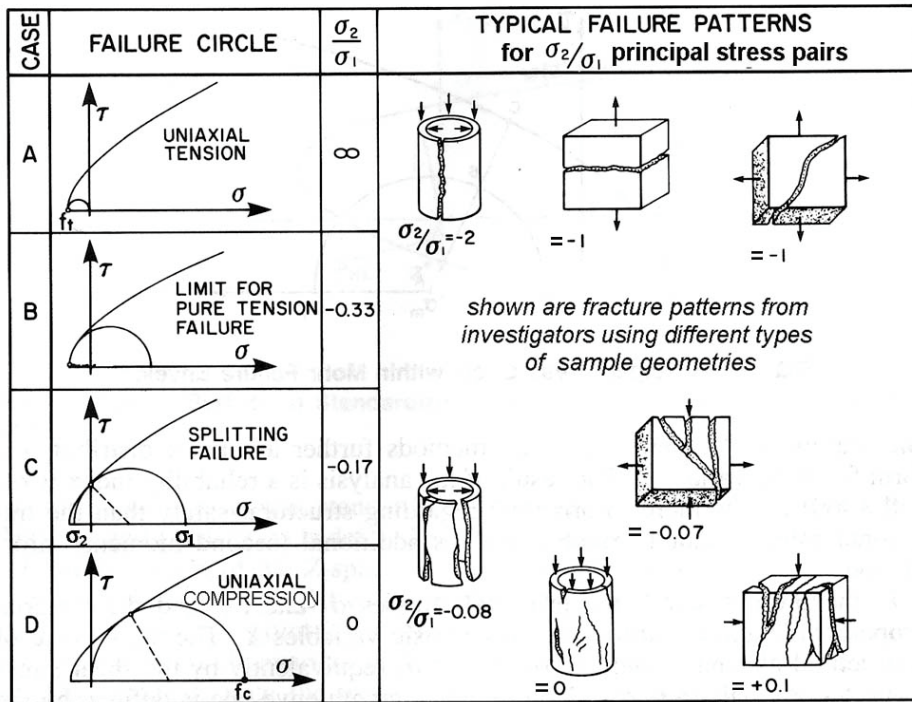


Fig. 2.16 – Typical failure pattern and corresponding Mohr circle representation [2.56]

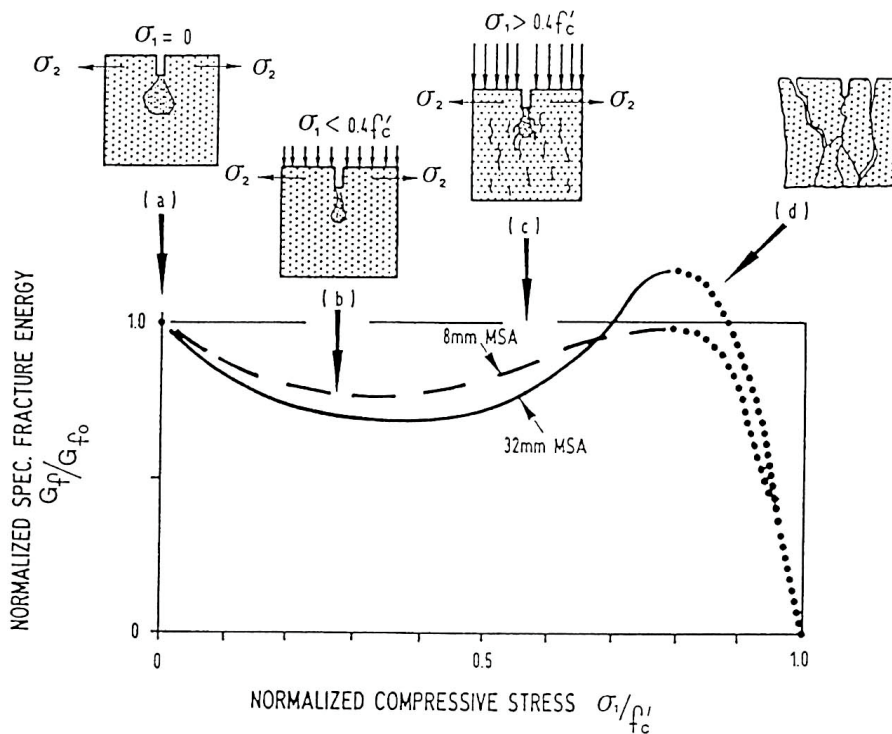


Fig. 2.17 - Development of fracture energy under biaxial loading[2.57] <sup>1</sup>

<sup>1</sup>  $G_{f0}$  is the fracture energy under corresponding uniaxial loading

### 2.4.8 Use of tensile strength in mathematical models

The development of mathematical models calls for performing laboratory testing of strength parameters to be used in constitutive models. This is particularly relevant for tensile strength parameters.

#### 2.4.8.1 Linear elastic analysis

In many cases a **linear-elastic stress analysis** will be a most adequate representation of reality. In this case it has to be considered that a uniaxial tension test will give a nonlinear stress-strain relationship, different to what is assumed in the model. The same is true for a flexural test: the load deflection response will be non linear (Fig. 2.18). To be consistent with a linear analysis, the stress difference between point A (linear analysis) and B (test result) has to be considered by conversion factors for the stress ratios AB. These factors can be obtained from pure tension, flexural tension tests or wedge splitting tests. Factors between 1.2 and 1.4 can be expected from tensile test series for mass concrete of dams.

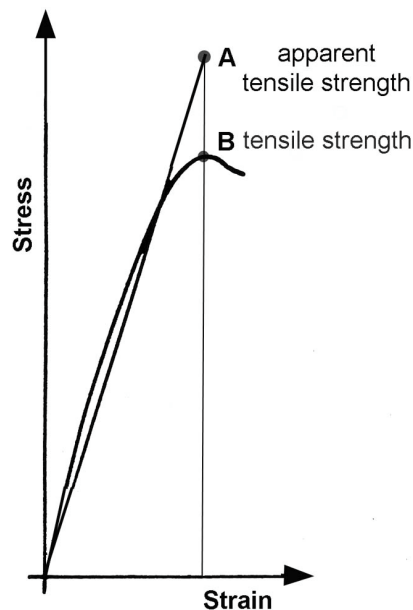


Fig. 2.18 - Apparent tensile strength (in a linear analysis) compared to tensile test results [2.58]

#### *2.4.8.2 Non linear analysis*

To conduct a **nonlinear analysis**, the present state-of-the-art includes the ability to formulate:

- plastic straining under compressive and tensile states of stress,
- tensile strain softening,
- material degradation due to a-priori strain histories,
- influence of creep,
- viscoplastic bi- or triaxial stress-strain solutions with cycles to reach conversion at time-dependent plastic strain conditions (for seismic loading).

Here the validation of constitutive strength modelling via experimental data is more cumbersome and delicate. Fig. 2.19 shows the example for validating tensile strain softening by means of wedge splitting tests. The sequence of actions comprises:

**1** Sample extraction from the dam. Standard diameters are 200mm. Several cores should be extracted to average the scatter of strain softening curves. This scatter can be large given the influence of paste-large aggregate heterogeneity on the fracture mechanism. Curing immediately after core extraction can influence the result. It is suggested to follow curing conditions of test standards such as RILEM[2.59] or ACI [2.60].

**2+3** Fig. 2.19 shows a wedge splitting test on cores, as an example, and the force-crack opening diagram as the result of such a test. Equally, this test is commonly performed also on beams or cubes [2.59].

**4** The post-peak response of the material has to be transferred into a constitutive model by FE-discretization. This means that the computed and measured fracture energy ( $G_f$ ) during testing (surface under the post-peak softening curve) must comply. This needs consideration of the size effect relating the in-situ strength to the laboratory-determined strength [2.61], and it generally needs mesh adaptations[2.62]. Shown on **4** are stress contours obtained from FE-analysis, which best match, the experimentally found softening curve.

**5** Example of a bilinear strain softening relation to be used in a plasticity-based model. It is obtained by numerical compliance to experimental data. The kink indicates that energy is consumed by two different fracture mechanisms: the upper branch of the curve is due to microcracking, the lower branch by overcoming friction and tortuosity of aggregate interlock.

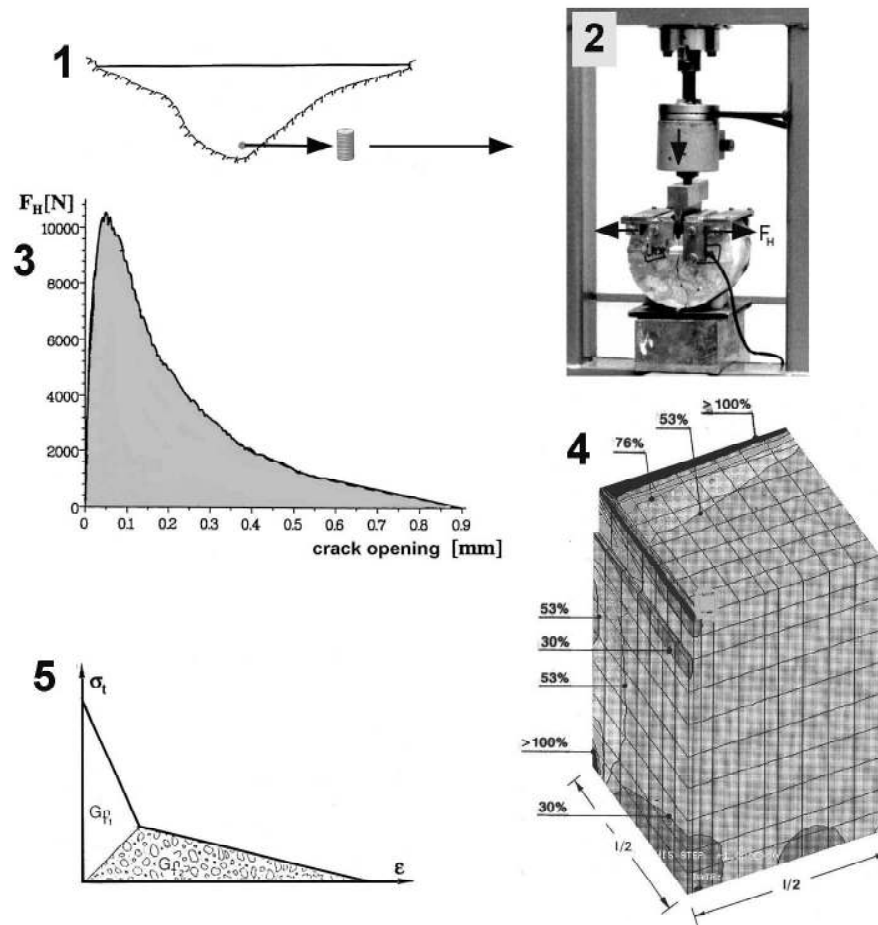


Fig. 2.19 - Strain softening: tensile strength testing for FE-validation. **1:** core extraction, **2:** wedge splitting testing, here shown on a core, with  $F_H$  the tensile force, **3:** strain softening curve from wedge splitting test, **4:** FE-discretization of concrete test sample, here a quarter-cube of a wedge splitting test with some stress contours in % of uniaxial compressive strength, **5:** bilinear softening diagram which best fits the measured softening curve for input into a nonlinear FE-stress analysis, indicating two types of crack propagation:  $G_{f1}$  strain softening due to microcracking, and  $G_{f2}$  continued cracking due to debonding of aggregate interlock [2.17].

## 2.5 SHEAR STRENGTH

The significance of shear strength in dam concrete is practically limited to discontinuities in the concrete mass (joints, cracks) and to the rock-concrete contact. Shear strength depends on the adhesion between the substrate material and the grout (in the case of grouted block joints), and the cohesive strength of the lift joint surfaces.

Shear strength is usually assumed to follow the Mohr-Coulomb<sup>1</sup> relationship

$$T=c.A + \tan\phi.N$$

where

T= shear force,

c= cohesion of intact lift surface or contraction (block) joint surface accounting for shear key, if constructed,

A= intact area, e.g. total area times a coefficient assessing the efficiency of joint curing, roughness or joint grouting,

$\tan\phi$  = friction coefficient,

N normal force.

The Mohr-Coulomb relationship is an appropriate presentation for shear resistance, since shearing strength is represented by the point where the failure envelope intersects the vertical shear axis in a  $\sigma$ - $\tau$  (normal stress-shear) diagram.

If doubts about effective joint treatment (e.g. thermal cracking due to lacking curing) or if block joints are taking no or little grout, c can conservatively be put to zero.

Shear resistance of the grout material (in block joints or at the concrete-rock contact) depends on the water-cement ratio and thus on the compressive strength  $f_c$ . In absence of test results a shear value of  $\tau=0.15.f_c$  can be assumed, with  $\tau$  being the intercept of the failure envelope, as mentioned above.

In addition to the Mohr-Coulomb failure envelope, a bilinear shear resistance criterion is meaningful for assessing the shear resistance in shear-keyed block joints. The lower, steeper branch in the  $\sigma$ - $\tau$  diagram is for shear resistance of the plain concrete surface within the keys (high  $\phi$ , no cohesion), whereby the higher flatter branch is for shear resistance of the joint surface (lower  $\phi$  and some  $c= f$  [total block joint surface to shear-keyed surface]). This implies that the steeper branch being the shear resistance of concrete, say  $\tau_c=0.2.f_c$  and the flatter branch a function of the key geometry.

For intact concrete a curved Mohr rupture diagram can be assumed enveloping the two uniaxial Mohr circles for compressive and tensile strength.

Quality of bonding at joint surfaces is generally checked by shear tests from cores drilled through joints. As may be expected, such shear tests demonstrate a wide range of joint quality values between low-shear strength (core separation) and full material strength (invisible joints).

---

<sup>1</sup> The common terminology relates a curved envelope to the Mohr rupture diagram (constructed by the uniaxial compression and tension circles) whereby the term Coulomb relates to a linear/bilinear failure criterion

A fine survey of joint treatment in dams and their benefits are found in [2.63].

Test results can be evaluated to render several resistance parameters. Fig. 2.20 shows the result of a simple shear test along a discontinuity, providing:

- a peak shear value
- a residual shear value (from a second test),
- displacement at peak shear value, and
- degree of separation from the inspection of the shear surface.

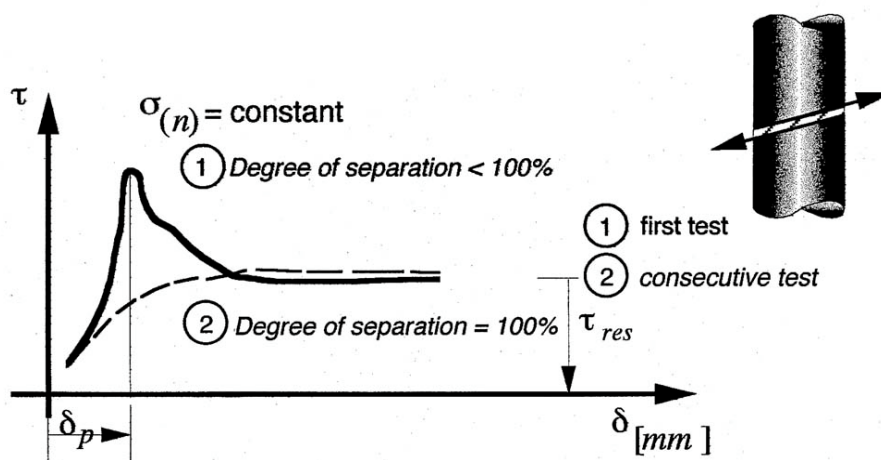


Fig. 2.20 - Shear results from core testing

Such shear test results can then be used for modelling shear resistance envelopes in a  $\sigma$ - $\tau$  diagram according to the anticipated shear resistance parameters, say, of block joints with questionable grouting success or of "cold" construction joints (Fig. 2.21).

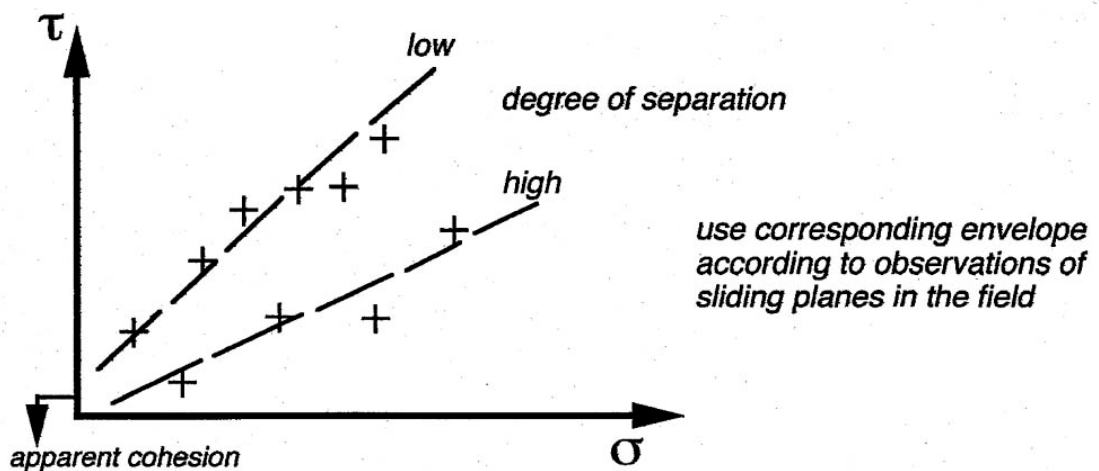


Fig. 2.21 - Reduction of test data into a Coulomb  $\sigma - \tau$  diagram.

## 2.6 DYNAMIC STRENGTH

This section concentrates on strength at loading rates which are related to strong earthquakes, e.g. at strain rates of  $10^{-3}$  to  $10^{-2}$  /s. Corresponding results from several test series under static and dynamic loading are summarised as static/dynamic strength ratios in Tab. 2.12.

A caveat needs to be added using these strength ratios. What is not shown explicitly in this Table is the larger scatter of dynamic strength values as compared to static strength testing. This means that dynamic strength is less reliable than the static strength. This has a bearing on the stipulated dynamic strength for safety analyses. Ratios from experimental tests, like those in Tab. 2.12, should therefore be cautiously chosen (e.g. lower bounds be taken) when using them for safety assessment.

Tab. 2.12 – Examples for Static/Dynamic Strength Ratios

Parameter	Dyn./stat.			Comments
	max.	av./single	min.	
<b>Young's</b>		1.25		Bureau's of Reclamation test series, rep. in Ref. [2.64]
	1.57	1.42	1.28	Big Tujunga dam, cores drilled from the dam. 2
	1,48	1.38	1,32	concrete types: 25 (1. row) ; 36 MPa strength (2. row)
		1.18		Crystal Springs Dam as reported by J. Raphael [2.49]
		1.15		Tests on Swiss dams, Ref. [ 2.65]
<b>Compressive strength</b>	1.60		1.00	Uniaxial loading from Ref. [2.66]
		1.50		Multiaxial loading from Ref. [2.66]
		1.20		Auburn Dam (Bureau of Reclamation)
	1.20		1.60	Ref.[2.67] for saturated dam
	1.28	1.15	1.00	Big Tujunga dam, cores drilled from the dam. 2
	1.27	1.12	1.00	concrete types: 25 (1. row) and 36 MPa
		1.32		Crystal Springs Dam ( J. Raphael) 32 MPa
<b>Flexural strength</b>	1.40	1.29	1.23	Ref.[2.51] with reference to size
	1.73	1.48	1.21	Bureau's extensive tests on Auburn dam (1977/78)
<b>Splitting strength</b>		1.31		Crystal Springs Dam as reported by J. Raphael [2.49]
		1.50		Ref. [2.68]: testing for evaluating blasting impacts:
		1.28		value for 20 MPa and lower value for 50MPa concrete
<b>Pure tension</b>		1.48		Santa Anita Dam as reported by J. Raphael [2.49]
		1.83		Big Tujunga Dam as reported by J. Raphael [2.49]
	1.13	1.06	1.00	Ref.[2.69] with tests on dry (1. row) and saturated
	1.46	1.33	1.16	Specimen (2.row)
	1.50	1.17	1.07	Zervreila Dam (Switzerland): cores drilled from the dam
		2.0*)		Reinhard [2.70] suggests a ratio $r = 14.f_c'^{-0.57}$ respecting the dependence of r on the compressive strength. CEP has a similar proposal. *)for $f_c'=30\text{MPa}$

The US Bureau of Reclamation performed an extensive test series for dynamic properties from cores of existing dams [2.71]. Main results are summarized in Table Tab. 2.13. This is the most complete data series available for dynamic/static strength ratios for dams.

Tab. 2.13 – Dynamic Concrete Properties from Dam Cores

Parameter	Ratio dynamic/static (mean ± coefficient of variation)	Max. ratio	Min. ratio
Compression	1.07±0.20	1.45	0.73
Young's Modulus	0.89±0.17	1.1	0.7
Failure strain	0.93±0.12	1.58	0.78
Poisson ratio	1.09±0.29	1.69	0.69
Splitting strength	1.44±0.15	1.73	0.98

The values are from 103 specimens of 10 dams constructed between 1916 and 1995. The test data reflect a high variability due to the highly variable mix proportions and due to different degrees of saturation of the specimens.

Evidently, one has to link these test results to what might happen in the dam. Not considered in laboratory-obtained strength ratios is the dam's strength margin during strong shaking due to the concrete's ability of plastic straining (strain softening) before failure becomes imminent.

Here one is faced with two phenomena: one is the pure material response under dynamic loading (obtained from small samples), the other is the large-scale structural response. This means that the designer has to weight the compatibility of these phenomena on a safety outcome, e.g. by tuning the choice of static/dynamic strength ratios with the ability of the constitutive model to consider the above mentioned structural safety margin.

### **2.6.1 Dynamic Compressive Strength**

A number of test results exist about the dynamic-to-static strength ratio:

- A state-of-the-art paper is [2.66]. This well documented publication concludes that the predominant parameter influencing the ratio is static compressive strength (and not mix proportions, w/c ratio type of aggregate etc.). Again the scatter of evaluating some 30 test series is high and varies between a ratio of 1.3 and 0.9 for strain rates between  $10^{-3}$  to  $10^{-2}$  /s, with high strength concrete tending towards the lower ratios of the above range and low strength concrete towards the higher ratios. This is as expected, given the higher ductility of low strength concrete.



- In 1975 tests were performed with the concrete of Big Tujunga dam in California on cores drilled from different quality concrete [2.72]. A strain rate of 0.04s was applied corresponding to the 1/4 of the assumed earthquake cycle. The results from 6 dynamic tests are as shown in the following Tab. 2.14.

Tab. 2.14 - Ratio between dynamic and static strength

Static strength (MPa)	Dynamic strength (MPa)	Ratio
24.9	28.8	1.16
26.7	34.3	1.28
22.8	22.4	0.98
38.2	37.8	0.99
36.8	46.9	1.27
36.7	40.6	1.11

Given this information the a caution approach suggests using a ratio close to unity for any analytical consideration unless test are performed for the particular dam.

### **2.6.2 Dynamic Tensile Strength**

Commonly the 2/3-power law is used for the relation between tensile and compressive strength, both for static and dynamic load.

Reference [2.49] uses the same power law for assessing dynamic tensile strength,  $f_t$ :

$$f_t = 1.07 \cdot f_c^{2/3} \text{ [kg/cm}^2\text{]}$$

$$f_t = 0.5 \cdot f_c^{2/3} \text{ [MPa]}$$

with

$f_t$  dynamic tensile strength from pure tension tests

$f_c$  compressive cylinder strength

The comparison with Tab. 2.11 shows that this formula suggests a 50% increase of dynamic against static strength.

Again, such high ratios should be used with caution and in combination with the mathematical model to be employed for stress analysis, as mentioned earlier. Another

factor influencing the static/dynamic strength ratio is compressive strength. Studies at Delft University indicate a decreasing static/dynamic strength ratio with stronger, more brittle concrete, expressed by the formula

$$f_t = 3.2 \cdot f_c^{0.1} \text{ [MPa]}$$

for earthquake loading, see Fig. 2.22 [2.70].

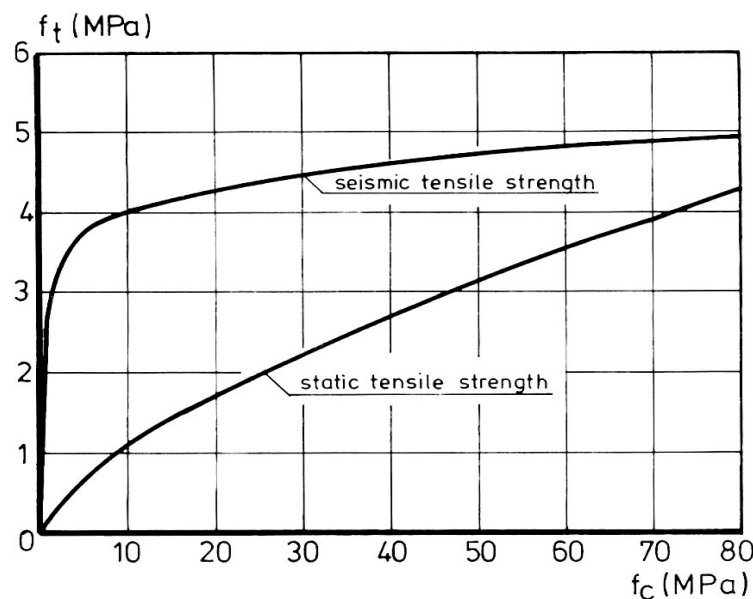


Fig. 2.22- Tensile (static/seismic) vs. compressive strength [2.70]

Besides the above mentioned post-earthquake strength margin, the dynamic tensile strength is also an ambiguous material parameter as soon as it is used as input in linear stress analysis. If a linear stress-strain relation is used on a material, which actually behaves nonlinearly at high stresses, then the analysis will predict failure at a higher stress than the test value (peak of the stress-strain softening curve). The linear high strength was termed apparent tensile strength [2.58].

The difference between apparent (linear) and nonlinear peak at ultimate strain can be considerable, both for static and dynamic tensile strength. In [2.3] a ratio of 1.35 for dynamic loading and for common dam concrete ( $f_c \approx 20$  MPa) is suggested.

The strain-rate effect on the tensile strength for different concretes, with maximum aggregate size up to 25 mm, is shown in Fig. 2.23 [2.73]. The range of strain rates might be very large; typically from  $\sim 10^{-2} \text{ s}^{-1}$  of earthquakes to  $\sim 10^2 \text{ s}^{-1}$  of impacts.

The increase of the tensile strength with increasing relative humidity was observed [2.74].

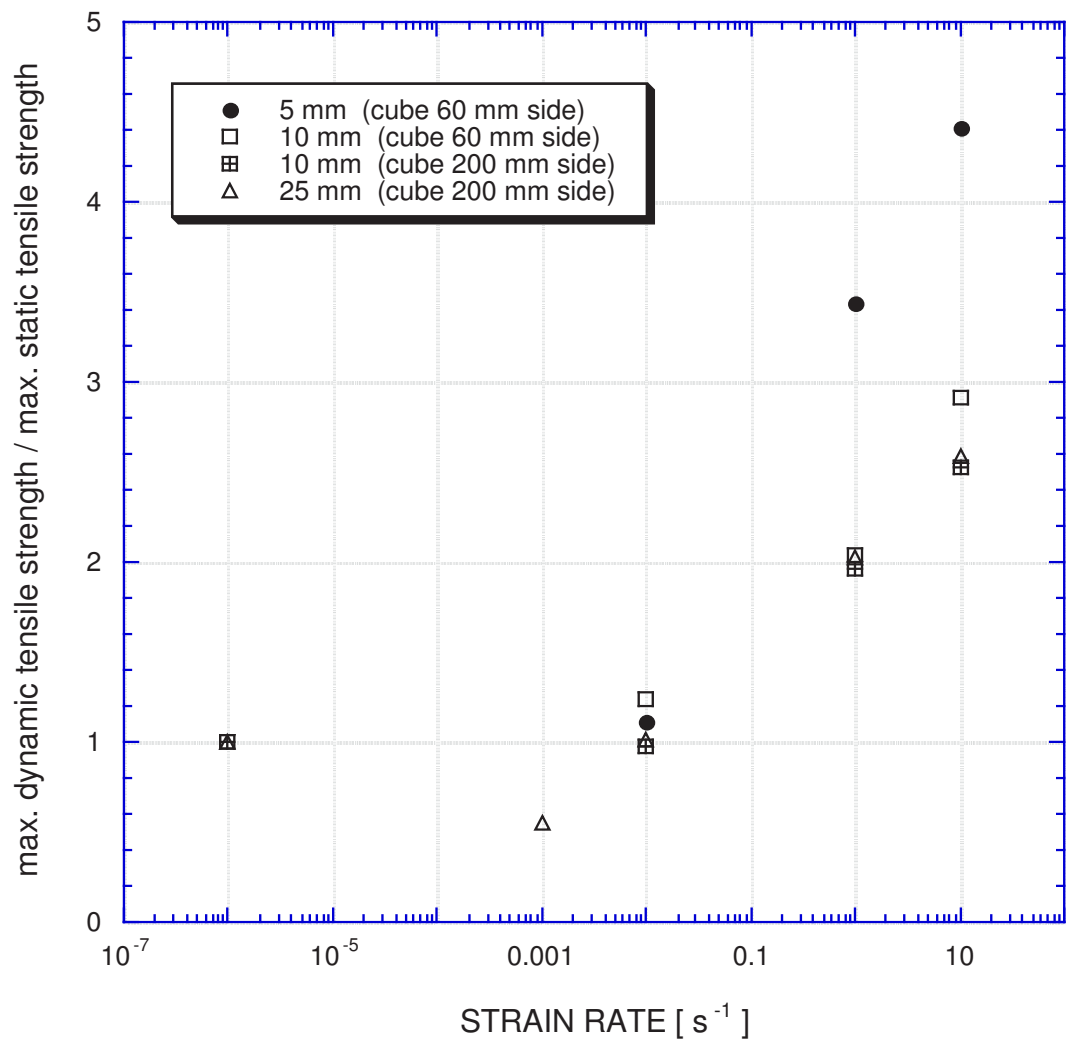


Fig. 2.23 – Dynamic/static tensile strength at different strain rates [2.73]

### 2.6.3 Dynamic Shear Strength

No increase for dynamic as compared to static shear parameters is generally assumed. From an engineering aspect the friction coefficient should be larger for short term loading which leads occasionally to accept an increase of 10%.

## 2.7 REFERENCES

- [2.1] Vilardell, J., Morreu, H., "Estimation of the modulus of elasticity for dam concrete", *Cement and Concrete Research*, Vol. 28, n°1, 93-101, 1998.
- [2.2] Experience from Swiss dams: *Bulletin Technique de la Suisse Romande*, 1956, p.77.
- [2.3] Raphael J. "The Nature of Mass Concrete in Dams", ACI SP 55-6.
- [2.4] US Bureau of Reclamation: "Concrete Manual" ,8th ed., J. Wiley, New York, 1981
- [2.5] Soares de Pinho, J., et al. "Control of Mass Concrete for Dams: Full- mix and Wet-screened Concrete Tests", 16. ICOLD Congress Proc. Q.62, R.27, San Francisco 1988.
- [2.6] LERM (Laboratoire d'études et de recherches sur les matériaux), "Contrôle des bétons durcis in situ - Etat de l'art", LERM rapport d'étude n° 01.5529.001.01.A, Arles, July 2001.
- [2.7] Neville, A., "Core Tests: Easy to Perform, Not Easy to Interpret", *Concrete International*, American Concrete Institute (ACI), Nov. 2001, 59-68.
- [2.8] American Concrete Institute, "In Place methods to Estimate Concrete Strength", *ACI Manual of Concrete Practice*, 228.1R, Vol. 2.
- [2.9] Paolina, R., Appendino, M., Baldovin, E., Berra, M., Bianchini, Carabelli, Posta, Vielmo. I., "Deterioration problems for concrete and masonry dams in Italy", 17th ICOLD Congress, Vienna, June 1991, Q.65, R.43.
- [2.10] Barlett, F. M., MacGregor, J. G., "Effect of Core-Length-to-Diameter Ratio on Concrete Core Strength", *ACI Material Journal*, Vol. 91, No.4, Aug. 1994, 339-348.
- [2.11] Ahmed A.E. "Does Core Size Affect Strength Testing?", *Concrete International*, Aug. 1999, 35-39.
- [2.12] ASTM C 42-99: "Standard Test Method for Obtaining and Testing Drilled Cores and Sawed Beams of Concrete", *Annual Book of ASTM Standards*, Section 4, Vol. 04.02
- [2.13] EN 12504: "Essais pour béton dans les structures (Testing of concrete in structures)", Norme européenne, Paris, August 2000.
- [2.14] American Concrete Institute, "ACI Building Code Requirements for Structural Concrete", ACI 318R-95, Part 3, Chapter 5, 1998
- [2.15] Akers, D.J. "Testing practice affects concrete's perceived quality", *Concrete International*, April 1990, 42-45.
- [2.16] Widmann, R., "How to avoid thermal cracking of mass concrete", 15th ICOLD Congress on Large Dams, Q.57, R.15, Lausanne 1985.
- [2.17] Kreuzer H., Tschegg E., Wilk W., "Fracture Energy of Concrete under Biaxial Loading", *Proc. of the International Conference on Dam Fracture*, eds. V. Saouma, R. Dungar, M. Morris, Sep. 1991, Boulder, Colorado, 447-457.
- [2.18] American Concrete Institute, "Mass Concrete", ACI Publication, 207.1R-96.

*ICOLD Bulletin: The Physical Properties of Hardened Conventional Concrete in Dams*  
Section 2 (Strength properties)

- [2.19] Tuthill, L.H. et al. "Better concrete for dams: recent experiences and trends in California", 10th ICOLD Congress on Large Dams, Q.39, R.11, Montreal 1970.
- [2.20] Portland Cement Association (PCA), "Concrete Information", Skokie III, USA, 1987.
- [2.21] Kreuzer, H., Collected from several publications.
- [2.22] ANIDEL, Le dighe di ritenuta negli impianti idroelettrici italiani, vol. 1, 1951.
- [2.23] American Concrete Institute, "Recommended Practice for Evaluation of Strength Test Results of Concrete", ACI Publication, 214, Manual of Concrete Practice, Vol. 2.
- [2.24] ISO 2859 - Sampling procedures for inspection by attributes.
- [2.25] ISO 3951 - Sampling procedures for inspection by variables.
- [2.26] ISO 5479 - Statistical interpretation of data -- Tests for departure from the normal distribution.
- [2.27] Comité Euro-International du Béton (CEB): CEB-FIP Model Code, 1990.
- [2.28] Lambotte H., Morreu H., "Contrôle de la qualité du béton chantier et en usine", C.S.T.C.-Revue No. 3, Sept. 1979.
- [2.29] Lombardi G. "Distributions a double borne logarithmique", 16th ICOLD Congress, Proc. Vol.5, San Francisco, 1988.
- [2.30] Kreuzer H., Bury K. "The effect of distribution bounds on dam safety evaluation", International Workshop on Dam Safety Evaluation, Grindelwald April 1993, Vol.3, 49-54.
- [2.31] Rüschi, H., Rackwitz, R. (1969), "Statistische Analyse der Betonfestigkeit" (Statistical Analysis of Concrete Strength), Deutscher Ausschuss für Stahlbeton, Heft 206, W. Ernst, Berlin.
- [2.32] Swiss Committee on Dams, "Concrete of Swiss dams", edited to the 20<sup>th</sup> ICOLD congress, Beijing, September 2000.
- [2.33] American Concrete Institute, "Standard Practice for Selecting Proportions for Normal, Heavyweight and Mass Concrete, ACI 211.1-91 (Re-approved 2002).
- [2.34] Popovics S., "Analysis of the concrete strength vs water/cement ratio relationship", ACI Material Journal. September – October 1990, 512 – 529.
- [2.35] AFNOR Association Française de Normalisation: "Béton prêt à l'emploi", XP P 18-305, August 1996
- [2.36] Higginson, E.C., et al., "Maximum size of aggregates affects strength of concrete", Civil Engineering, Nov. 1963
- [2.37] Gordon, W.W., Gillespie, H.A., "Variables in Concrete Aggregates and Portland Cement Paste with influence on Strength of Concrete", Journal of ACI, Aug. 1963, 1429
- [2.38] Leemann, A., et al., "Gebrochene Zuschlagstoffe" [Crushed Aggregates], Schweizer Ingenieur und Architekt (SIA), Nr. 24, June 1999, 532-536.
- [2.39] Huber, H., "Die Kölnbreinsperre – Neue Wege in der Technik des Massbetons" [Kölnbrein Arch Dam – Recent Developments in Mass Concrete Technology], Beton & Stahlbeton, Heft 5, 1979.

*ICOLD Bulletin: The Physical Properties of Hardened Conventional Concrete in Dams*  
Section 2 (Strength properties)

- [2.40] American Concrete Institute, "Standard Practice for Curing Concrete", ACI Manual of Concrete Practice, 308 -92, Vol. 2, 1998.
- [2.41] Haque, M.N., "Give it a week: 7 day initial curing", ACI Concrete International, Sep. 1998.
- [2.42] Huber, H., "Neue Wege in der Technik des Massenbetons" [New developments in mass concrete technology], SIKA Information, No.3, Dec. 1977.
- [2.43] Rüschi, H., "Der Einfluss der Deformationseigenschaften des Betons auf den Spannungszustand (the influence of deformation properties on the state of stress in concrete)", *Schweizerische Bauzeitung*, Jg. 77, Heft 9, Febr. 1959
- [2.44] Kupfer, H.B., Gerstle, K.H., "Behaviour of Concrete under Biaxial Stress" Journal of Engineering mechanics Div., ASCE, Vol. 99, n° EM4, Paper 9917, Aug. 1973, 853-866.
- [2.45] Bertacchi, P., Bellotti, R., " Experimental research on deformation and failure of concrete under triaxial loads", Colloque Rilem, Cannes, 4-6 October 1972.
- [2.46] Berra, M., Faticcioni, A., Ferrara, G., "Triaxial behaviour of concretes of different weights" Int. Conf. on concrete under multiaxial conditions, Toulouse, 22-24 May 1984.
- [2.47] Hellmann, H.G., "Beziehung zwischen Zug-und Druckfestigkeit des Betons", *Beton*, 2-69, 1969, 68-70.
- [2.48] Metha, P.K., "Durability – Critical Issue for the future", ACI Concrete International, July 1997.
- [2.49] Raphael J. "Tensile Strength of Concrete", ACI Journal, March, April 1984, 158-165.
- [2.50] Khan A., et. al., "Tensile strength of low, medium and high strength concrete at early ages", ACI Material Journal Sep./Oct. 1996, 487-493.
- [2.51] Bazant, P., Gettu, R., "Rate Effect and Load Relaxation in Static Fracture of Concrete" ACI Material Journal, Vol. 89, n°5, Sept.-Oct. 1992, 456-468.
- [2.52] Dungan, R., Kreuzer, H., "Apparent tensile strength for arch dam design: a review for rate, size and strength dependency" *Dam Engineering*, Vol. III, Issue 3, Aug. 1992.
- [2.53] The National Academy of Sciences, "Earthquake Engineering for Concrete Dams: Design, Performance, and Research Needs", Commission on Engineering and Technical Systems, USA, 1991.
- [2.54] Liu, T.C., Mc Donald, J.M., "Prediction of tensile strain capacity of mass concrete", *Journal ACI*, 75, n° 5, 1978.
- [2.55] Newman, K., Newman, J.B., "Failures theories and design criteria for plain concrete", Proc. of the Southampton 1969 Civil Engineering Materials Conference, ed. M. Teeni, 1971.
- [2.56] Kreuzer, H., Bury, K., "Reliability analysis of the Mohr failure criterion", *Journal of Engineering Mechanics*, Vol. 115, n°3, ASCE, 1989.
- [2.57] Tschegg, E. et al. "Fracture in concrete under biaxial loading – numerical evaluation of wedge splitting test results", Proc. of the Conference on Fracture mechanics of Concrete Structures, Z.B. Bazant ed., FramCos 1, Breckenridge 1992, Eseevier Applied Science, London, 455-460.

*ICOLD Bulletin: The Physical Properties of Hardened Conventional Concrete in Dams*  
Section 2 (Strength properties)

- [2.58] Dungar, R., "El Cajon Hydroelectric Powerplant, Arch Dam Final Design, Static and Dynamic Stress Analysis, May 1981 (unpublished). See also comment to this reference in [2.3].
- [2.59] RILEM Report 5, "Fracture mechanics test methods of concrete", ed. S.P. Shah and A. Carpinteri, Chapman & Hall, 1989.
- [2.60] ACI 446.3R-97, "Finite Element analysis of fracture in concrete structures", American Concrete Institute, Manual of Concrete Practice, Part 4, 1998.
- [2.61] Bazant, z.P., He, S., Plesha, M.A., Gettu, r., Rowlands, R.E., "Rate and size effect in concrete fracture: implications for dams", Dam Fracture, Proc. of International Conference, Boulder CO, Sept. 1991.
- [2.62] Gunn, R.M., "Non-linear design and safety analysis of ach dams using damage mechanics", Hydropower & Dams, Issue 3, 2001.
- [2.63] Pacelli, W. A. et al., "Treatment and performance of construction joints in concrete dams", Water Power & Dam Construction, Nov. 1993.
- [2.64] Tarbox G. et al. "Seismic Analysis of Concrete Dams", 13 ICOLD Congress Proc. Q.51 R.12, New Dehli 1979.
- [2.65] Brühwiler E., "Fracture Mechanics of Dam Concrete Subjected to Quasi-static and Seismic Loading Conditions", Ph.D. Thesis no. 739, Ecole Polytechnique Federale de Lausanne, 1988.
- [2.66] Bischoff, P.H., Perry, S.H., "Compressive behavior of concrete at high strain rates", RILEM Materials and Structures, 1991, 24.
- [2.67] Hatano T. "Aseismic design criteria for arch dams in Japan", 9. ICOLD Congress Proc. Q.35 R.1, Istanbul 1967.
- [2.68] Harris, D.W. et al., "Dynamic Properties of Mass Concrete Obtained from Dam Cores", ACI Materials Journal, Vol. 97, No.3, May-June 2000.
- [2.69] Saucier K.L., Carpenter L. "Dynamic Properties of Mass Concrete", ASTM STP 654, 1978, 163-178.
- [2.70] Discussion by H.W. Reinhard and others included in ACI Jan.-Febr. 1995, 94-98. In Ref. [2.3]
- [2.71] Bureau of Reclamation (Mohorovic, C. Harris D.W. Dolen T.P.), "Dynamic Properties of Mass Concrete Obtained from Dam Cores" Dam safety Office, 1999.
- [2.72] Lindvall, Richter & Ass., "Final Report for Investigations of the Big Tujunga Dam", Los Angeles 1975 (unpublished).
- [2.73] Berra, M., Albertini, Cadoni, Labibes, Giangrasso, " High strain-rate tensile concrete behaviour ", Magazine of Concrete Research, Vol. 52 – n°5 – Oct.. 2000 – pp. 365-370.
- [2.74] Berra, M., Albertini, Cadoni, Labibes, Giangrasso, " Strain-rate effect on the tensile behaviour of concrete at different relative humidity levels ", RILEM Materials and Structures, Vol.34 - n° 235 - January-February 2001 - pp. 21 – 26.

### 3 ELASTIC PROPERTIES

<b>3 ELASTIC PROPERTIES.....</b>	<b>1</b>
<b>3.1 GENERAL.....</b>	<b>2</b>
<b>3.2 STATIC MODULUS OF ELASTICITY.....</b>	<b>4</b>
3.2.1 <i>Typical behaviour and definitions.....</i>	4
3.2.2 <i>Internal mechanisms affecting the behaviour.....</i>	5
3.2.3 <i>Factors affecting the elastic modulus.....</i>	6
3.2.3.1 Aggregates.....	6
3.2.3.2 Cement paste matrix.....	8
3.2.3.3 Transition zone.....	8
3.2.3.4 Test conditions.....	9
3.2.3.5 Age.....	10
3.2.3.6 Damage conditions.....	11
3.2.4 <i>Estimation of the elastic modulus.....</i>	12
3.2.4.1 Experimental determination in laboratory.....	12
3.2.4.2 Prediction based on elastic models.....	13
3.2.4.3 Empirical expressions through correlation with the compressive strength.....	14
<b>3.3 DYNAMIC MODULUS OF ELASTICITY.....</b>	<b>17</b>
3.3.1 <i>Modulus of Elasticity under Seismic Loading.....</i>	17
3.3.2 <i>Dynamic Ultrasonic Modulus of Elasticity.....</i>	18
<b>3.4 POISSON'S RATIO.....</b>	<b>19</b>
<b>3.5 SIGNIFICANCE OF ELASTIC PROPERTIES ON DAM BEHAVIOUR.....</b>	<b>23</b>
<b>3.6 USE OF ELASTIC PROPERTIES IN MATHEMATICAL MODELS FOR DAM STRUCTURAL ANALYSIS.....</b>	<b>24</b>
<b>3.7 REFERENCES.....</b>	<b>28</b>



### 3.1 GENERAL

The elastic characteristics of a material define how the material will deform when various loads are applied. Elastic properties provide a measure of the stiffness of a material. Concrete has a non-linear stress-strain curve, however to a certain degree it may be considered an elastic material (Fig. 3.1).

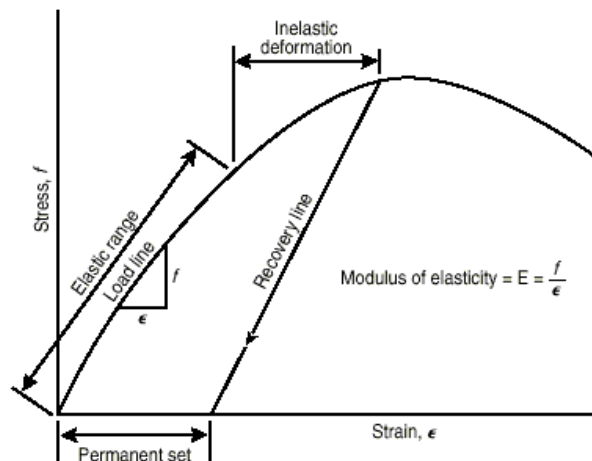


Fig. 3.1 - Generalised stress-strain curve for concrete [3.1]

Prior to discussing the elastic properties of concrete, it is useful to present a brief summary of other constitutive models which have been used to determine the stress-strain response of concrete structures.

Concrete is variously characterised theoretically as “elastic”, “visco-elastic”, “elastic-plastic”, “poro-plastic” or otherwise depending on the behavioural model assumed. “Elastic” (see for example [3.1] and Timoshenko and Goodier [3.2])

behaviour by definition has the property that the strains appear and disappear immediately on the application and removal of stress. Elastic behaviour does not imply a linear stress-strain relationship. In non-linear elastic models, the elastic properties may vary depending on the level of stress or other controlling parameters. “Viscoelastic” (for example Neville et al. [3.3]) behaviour includes treatment of time dependent deformation such as creep. Viscoelastic rheological material models are applied to concrete when the stresses are relatively low which is similar to the range of applicability of linear elastic material models. At higher stress levels the time dependent behaviour of concrete is non linear. Creep of concrete is discussed further in Section 4. “Elastic-plastic” behaviour (see for example, Bangesh [3.4] and Chen [3.5]) includes permanent deformations and a plastic flow rule subsequent to “yielding”. “Poro-plastic” (see for example, e.g. Fauchet et al.[3.6]) behaviour includes the effects of fluid pressure in the pore spaces of an elastic-plastic material.

Fig. 3.2 shows a rheological equivalent of the above mentioned stress-strain response. It shows, among others, the typical stress transfer between the damping (viscosity) and

the friction element, hereby, with time, stress will be completely transferred from the first to the latter resulting in irreversible (plastic) strain. Plastic strain continues until the accumulated strain is enough to activate resisting stress. This kind of process can then be simulated in a non linear stress-strain relation for Finite Element-modelling.

In addition, it is necessary to select further idealisations in terms of homogeneity and isotropy. Homogeneity is frequently assumed at a macro level but of course at the particle level the grains and aggregate form a very inhomogeneous mixture. In structures where distinctly different concrete mixes were used, then selected volumes may be assumed to be homogeneous within themselves but may vary from volume to volume. In some instances, inhomogeneity may develop with time due to deterioration mechanisms varying spatially. Isotropy is usually assumed in conventional mass concrete. In fact it can be shown that strength parameters (compressive strength, Young's modulus) are only insignificantly (if ever) different when comparing their values parallel or perpendicular to the direction of concrete placement.

The classic and simplest constitutive material model is one of linear elasticity in an isotropic homogeneous material in which the behaviour can be characterised by two parameters, the modulus of elasticity ( $E$ ) and the Poisson's ratio ( $\nu$ ). A material is isotropic when its elastic properties are identical in all directions.

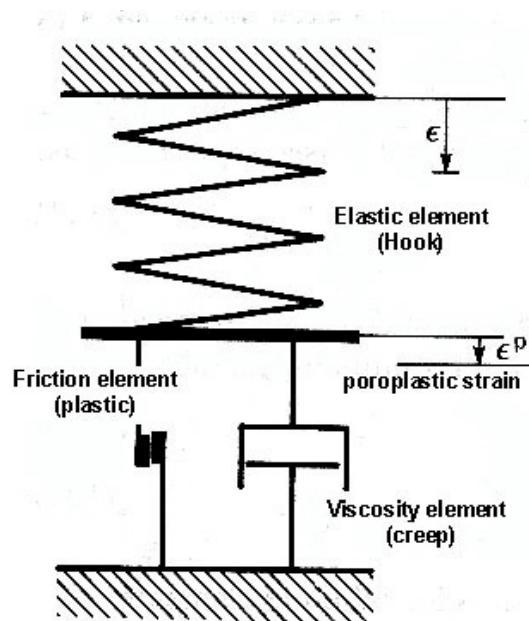


Fig. 3.2 - Rheological equivalent of typical stress-strain response in concrete [3.7]

The above models consider the concrete as “continua” but in fact internal cracking due to shrinkage or other source of tension may introduce discontinuities. Moreover, vertical block joints or weak horizontal lift joints are marked discontinuities too. These discontinuities may be modelled as equivalent continua as “no tension” models, with “smeared cracks” and strain-softening or as discrete cracks depending on the level of detail available and behaviour desired.

The behaviour of concrete is usually characterised differently for static and dynamic loading. This will depend on the rate of loading and the idealisation. In some cases, such as blast loading, the rate effects are significant in themselves, in others the distinction is related to modelling assumptions and strain magnitude, for example, the use of secant modulus for static loading versus tangent modulus for dynamic loading of small amplitude.

Here we discuss the use of the two parameter model, using a modulus of elasticity and Poisson's ratio to include certain elastic and inelastic behaviours exhibited by concrete.

## **3.2 STATIC MODULUS OF ELASTICITY**

### **3.2.1 Typical behaviour and definitions**

The behaviour of concrete in compression is shown diagrammatically in Fig. 3.3 (from Mehta [3.8]).

Since the curve is non-linear, various definitions of elastic moduli are possible as illustrated. These are:

1. the tangent modulus given by the slope of the line drawn tangent to the stress-strain curve at any point, or stress level, on the curve. The tangent modulus is of little practical significance since it applies to very small stress-strain conditions. However, with respect to using elastic moduli in finite element analyses (FEA), the tangent modulus is a choice when non-linearities are taken as rate-dependent (e.g. in a viscoplastic model) or for short term loading, for which the modulus is regarded being higher than long term loading.
2. the secant modulus given by the slope of the line drawn from the origin to the point on the curve at the stress level, and,
3. the chord modulus (or an incremental modulus) given by the slope of the line between two points. It is the modulus defined in most standards, in which the strain is measured between stipulated load percentages (see 3.2.4).

Concrete in dams will exhibit time dependent straining (creep) and the notion of an elastic modulus does not strictly apply. However, in a linear-elastic FEA the artifice to choose a secant modulus, including creep effects, is fully justified.

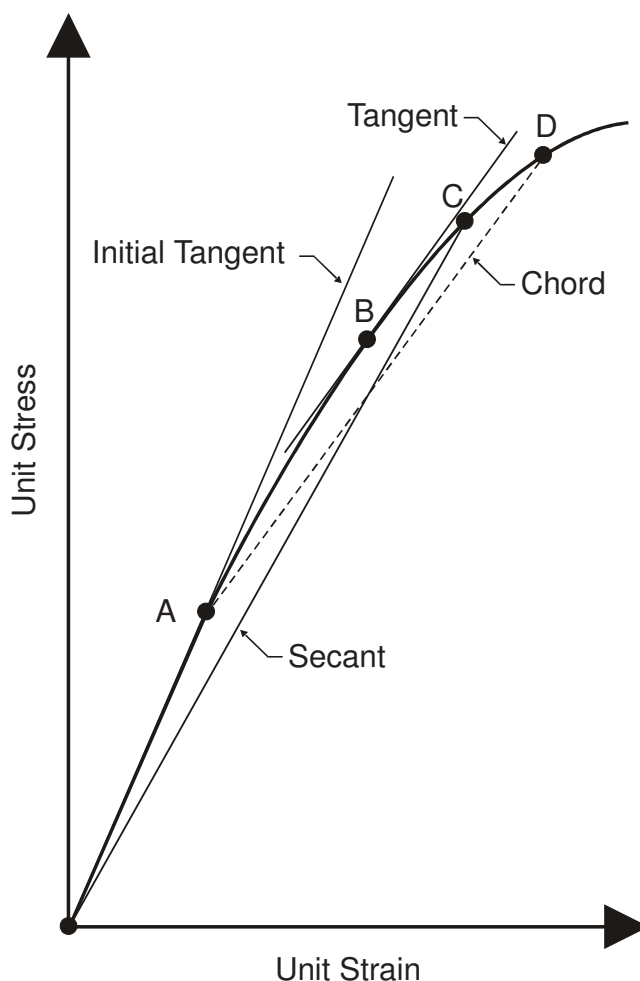


Fig. 3.3 - A typical concrete stress-strain curve and various definitions of elastic moduli

### 3.2.2 Internal mechanisms affecting the behaviour

The non-linear stress-strain behaviour has been explained in terms of the progression of micro-cracking of concrete through four stages [3.8]. Initially, before the application of external load, the concrete would contain micro-cracks in the transition zone between the matrix and the coarse aggregate. The number and extent would depend on the mix proportion, curing history and strength of the material and consist of drying shrinkage, chemical shrinkage (autogenous volume change) and thermal cracks. Up to a certain level depending on the placing, mix design and curing, the micro-cracks will be stable and the modulus will be approximately constant, i.e. essentially linear. Then as the strain progresses, the micro-cracks increase in length, although they may still be stable, and non-linear behaviour becomes apparent. Subsequently the micro-cracks become unstable and non-linearity is stronger and eventually spontaneous crack growth and large strains occur which could eventually lead to failure. In this Section, the discussion mainly pertains to linear elastic behaviour which occurs at low level of strain and when micro-cracking is small.

### 3.2.3 Factors affecting the elastic modulus

These are aggregates, cement paste matrix, aggregate – cement paste interface (transition zone), test conditions (humidity, temperature, loading rate application), age and damage conditions.

#### 3.2.3.1 Aggregates

The relationship between the concrete static modulus and the aggregate used for the concrete can be obtained through the volumetric contents of both cement paste and aggregates, and their relative static moduli. In particular this relationship can be expressed with the two-phase composite models, which combine elements with parallel (Voigt model) and series (Reuss model) phases (Fig. 3.4) [3.9].

The parallel system is the upper bound for elastic properties of interest while the series system provides the lower bound. Concrete made with natural aggregate in a soft paste conforms more closely to the lower bound, i.e. the series model.

However other more realistic models for concrete have been suggested as those by Hirsch and Counto (Fig. 3.4) [3.9] or that one consisting of spherical particles in a continuous matrix [3.10]. This last can be expressed as:

$$E_c = \left[ \frac{(1-V_a)E_m + (1+V_a)E_a}{(1+V_a)E_m + (1-V_a)E_a} \right] E_m$$

These models depend on the assumptions that (1) the concrete is a three-dimensional combination of the two homogeneous and isotropic phases, the matrix and the coarse aggregate, (2) each phase behaves linearly in the linear elastic regime, (3) there is no interaction between the aggregate particles, and (4) that there is a perfect bond between aggregate and the matrix. These assumptions are not all always valid.

For good quality normal weight aggregates, such as those used in dams,  $E_a$  is considerably higher than  $E_m$  and the true value for  $E_c$  should lie between the theoretical lower limit (series model) and the spherical model.

The porosity of the aggregate is another aggregate parameter able to influence the concrete elastic modulus. In fact it directly affects the aggregate stiffness,  $E_a$ . A dense aggregate has a high elastic modulus and this also produces a concrete with a higher modulus. Aggregates from low porosity rock such as basalt and granite have  $E_a$  greater than 60 – 70 GPa while aggregates from more porous rocks, like for example sandstone, are characterised by a lower  $E_a$  (8 - 25 GPa). The aggregates coming from rocks with variable porosity, like for example limestones, are consequently characterised by more variable values of  $E_a$ , between 10 and 60 GPa.

The higher is the concrete grade (e.g. facing concrete) the greater is the porosity importance of the aggregate.

Other aggregate properties that influence the elastic modulus of concrete are the maximum size and size distribution, the shape, the surface texture and mineralogical composition. These last through the influence of micro-cracking in the transition zone between aggregate and cement paste (see 3.2.3.3).

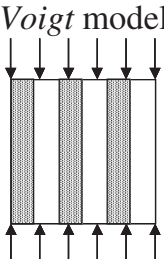
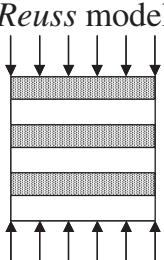
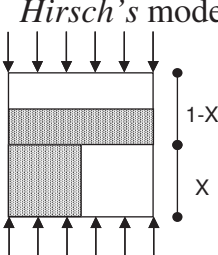
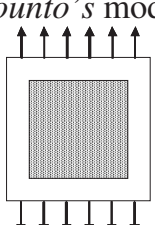
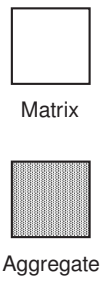
Model	Equation	
<p><i>Voigt model</i></p> 	$E_C = V_m \cdot E_m + V_a \cdot E_a$	Assumes $\epsilon$ is the same in aggregate and matrix
<p><i>Reuss model</i></p> 	$\frac{1}{E_C} = \frac{V_m}{E_m} + \frac{V_a}{E_a}$	Assumes $\sigma$ is the same in aggregate and matrix
<p><i>Hirsch's model</i></p> 	$\frac{1}{E_C} = X \cdot \frac{1}{V_m \cdot E_m + V_a \cdot E_a} + (1-X) \cdot \left( \frac{V_m}{E_m} + \frac{V_a}{E_a} \right)$	
<p><i>Counto's model</i></p> 	$\frac{1}{E_C} = \frac{1 - \sqrt{V_a}}{E_m} + \frac{\sqrt{V_a}}{(1 - \sqrt{V_a}) \cdot E_m + \sqrt{V_a} \cdot E_a}$	
	<p><math>E_C</math>    Elasticity modulus of concrete [MPa]  <math>E_m</math>    Elasticity modulus of matrix [MPa]  <math>E_a</math>    Elasticity modulus of aggregate [MPa]  <math>V_m</math>    Volumetric fraction of matrix in concrete  <math>V_a</math>    Volumetric fraction of aggregates in concrete  <math>X</math>    Arbitrary parameter for combination of parallel and series composition within <i>Hirsch's</i> model</p>	

Fig. 3.4 - Concrete two-phase composite models and computation of elastic modulus [3.9]

### 3.2.3.2 Cement paste matrix

Similarly the capillary porosity of the cement paste matrix controls the concrete elastic modulus. The porosity of the cement paste matrix is affected by the water/cementitious ratio, air content and mineral admixtures. The modulus of the cement paste matrix is generally in the range of 10 GPa to 30 GPa.

It should be noted that these values are similar to the elastic moduli for low quality high porosity aggregates.

### 3.2.3.3 Transition zone

Fig. 3.5 schematically shows the typical stress – strain curve for a concrete and its main components (cement matrix or paste and aggregate). As for all composite materials, the concrete curve lies between those of the two components but while these two last ones are substantially linear elastic, in the considered concrete stress range, the concrete curve is not. The reason of this is the behaviour of the cement paste – aggregate interface or transition zone.

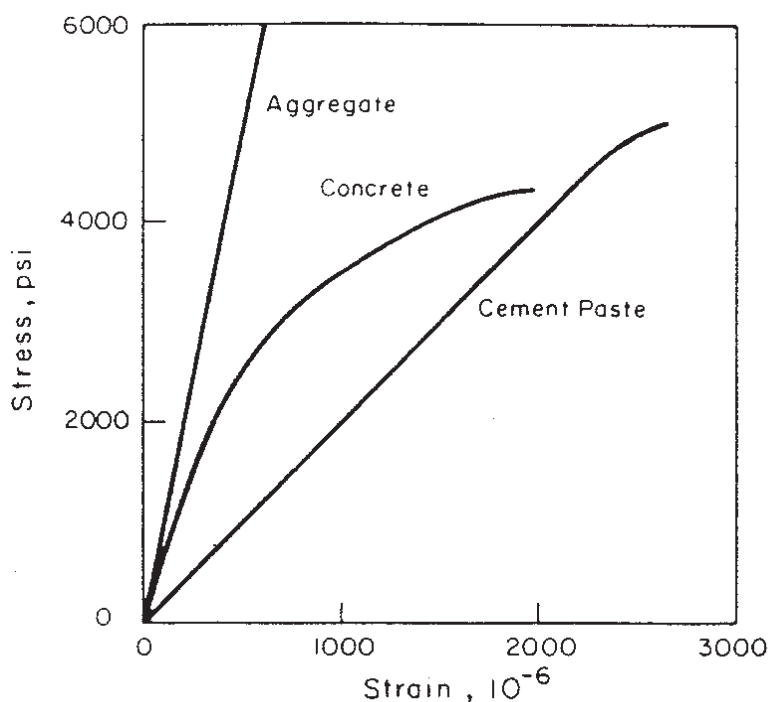


Fig. 3.5 – Typical stress-strain behaviour of cement paste, aggregate and concrete [3.8]

The transition zone contains void spaces, micro-cracks and calcium hydroxide crystals, whose amount is related to degree of consolidation and degree of hydration and type of curing. They already exist in this interface zone even before the application of external loads but generally they remain stable up to about 1/3 of the ultimate load. This is approximately the range where stress-strain curve remains linear (Fig. 3.5) and an elastic modulus  $E_C$  can be measured.

Above this range, the transition zone microcracks begin to increase in length, width and numbers and the higher the stress level the lower the stability of the microcracks system. This is reflected by a clear non linearity in the concrete curve of Fig. 3.5. Above 50 – 60 % of the ultimate load cracks begin to form also into the cement matrix and then very high strain are finally developed up to failure [3.9].

#### *3.2.3.4 Test conditions*

The test conditions also affect the value of measured elastic modulus. Tests conducted under dry conditions indicate approximately 15 to 20 per cent lower elastic modulus than corresponding samples tested in the wet conditions, depending on the saturation degree [3.8] [3.11].

There are several authors that have experimented this phenomena. Gorisse [3.12] has established the following relationship that quantifies the value of the E modulus.

$$E (\text{saturated}) = E (\text{dry}) + 3 \text{ GPa.}$$

The dry samples are adversely affected by drying which increases the amount of micro-cracking in the transition zone. It is worth to note an apparent inconsistency in that the compressive strength under dry conditions is, on the contrary, higher than in wet conditions, due to the wedge effect produced by the presence of water inside the concrete porosity.

For this reason it is important, when taking cores from concrete dams, to maintain their in situ moisture content during specimen preparation and transportation to the laboratory (for example wrapping them with plastics and moist towels).

The modulus of elasticity varies also with changes in temperature and a tendency of decreasing values with increasing temperature conditions have been found [3.3]. The influence of temperature on elastic modulus is not direct, because there are other aspects that must be considered at the same time, such as the humidity degree and the sealing degree. In the most cases that have been analysed, a dry concrete has a reduction of elastic modulus that varies with the temperature in quasi-linear way when the value exceeds 50°C, and reaching 400°C, the modulus has lost 60% of the initial value.

In case of saturation of the concrete, and the moisture doesn't decreases, the value modulus can fall quickly, and at 150°C the 60% of the initial value can be lost.

However, between the normal range of temperatures (0°C-50°C) the effect of the temperature on the modulus is less important.



The rate of loading application is another important factor that influence the concrete elasticity modulus. In fact, under instantaneous loading only a little strain can occur prior to failure and the modulus of elasticity is higher than in static conditions [3.8] (see also the paragraph 3.3 on the dynamic modulus of elasticity and Figure 2.11 in Section 2).

For very slow loading rates, the elastic modulus is, on the contrary, lower than in static conditions, also due to the significant creep effects. In fact creep strains would be superimposed, thus lowering the elastic modulus further [3.8] (see also the Section 4 on creep properties).

### 3.2.3.5 Age

The concrete modulus varies with time and numerous investigators have presented results of tests and equations to describe this behaviour.

For example a commonly accepted expression developed by Geen and Swanson [3.13] is as follows:

$$E(\tau) = E \left\{ 0.4 + 0.6 \left[ \frac{f(\tau)}{f_{cu}} \right] \right\}$$

where  $E$  = Young's modulus at 28 days,  $f(\tau)$  = cube strength of concrete at time  $\tau$  and  $f_{cu}$  = cube strength of concrete at 28 days.

Investigations on dam concrete show a considerable increase in moduli with age. ACI 207 ("Mass Concrete") [3.14] shows elastic properties (modulus of elasticity and Poisson ratio) for 13 dams. An increase between 105% and 138% within the period of 28 days and one year is reported.

Raphael in his "The nature of mass concrete in dams" [3.15] reports results for ratios "modulus under sustained load after one year to the instantaneous modulus after 28 days". The average increase within this period is 122% with a low coefficient of variation of 7.5% (Fig. 3.6).

The effect of an increase of the modulus of elasticity with time even beyond an age of 90 days is particularly pronounced when pozzolanic materials are used within the cementitious content of the concrete mix.

Research has also shown that concrete modulus of elasticity tends to increase with time at a faster rate compared to the compressive strength [3.9]. This is though to depend on the density improvement of the transition zone, because of the slow chemical beneficial interactions between cement paste and aggregate, that still can continue even after a long time.

Fig. 3.6 also indicates some cases where the modulus of elasticity increases during the period of cement hydration (say until an age of 90 days) and is constant thereafter. Because all laboratory samples show significant increase with age, such cases of no modulus increase on core samples may be related to eventual micro-cracking on sample from coring.

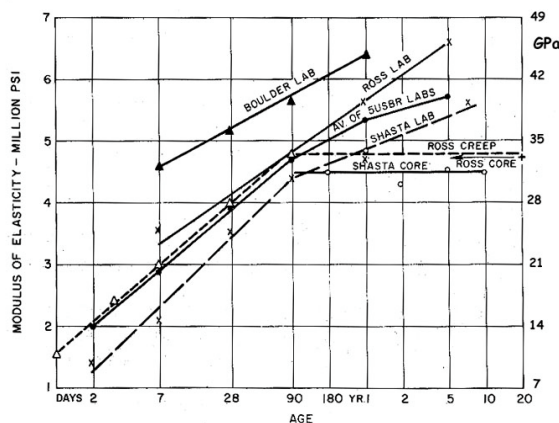


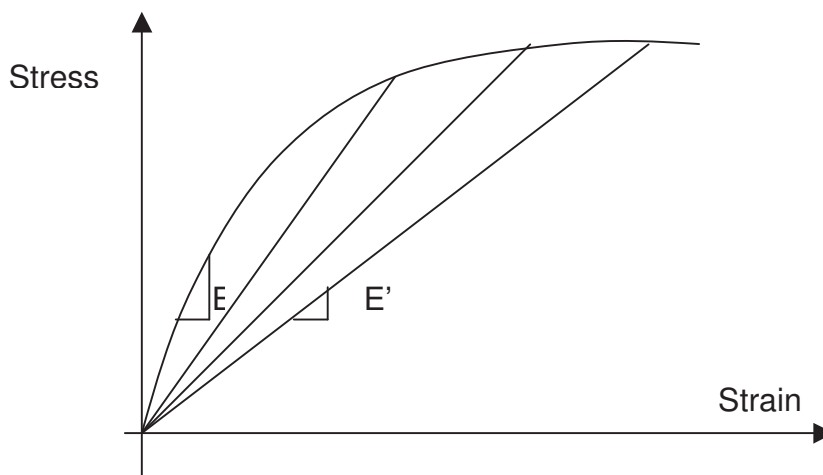
Fig. 3.6 - Increase of modulus of elasticity with age [3.15]

### 3.2.3.6 Damage conditions

If concrete is damaged or plasticized (because of high loads, fatigue, chemical or physical deterioration etc.), its elasticity modulus becomes, of course, lower compared to that in no damage conditions. A reduction of this parameter, as the damage proceeds, can be observed through the changing of slope of loading and unloading cycles, both in tension and compression. From Fig. 3.7 can be observed how the elastic parameter can evolve due to the effects, for example of micro-crackings.

However, one has to be cautious in not relating an E-modulus reduction to a corresponding reduction in strength. As fracture mechanics testing shows, damaged concrete can mobilize margins of strength due to aggregate interlock of a micro-cracked concrete. Such strength margins are of particular interest for judging post-earthquake stabilities in dams.

Fig. 3.7 – Elastic modulus evolution due to damage increase



### **3.2.4 Estimation of the elastic modulus**

The elastic modulus of a concrete is conventionally measured using standardised tests directly based on concrete samples subjected to uniaxial loading (paragraph 3.2.4.1). The sizes of these samples should be at least three times the maximum size of the aggregate used in concrete. However, from an experimental point of view, this is not always easy: in fact the maximum size aggregate usually ranges from 80 to 200 mm and large specimens, for example cylinders of 45 x90 cm, should be required [3.16].

Due to the practical difficulties in performing such tests, dam concrete is usually wet-screened, removing aggregates larger than 40 mm, and using standard cylinders of 15x30 cm (2.2.1 in Section 2).

However this procedure can result in a incorrect estimation of the elasticity values. A method has been recently proposed [3.17] in order to predict the modulus of the real size aggregate concrete from the experimental results obtained from the wet-screened concrete specimens (paragraph 3.2.4.2). It is based on the application of the simple elastic models presented in the paragraph 3.2.3.1.

Furthermore empirical approaches can be used to estimate the elastic modulus, less complicated and time-consuming compared to the experimental determination. A lot of empirical relationships have been proposed and recommended by national and international standards, estimating the elastic modulus directly from the concrete compressive strength (paragraph 3.2.4.3).

#### *3.2.4.1 Experimental determination in laboratory*

Dam concrete is designed for a compressive stress state, therefore the static modulus of elasticity is typically measured with concrete in compression. For example, the ASTM C469 [3.18] provides the static Young's Modulus and Poisson's Ratio using a compressive test procedure.

It stipulates the use of chord modulus with a lower point at strain of 50  $\mu\epsilon$  and the upper point corresponding to 40 per cent of the compressive strength at the time of loading. The lower and upper chord modulus points are chosen to avoid seating effects and also the modulus is obtained in the "elastic" range of the stress-strain curve. ASTM C 469 uses 6 by 12 inch (15 by 30 cm) cylinders.

For drilled core specimens, only diamond drilled cores with length-to-diameter ratios of greater than 1.5 are used. The strains along the axis of compression should be measured with two or more gage lines such that eccentric loading and non-uniform response can be monitored. The gage length for strain measurement is an important consideration. ASTM C469 specifies that the gage shall not be less than three times the maximum size of aggregate or more than 2/3 the height of the specimen. The preferred gage length is typically about one half the height of the specimen.

Before loading the specimen it is important to follow a specific centering sequence, accurately placing the test specimen in the centre of the loading platens of the testing machine and monitoring the strains values provided by the gauges. If these strains excessively differ by more than 20% from their mean value. It is recommended to re-centre the test specimen and repeat the test.

This preloading procedure, with loading and unloading cycles, is also effective in order to stabilise the concrete behaviour and reduce the creep effect that can be induced by the strain-time diagram used for the determination of the elastic modulus.

The static modulus of elasticity in compression,  $E_c$ , in MPa, is given by the formula

$$\frac{\Delta\sigma}{\Delta\varepsilon} = \frac{\sigma_a - \sigma_b}{\varepsilon_a - \varepsilon_b}$$

where

$\sigma_a$  is the upper loading stress, in MPa (for ASTM C469:  $\sigma_a = 0.4 f_c$ );

$\sigma_b$  is the initial stress (for ASTM C469: stress corresponding to a strain  $\varepsilon_b$  of 50  $\mu\varepsilon$ )

$\varepsilon_a$  is the mean strain under the upper loading stress:

$\varepsilon_b$  is the mean strain under the initial loading stress (for ASTM C469: 50  $\mu\varepsilon$ ).

An interesting aspect of the stress strain curve obtained from such a test is that the sample fails suddenly shortly after the maximum load is obtained. Such a response is related to the properties of the testing machine rather than the behaviour of the tested concrete specimen. The use of a stiff testing machine will result in gradually softening behaviour in the post-peak response stages of the test.

The modulus of elasticity in tension and flexure is typically taken to be equal the value obtained from compression tests. Data from tension and flexure tests indicate that this is a reasonable approach.

#### *3.2.4.2 Prediction based on elastic models*

A valuable proposal for predicting the elasticity modulus of a real dam concrete from the experimental results of tests carried out on standard wet-screened concrete specimens (e.g. cylinders of 15x30 cm) is presented in [3.17]. It is less complicated and time-consuming than testing on large size specimens.

On the basis of an experimental research on dam concrete, it was found that this aim can be easily obtained by simply using the wet-screened concrete data, along with estimations of the aggregate modulus, in a multiphase concrete model such as the Hirsch model presented in paragraph 3.2.3.1.

By taking the matrix phase as the wet-screened concrete (15x30 cm cylinders with aggregate size up to 40 mm) and the gravel above 40 mm (40 - 120 mm) as the aggregate phase, the elastic moduli calculated for the real size concrete were quite close to those experimented on large size specimens (45x45x90 prisms with aggregate 0-120 mm) of real concrete.

A synthesis of the comparison between the experimented and calculated results is reported in Tab. 3.1, with two different values of aggregate moduli (50 and 65 GPa). In this case the calculated error is less than 10%. More detailed information on this procedure can be found in [3.17].

Tab. 3.1 – Comparison between the predicted moduli of the real concrete (Hirsch model) and the experimental ones (at different ages and for two aggregate moduli)

Age (days)	$E_m$ (GPa) Wet-screened concrete	$E_a$ (GPa) Aggregate	$E_c$ (GPa) Real concrete predicted	$E_c$ (GPa) Real concrete experimented	Error
7	24.8	50	30.2	30.3	-0.3%
		65	32.6		7.6%
28	34.5	50	38.2	37.3	2.4%
		65	41.2		10.5%
90	35.1	50	38.7	43.0	-10.0%
		65	41.7		-3.0%
180	37.2	50	40.3	42.2	-4.5%
		65	43.4		2.8%

### 3.2.4.3 Empirical expressions through correlation with the compressive strength

The concrete modulus of elasticity is usually and widely expressed as a function of concrete uniaxial compressive strength. Different national building codes propose various formulas for normal strength concrete (NSC) and high strength concrete (HSC). Among the relationships for NSC the equations of American Concrete Institute (ACI Building Code 318), British Standard BS 8110 and Eurocode 2 (Design of concrete structures) are here presented, where the  $f_{ck}$  is the characteristic compressive strength (in MPa) from 15x30 cm cylinders and  $E$  is the average modulus of elasticity in compression (in GPa) at the same age (28 days).

1. ACI Building Code (ACI Committee 318) [3.19]:

$$E=4.37 f_{ck}^{1/2}$$

This formula applies for normal density concrete with unit weight of 2,300 kg/m<sup>3</sup>

2. The British Code of Practise (CP 110, Part 1) [3.20]:

$$E=9.1. f_{ck}^{1/3}$$

3. Eurocode 2 (Design of concrete structures) [3.21]:

$$E=9.5 * (f_{ck} +8)^{1/3}$$

*ICOLD Bulletin: The Physical Properties of Hardened Conventional Concrete in Dams*  
Section 3 (Elastic properties)

According to the Eurocode 2, the elastic modulus can be calculated even at a later age, if  $f_{ck}$  is replaced by the effective strength at the considered time.

Common to all equations is a high coefficient of variation.

Typical estimates of static modulus of elasticity obtained from the ACI and British codes is given in Tab. 3.2.

Tab. 3.3 shows the elastic moduli calculated according to the Eurocode 2 for the different concrete grades, from C12/15 to C50/60 (cylinder strength / cube strength in MPa).

Tab. 3.4 shows modulus of elasticity values for concretes from German and Swiss dams, compared to their compression strength. Information on concrete mix design and time of testing are also provided.

Tab. 3.2 - Typical estimates of static modulus versus compressive strength [3.8]

ACI Building Code 318		British Code of Practice (CP 110)	
$f'_{ck}$ MPa (psi)	E GPa (x 10 <sup>6</sup> psi)	$f_{ck}$ MPa (psi)	E GPa (x 10 <sup>6</sup> psi)
20 (3,000)	21 (3.1)	20 (3,000)	25 (3.6)
27 (4,000)	25 (3.6)	30 (4,500)	28 (4.1)
40 (6,000)	30 (4.4)	40 (6,000)	31 (4.5)
53 (8,000)	35 (5.1)	50 (7,500)	34 (4.9)
67 (10,000)	39 (5.7)	60 (9,000)	36 (5.2)

Tab. 3.3 – Elastic moduli for different concrete grade according to Eurocode 2 [3.21]

Concrete grade	C 12/15	C 16/20	C 20/25	C 25/30	C 30/37	C 35/45	C 40/50	C 45/55	C 50/60
E (GPa)	26	27.5	29	30.5	32	33.5	35	36	37

Tab. 3.4 - Compressive strength vs elastic modulus from German and Swiss dams

Project	Dam Type	Country	Mix Design	Cube Compres. Strength		Static Elastic Modulus		Ref.	Remark
				Age [d]	fc [MPa]	Age [d]	E [GPa]		
Leibis Lichte	CVC Gravity	Germany, 2004	Greywacke, NMSA 125mm, C 120kg/m <sup>3</sup> , FA 40kg/m <sup>3</sup> , Water 103kg/m <sup>3</sup>	3	10.9	4		[3.22]	Quality control programme; cube compr. strength, split tensile strength, density on 300x300x300mm cubes, flexural strength, modulus on 200x200x800 mm beams
				7	16.3	7	17.0		
				28	26.7	28	27.6		
				90	30.6	90	30.2		
				180	32.8				
				360	35.2				
Leibis Lichte	CVC Gravity	Germany, 2004	Greywacke, NMSA 125mm, C 150kg/m <sup>3</sup> , FA 50kg/m <sup>3</sup> , Water 110kg/m <sup>3</sup>	3	10.7	4	20.7	[3.22]	Quality control programme; cube compr. strength, split tensile strength, density on 300x300x300mm cubes, flexural strength, modulus on 200x200x800 mm beams
				7	15.4	7	21.9		
				28	24.5	28	27.3		
				90	29.1	90	30.2		
				180	31.8				
				360	34.0				
Albigna	CVC Gravity	Switzerland, 1959	Granite, NMSA 150mm, C 140kg/m <sup>3</sup> , Water ca. 115kg/m <sup>3</sup>	90	25.3	365	24.0-28.0	[3.23]	Cube compr. strength C20 on 200x200x200mm cubes
Emosson	CVC Arch	Switzerland, 1974	Granite, NMSA 120mm, C 160kg/m <sup>3</sup> , Water ca. 130kg/m <sup>3</sup>	90	27.5	365	30.2-37.7	[3.23]	Cube compr. strength C30 on 300x300x300mm cubes
Grand Dixence	CVC Gravity	Switzerland, 1961	Gneiss, NMSA 100mm, C 140kg/m <sup>3</sup> , Water ca. 130kg/m <sup>3</sup>	90	16.3 / 18.7	365	32.5	[3.23]	Cylinder compr. strength CYL(30x45) on d=300xh=450mm cylinder
Zeuzier	CVC Arch	Switzerland, 1956	Limestone, NMSA 100mm, C 140kg/m <sup>3</sup> , Water ca. 120kg/m <sup>3</sup>	90	32.3 3)	365	44	[3.23]	Cube compr. strength C20 on 200x200x200mm cubes
Zervreila	CVC Arch	Switzerland, 1957	Gneiss, NMSA 100mm, C 140kg/m <sup>3</sup> , Water ca. 135kg/m <sup>3</sup>	90	23.6	365	13.8-15.9	[3.23]	Cube compr. strength C20 on 200x200x200mm cubes
Mauvoisin	CVC Arch-Gravity	Switzerland, 1957	Gneiss, NMSA 120mm, C 140kg/m <sup>3</sup> , Water ca. 105kg/m <sup>3</sup>	90	30.0 / 32.5	365	38.5	[3.23]	Cube compr. strength C30 on 300x300x300mm cubes
Mauvoisin	CVC Arch-Gravity (Height ening)	Switzerland, 1991	Gneiss, NMSA 63mm, C 140kg/m <sup>3</sup>	90	29.7			[3.23]	Cylinder compr. strength CYL(16x32) on d=160xh=320mm cylinder
Moiry	CVC Arch	Switzerland, 1958	Gneiss, NMSA 150mm, C 140kg/m <sup>3</sup> , Water ca. 110kg/m <sup>3</sup>	90	25.9			[3.23]	Cylinder compr. strength CYL(30x45) on d=300xh=450mm cylinder

### 3.3 DYNAMIC MODULUS OF ELASTICITY

An important characteristic of concrete is its behaviour under short term loading such as experienced during earthquakes (e.g. strain rates of  $10^{-3}$  to  $10^{-2}$  /s). ASTM C469 [3.18] states that the modulus of elasticity values obtained under rapid load application (dynamic or seismic rates) are usually higher than moduli in the static conditions. The dynamic modulus can be considered as approximately equal to the initial tangent modulus while the static modulus is equal to the cord modulus (Fig. 3.3). In the dynamic condition, the strain behaviour of concrete is not influenced by the micro-cracking and creep, as it happens in the case of static modulus in presence of applied stresses [3.10].

#### 3.3.1 Modulus of Elasticity under Seismic Loading

Several investigations were carried out to study values and relations between static and seismic moduli. Some of them, specifically concerning dam concrete, are summarised in Tab. 3.5.

Tab. 3.5 - Results from investigations for seismic moduli of elasticity [3.24]

Dynamic/static Ratio			Reference
max.	av./single value	min.	
	1.25		Bureau's of Reclamation test series
1.57	1.42	1.28	Big Tujunga dam, cores drilled from the dam. 2 concrete types: 25 MPa (1. row) and 36 MPa strength (2. row)
1,48	1.38	1,32	
1.10	0.89	0.66	Bureau's of Reclamation test series
	1.18		Crystal Springs Dam
	1.15		Tests on Swiss dams
	1.04		extensive testing for Zervreila Dam (Switzerland)

For a better evaluation of the results of such investigations, the following considerations can be drawn:

- In general, the observed high scatter comes mainly from difficulties to test specimens under short rates of load application and from the influence of the individual granular texture and size distribution in the generally small test sections.
- The ICOLD Bulletin 52 [3.25] mentions on p. 105 that "... indiscriminate application of increased [tensile] strength criteria in analysis should be treated with caution as incipient cracks in most dams exist due to static thermal loading...". Such a note of caution certainly can also be applied to the ratio between seismic and static moduli.



- Nagayama et al. report in [3.26] that the modulus of elasticity is not affected by loading rate.
- Harris et al. [3.27] comment about test series with cores from 10 US dams: “the average dynamic to static modulus of elasticity was 0.89 with a coefficient of variation of 17%”. “Consequently the average dynamic modulus did not tend to increase as the dynamic strength increased”.

Another characteristic for concrete exposed to reversed straining, as it is common during high intensity earthquake loading, is that irreversible plastic straining will occur together with reversible elastic deformations. This will result in hysteresis effects, which may broadly be characterised in Finite Element Analysis by a lowering of the equivalent elastic modulus (together with an increase of damping).

All this demonstrates that the ratio between seismic and static modulus of elasticity is burdened with a high scatter. This means that the reliability of assessing values for the modulus of elasticity under seismic loading is lower than that for static loading. A conservative approach would therefore tend to use lower bounds when applying corresponding reference data or test results.

### **3.3.2 Dynamic Ultrasonic Modulus of Elasticity**

The dynamic ultrasonic modulus of elasticity of concrete, as determined according to the national standards, for example ASTM C 597 [3.28], is greater than the static modulus, typically around a value of 25 per cent. Other authors report figures as high as 40% [3.8].

The determination of the dynamic modulus of elasticity  $E_d$  is based on the studies on the sound wave propagation and is related to the propagation velocity of longitudinal stress wave pulses through concrete.

$E_d$  can be expressed as follows:

$$E_d = \rho * V^2 \frac{(1 + \nu) * (1 - 2\nu)}{(1 - \nu)}$$

where:

$\rho$  = concrete density

$V$  = pulse velocity

$\nu$  = Poisson coefficient

Two ultra-sonic test methods are currently used to determine the concrete modulus in the high frequency range i.e., ultrasonic pulse velocity method and the cross hole sonic logging method. In the ultrasonic pulse velocity method an ultrasonic pulse is emitted by a transducer coupled to the structure surface. A receiving device detects the ultrasonic pulse and the transit time is determined. The path length is known and the ultrasonic pulse velocity is computed. The velocity is used to compute the dynamic modulus for high frequency excitation. The range is dependent on the transmitter energy with a range of 3 m for low powered systems and 10 m for high powered systems. The cross

hole sonic method is a down-hole version of the previous method. This method is useful if a particular zone in the structure is to be investigated.

As already stated in Section 2 (Strength Properties), non-destructive sonic methods can also be used also for compressive strength evaluation and diagnostic investigations on concrete in existing dams.

Another possible test method for determining the dynamic modulus of elasticity is that based on measurements of the fundamental transverse, longitudinal, and torsional frequencies of concrete cylinders and prisms. In fact the resonant frequency of a structure is directly related to its dynamic modulus and hence its mechanical integrity. National Standards cover this testing method as, for example the ASTM C215 [3.29].

### 3.4 POISSON'S RATIO

Poisson's ratio is the ratio between lateral strain accompanying an applied axial strain (Fig. 3.8). Also, Poisson's ratio must be determined from strains which are within the elastic range of the stress-strain curve.

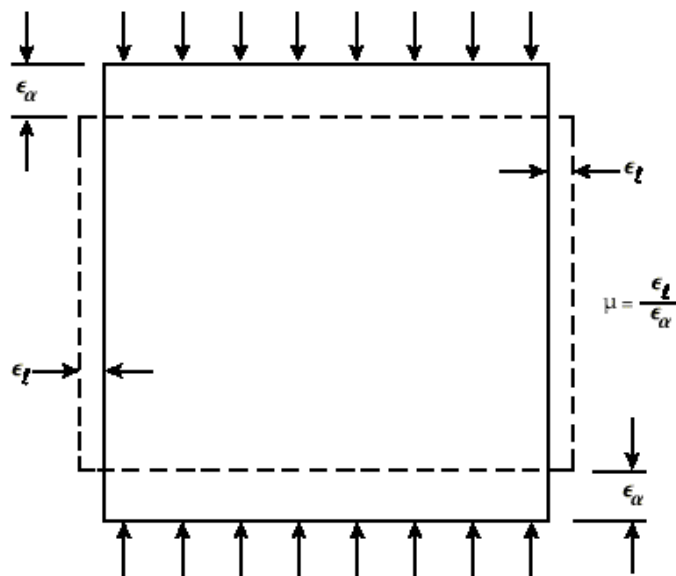


Fig. 3.8 - The Poisson coefficient as ratio between lateral and axial strain [3.1]

Under high loads, Poisson's ratio increases rapidly due to the level of cracking within the section. However this response is non linear and indicative of near-failure conditions. Under static conditions, for static stresses below 40 percent of the compressive strength, the Poisson's ratio varies in the range of 0.11 to 0.21 (and generally from 0.15 to 0.20) based on strain measurements for normal concrete [3.11].

In the German Specification DIN 4227 [3.30], Poisson's ratio is related to the elastic modulus E as follows (Tab. 3.6):

Tab. 3.6 - Typical estimates of compressive strength versus Poisson's ratio

E (MPa)	24,000	30,000	35,000
$\nu$	0.15-0.18	0.17-0.20	0.20-0.25

The elastic modulus of concrete in mass concrete is typically in the range of 24 to 30 GPa, therefore this also indicates that Poisson's ratio will vary from 0.15 to 0.20.

Poisson's ratio is higher for dynamically loaded concrete. A dynamic determination of Poisson's ratio yields an average value of 0.24 which is significantly different than the static value.

However the tests carried out by Harris [3.27] from 16 dam core samples showed an average ratio dynamic/static Poisson of 1.07 with coefficient of variation of 31%. Again this demonstrates the high scatter inherent in dynamic test methods. It is therefore not recommended increasing the Poisson ratio for dynamic loading from 0.15/0.20 to 0.24.

Tab. 3.7 shows modulus of elasticity values for concretes from US and Brazilian dams, together with their Poisson ratio. Information on concrete mix design and time of testing are also provided.

*ICOLD Bulletin: The Physical Properties of Hardened Conventional Concrete in Dams*  
 Section 3 (Elastic properties)

Tab. 3.7 - Elastic Modulus vs Poisson's ratio from US and Brazilian dams (part I)

Project	Dam Type	Country	Mix Design	Static Elastic Modulus		Poisson Ratio		Ref.
				Age [d]	E [GPa]	Age [d]	Ratio [-]	
Hoover			Limestone & Granite, NMSA 225mm, C 225kg/m <sup>3</sup> , Water 130kg/m <sup>3</sup>	28	38.0	28	0.18	[3.31]
				90	43.0	90	0.20	
				365	47.0	365	0.21	
Grand Coulee	CVC Gravity	USA, 1942	Basalt, NMSA 150mm, C 224kg/m <sup>3</sup> , Water 134kg/m <sup>3</sup>	28	32.0	28	0.17	[3.31]
				90	42.0	90	0.20	
				365	41.0	365	0.23	
Glen Canyon	CVC Arch Gravity	USA, 1963	Limestone, Chert, Sandstone, NMSA 150mm, C 111kg/m <sup>3</sup> , P 53kg/m <sup>3</sup> , Water 83kg/m <sup>3</sup>	28	37.0	28	0.15	[3.31]
				90	43.0	90	0.15	
				180	46.0	180	0.19	
Flaming Gorge	CVC Arch Gravity	USA, 1962	Limestone, Sandstone, NMSA 150mm, C 111kg/m <sup>3</sup> , P 56kg/m <sup>3</sup> , Water 88kg/m <sup>3</sup>	28	24.0	28	0.13	[3.31]
				90	30.0	90	0.25	
				180	32.0	180	0.20	
Yellowtail	CVC Arch Gravity	USA, 1965	Limestone, Andesite, NMSA 150mm, C 117kg/m <sup>3</sup> , P 50kg/m <sup>3</sup> , Water 82kg/m <sup>3</sup>	90	42.0	90	0.24	[3.31]
				180	37.0	180	0.26	
				365	43.0	365	0.27	
Morrow Point	CVC Arch	USA, 1967	Andesite, Tuff, Basalt, NMSA 114mm, C 221kg/m <sup>3</sup> , Water 93kg/m <sup>3</sup>	28	30.0	28	0.22	[3.31]
				90	34.0	90	0.22	
				180	37.0	180	0.23	
				365	32.0	365	0.20	

ICOLD Bulletin: The Physical Properties of Hardened Conventional Concrete in Dams  
Section 3 (Elastic properties)

Tab. 3.8 - Elastic Modulus vs Poisson's ratio from US and Brazilian dams (part II)

Project	Dam Type	Country	Mix Design	Static Elastic Modulus		Poisson Ratio		Ref.
				Age [d]	E [GPa]	Age [d]	Ratio [-]	
Lower Granite	CVC Gravity	USA, 1973	Basaltic Gravel, NMSA 150mm, C 86kg/m <sup>3</sup> , P 29kg/m <sup>3</sup> , Water 82kg/m <sup>3</sup>	28	19.0	28	0.19	[3.31]
				90	27.0	90	0.20	
Libby	CVC Gravity	USA, 1972	Quartzite Gravel, NMSA 150mm, C 88kg/m <sup>3</sup> , P 29kg/m <sup>3</sup> , Water 79kg/m <sup>3</sup>	28	22.0	28	0.14	[3.31]
				90	28.0	90	0.18	
Dworshak	CVC Gravity	USA, 1972	Granite Gneiss, NMSA 150mm, C 125kg/m <sup>3</sup> , P 42kg/m <sup>3</sup> , Water 97kg/m <sup>3</sup>	90	26.0	90		[3.31]
				365	26.0	365		
Ilha Solteira	CVC Gravity	Brazil, 1974	Quartzite Gravel, Basalt, NMSA 150mm, C 82kg/m <sup>3</sup> , P 27kg/m <sup>3</sup> , Water 82kg/m <sup>3</sup>	28	35.0	28	0.15	[3.31]
				90	41.0	90	0.16	
Itaipu	Hollow Gravity Buttress	Brazil / Paraguay, 1982	Basalt, NMSA 150mm, C 108kg/m <sup>3</sup> , P 13kg/m <sup>3</sup> , Water 85kg/m <sup>3</sup>	28	38.0	28	0.18	[3.31]
				90	43.0	90	0.21	
				180	43.0	180	0.22	
				365	45.0	365	0.20	
Theodore Roosevelt Modification	CVC Arch Gravity	USA, 1995	Granite, NMSA 100mm, C 128kg/m <sup>3</sup> , P 32kg/m <sup>3</sup> , Water 85kg/m <sup>3</sup>	28	31.0	28	0.20	[3.31]
				90	37.0	90	0.21	
				365	43.0	365	0.21	

### **3.5 SIGNIFICANCE OF ELASTIC PROPERTIES ON DAM BEHAVIOUR**

The modulus of elasticity is an important concrete parameter, vital for structural analysis and for evaluating the strain distributions and deformations in concrete dams, especially when their design is based on elasticity considerations [3.17].

The concrete deformation that occurs immediately after the load applications depends on the “instantaneous” elastic modulus. The subsequent development of the deformation, over a period of time with constant load, is the result of creep. Sometimes this last one is generally accounted for by determining a “sustained” modulus of elasticity to be used in static analyses [3.32].

From the experimental point of view, the sustained modulus of elasticity should be evaluated from the concrete specimens with the same testing procedure prescribed for the instantaneous elastic modulus [3.18], except for the testing time that can attain two years or more, under constant sustained loads. These sustained moduli are further discussed in Section 4 (paragraph 4.5 modelling creep in structural analysis).

As already discussed in paragraph 3.2.3.5, the elasticity modulus has an appreciable increasing trend with time, particularly in pozzolanic cement concrete, and could be even faster than for compressive strength (Section 2). From a series of laboratory modulus data at different ages (up to 365 days) from more than 50 Brazilian dam concretes [3.34], it was found that, in the presence of mineral admixtures, the average ratio between the elasticity modulus at 365 days and at 90 days is about 1.2. Single values can even attain ratios in excess of 1.5. This fact could also have a detrimental effect in highly hyper-static structures such as dams and especially arch dams that have a complex relation with their foundation.

For these structures, in fact, problems could arise in transferring direct loads to the foundation rock or in reacting to imposed deformations like thermal loads. Different stress levels and distributions, compared to those predicted in the design phase, can appear and cracks could develop. Thus, in order to avoid extreme situations that are not expected, it is recommended to consider the possible increase of the concrete elastic modulus already in the design stage. This problem should be taken into account also in the monitoring and interpretation of the dam behaviour [3.33].

### 3.6 USE OF ELASTIC PROPERTIES IN MATHEMATICAL MODELS FOR DAM STRUCTURAL ANALYSIS

The degree of refinement of the mathematical model used for static and earthquake loading influences the choice of the modulus of elasticity. Most important is the effect of rate of loading as it both influences strength and elasticity.

Fig. 3.9 illustrates that different loading rates and situations result in different “apparent elasticities”. The shown relations refer to mathematical modelling as follows:

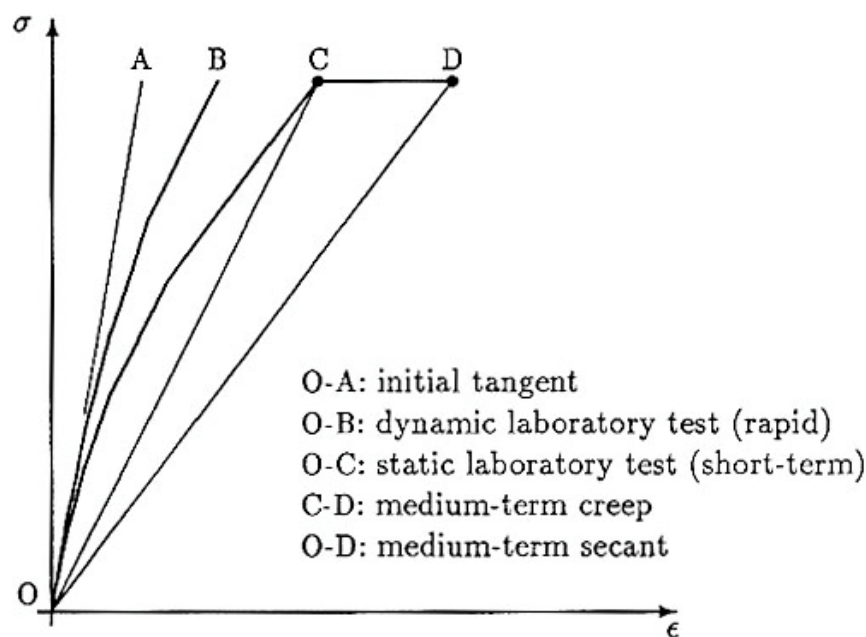


Fig. 3.9 - Definitions of apparent moduli of elasticity used in mathematical models

- Static correlations: medium-term creep strain is often included in the secant modulus (O-D), but for some models creep can be explicitly calculated with respect to the initial tangent elasticity [3.35].
- differences exist between static (O-C) and dynamic (O-B) laboratory tests due to strain rate dependency. These differences can be modelled by a visco-plastic model [3.36].
- Tangent moduli (O-A) are required for modelling when non-linearity is taken as a rate-dependent (e.g. visco-plastic) phenomenon.

In this respect the following references to other Sections of the Bulletin are in order:

- reference to Section 2 - 2.4.8 Use of tensile strength in mathematical models - linear elastic analysis and non linear analysis
- reference to Section 4 - C.4.5 Modelling creep in structural analysis (concept of sustained modulus of elasticity)

*ICOLD Bulletin: The Physical Properties of Hardened Conventional Concrete in Dams*  
Section 3 (Elastic properties)

Even if linear elastic analysis is the standard method for dam structural analysis, in several conditions such as seismic loading, deterioration, loading beyond capacity, the structural dam behaviour is better modelled with non-linear analysis. This is particularly important if damage prone conditions are to be expected for existing dams. Reference [3.38] uses the principles of damage mechanics to analyse non-linear static or dynamic behaviour.

However, data obtained from standard elastic material tests are still important because they can be used, as suggested by the Bureau of Reclamation [3.37], to provide a comprehensive stress-strain diagram, able to represent different failure states of the concrete.

As an example, in Fig. 3.10 typical experimental compressive-stress-strain curves for a Bureau of Reclamation dam are reported, together with a comprehensive “failure state diagram”, derived from the best fitting of experimental behaviours of sample population. It allows a rational evaluation on the need for either linear or non-linear modelling.

The working stress zone, with an elastic pattern, is that below the stress corresponding to 40% of the average ultimate strength, as defined by the ASTM C469 [3.18]. The zone above this level represents a transition zone to non-linear behaviour, characterised by accumulated non recoverable strains. Both linear and non-linear laboratory tests are recommended in this zone. Some supplemental tests to represent the non-linear behaviour is suggested by [3.37], based on loading and unloading cycles (Fig. 3.11).

Post failure tests and fracture energy special testing are required for the cracked zone.



ICOLD Bulletin: The Physical Properties of Hardened Conventional Concrete in Dams  
 Section 3 (Elastic properties)

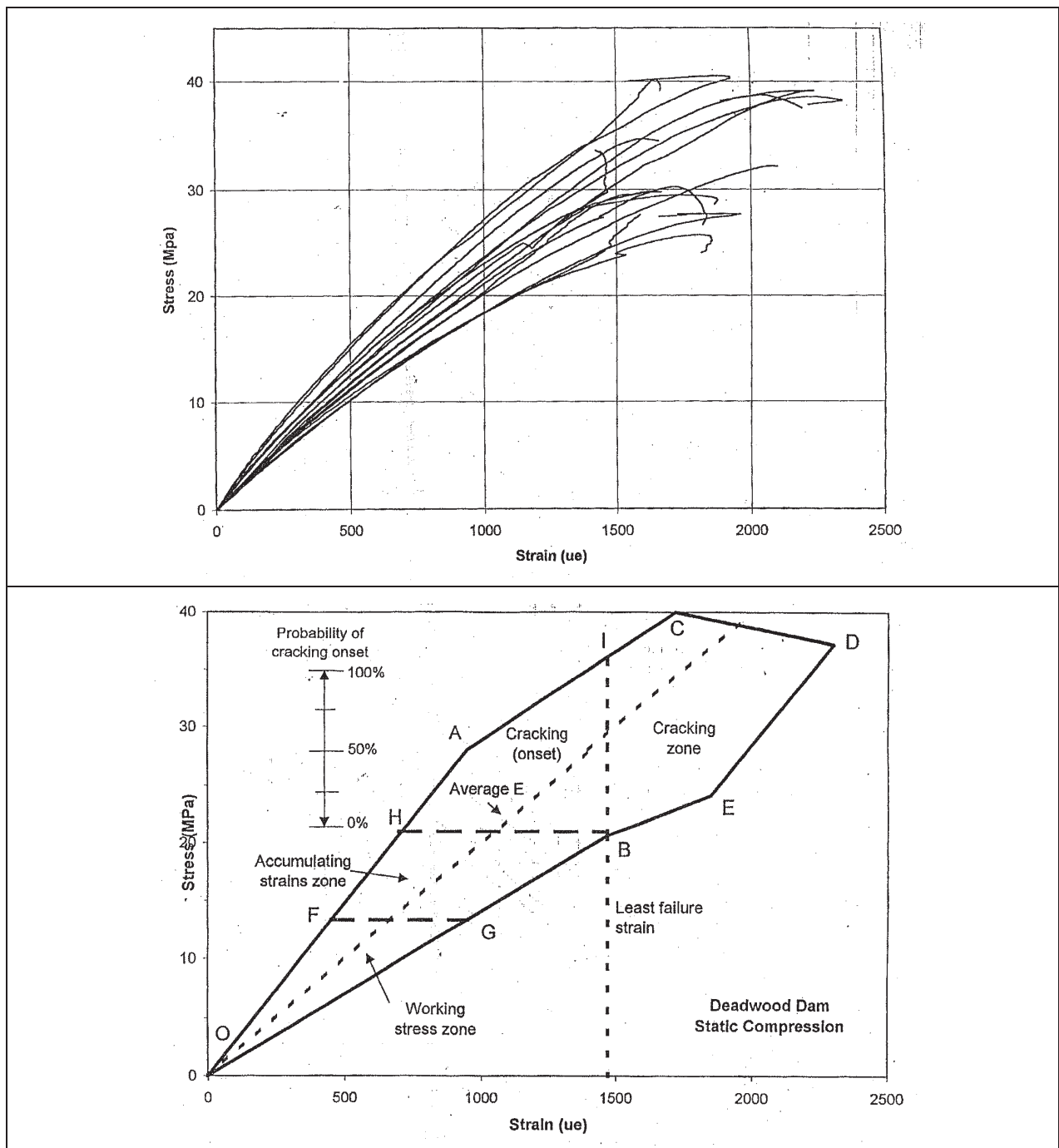


Fig. 3.10 - Compressive-stress-strain curves for the Deadwood dam (Bureau of Reclamation dam) and the obtained "failure state diagram" [3.37]

*ICOLD Bulletin: The Physical Properties of Hardened Conventional Concrete in Dams*  
Section 3 (Elastic properties)

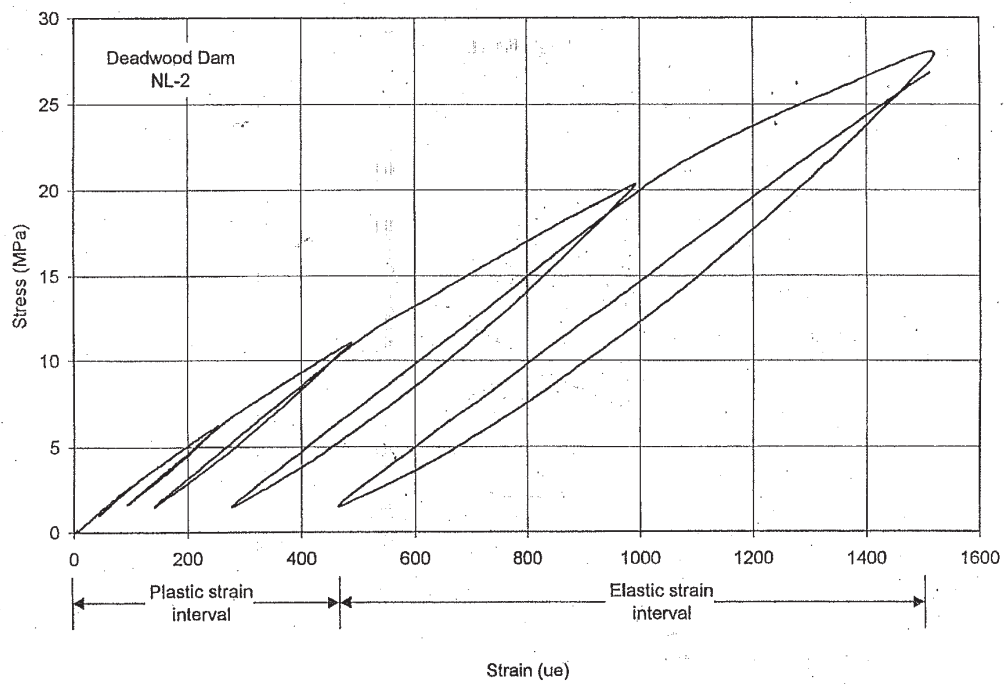


Fig. 3.11 – Loading and unloading cycles testing of concrete cores to evaluate non linear pre-failure parameters [3.37].

### 3.7 REFERENCES

- [3.1] Cement Association of Canada - <http://www.cement.ca/cement.nsf/>
- [3.2] Timoshenko, S.P. and Goodier, J.N., "Theory of Elasticity", McGraw-Hill Book Company, New York, 1934.
- [3.3] Neville, A.M, Dilger, W.H. and Brooks, J.J., "Creep of Plain and Structural concrete", Construction Press, Longmann Group Limited, 1983.
- [3.4] Bangash, M.Y., "Concrete and Concrete Structures: Numerical Modelling and Applications", Elsevier Applied Science, London, 1989.
- [3.5] Chen, W.F. "Plasticity in Concrete", McGraw-Hill Book Company, New York, 1982.
- [3.6] Fauchet, B., Coussy, O., Carrere, A. and Tardieu, B., "Poroplastic Analysis of Concrete Dams and their Foundations", Dam Engineering, Volume II, Issue 3, 1991.
- [3.7] Franklin Dusseault "Rock Engineering" (1991), p. 321.
- [3.8] Metha, K.P., "Concrete: Structure, Properties and Materials", Prentice-Hall, Inc, Englewood Cliffs, New Jersey, 1986.
- [3.9] Mindess, S.; Young, J.F.; Darwin, D.: Concrete. Second edition, ISBN 0-13-064632-6, Prentice Hall, Upper Saddle River, 2003.
- [3.10] The University of Memphis, Department of Civil Engineering, [http://www.ce.memphis.edu/1101/notes/concrete/everything\\_about\\_concrete/11\\_-\\_compositee.html](http://www.ce.memphis.edu/1101/notes/concrete/everything_about_concrete/11_-_compositee.html).
- [3.11] Neville, A., M., "Properties of Concrete", Sir Isaac Pitmann & Sons LTD, London, 1963.
- [3.12] Gorisse, F., "Ensayos y control de hormigones", Ed. ETA
- [3.13] Geen, S.J. and Swanson, S.R., "Static Constitutive Model for Concrete in compression", Technical Report AFWC-TR-72, 1973.
- [3.14] American Concrete Institute, "Mass Concrete", ACI Publication, 207.1R-96.
- [3.15] Raphael J. "The Nature of Mass Concrete in Dams", ACI SP 55-6.
- [3.16] Tuthill, L.H., Sarkaria, G.S., Cortright, C.J., Proceedings of 10<sup>th</sup> ICOLD International Congress, Montréal, 1970, Vol. IV, pp. 181-197.
- [3.17] Vilardell, J., Aguado, A., Agullo, L., Gettu, R., "Estimation of the modulus of elasticity for dam concrete", Cement and Concrete Research, 1998, Vol. 28, n° 1, pp. 93-101.
- [3.18] ASTM C469-02e1, "Standard Test Method for Static Modulus of Elasticity and Poisson's Ratio of Concrete in Compression", 2002.
- [3.19] ACI 318-95 Building code requirements for structural concrete. ACI Manual of Concrete Practice Part 3: Use of concrete in Buildings – Design, Specifications, and Related Topics. Detroit, Michigan; 1996.
- [3.20] British Code of Practice, CP 110, Part 1
- [3.21] Eurocode 2, "Design of concrete structures", 1993.

*ICOLD Bulletin: The Physical Properties of Hardened Conventional Concrete in Dams*  
Section 3 (Elastic properties)

- [3.22] Wagner, J.-P.; Massenbetone für die Gewichtsstaumauer Talsperre Leibis/Lichte; Beton-Informationen 2/3 2004; Deutscher Beton-Verein; 2004.
- [3.23] Kreuzer, H.; Email Communication with M. Conrad, 23.12.2007; Concrete Data Basis for Bulletin "Concrete of Swiss Dams"; Swiss Committee on Dams, 2001, partially published.
- [3.24] US Bureau of Reclamation: "Concrete Manual" ,8th ed., J. Wiley, New York, 1981.
- [3.25] ICOLD Bulletin n°52, Earthquake analysis for dams, 1986.
- [3.26] "Experimental study on tensile strength of concrete for dams", Proc. of 2<sup>nd</sup> US-Japanese Workshop on Advanced Research on Earthquake Engineering for Dams, Technical Memorandum of PWRI, 1999.
- [3.27] Harris, D. W., Mohorovic, C. E., Dolen, T.P., "Dynamic Properties of Mass Concrete Obtained from Dam Cores", ACI Materials Journal, Vol. 97, N°3, May-June 2000.
- [3.28] ASTM C597-02, " Standard Test Method for Pulse Velocity Through Concrete".
- [3.29] ASTM C215-02 "Standard Test Method for Fundamental Transverse, Longitudinal, and Torsional Frequencies of Concrete Specimens".
- [3.30] German Specification DIN 4227, " Prestressed concrete; prestressed lightweight concrete structural members".
- [3.31] ACI 207.1R-05 Mass Concrete; American Concrete Institute ACI, 2005".
- [3.32] Bureau of Reclamation "Design criteria for concrete arch and gravity dams", a water resource technical publication, Engineering Monograph n° 19.
- [3.33] Buil Sanz, J. M, personal communication, 2002.
- [3.34] Filho J. M., J. M, personal communication, 2007.
- [3.35] Dungar, R., "The effect of cyclic creep on the ageing of arch dams", Proc. ICOLD, 17. Congress, Vienna, 1991, Q.65, R.9.
- [3.36] Dungar, R., Studer, J.A., "Numerical Models in Geomechanical Engineering Practice", A..A Balkema, Rotterdam, 1985.
- [3.37] Harris, D.W., Dolen T. P., Mohoroovic C.E., "Failure states from concrete stress-strain data for use in analysis"; 1998.
- [3.38] Gunn R.M., "Non-linear design and safety analysis of arch dams using damage mechanics", Hydropower & Dams, Issue 2, 2001.

## 4 CREEP PROPERTIES

<b>4 CREEP PROPERTIES.....</b>	<b>1</b>
<b>4.1 GENERAL .....</b>	<b>2</b>
<b>4.2 FACTORS INFLUENCING CREEP .....</b>	<b>3</b>
4.2.1 Aggregate .....	3
4.2.2 Cement .....	4
4.2.3 Strength and mixture proportions .....	4
4.2.4 Age at loading.....	5
4.2.5 Level of stress .....	5
4.2.6 Ambient humidity .....	5
4.2.7 Temperature .....	6
4.2.8 Specimen size .....	6
4.2.9 Creep under different states of stress.....	6
<b>4.3 MEASUREMENT OF CREEP.....</b>	<b>6</b>
<b>4.4 SIGNIFICANCE OF CREEP PROPERTIES ON DAM BEHAVIOUR .....</b>	<b>9</b>
<b>4.5 MODELLING CREEP IN STRUCTURAL ANALYSIS .....</b>	<b>11</b>
<b>4.6 REFERENCES .....</b>	<b>14</b>

#### 4.1 GENERAL

Creep is time-dependent deformation due to sustained load [4.1]. The nature of the concrete behaviour can be shown schematically in Fig. 4.1.

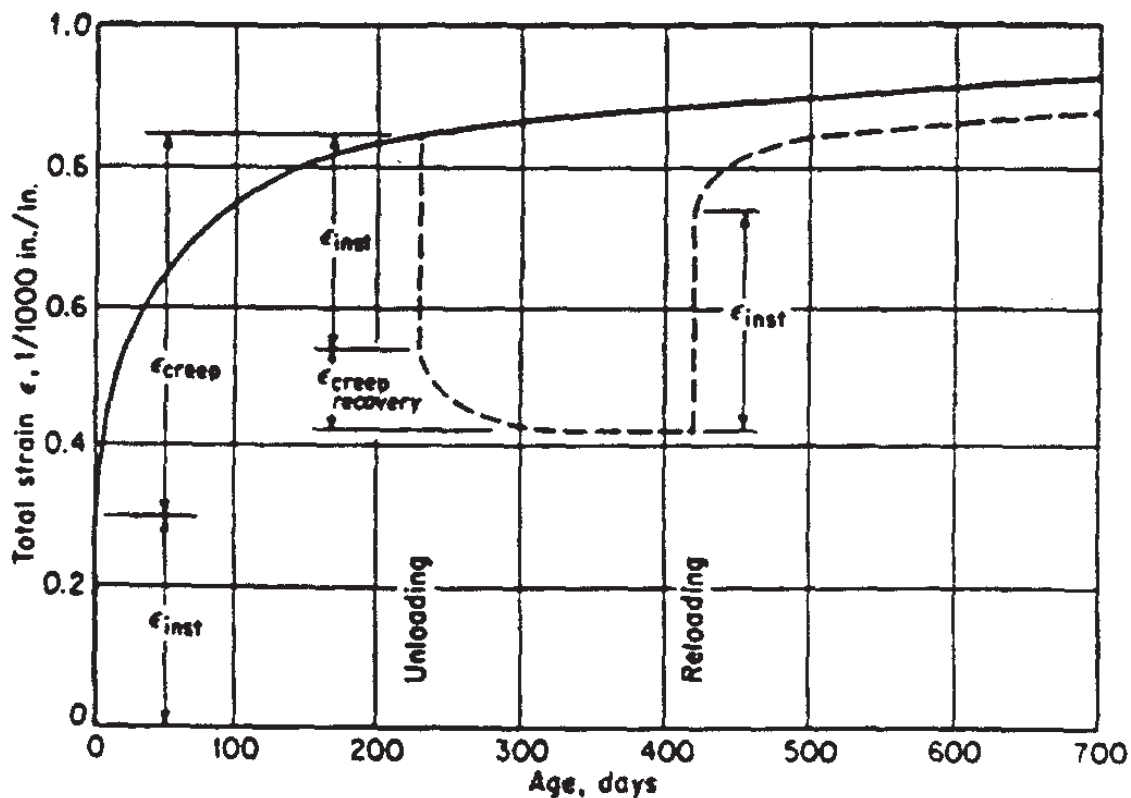


Fig. 4.1 - Typical concrete creep curve [4.2]

This particular concrete was loaded at age 28 days with resulting instantaneous strain  $\epsilon_{inst}$ . The load was then maintained for 230 days, during which time creep is seen to have increased the deformation to  $\epsilon_{creep}$  which is almost 3 times its instantaneous value. If the load were maintained, the deformation would follow the solid curve. If the load is removed, as show by the dashed curve, the elastic instantaneous strain  $\epsilon_{inst}$  is recovered, and some creep recovery is seen to occur. If the concrete is reloaded at some later date, the instantaneous and creep deformations develop again as show [4.2].

Although several hypotheses of creep, based on certain observed mechanisms of deformation, have been proposed, it is generally accepted that concrete creep is a paste property, i.e. a rheological phenomenon associated with the gel-like structure of cement paste [4.3] [4.4]. The movement of water into and out of the gel in response to changes in ambient humidity produces the well-know shrinking and swelling behaviour of concrete. In creep, gel water movement is caused by changes in applied pressure instead of differential hygrometric conditions between the concrete and its environment.

This concept is supported by the similar manner in which creep and shrinkage are affected by such factors as water-cement ratio, mixture proportions, properties of aggregate, compaction, curing conditions, and degree of hydration [4.5]. Creep deformation can also be explained partly in terms of visco-elastic deformation of cement paste and to the gradual transfer of load from the cement paste to the aggregate. This concept offers explanations for the linearity of creep strain over a wide range of stress, the reduction in strain rate with time, and the sensitivity of creep to temperature [4.6].

Creep has been classified as “basic creep” and “drying creep” [4.3]. In basic creep no exchange of water from the concrete specimen to the environment is possible and only permanent and irreversible strain occur. It is not influenced by humidity, size and ambient temperature conditions. Drying is the other creep that develops in concrete. It is partly reversible and partly irreversible

## 4.2 FACTORS INFLUENCING CREEP

Creep is influenced by properties of aggregate and cement, and by strength, mixture proportions, age of loading, level of stress, and conditions of storage of the concrete. Most of the creep studies that have been conducted have been for the purpose of determining the effect for one or more of these variables on creep. This section briefly summarises the current state of knowledge regarding the major factors that influence the creep of concrete.

### 4.2.1 Aggregate

Since the cement paste is subject to creep and the aggregate generally is not, the effect of aggregate is to reduce the effective creep of concrete. Creep of concrete,  $c$ , and the volumetric content of aggregate,  $g$ , are related by [4.7]:

$$\log \frac{c_p}{c} = \alpha \log \frac{1}{1-g} \quad (4.1)$$

where  $c_p$  is creep of neat cement paste of the same quality as used in concrete and  $\alpha$  is defined as follows:

$$\alpha = \frac{3(1-\mu)}{1+\mu+2(1-2\mu_a)\frac{E}{E_a}} \quad (4.2)$$

where

$\mu_a$  = Poisson's ratio of aggregate

$\mu$  = Poisson's ratio of the neat cement paste

$E_a$  = Modulus of elasticity of aggregate, and

$E$  = Modulus of elasticity of the neat cement paste

As evident from Eq. (4.2), the modulus of elasticity of aggregate affects the creep; the higher the modulus, the greater the restraint offered by the aggregate to the creep of concrete.

Tests indicated that the influence of the type of rock of which the aggregate is composed has an effect on creep primarily through the modulus of elasticity of the rock [4.8]. Typical rocks used as aggregates in the order of increasing creep are limestone, quartzite, granite, basalt, and sandstone. Concrete made with sandstone aggregate exhibited creep more than twice as much as concrete made with limestone aggregate.

Examples of creep data in dam concretes characterised by different types of aggregates are shown in 4.3 (Tab. 4.1).

#### **4.2.2 Cement**

Creep is generally not influenced by the type and composition of cement if the concrete, at the time of loading, is fully hydrated. Since the usual Portland cements differ from one another primarily in the rate of hydration (gain of strength), for a constant applied stress at the same early age, creep increases in order for ASTM Types III, I, and II, V and IV. I.e. type III has the highest, Type IV the lowest early strength.

The influence of the cement type on creep is less significant for dams than for common civil structures due to the late hydrostatic loading (early creep only due to self weight).

Fineness of cement affects the strength development at early ages and thus influences creep. The amount of gypsum in the cement may affect creep in a manner similar to its influence on shrinkage [4.7]. This means that finer cements need more gypsum, which influences creep. Creep as a function of gain of strength is also valid for all kinds of blended cements.

#### **4.2.3 Strength and mixture proportions**

Strength is a convenient, but approximate, measure of the water-cementitious material ratio and degree of hydration of the cement in concrete. For a constant cement paste content and the same applied stress, creep is inversely proportional to the strength of concrete. Therefore, it can also be stated that creep increases with an increase in water-cementitious material ratio of the concrete mixture.

The relationship between creep and cement paste content is of particular interest in the field of mass concrete for dams. Mass concrete for dams commonly contains large size (e.g., 150-mm) aggregate. Fabrication and testing of concrete specimens containing such large aggregate are expensive. For paste contents normally used in mass concrete, the creep of sealed specimens, having identical water-cementitious material ratio and air contents in the mortar phase but different amounts and size of a given coarse aggregate, is proportional to the amount of paste [4.9] [4.10]. This finding has made it possible to develop significant data for mass concrete from small specimens.



#### 4.2.4 Age at loading

Age of concrete at loading is a factor in creep in so far as age influences the degree of hydration and the development of strength. At later ages when the degree of hydration remains substantially constant, the rate of creep becomes independent of the age at loading.

#### 4.2.5 Level of stress

It is generally accepted that there is a nearly linear relation between creep and the applied stress up to stress-strength ratios of approximately 0.35 to 0.40. Above the limit of proportionality, creep increases with an increase in stress at an increasing rate, and there exists a stress-strength ratio above which creep resulting from sustained load causes failure [4.11]. This stress-strength ratio is in the range of 0.8 to 0.9.

#### 4.2.6 Ambient humidity

Creep increases with a decrease in the ambient relative humidity (RH) as shown in Fig. 4.2 [4.12]. Strictly speaking, the ambient RH only affects creep if drying takes place while the specimen is under load. If concrete has reached moisture equilibrium prior to loading, the magnitude of creep will be independent of the RH [4.6].

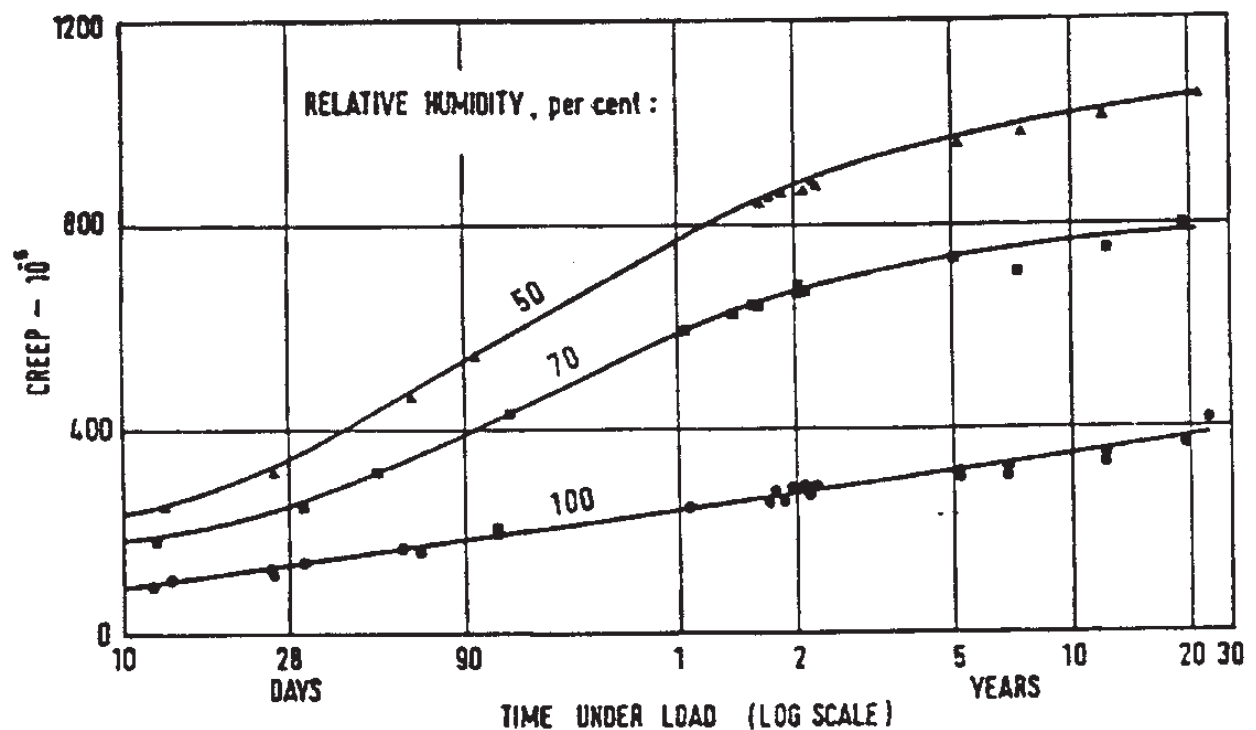


Fig. 4.2 - Creep of concrete at different relative humidities [4.12]

#### **4.2.7 Temperature**

The effect of concrete temperature on creep is of importance for mass concrete in dams where later temperatures can be significantly higher than the concrete placement temperatures due to heat of hydration. The rate of creep increases with increasing temperature. Test results indicate that the rate of creep increases approximately 3.5 times when temperature increases from 21°C to 70°C [4.13]. Laboratory investigations have shown that when the temperature alternates creep is higher than at either extreme of the alternating temperatures [4.14]. This is similar to the behaviour of concrete at alternating humidity.

#### **4.2.8 Specimen size**

It has been demonstrated [4.9] that creep of sealed specimens is independent of specimen size. For unsealed specimens exposed to drying environment, it is evident that there must be a size effect associated with the moisture gradients within the specimen. It was reported that shrinkage and creep were dependent only on the ratio of surface to volume but independent of the shape of the specimen [4.15].

#### **4.2.9 Creep under different states of stress**

Most creep testing has been concerned with specimens subjected to compression. Creep was less under multi-axial compression than under a uniaxial compression of the same magnitude in the given direction [4.16]. McDonald reported that the average values of compressive creep differed by a factor of 1.00:0.84:0.69:0.45 for uniaxial, biaxial, triaxial, and hydrostatic loading, respectively [4.17].

Creep in saturated concrete is larger than in dry concrete. This is advantageous against the development of tensile stresses at the upstream toe of dams.

For creep under tension there are only conflicting results reported [4.4].

### **4.3 MEASUREMENT OF CREEP**

The method normally used to measure creep is based on the application of a constant load to concrete cylinders or prisms placed in a loading frame. The constant load, which may be applied for several months or even years, can be maintained through loaded springs or hydraulic systems. Loads may be applied at different ages and can be decreased or removed when desired to investigate creep recovery. The strains can be measured periodically by means of internal strain gages or by demountable mechanical extension gages applied to the external faces of the prism. Since the amount of creep is influenced by humidity and temperature, creep tests should be carried out in conditions appropriate to those existing in the structure. It is clearly not possible to reproduce these conditions exactly, particularly in the case of the temperature, which will vary. As regards to the humidity conditions for mass concrete in dams, it is generally considered appropriate to carry out the test in a sealed specimen to prevent moisture loss from the concrete (basic creep). Both cylinder and prism creep specimen

subjected to constant loads have been enclosed in sheer copper casing with soldered joints, polyethylene plastic bags, or neoprene or butyl rubber encasements.

A device for in-situ measurement of creep and its back analysis by the LNEC (Portugal) is reported in [4.18].

The strain measurements obtained in creep tests must be processed to take account of the immediate elastic strain due to loading and, in the case of unsealed specimens, the shrinkage strain. Creep and shrinkage are difficult to separate in measurements of deformation during testing of unsealed specimens because they are inter-related. The usual approach is to determine the shrinkage by making a parallel set of concrete cylinders or prisms, which are kept in the same environment as the creep test specimens but which remain unloaded. In this way, strains resulting purely from shrinkage are measured directly.

It is common to plot creep test results on a semi-logarithmic graph in which the linear axis represents creep strain and the logarithmic axis represent time. Many sets of data show an approximately straight line over a considerable period of time. This has led to the development of numerous logarithmic equations for creep. An example of a typical creep equation is shown below:

$$\epsilon = \frac{1}{E} + F(K) \ln(t+1)$$

where:

$\epsilon$  = total strain per unit stress;

$E$  = instantaneous elastic modulus at the age when it is first loaded;

$F(k)$  = creep rate, calculated as the slope of a straight line representing the creep curve on the semi-log plot; and

$t$  = time after loading, in days (duration of loading).

While it is not intended that a theoretical logarithmic law should be inferred from the equation, the slope of the least squares line is a convenient parameter for comparing the creep characteristics of different concretes.

For a large concrete dam project, it is generally necessary to conduct creep tests on sealed specimens in the laboratory at enough ages of loading so that a complete knowledge of rheological behaviour is available. Such data can be represented pictorially by a creep surface such as that shown in Fig. 4.3 [4.5].

Seasonal reservoir storage schemes are typically subjected to cycling load variation depending on the year period. In addition the cycling nature of the hydrostatic load, temperature effects also have a cycling variation, at least at near the upstream and downstream dam faces. These accumulated effects are to be taken into consideration, when interpreting laboratory test results for creep in real dam behaviour [4.19].

Some creep data from Brazilian concrete dams are reported in reference [4.20] and briefly summarised in Tab. 4.1. Other valuable creep test results on dam concrete can be found in references [4.19] [4.21] and, for Swiss Dams, in Fig. 4.4 [4.22] [4.23] and in reference [4.24].

Tab. 4.1 Creep values for Brazilian mass concrete [4.20]

Age at time of loading (Days)	Schist		Quartzite		Basalt		Greywacke	
	1/E	F(k)	1/E	F(k)	1/E	F(k)	1/E	F(k)
	10 <sup>-6</sup> /MPa		10 <sup>-6</sup> /MPa		10 <sup>-6</sup> /MPa		10 <sup>-6</sup> /MPa	
2	23.3	18.8	12.7	9.6	6.1	6.7	6.0	9.0
7	22.3	10.5	9.5	8.4	6.0	5.5	3.5	8.3
28	13.2	8.13	6.8	6.3	3.5	4.1	3.1	7.2
90	9.2	5.9	5.7	4.5	-	-	-	-
365	6.9	3.4	-	-	-	-	3.1	4.8

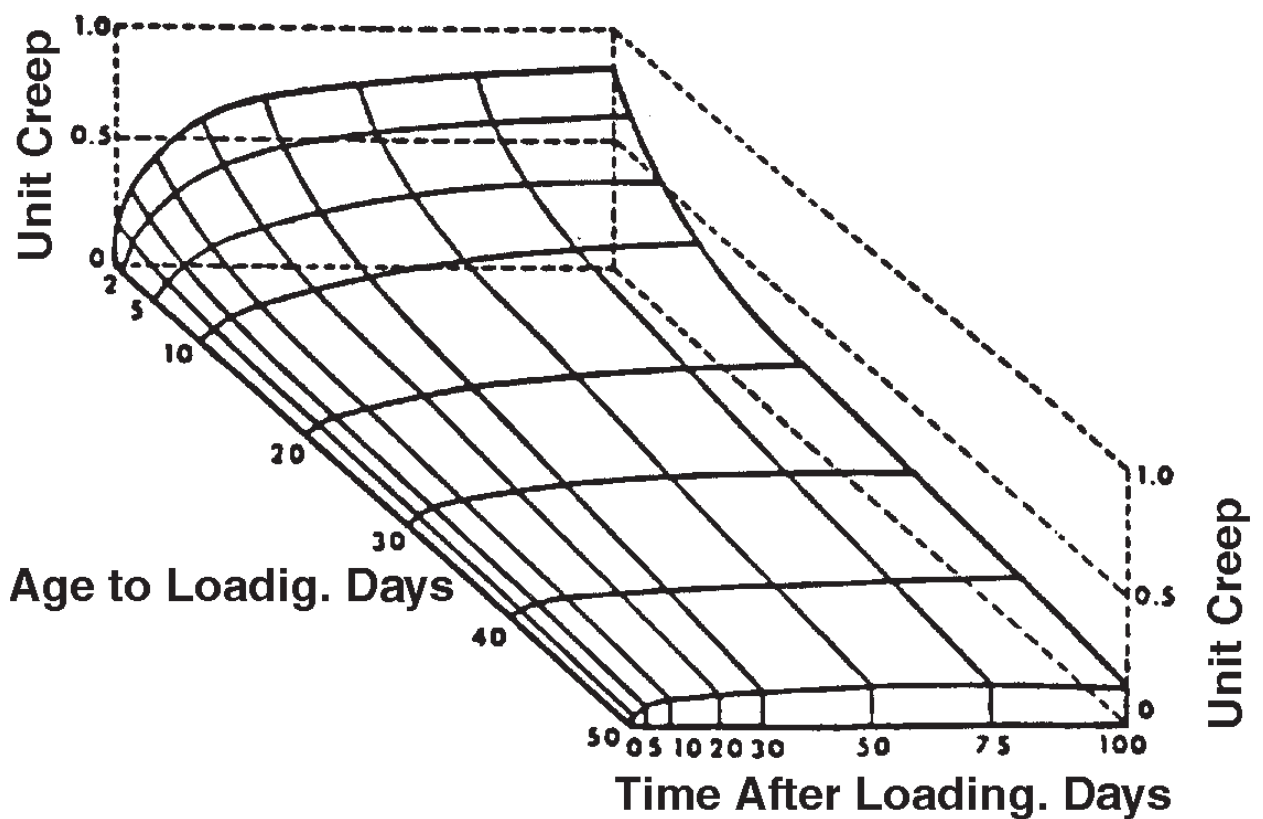


Fig. 4.3 - Typical Creep surface [4.5]

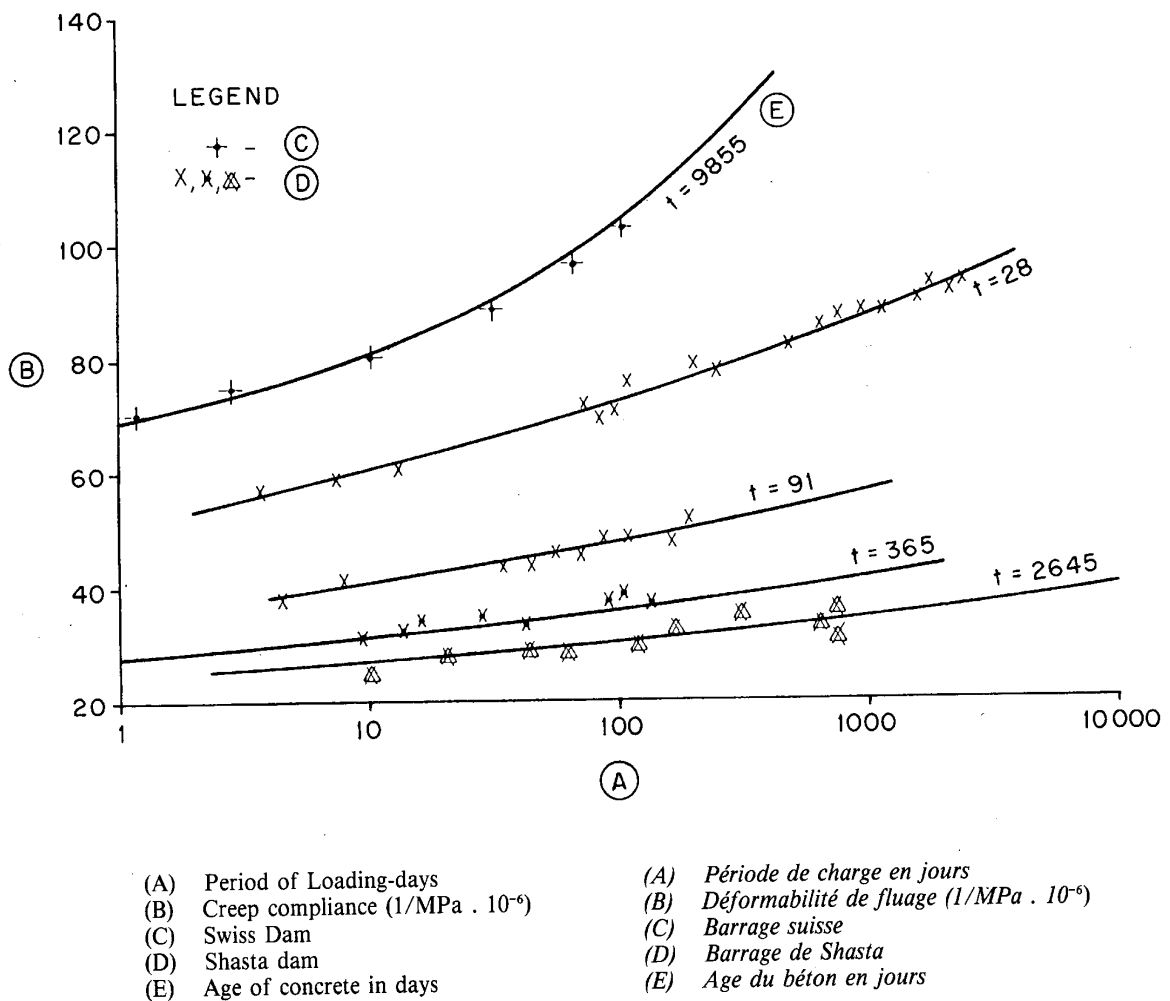


Fig. 4.4 – Comparison of results of creep tests on two different types of dam concrete (Swiss dam and Shasta dam) [4.22] [4.23]

#### 4.4 SIGNIFICANCE OF CREEP PROPERTIES ON DAM BEHAVIOUR

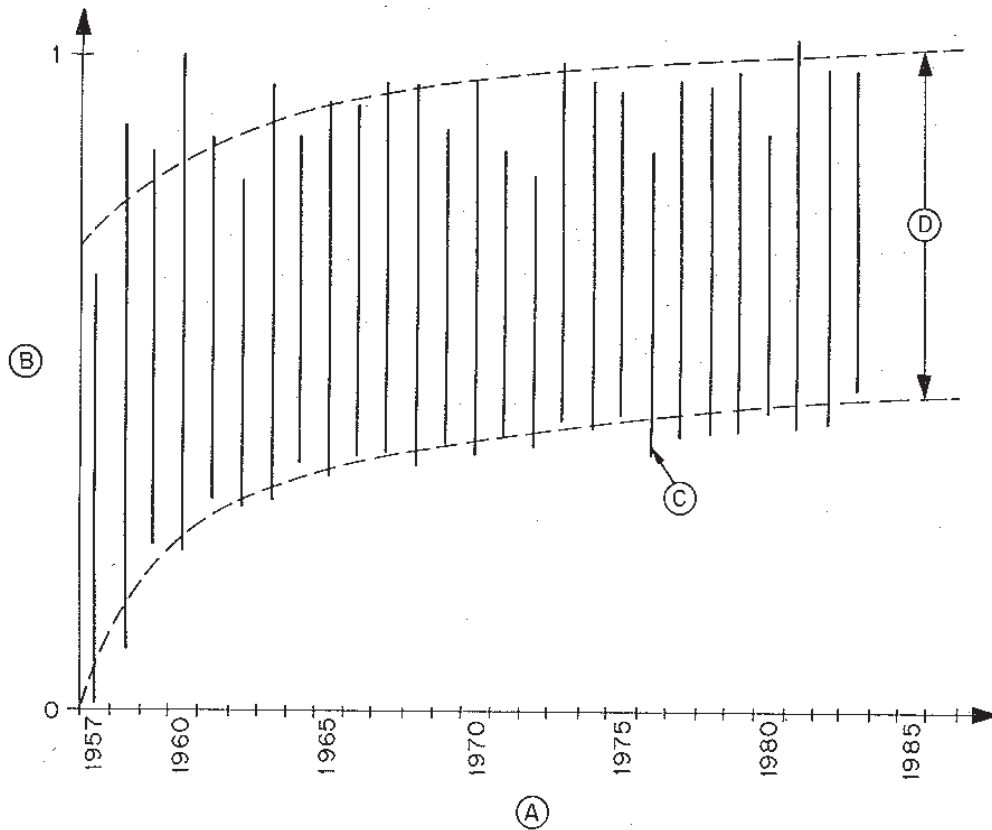
Due to the special conditions of concrete in dams, as for example the high temperature in the body mass and the high sustained load (self-weight) at early ages, the cycling hydrostatic loading, the low cement content, with higher strain at equal stress, etc., creep in dams is usually larger than in other civil structures and needs a careful estimation.

In particular, information on creep properties is of relevance to an understanding of the mechanism leading to the prediction of potential thermal cracking of mass concrete when undergoing thermal cycles due to the heat of hydration and ambient conditions. Therefore, the most extensive use of creep data has been in the thermal stress analysis for concrete dams.

The effect of creep strain of a dam concrete, particularly due to the cycling loading conditions, together with the changes in the mechanical material properties, plays also

an important role in the ageing of concrete dams [4.22]. In fact, the creep effect does not stabilise rather quickly for thick structures like dams and creep is very close to the so called “basic creep” for which no evidence of complete stabilisation is obtained after several decades of loading [4.25]. For example creep tests carried out on 27 year old concrete samples of the Zervreila arch dam, in Switzerland, have shown that creep deformation can form an important contribution to the total deformation process for many years [4.26].

This is clearly shown in Fig. 4.5 where the radial displacement at the top of the crown cantilever of the arch dam was chosen as a measure for the correlation of the irreversible creep strain with age. In this case the effect of creep deformation has been assessed taking into account the creep recovery, which occurs when the structures is unloaded (seasonal variation of the loads) [4.22].



- |   |  |
|---|--|
| (A) Year of measurement                 | (A) <i>Années de mesure</i>                        |
| (B) Normalised deformation              | (B) <i>Déformations relatives</i>                  |
| (C) Deformation range for one year      | (C) <i>Déformations annuelles</i>                  |
| (D) Envelope of recoverable deformation | (D) <i>Enveloppes des déformations réversibles</i> |

Fig. 4.5 – Normalised radial deformation of a Swiss arch dam, assumed as a measure of the irreversible creep strain over the years [4.22]

Information on creep properties is also of particular interest to evaluate the stress behaviour and the structural safety of a mass concrete dam when subjected to the expansion phenomena due to Alkali-Aggregate Reaction (AAR). Literature and field data seem to indicate that AAR expansion tends to increase the rate in concrete [4.27].

#### 4.5 MODELLING CREEP IN STRUCTURAL ANALYSIS

One method of expressing the effect of creep in structural finite elements analysis is the sustained modulus of elasticity in which the stress is divided by the total deformation (i.e., instantaneous deformation plus creep deformation) for the time under the load (see Fig. 4.1).

Typical instantaneous and sustained moduli of elasticity of mass concrete are given in Tab. 4.2. It can be seen that the values for sustained moduli of elasticity are approximately one-half those for the instantaneous moduli when loads are applied at early ages and slightly higher percentage of the instantaneous moduli when loading age is 90 days or greater. The sustained modulus of elasticity has been used, for example, in simplified linear thermal stress analyses to account for the creep effects. It allows a quick approximate determination of thermal stresses resulting from heat of hydration of cement and ambient conditions.

Tab. 4.2 - Typical instantaneous and sustained modulus of elasticity values (GPa) for mass concrete [4.28]

Age at time of loading (Days)	Basalt		Andesite & Slate		Sandstone		Sandstone & Quartzite	
	E	E'	E	E'	E	E'	E	E'
2	12	5.7	9.7	3.7	19	10	9.7	4.3
7	16	7.6	14	6.9	29	13	15	6.5
28	24	12	24	12	31	18	25	12
90	28	17	30	19	36	22	29	18
365	34	21	32	24	39	25	32	21

REMARKS (All concrete mass mixed, wet screened over 37.5 mm sieve):

E= instantaneous modulus of elasticity at time of loading, GPa

E'= sustained modulus of elasticity after 365 days under load, GPa

The experimentally generated creep surface (Fig. 4.3) can be also used to formulate the creep equation required in thermal and structural stresses in the mass concrete of dams.

Even more elaborated models have been proposed in the technical literature, able to predict, in a general and comprehensive way, the long term creep strain of concrete: in fact this last can play, together with the changes in the mechanical material properties, an important role in the ageing of concrete dams [4.22], particularly in presence of cycling loading conditions [4.29]. Among the models, those proposed by ACI (American Concrete Institute) Committee 209 [4.30], by CEB (Comité Euro-international du Béton) [4.31] and by other Authors [4.32] [4.33] [4.34] [4.35] can be reported.

For example the so called “double power” creep model of Bazant [4.33] describes a creep compliance function  $J(T, \tau)$  which represent the total strain (elastic + creep) per unit stress, at age “T”, caused by an uniaxial constant stress acting since age “ $\tau$ ”.

$$J(T, \tau) = \frac{1}{E} (1 + \Phi(\tau^{-m} + \alpha)(T - \tau)^n)$$

where E and n are the Elasticity modulus and a power constant respectively, while  $\Phi$ , m and  $\alpha$  are materials parameters. Examples of the values of such parameters for some dams are shown in Tab. 4.3.

Tab. 4.3 – Values of the parameters of the creep compliance function for some dams [4.22] [4.33]

	E (GPa)	m	n	$\alpha$	$\Phi$
Canyon Ferry	85.26	0.3222	0.115	0.10	7.267
Ross Dam	24.56	0.451	0.114	0.01	2.814
Dworshak Dam	43.03	0.353	0.058	0.00	13.510
Shasta Dam	41.52	0.701	0.099	0.032	17.46

This model [4.33] has also been extended to consider the cyclic creep caused by the cycling loading conditions of dams [4.22]. The following correction function was then included in the creep compliance function, taking into account a  $T_f$  relaxation time constant.

$$J(T, \tau) = \frac{1}{E} (1 + \Phi(\tau^{-m} + \alpha)(T - \tau)^n * (K_1 + K_2(1 - e^{-\frac{T-\tau}{T_f}})))$$

$K_1$  is the fraction of elastic strain which is instantaneously recovered on unloading  $K_1 + K_2 = 1$ .

The principle of superposition was involved and the effect of unloading was simply added to that of loading.



Based on this function, in the structural analysis of the Zervreila arch dam [4.22], it was possible to obtain a suitable correlation between the calculated cyclic total strain and the normalised chosen function (deformation of the crown cantilever crest of the dam). This calculated normalised strain due to seasonal variation of loading, including creep effects, is shown in the following Fig. 4.6, to be compared with the experimental data of the previous Fig. 4.5.

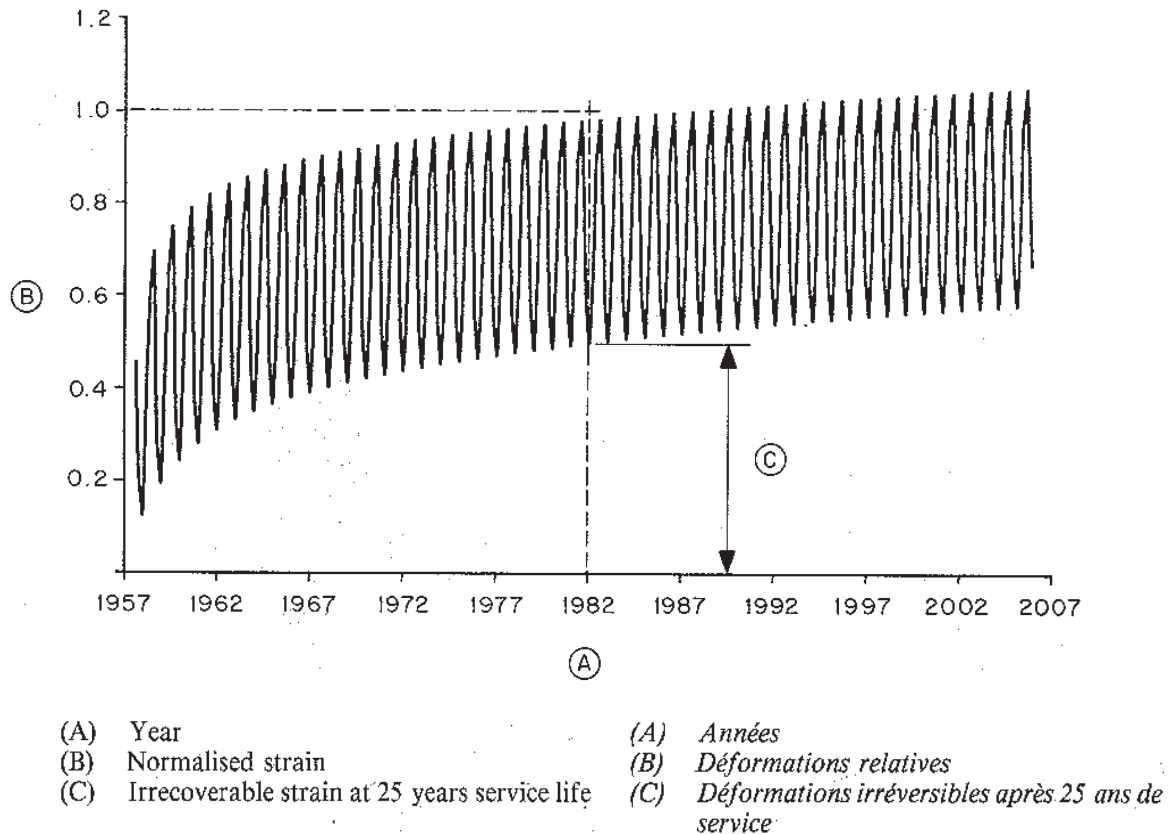


Fig. 4.6 - Calculated normalised strain due to seasonal variation of loading, including creep effects, at Zervreila arch dam [4.22]

In the case of expansion phenomena due to Alkali-Aggregate Reaction (AAR), again, if the instantaneous modulus of elasticity is used in the mathematical models, very high stress states come up, not consistent with the real stress behaviour at the dam site [4.36] [4.37]. Redistribution effects caused by creep are to be taken into consideration in the evaluating criteria. Alternative to models with more or less complicated creep laws is the simple approach, usually adopted, based on the use of a sustained elastic modulus lower than the instantaneous modulus of elasticity. Even lower ratio than those presented in Tab. 4.2 are reported in the literature. In the case of Mactaquac, for example, in order to evaluate the stress within the mass concrete structure, a sustained modulus of elasticity of about one third of the instantaneous modulus was used for the evaluation of the long term loading effects (concrete grows loads) [4.38].

#### 4.6 REFERENCES

- [4.1] American Concrete Institute, "Cement and Concrete Terminology", ACI 116R-90, ACI Manual of Concrete Practice, Part 1, American Concrete Institute, Detroit, Michigan, USA, p.1-68, 1990.
- [4.2] Winter, G. and Nilson, A. H., "Design of Concrete Structures" McGraw-Hill Book Company, New York, NY, 1979.
- [4.3] Smerda, Z., Fristek, V., "Creep and Shrinkage of Concrete Elements and Structures", Developments in Civil Engineering, Vol. 21, published by Elsevier, 1988.
- [4.4] Neville, A.M., "Properties of Concrete", published by Wiley, third edition, 1983.
- [4.5] Philleo, R.E., "Elastic Properties and Creep," Significance of Tests and Properties and Concrete and Concrete-Marking Materials, ASTM STP 169C, American Society for Testing and materials, Philadelphia, PA, USA, p. 192-201, 1994.
- [4.6] Ali I. And Kesler, C. E., "Mechanisms of Creep in Concrete," Symposium on Creep of Concrete, ACI SP-9, American Concrete Institute, Detroit, Michigan, USA, p.35-57, 1964.
- [4.7] Neville, A. and Meyers, B., "Creep of Concrete: Influencing Factors and Prediction," Symposium on Creep of Concrete, ACI SP-9, American Concrete Institute, Detroit, Michigan, USA, p. 1-33, 1964.
- [4.8] Rusch, H., Kordina, K., and Hillsdorf, H., "Der Einfludd des mineralogischen Charakters der Zuschlage auf das Kriechen von Beton," Deutscher Ausschuss fur Srahlbeton, Bulletin No. 146, 134 pp., 1963.
- [4.9] McCoy, E. E., "Investigation of Creep in Concrete – Creep of Mass Concrete," Miscellaneous Paper No. 6-132, Report 3, U.S. Army Engineer Waterways Experiment Station, Vicksburg, Mississippi, USA, 22 pp., 1958.
- [4.10] Polivka, M., Pirtz, D., and Adams, R.F., "Studies of Creep in Mass Concrete," Symposium on Mass Concrete, ACI SP-6, American Concrete Institute, Detroit, Michigan, USA, pp. 257-283, 1963.
- [4.11] Neville, A.M., "Hardened Concrete: Physical and Mechanical Aspects," American Concrete Institute Monograph No. 6, American Concrete Institute, Detroit, Michigan, USA, 260 pp., 1971.
- [4.12] Troxell, G.E., Raphael, J.M., and Davis, R.E., "Long-time Creep and Shrinkage Tests of Plain and Reinforced Concrete," Proceedings, American Society for Testing and Materials, Vol 58, 1943, p. 1101-1120, 1943.
- [4.13] Nasser, K.W. and Neville, A.M., "Creep of Concrete at Elevated Temperatures," Proceedings, ACI Journal, Vol 62, No. 12, p. 1567-1579, 1965.
- [4.14] Johansen, R. and Best, C.H., "Creep of Concrete with and without Ice in the System," RILEM Bulletin (Paris), New Series No. 16, p. 47-57, 1962.
- [4.15] Hansen, T.C. and Mattock, A. H., 1966: "The Influence of Size and Shape of Member on the Shrinkage and Creep of Concrete," Proceedings, ACI Journal, Vol 63, p. 267-290, 1966.

*ICOLD Bulletin: The Physical Properties of Hardened Conventional Concrete in Dams*  
Section 4 (Creep properties)

- [4.16] Gopalakrishnan, K.S., Neville, A.M., and Ghali, A., "A Hypothesis on Mechanism of Creep of Concrete with Reference to Multi-axial Compression", Proceedings, ACI Journal, Vol 67, No. 1, p. 29-35, 1970.
- [4.17] McDonald, J.E., "Time-Dependent Deformation of Concrete Under Multiaxial Stress Conditions", Technical report C-75-4, U.S. Army Engineer Waterways Experiment Station, Vicksburg, Mississippi, 306 pp., 1975.
- [4.18] Ramos, J.M., Soares de Pinho J., "Delayed effects observed in concrete dams", Proc. ICOLD 15. Congress, Lausanne, 1985, Q.56, R.38.
- [4.19] Raphael, J., M., "The Nature of Mass Concrete in Dams", American Concrete Institute, SP 55, 1976.
- [4.20] Guerra, E.A., Fontoura, J.T.F., Bittencourt R.M. and Pacelli, W.A., "Mass Concrete Properties for Large Hydropower Constructions"- FURNAS CENTRAIS ELETRICAS SA.
- [4.21] Gunn, R.M., Bossoney, C., "Creep analysis of Mass Concrete Dams", Hydropower & Dams, Issue six, 1996, 73-79.
- [4.22] Dungar, R., "The effect of cyclic creep on the ageing of arch dams", Proc. ICOLD, 17. Congress, Vienna, 1991, Q.65, R.9.
- [4.23] USBR Concrete Laboratory Report n° SP-38, "A 10 year study of creep properties of concrete"; Denver, July 1953.
- [4.24] Swiss Committee on Dams, "Concrete of Swiss Dams – Experiences and Synthesis", edited for the ICOLD Congress in Beijing, 2000.
- [4.25] Sinniger, R. et al. "Ageing of Dams – Swiss Experience", Proc. ICOLD, 17. Congress, Vienna, 1991, Q.65, R.10.
- [4.26] Dungar R., "Observed and computer-simulated movements in the 157 m high Zervreila Arch Dam (2-creep and plasticity of mass concrete)", "Arch Dams", Balkema 1990, 462-472.
- [4.27] Blight, G.E., Mciver, J.R., Schuttle, W.K., Rimmer, R., "The effects of Alkali-Aggregate Reaction of Reinforced Concrete Structures made with Witwatersrand Quartzite Aggregate", Conference on Alkali-Aggregate Reaction in Concrete, Cape Town, South Africa, 1981.
- [4.28] American Concrete Institute, "Cooling and Insulating Systems for Mass Concrete," ACI 207.4R-93, ACI Manual of Concrete Practice, Part 1, American Concrete Institute, Detroit, Michigan, USA, 1993.
- [4.29] Gunn, R.M., Bussoney, C. "Creep analysis of mass concrete dams", International Journal on Hydropower and Dams, Issue six, 1996, pp. 73-79.
- [4.30] ACI, "Prediction of Creep, Shrinkage, and temperature effects in concrete structures", ACI 209R-92, ACI Manual of concrete practice - Part 3, 1993.
- [4.31] CEB, "Evaluation of the time dependent behaviour of concrete", Bulletin d'information n°199, 1990.
- [4.32] Brooks, J.J., Neville, A.M., "Predicting long-term creep and shrinkage from short-term tests", Magazine of Concrete Research, V. 30, n° 103, June 1978.

*ICOLD Bulletin: The Physical Properties of Hardened Conventional Concrete in Dams*  
Section 4 (Creep properties)

[4.33] Bazant, Z.P. "Triple Power law for Concrete Creep" ASCE Journal of Eng. Mech., Vol. 111, n° 1, 1985.

[4.34] Bazant, Z.P. "Creep and shrinkage prediction model for analyses and design of concrete structures – Model B3", Materials and Structures, vol. 28, 1995.

[4.35] Gardner, N.J., Lockman, M.,J. "Design provisions for drying shrinkage and creep of normal-strength concrete", ACI Materials Journal, V.98, March-April 2001, pp159-167.

[4.36] Garner, S.B. and Hammons, M.I., "Development and Implementation of a Time-Dependent Material Model for Concrete", Technical Report SL 91-7, U.S. Army Engineer Waterways Experiment Station, Vicksburg, Mississippi, 1991.

[4.37] ICOLD European Club, Working Group on Ageing on Concrete Dams, " Ageing on Concrete Dams", final report, 2004.

[4.38] Thompson, G.A., Charlwood, R.G., Steele, r.R., Curtis, D.D., "Mactaquac Generating Station Intake and Spillway Remedial Measures", Proceedings 18<sup>th</sup> ICOLD Congress, Q. 68, R. 24, Durban, 1994.

## 5 SHRINKAGE

<b>5 SHRINKAGE</b> .....	<b>1</b>
<b>5.1 GENERAL</b> .....	<b>1</b>
<b>5.2 TYPES OF SHRINKAGE</b> .....	<b>2</b>
<b>5.3 CAUSES AND MECHANISM OF DRYING SHRINKAGE</b> .....	<b>3</b>
<b>5.4 FACTORS AFFECTING DRYING SHRINKAGE</b> .....	<b>5</b>
5.4.1 <i>Materials and mix design</i> .....	5
5.4.2 <i>Time, humidity and temperature</i> .....	7
5.4.3 <i>Geometry</i> .....	9
<b>5.5 ESTIMATION OF DRYING SHRINKAGE</b> .....	<b>10</b>
5.5.1 <i>Laboratory methods</i> .....	10
5.5.2 <i>Site measurements</i> .....	11
5.5.3 <i>Prediction models (ACI, CEB/FIP, etc.)</i> .....	12
<b>5.6 EFFECT OF SHRINKAGE ON CRACKING</b> .....	<b>15</b>
<b>5.7 EFFECT OF SHRINKAGE ON CONCRETE DAMS</b> .....	<b>16</b>
<b>5.8 REFERENCES</b> .....	<b>17</b>

### 5.1 GENERAL

Volume changes in concrete can be caused by a series of mechanical, physical and chemical processes such as stresses from applied loads, moisture variations, temperature variations, cement hydration, carbonation and phenomena like sulphate attack or alkali-aggregate reaction. Some of them are characterised by a volume decrease (shrinkage) while others by a volume increase (swelling). However, when becoming excessive, they are detrimental to the concrete, inducing deformations in the dam, which are transmitted to its foundations to a greater or lesser extent, according to the relative rigidity of the foundations and the type of the dam. Because in practice these deformations are usually partially or wholly restrained, stresses are developed and cracks may therefore appear, depending also on concrete ultimate strain capacity. The ability of the concrete itself to withstand its design loads could then be affected and its durability compromised.

In this section the volume decrease due to the moisture variations in hardened concrete (drying shrinkage) will be essentially dealt with. The volume decrease due to moisture variations in fresh concrete (plastic shrinkage), due to hydration of cement (autogenous shrinkage) and carbonation (carbonation shrinkage) will be only rapidly touched on. Other processes are instead specifically treated elsewhere in this ICOLD Bulletin (i.e. elastic, creep, thermal and durability properties). However it should be remembered that some of these processes are inter-dependent and influenced by common factors. Both shrinkage and creep, for example, depend on moisture migration within the concrete and can hardly be completely isolated. The magnitude of creep can be affected by concurrent shrinkage and the two phenomena are influenced by a common process during drying. Creep does not add to shrinkage but combines with it [5.1].

As further discussed in the paragraph 5.7, the volume changes in concrete dams due to drying shrinkage are usually to be considered as belonging to the indigenous physiological behaviour of concrete and should not be considered as pathologic. Moreover, as they concern only the external part of the massive concrete, they are usually of minor importance in dams, even if cracks can develop on concrete surfaces exposed to air, further enhancing the risk of other deterioration phenomena such as for example leaking. Therefore, if cracking of concrete due to drying shrinkage is not dealt with, the cracking advances and may cause serious problems.

## 5.2 TYPES OF SHRINKAGE

A first shrinkage phenomenon occurs when concrete is still plastic. The loss of water through evaporation from the surface, drainage of forms and suction by drying concrete below, cause a volumetric reduction named *plastic shrinkage*. Taking place on plastic and not on hardened concrete, it is beyond the scope of the Bulletin.

On the contrary *autogenous shrinkage* occurs on hardened concrete and can be defined as the decrease of volume when no moisture movement to or from hardened concrete is possible, as typically happens inside the massive concrete of dams. Autogenous shrinkage is caused by the initial water content of the concrete mix when this water is used up in the cement hydration. The decrease of volume is the result of the formation of hydrated final products that are characterised by lower volume than that of the initial component materials (cement and water). Autogenous shrinkage is very small, typically  $40 \cdot 10^{-6}$  after 1 month curing to  $100 \cdot 10^{-6}$  after 5 years and it is generally not distinguished from more relevant drying shrinkage [5.2]. Increasing values are to be expected with high cement content, low water/cement ratio and at high temperatures.

Also carbonation, that is the reaction of  $\text{CO}_2$  with  $\text{Ca(OH)}_2$  of hydrated cement to form  $\text{CaCO}_3$ , produces a shrinkage, named *carbonation shrinkage*. It is usually measured together with drying shrinkage but its mechanism is different. In fact the progressive decomposition of  $\text{Ca(OH)}_2$  increases the compressibility of the cement paste and then foster the ability of drying concrete to shrink. Carbonation shrinkage is strongly influenced by relative humidity of the environment: it is negligible at low (25%) and high (100%) values of R.H., when carbonation process is hindered, while it is considerable at intermediate humidities (50%). Since  $\text{CO}_2$  does not penetrate deep into the mass concrete (rarely more than 20-40 mm), this type of shrinkage is usually of minor importance.

*Drying shrinkage* is the effect of loss of water by evaporation from hardened concrete stored in unsaturated air and consequent moisture variations inside the concrete itself. Compared to the other shrinkage types, this is the more relevant one for both conventional and mass concrete. However drying shrinkage becomes negligible in conditions approaching 100% of relative humidity or when drying is prevented. The total drying shrinkage potential of a dam concrete specimen exposed to 50% relative humidity is in the range of  $200 - 800 \cdot 10^{-6}$ , depending on the several factors influencing shrinkage and discussed in the following. As in most cases only drying shrinkage is of engineering importance, it will be specifically considered and more accurately examined.

### **5.3 CAUSES AND MECHANISM OF DRYING SHRINKAGE**

Drying shrinkage is related to the gel and capillary porosity of cement paste that allow evaporable water to be contained inside the concrete. At low relative humidity the loss of free water (not physically bound), which takes place first in the large size capillaries, causes little or no shrinkage as its effect is limited by the paste structure. Only when the adsorbed water is removed from the hydrated gel a volume decrease occurs, connected to a gel contraction. Shrinkage is therefore directly associated with the water held by small gel pores in the range of 3 to 20 nm [5.3].

As shown in Fig. 5.1, if concrete is successively wetted, it again swells but only a part of the initial shrinkage is reversible and subsequent cycles of wetting and drying are characterised by lower volume changes (moisture movement).

The reversible part of shrinkage ranges between 40 and 70% of the initial shrinkage, depending also on the age of the onset of first drying and on the extension of concurrent carbonation. The irreversible drying shrinkage is probably due to the development of new chemical bonds within the paste structure as a consequence of drying.

Drying is generally very much slower than wetting. This can be justified by considering that when the water flows outwards through gel and capillary pores, the adsorption bonds of water particles increases as the water content decreases.

Massive concrete is characterised by an even lower rate of drying and the deeper is the concrete layer considered the lower is the loss of water and then its shrinkage. Fig. 5.2 shows that, although the drying penetration depends obviously also on environmental relative humidity, in practice concrete underneath 50 - 60 cm is not subjected to any loss of water and drying shrinkage. It is therefore evident that a gradient of relative humidity will be established between the surface and the internal part of a massive concrete, inducing stresses and possible cracks.

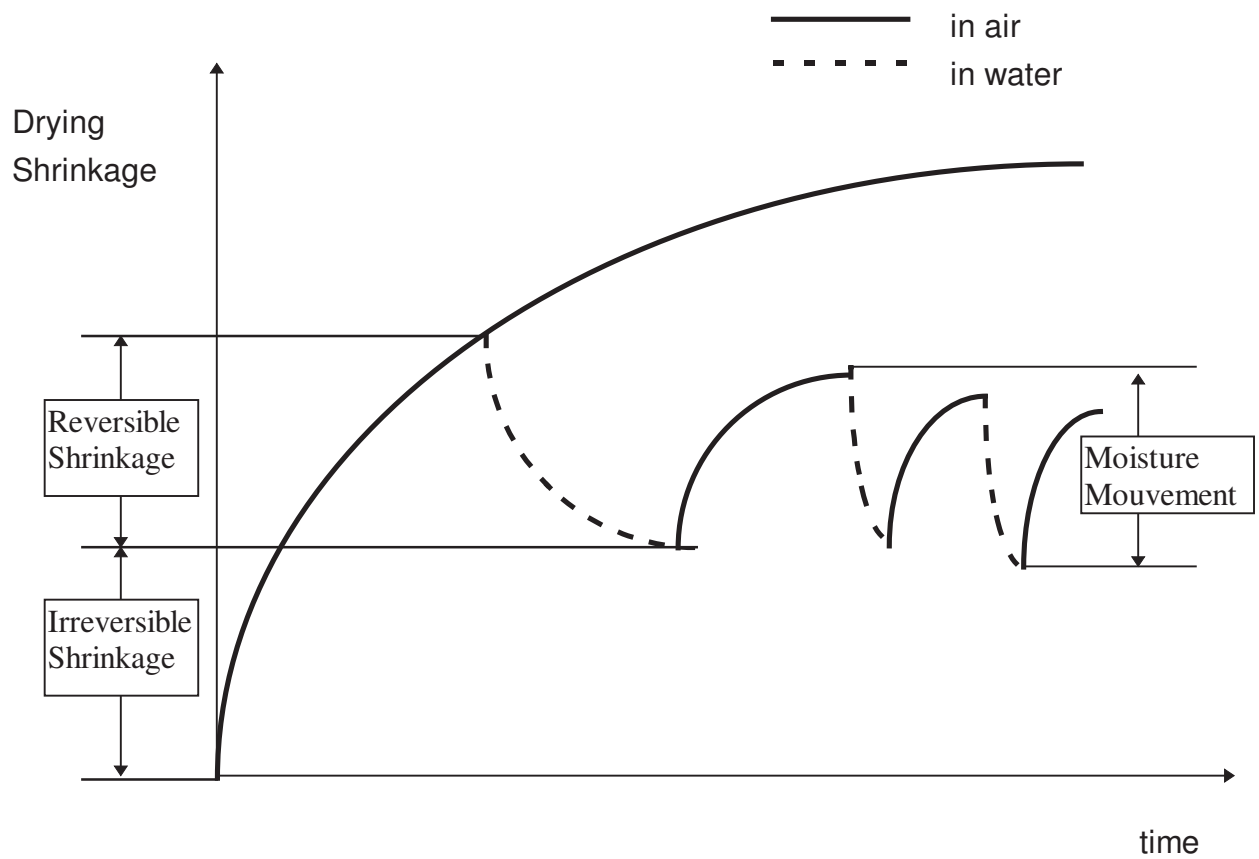


Fig. 5.1 - Volume changes and humidity conditions (just qualitative behaviour)

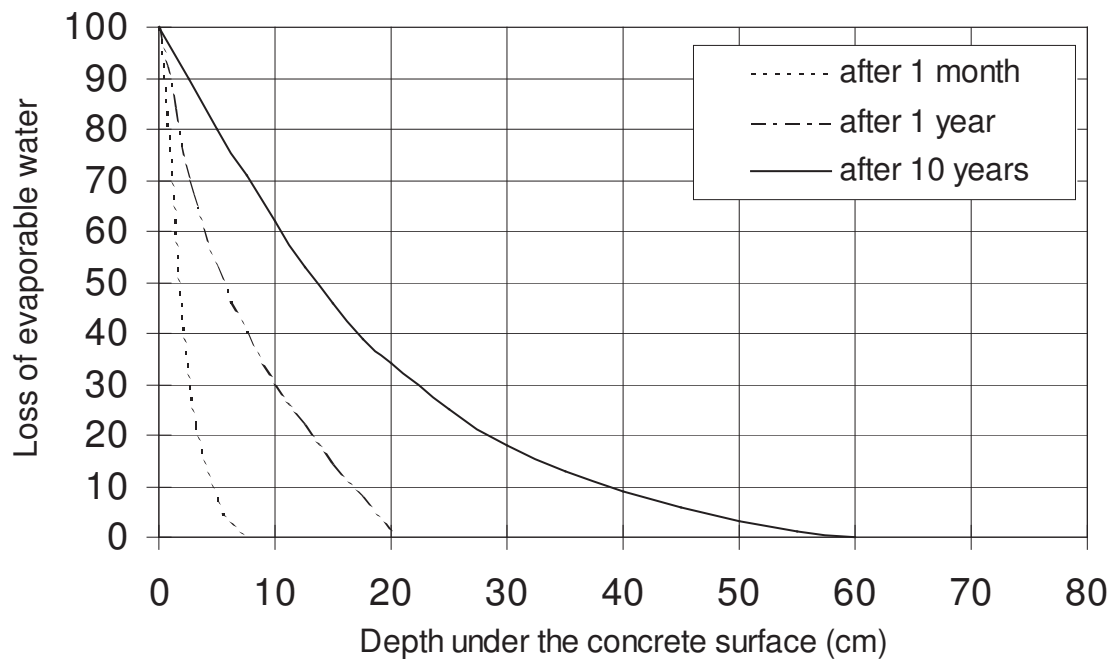


Fig. 5.2 - Loss of water at different depths from a massive concrete at 50% R.H.



## **5.4 FACTORS AFFECTING DRYING SHRINKAGE**

Drying shrinkage is affected by several factors that very often act simultaneously [5.4]. To assess its influence it is necessary to consider them separately, also because their interrelations are quite complex and not still completely understood.

### **5.4.1 Materials and mix design**

The main source of concrete drying shrinkage is its hydrated cement paste: the higher the water content and the higher its porosity and the larger the resulting shrinkage.

However the shrinkage of concrete is considerably less than that of cement paste owing to the restraint against deformation of the surrounding aggregates. The ratio of the concrete shrinkage ( $S_c$ ) and the relative cement paste shrinkage ( $S_p$ ) can be estimated through the relation  $S_c = S_p * (1-a)^n$  where “a” is the volume fraction of aggregate and n a value depending on the elastic modulus of [5.5]. The higher the aggregate modulus the lower the concrete shrinkage (Fig. 5.3). Therefore quartz or granite (high modulus of elasticity) generally give a concrete with less shrinkage than sandstone (low modulus of elasticity). Granite and sandstone aggregate used in some concrete investigations on Guri dam (Venezuela) indicated shrinkage values at 90 days passing respectively from 340 to  $750 * 10^{-6}$ , other conditions being constant [5.6]. An increase of water content also reduces the volume of restraining aggregate and thus results in higher shrinkage.

The aggregate content of the concrete, the aggregate modulus of elasticity and the water content are therefore the most important material factors influencing concrete drying shrinkage. The water content of a mix would just indicate the order of shrinkage to be expected: some indications for normal concrete are reported in Fig. 5.4. For dam concrete, water contents even lower than the value of  $160 \text{ kg/m}^3$  reported in Fig. 5.4 are used but shrinkage values below  $200 * 10^{-6}$  are hardly to be obtained.

Other parameters can indirectly have an influence through their effect on the aggregate content of concrete and on the compactability of concrete mixture. For example the maximum aggregate size and grading control the amount of cement paste in a properly designed concrete mix. Therefore larger maximum size aggregates allow the use of leaner mixes, at a constant water/cement ratio, and then lead to a lower drying shrinkage. In some cases the importance of the shrinkage of the aggregate on the shrinkage of concrete has been emphasised [5.7] [5.8]. Aggregates with low modulus of elasticity and high absorption capacity could exhibit significant changes in volume from the wet to the dry state an vice versa.

The properties of cement have minor influence on concrete shrinkage. For example fineness and composition of Portland cement affect mainly the rate of hydration but not the characteristics of the hydration products [5.2]. Mineral additions as granulated slag and pozzolans and accelerators admixtures as calcium chloride seem to increase the drying shrinkage as the result of pore refinement of cement paste. Mineral admixtures may increase the shrinkage also because of their increased water demand. Water reducing admixtures have naturally a significant effect on limiting the concrete shrinkage while air entrainment admixtures has not been found to have a significant influence.

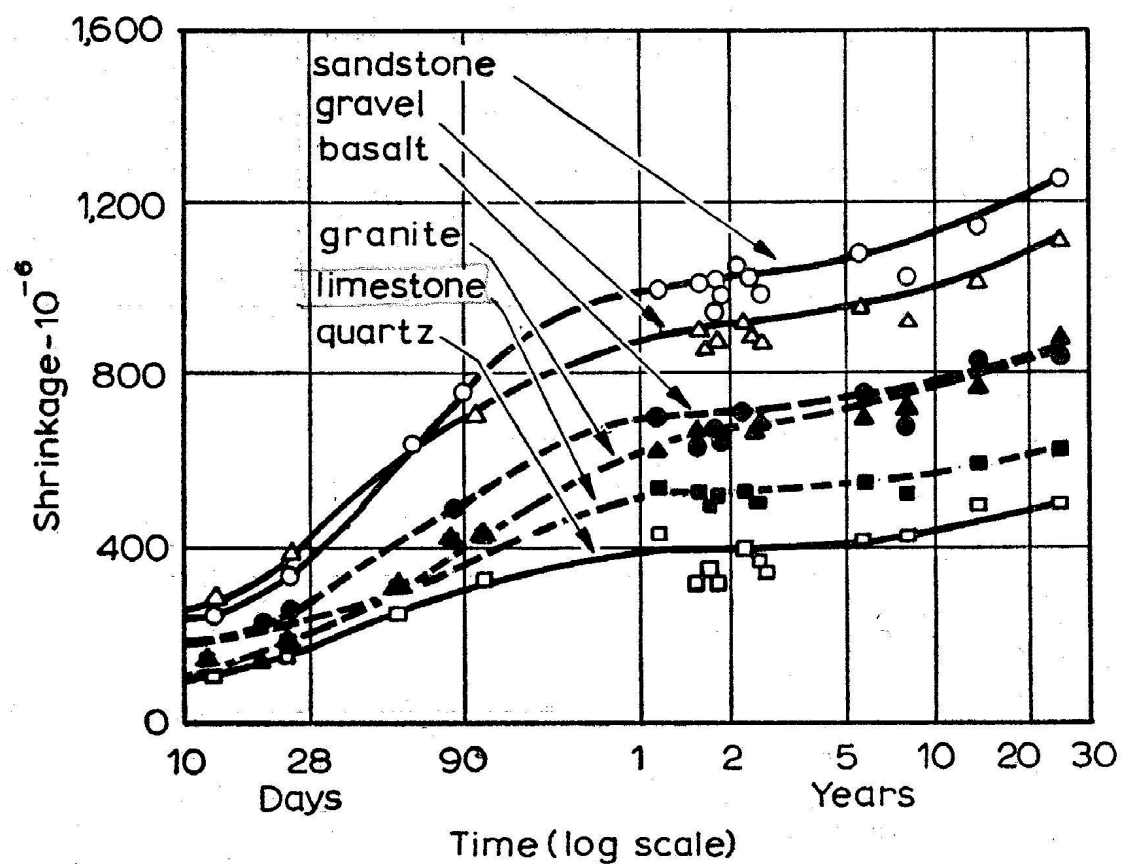


Fig. 5.3 – Shrinkage of concretes with different aggregates and stored in air at 21 °C and 50% relative humidity [5.2]

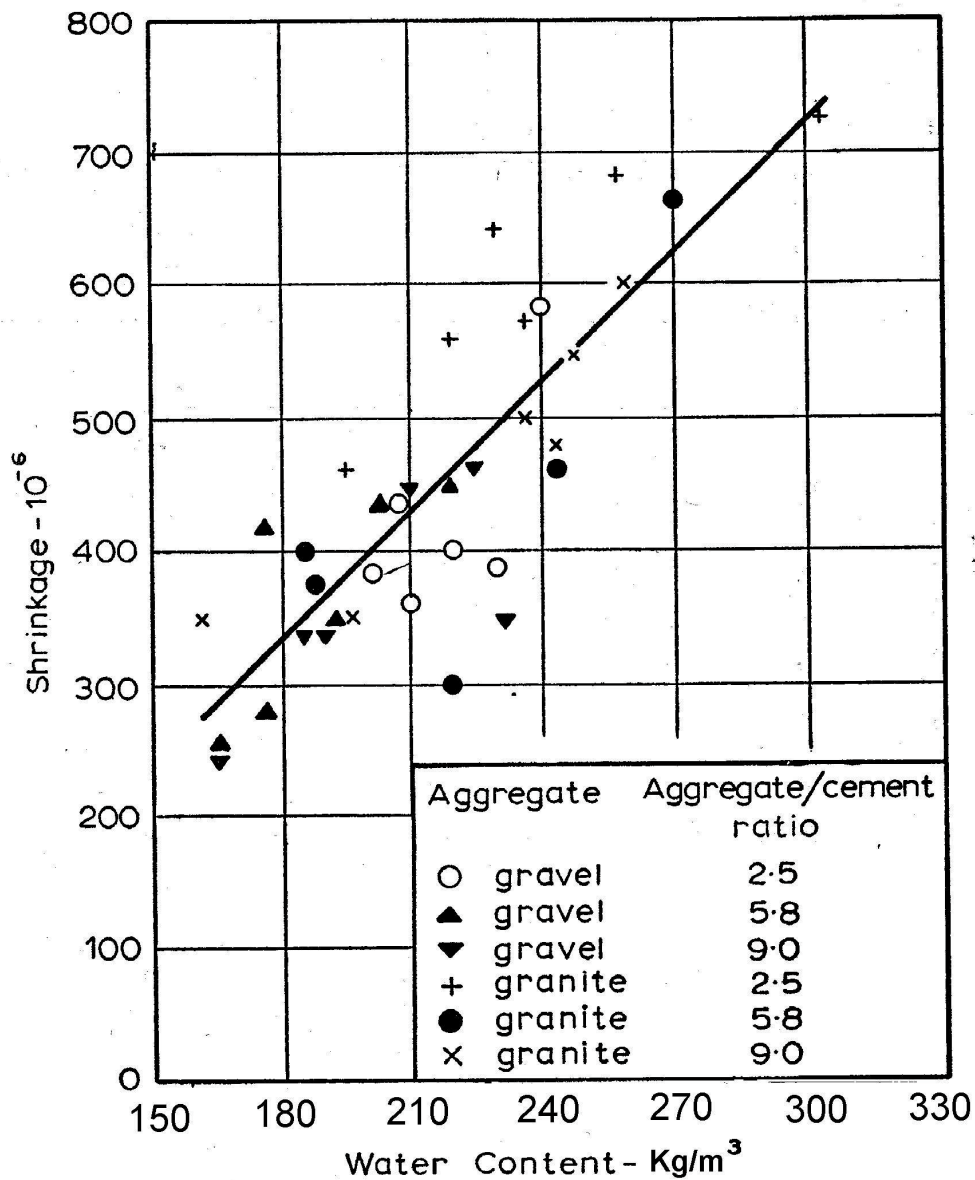


Fig. 5.4 – Relation between water content of fresh concrete and drying shrinkage for different aggregate types and aggregate/cement ratio [5.2]

**5.4.2 Time, humidity and temperature**

It is well known that shrinkage takes place over a considerably long period of time (20 to 30 years) but the rate of increasing of shrinkage decreases with time. Most of the total shrinkage occurs in the first years. Fig. 5.3 shows an example of concrete drying shrinkage over a period of 30 years for concretes of fixed mix proportions but made of different aggregates and stored in air at 21 °C and 50% relative humidity, after an initial wet curing of 28 days [5.3].

A prolonged moist curing before drying delays the shrinkage development but contradictory results on the final shrinkage magnitude of concrete have been reported. It is generally assumed that long initial moist curing tends to reduce the shrinkage.

On the contrary, the relative humidity of the environment surrounding the concrete greatly affects its drying shrinkage. Therefore much attention should be given to keep the concrete surfaces from drying out during construction.

There is a theoretical hygrometry equilibrium at 94% relative humidity at which does not occur neither weight nor volume changes. At lower humidity the water flows from the interior to the outer surface of concrete and the shrinkage increases as the humidity decreases. For a given exposure time, the effects of relative humidity of air on drying shrinkage of a structural concrete are shown in Fig. 5.5. In the above quoted concrete investigations carried out on Guri dam (Venezuela), the ratio between the shrinkage value at 70 % and 50% was about 0.7 as reported in Tab. 5.1 [5.6], confirming the trend of curve in Fig. 5.5.

Temperature is generally less important than relative humidity, affecting mainly the rate of concrete ageing due to the more rapid development of cement hydration.

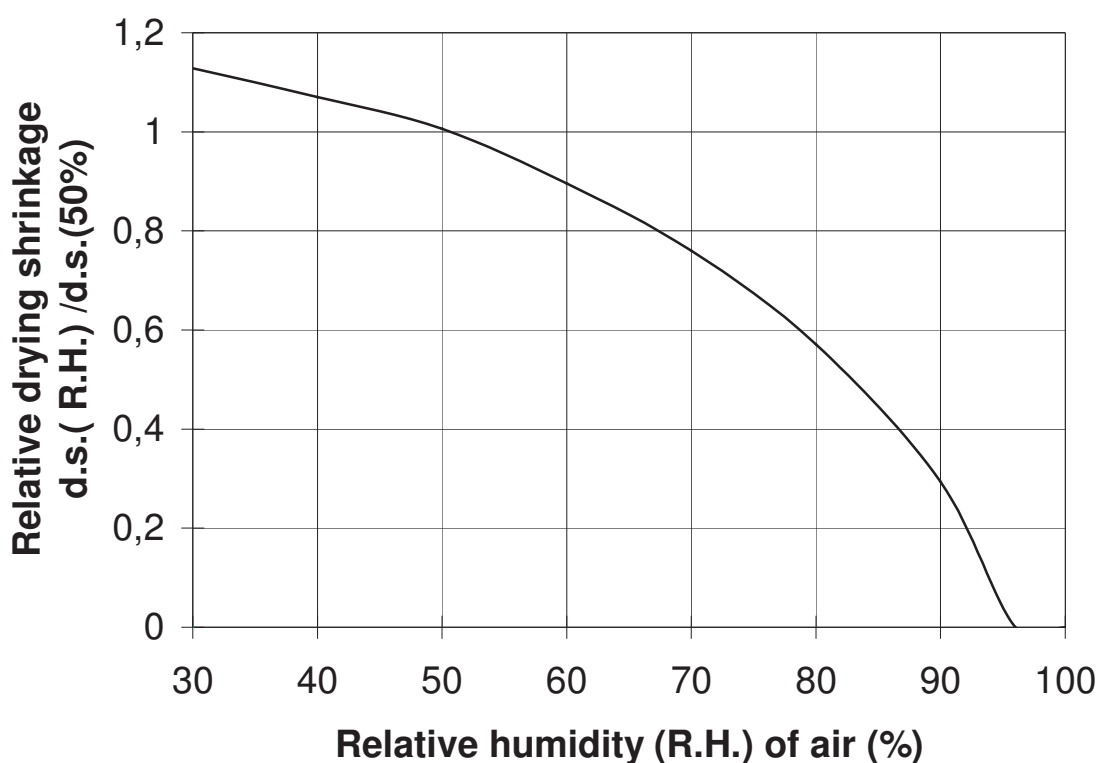


Fig. 5.5 – General trend of the effect of relative humidity of the environment upon drying shrinkage [5.9]

Tab. 5.1 – Range of drying shrinkage for different concrete compositions and different environmental conditions

Variable	Range of variable	Range of shrinkage at age of 90 days [10 <sup>-6</sup> ]
Water content	110/160, l/m <sup>3</sup>	250/650
Fineness of cement:	Spec. surface, cm <sup>2</sup> /g	
ASTM I	2200/1300	800/700
ASTM IV	2200/1300	1050/850
Aggregates	sandstone granite	750 340
Ambient humidity	fog/water curing 70% RH 50%RH	±zero 500 700
Duration of moist curing	28 days 90 days	300 250
<p><b>Conditions:</b> concrete with MSA=20mm, water/cement ratios between 0.59 and 0.62, 28 days fog curing, thereafter in 50% rel. humidity (RH) at 21 °C.</p>		

### 5.4.3 Geometry

For a given period of time, at a constant relative humidity and temperature and with a fixed concrete mix composition, the magnitude of shrinkage depends on both size and shape of the concrete element. In fact they influence the length of the path travelled by the water diffusing from the interior of the concrete to the atmosphere.

The shrinkage increases as the ratio between volume and surface area decreases. The shrinkage of a concrete element with a ratio of 150 mm is about one half of that showed by the same concrete in an element with a volume/surface ratio of 25 mm [5.10], [5.4].

Therefore for practical purposes drying shrinkage cannot be considered as purely an inherent property of concrete without reference to the size and shape of the element.

## **5.5 ESTIMATION OF DRYING SHRINKAGE**

### **5.5.1 Laboratory methods**

The measurement of drying shrinkage is covered by several National Standards. For example ASTM C 157 [5.11] prescribes the use of concrete prisms of 100 mm square cross section and 285 mm long. After 28 days of moist curing, the specimens are stored in a dry room at a temperature of 23 °C and a relative humidity of 50% up to 64 weeks. The magnitude of shrinkage can be determined by means of a measuring frame fitted with micrometer gauges or inductive transducers. ASTM C 341 [5.12] provides for similar procedures in the case of specimens cored from a structure.

Nevertheless these specimens are usually not suitable for a dam concrete, due to their small sizes in comparison with the typical aggregate maximum size used in dam construction. Larger specimens should then be considered and, if necessary, the concrete be sieved.

Some results obtained by the Bureau of Reclamation on mass concrete for dams are reported in Tab. 5.2. The tests were conducted on 100 x 100 x 705 (or 1000) mm specimens from concrete wet screened from the mass mix to contain 38 mm maximum size aggregate. Drying shrinkage specimens were fog cured for 14 days after fabrication and then allowed to dry in a room at 50 % relative humidity and 23 °C. In Tab. 5.2 autogenous shrinkage results are also reported. They were obtained in on specimens sealed in soldered copper jackets and maintained at 23°C [5.13].

However the results obtained on concrete test specimens in the laboratory are of limited value in determining the amount of shrinkage which actually takes place in the concrete of a dam. This is due to the fact that shrinkage is very much dependent on the size of specimens being tested and on the humidity and temperature conditions. The rate and magnitude of shrinkage of a small laboratory specimen will be much greater than that obtained on the concrete in the structures. Furthermore, even if carbonation shrinkage has a minor importance in the overall shrinkage of a concrete dam, it plays an important role in the shrinkage of small specimens, particularly when subjected to long term exposure to drying in laboratory [5.14].

Therefore it is a common practice to estimate drying shrinkage from empirical formulas as herein described.

Tab. 5.2 – Drying shrinkage of mass concrete in Bureau of Reclamation dams [5.13]

Dam	Drying shrinkage at 1 year (* 10 <sup>-6</sup> )	Autogenous shrinkage at 1 year (* 10 <sup>-6</sup> )
Hoover	270	-
Grand Cooley	420	-
Angostura	390*	0
Kortes	600	23
Hungry Horse	520	52
Canyon Ferry	397*	37
Monticello	998	38
Anchor	588*	36
Glen Canyon	459	61
Flaming Gorge	496	-
Yellowtail	345#	38

\* cured 90 days instead of 14 days

# 9 month shrinkage

### 5.5.2 Site measurements

The shrinkage of concrete for dams may be directly determined in site by instruments placed in the dam. A possible way is by means of so-called “no stress” strain gauges [5.15]. These are gauges which are embedded in the concrete with a space on all sides, except one, to prevent stresses being carried through to the strain gauge. Standard designs of electric strain or acoustic strain (vibrating wire) are normally used for “no-stress” gauges. With suitable choice of dimensions for the isolated blocks of concrete, they should enable concrete shrinkage in dams to be measured with a fair degree of accuracy [5.16].

However experience has shown that site measurements of shrinkage are often difficult to attain. In fact it is only in the interpretation of results that the effects of shrinkage can sometimes be separated from other effects, for example temperature variations and creep. To this aim it may be necessary to take into account the differential expansion of concrete relative to the gauge due to temperature changes.

### 5.5.3 Prediction models (ACI, CEB/FIP, etc.)

Different models have been proposed and are commonly used to predict the drying shrinkage. They generally are formed from two parts: the shape of the shrinkage-time curve and the scaling terms.

The following simplified expression was suggested by ACI (American Concrete Institute) Committee 209 [5.17] [5.18] for predicting the drying shrinkage of concrete (after 7 days moist curing):

$$\epsilon_{sh}(t, t_{sho}) = \frac{(t - t_{sho})}{35 + (t - t_{sho})} (\epsilon_{sh})_u$$

where:

$\epsilon_{sh}(t, t_{sho})$  is the shrinkage strain, at time  $t$  with reference to time  $t_{sho}$

$t$  is the time (in days)

$t_{sho}$  is the time (in days) at start of drying

$(\epsilon_{sh})_u$  is the ultimate shrinkage strain

This design approach refers to standard conditions and to correction factors.

The average value of the ultimate shrinkage suggested for a concrete with a specific composition, 7 days of moist curing, drying at 40% R.H., minimum thickness of member of 150 mm, volume/surface ratio of 38 mm and temperature of 23°C is  $780 \cdot 10^{-6}$ . Correcting factors  $\gamma$  are applied to this ultimate value for different conditions and concrete compositions.

This ACI equation is simple but when selecting reasonable values for ultimate shrinkage it has to be kept in mind that laboratory results are much higher than those to be expected in the dam.

According to the method proposed by CEB/FIP (Comité Euro-International du Béton / Fédération Internationale de la Précontrainte) in the Model Code 1990 for Concrete Structures [5.19] [5.18], and included in the ENV EC 2 (Eurocode 2 for Concrete Structures), the drying shrinkage  $\epsilon_{cs}$  developed in a period of time  $t-t_s$  can be estimated from the formula:

$$\epsilon_{cs}(t, t_s) = \epsilon_{cso} * \beta_s(t-t_s)$$

where:

$t$  is the age of concrete (in days) at the time considered

$t_s$  is the age of concrete (in days) at the time of initial drying

$\epsilon_{cso} = \epsilon_s(f_{cm}) * \beta_{RH}$  is the notional shrinkage coefficient, depending on concrete strength, type of cement and relative humidity

$$\epsilon_s(f_{cm}) = [160 + \beta_{sc} * (90 - f_{cm})] * 10^{-6}$$

$f_{cm}$  = mean compressive strength of concrete in N/mm<sup>2</sup>

$\beta_{sc}$  = coefficient which depends on type of cement (4 for slowly hardening, 5 for normal or rapid hardening and 8 for rapid hardening high strength cement)



*ICOLD Bulletin: The Physical Properties of Hardened Conventional Concrete in Dams*  
Section 5 (Shrinkage)

$$\beta_{RH} = -1.55 [1 - (R.H./100)^3]$$

R.H.=Relative Humidity in %

The parameter strength of concrete, which has per se no effect upon shrinkage, has been introduced in the shrinkage prediction as a measure of the effect of the composition of concrete, in particular of the water/cement ratio.

$\beta_s(t-t_s)$  is the shrinkage-time curve

$$\beta_s(t-t_s) = \left[ \frac{t-t_s}{\beta_{SH} + t-t_s} \right]^{0.5}$$

$$\beta_{SH} = 0.035h_o^2$$

$h_o = 2 \cdot A_c / u$  is the theoretical thickness where  $A_c$  is the area of concrete section in  $mm^2$  and  $u$  is the perimeter in contact with the atmosphere in mm.

Relations to estimate the effect of ambient temperature both for the development and magnitude of shrinkage have been also proposed by CEB/FIP for a temperature range of 5-80 °C.

Some other prediction models have been proposed by Standard Organisations, for example by the Japan Concrete Standard Specification [5.20], by Australian Standard for Concrete Structures [5.21], by Brooks and Neville [5.22], or in the recent technical literature, for example by Bazant [5.23], Gardner and Lockman [5.24].

For Example the proposal of the Japan Concrete Standard Specification is as follows:

$$\varepsilon'_{cs}(t, t_0) = [1 - \exp \{ -0.108 (t - t_0)^{0.56} \}] * \varepsilon'_{sh}$$

where:

$$\varepsilon'_{sh} = -50 + 78 [1 - \exp (RH/100)] + 38 \log_e W - 5 [\log_e (V/S/10)]^2$$

$\varepsilon'_{sh}$ : final value of shrinkage strain ( $\times 10^{-5}$ )

$\varepsilon'_{cs}(t, t_0)$ : shrinkage strain of concrete from age of  $t_0$  to  $t$  ( $\times 10^{-5}$ )

RH: relative humidity (%) ( $45\% \leq RH \leq 80\%$ )

W: unit water content ( $kg/m^3$ ) ( $130 kg/m^3 \leq W \leq 230 kg/m^3$ )

V: volume ( $mm^3$ )

S: surface area in contact with outside air ( $mm^2$ )

V/S: volume-surface ratio (mm) ( $100 mm \leq V/S \leq 300 mm$ )

$t_0$  and  $t$ : temperature adjusted age (days) of concrete at the beginning of drying and during drying, values corrected by the following equation should used.

$$t_0 \text{ and } t = \sum_{i=1}^n \Delta t_i \exp \left[ 13.65 - \frac{4000}{273 + T(\Delta t_i)/T_0} \right]$$

$\Delta t_i$ : number of days when the temperature is  $T$  (°C);  $T_0 = 1$  °C

*ICOLD Bulletin: The Physical Properties of Hardened Conventional Concrete in Dams*  
Section 5 (Shrinkage)

The ACI 209-1992 and CEB/FIP 1990 model Code use the concept of an hypothetical ultimate shrinkage and a Ross-type equation to represent the effect of time. Brooks and Neville do not use the concept of an ultimate value and use a logarithmic expression of time to estimate the long-term shrinkage.

According to Bazant B3 model [5.23] the shrinkage prediction is based on a time function S(t) like

$$S(t) = \tanh \sqrt{\frac{t-t_0}{\tau_{sh}}}$$

t is the age of concrete (in days) at the time considered

t<sub>0</sub> is the age of drying started (in days)

τ<sub>sh</sub> is the half time shrinkage

and is calibrated by a computerized data bank comprising the relevant test data obtained in various laboratories. According to his results, the coefficient of variation of the deviations of the model from the data are distinctly smaller than those from the CEB Model (1990) and much smaller than those for the previous model in ACI 209. Details of the model are in reference [5.23].

According to Gardner and Lockman [5.24] the shrinkage data can be better represented by a Ross type term in the following way:

$$\epsilon_{sh} = \epsilon_{shu} * \beta(h) * \beta(t)$$

where:

ε<sub>sh</sub> is the shrinkage strain

ε<sub>shu</sub> is a constant value depending on type of cement and concrete mean compressive strength

β(h) = (1-1.18h<sup>4</sup>) correction term for the effect of humidity; for h<0.99 where h is the humidity expressed as a decimal

β(t) correction term for the effect of time; the following shrinkage-time curve is proposed:

$$\beta(t) = \left[ \frac{t-t_c}{t-t_c + 97 * (V/S)^{1/2}} \right] * 10^{-6}$$

t is the age of concrete (in days) at the time considered

t<sub>c</sub> is the age of drying started (in days)

V/S is the volume / surface ratio, mm

It could be expected that more complex the prediction model for shrinkage, the great would be it accuracy. However it has been shown that this is not necessarily the case [5.25]. For example the involvement of such factors as mix proportions does not necessarily lead to increase the accuracy as there are many other effects not yet accounted.

While these models yield reasonable results for laboratory conditions, a close correlation between the predicted deformations and the measurements from the field should not be expected. The degree of correlation can be improved if the prediction of the material response is based on test data from the actual materials used, under environmental conditions similar to those in the field.

## **5.6 EFFECT OF SHRINKAGE ON CRACKING**

If shrinkage could take place without any restraint, there would be no damage to the concrete. However, the concrete in a structure is always subject to some degree of restraints, internal or external. Therefore the combination of shrinkage and restraints causes tensile stresses that can ultimately lead to cracking [5.26]. As the mechanism is similar to thermal cracking and the crack pattern look also similar, shrinkage cracking is often mistaken by thermal cracking, even if it occurs at a later age [5.27].

When the cement paste shrinks, it places the surrounding aggregate under compression and itself become subjected to tensile stresses. In addition some internal restraints arise also from non uniform or differential shrinkage due to moisture gradients between the surface and the inside of concrete. This is the typical case of massive concrete where the length of moisture migration is considerable and the volume to surface ratio is large. The differential shrinkage causes tensile stresses near the surface and compressive stresses in the core. Assuming a surface shrinkage of  $300 \cdot 10^{-6}$ , a modulus of elasticity of 25 GPa and with the hypothesis of strains completely precluded by the concrete core, the differential shrinkage would induce a surface tensile stress of about 7 MPa. Since the stress arises gradually, it is relieved by creep but even so an extensive pattern of surface cracks may result. Normally they are small, extend only a short distance into the concrete and reinforcements are not particularly effective in altering the size or spacing of these cracks. The concrete durability could however be compromised.

Foundations or other parts of the structure represent the external restraints. While the internal restraints can rarely be avoided, the external ones can instead be reduced by careful design measures such as, for example, adequate contraction joints or facing concrete. Usually, for cracking considerations due to exterior restraints, the volume change caused by drying shrinkage is considered in terms of equivalent change in concrete temperature. In fact, the volume change for drying shrinkage is similar to volume change from temperature differences, except that the loss of moisture from hardened concrete is extremely slow, compared to the loss of heat. ACI Committee 207R [5.28] proposed an expression to evaluate the equivalent change in concrete temperature  $T_{DS}$  in the design of secondary reinforcements, when the length of moisture migration or volume to surface ratio is small, like for example in concrete slabs.

The amount of cracking caused by shrinkage will depend not only on the amount of shrinkage but also on the relative rates of development of tensile strength, modulus of elasticity and shrinkage itself and on the effect of the creep in reducing the tensile stresses [5.29] (see also Fig. 2.14 in Section 2). In mass concrete compressive stresses are developed during the very early period, when temperatures are rising, while tensile stresses appear only afterwards. However, due to the low strength of concrete at early ages, most of the creep takes place during the first week and

therefore concrete loses most of the stress relieving capacity before this is needed for preventing cracking induced by shrinkage. Furthermore rapid drying out does not allow a relief of stress by creep and may lead to more pronounced cracking.

## **5.7 EFFECT OF SHRINKAGE ON CONCRETE DAMS**

As already mentioned, the volume changes in concrete dams due to shrinkage are to be considered as belonging to the physiological behaviour of concrete and are not pathologic signs like, for instance, the swelling due to the alkali-aggregate reaction or the degradation due to the action of aggressive waters.

Shrinkage may proceed during a very long time (decades) because of the slow drying and the thickness of concrete in dams. In several cases, however, there is no easy way of distinguishing between shrinkage and creep that influence each other.

The shrinkage effects are usually less important for gravity dams than for arch, multiple arch and buttress dams [5.30] and in fact shrinkage problems are reported chiefly in connection with these last dams.

For arch dams in wide valleys contraction due to shrinkage may cause downstream tilting, which further reduces the low compressive stresses at the upstream dam heel, favouring the tendency of cracking in this zone, increasing the ingress of uplift pressures and inducing a progressive modification of the drainage curtain [5.31].

Experience has shown that this can be very often tolerated with only minor precautions but attention must always be given to the foundation conditions at the downstream toe where stress patterns and magnitudes and the hydraulic gradients may be seriously disturbed [5.32]. The shrinkage strains observed in an arch dam over a period of 16 years was of about  $40 \cdot 10^{-6}$  ( $30 \cdot 10^{-6}$  in the first 8 years and  $10 \cdot 10^{-6}$  in the remaining 8 years) equivalent to a uniform temperature drop of 4 °C. It was considered as 80% of the ultimate probable shrinkage value [5.33]. This shrinkage contraction tends to open the contact between dam heel and foundation, allowing uplift to develop. Similar shrinkage values are reported in [5.34].

In multiple arch dams, due to the reduced arch effect at the foundation level, the tilting tendency is much less important but some cracking in the concrete arches near the foundation could take place, depending on local geometric conditions.

In buttress dams the drying shrinkage of concrete makes surface cracks inevitable, at least near the foundation. Near-vertical cracks, sometimes with horizontal branches, can appear in the buttresses soon after the dam has been built but the dissipation of hydration heat increase the risk of cracking and the intensity of the cracking itself [5.35]. In fact both phenomena produce tensile stresses, particularly near the foundation restraints (where the cracks originate). Seasonal temperature cycles are responsible for cracks evolution. An extensive investigation was carried out with the Finite Element Method on a specific case of hollow gravity buttress dam in Italy to understand the cracks observed in site. The analyses were performed considering, in addition to the other load conditions, the combined effect of concrete shrinkage and cooling at 30 year from the date of construction, altogether assumed equivalent to a 50 °C temperature drop [5.36]. The results showed that the shrinkage and cooling were such as to justify the occurrence of cracks already during construction.

In all types of dams the cracks due to differential shrinkage, even if they do not necessarily penetrate deep into the mass concrete, could be detrimental because they may favour the access of aggressive agents and then compromise the concrete durability.

In general, shrinkage effects in dams are not impairing stability due to a number of reasons:

- shrinkage is a surface phenomenon and its effects reduce rapidly with concrete thickness;
- shrinkage is a early age phenomenon. It reduces with the rate of drying and it fades out during first impounding for common dams;
- shrinkage values from laboratory testing are much higher than those to be expected in the dam. The latter are only a fraction of those reported in the literature from common civil structures,
- in dams, concrete is less exposed to air (as compared to common civil structures), which leads to less drying shrinkage, and
- shrinkage will be reduced by creep recovery.

## **5.8 REFERENCES**

[5.1] Kovler K., "Interdependence of creep and shrinkage for concrete under tension", *Journal of Materials in Civil Engineering*, May 1995.

[5.2] Neville, A.M. "Properties of Concrete", Sir Isaac Pitman & Sons Ltd, London, 1965.

[5.3] Metha, P.K., "Concrete structure, properties, and materials", Prentice-Hall, 1986.

[5.4] ACI," Report on Factors Affecting Shrinkage and Creep of Hardened Concrete ", ACI 209.1R-05, 2005, p.12.

[5.5] Neville, A.M., Brooks, J.J., "Concrete technology", Longman Scientific Technical, 1987.

[5.6] Raphael J.M., "Drying shrinkage of mass concrete with particular reference to Guri Dam & Powerplant", Report to Harza Eng. Co., Chicago, Ill., June 1981, (unpublished).

[5.7] ACI, "Mass concrete", ACI 207.1R-90, ACI Manual of concrete practice - Part 3, 1993.

[5.8] Pike, D.C., "Standard for aggregates", Ellis Horwood, 1990.

[5.9] CEB, "Evaluation of the time dependent behaviour of concrete", *Bulletin d'information n°199*, 1990.

[5.10] Turriziani, R., "I leganti e il calcestruzzo", Edizioni Sistema, 1972 (in Italian).

[5.11] ASTM C157-89, "Standard test method for length change of hardened hydraulic-cement mortar and concrete", *ASTM annual book of Standards*, Section 4, 1990.

[5.12] ASTM C341-89, "Standard test method for length change of drilled or sawed specimens of hydraulic-cement mortar and concrete", *ASTM annual book of Standards*, Section 4, 1990.

*ICOLD Bulletin: The Physical Properties of Hardened Conventional Concrete in Dams*  
Section 5 (Shrinkage)

- [5.13] Bureau of Reclamation, "Properties of mass concrete in Bureau of Reclamation dams", Concrete Laboratory report n° C-1009, Denver, Colorado (USA), 1961.
- [5.14] ACI, "Control of cracking in concrete structures", ACI 224R-90, ACI Manual of concrete practice - Part 3, 1993.
- [5.15] Serafim, J. L., "New developments in the construction of concrete dams", 16th ICOLD Congress on Large Dams, GR. Q.62, San Francisco, USA, 1988.
- [5.16] ICOLD, "Methods of determining effects of shrinkage, creep and temperature on concrete for large dams", ICOLD Bulletin n° 26, 1976.
- [5.17] ACI, "Prediction of Creep, Shrinkage, and temperature effects in concrete structures", ACI 209R-92, ACI Manual of concrete practice - Part 3, 1993.
- [5.18] Bhal, N.s., Mital, M.K. "Effect of relative humidity on creep and shrinkage of concrete, The Indian Journal, January 1996.
- [5.19] CEB, "Evaluation of the time dependent behaviour of concrete", Bulletin d'information n°199, 1990.
- [5.20] Japan Concrete Standard Specifications, "Enacted 2002, Concrete Standard Specifications. Structure Performance Verification 3.2.8 Contraction".
- [5.21] SAA (Standard Association of Australia), "Australian Standard for concrete structures, AS3600", 1988.
- [5.22] Brooks, J.J., Neville, A.M., "Predicting long-term creep and shrinkage from short-term tests", Magazine of Concrete Research, V. 30, n° 103, June 1978.
- [5.23] Bazant, Z.P. "Creep and shrinkage prediction model for analyses and design of concrete structures – Model B3", Materials and Structures, vol. 28, 1995.
- [5.24] Gardner, N.J., Lockman, M.,J. "Design provisions for drying shrinkage and creep of normal-strength concrete", ACI Materials Journal, V.98, March-April 2001, pp159-167.
- [5.25] McDonald, D.B., Roper, H., "Accuracy of prediction models for shrinkage of concrete", ACI Materials Journal, V.90, n°3, May-June 1993.
- [5.26] ICOLD, "Concrete dams - Control and treatment of cracks", ICOLD Bulletin n° 107, 1997.
- [5.27] Concrete Society, "Non-structural cracks in concrete", Technical Report n°22, Third edition, 1992.
- [5.28] ACI, "Effect of restraint, volume change, and reinforcement on cracking of mass concrete", ACI 207.2R-90, ACI Manual of concrete practice - Part 3, 1993.
- [5.29] Orchard, D.F., "Concrete technology - Properties of materials", Vol. 1, 4th edition, Applied Science, 1979.
- [5.30] ITCOLD, "Processi di sviluppo dell'invecchiamento di dighe e loro fondazioni", Italian working group on dam ageing, 1994.
- [5.31] Monfort, L. et alii, "Eléments de méthodologie pour la détection et l'analyse du vieillissement illustrés par des exemples", 17th ICOLD. Congress on Large Dams, Q.65 - R.23, Vienna, Austria, 1991.

*ICOLD Bulletin: The Physical Properties of Hardened Conventional Concrete in Dams*  
Section 5 (Shrinkage)

[5.32] Combelles, J., "Ageing of dams and remedial measures", 17th ICOLD. Congress on Large Dams, GR. Q.65, Vienna, Austria, 1991.

[5.33] Bister, D. et alii, "Contribution au suivi des barrages en béton français sujets a gonflement ou retrait. Application a des ouvrages adultes (Chambon, Vouglans) at au béton jeune (cas du BCR)", 17th Int. ICOLD Congress on Large Dams, Q.65 - R.7, Vienna, Austria, 1991.

[5.34] ICOLD Bulletin N°. 26: "Methods of Determining Effects of Shrinkage, Creep and Temperature on Concrete for Large Dams", 1976.

[5.35] Paolina, R. et alii, "Deterioration problems for concrete and masonry dams in Italy", Proceedings 17th Int. Congress on Large Dams, Q.65 - R.43, Vienna, Austria, 1991.

[5.36] Appendino, M. et alii, "Specific and general trends of the ageing of buttress dams as revealed by investigations carried out on Ancipa dam", Proceedings 17th Int. Congress on Large Dams, Q.65 - R.22, Vienna, Austria, 1991.

## 6 THERMAL PROPERTIES

<b>6 THERMAL PROPERTIES .....</b>	<b>1</b>
<b>6.1 GENERAL .....</b>	<b>1</b>
<b>6.2 TEMPERATURE RISE OF YOUNG CONCRETE DURING HYDRATION OF CEMENTITIOUS MATERIALS .....</b>	<b>2</b>
6.2.1 Heat of solution technique .....	4
6.2.2 Isothermal conduction calorimetry .....	4
6.2.3 Adiabatic or Semi-Adiabatic Calorimetry .....	5
6.2.4 Comparison among different methods .....	6
<b>6.3 THERMAL CONDUCTIVITY OF HARDENED CONCRETE.....</b>	<b>10</b>
6.3.1 Effect of dry density .....	11
6.3.2 Effect of temperature .....	11
6.3.3 Effect of moisture content.....	11
6.3.4 Measurement method.....	12
<b>6.4 SPECIFIC HEAT OF HARDENED CONCRETE .....</b>	<b>12</b>
<b>6.5 THERMAL DIFFUSIVITY OF HARDENED CONCRETE .....</b>	<b>13</b>
6.5.1 Effect of dry density .....	14
6.5.2 Effect of moisture content.....	14
6.5.3 Effect of temperature .....	14
6.5.4 Measurement method.....	15
<b>6.6 COEFFICIENT OF THERMAL EXPANSION OF HARDENED CONCRETE.....</b>	<b>17</b>
<b>6.7 IN SITU MEASUREMENTS OF CONCRETE TEMPERATURES .....</b>	<b>20</b>
<b>6.8 REFERENCES .....</b>	<b>25</b>

### 6.1 GENERAL

Temperature has an important effect on the behaviour of concrete dams. Temperature gives rise to thermal stresses which can be, like in thin dams, comparable to stress procedure by other external loads. The evaluation of such types of stresses requires an analysis of two distinct phenomena:

- the hydration of the cement which causes an increase of temperature during the hardening phase of concrete;
- the environmental variations of temperature under the normal service conditions.



The hydration reactions of the cement develop and conclude during the early years of the life while the environmental variations of temperature continue to affect the structure throughout its lifetime.

In both cases a careful analysis of the temperature distribution in the dam must take into account the effective heat of hydration developed during the hardening phase of concrete, the thermal conductivity and diffusivity, the specific heat and the coefficient of thermal expansion of the concrete. All these parameters evolve during the setting time and depend on temperature and moisture content of concrete.

Some data on thermal properties of concrete dams can be found in reference [6.1].

## **6.2 TEMPERATURE RISE OF YOUNG CONCRETE DURING HYDRATION OF CEMENTITIOUS MATERIALS**

One of the most important factor associated with thermal cracking in concrete dams is the evolution and distribution of the rise in temperature at any time after pouring. The rise in temperature is a direct result of the heat evolved from the hydration of the cement.

In order to minimise the risk of thermal cracking in concrete dams a knowledge of the expected temperature rise during the hydration of cement is desirable. The temperature distribution in hardening concrete depends in a complex way on a large number of parameters: they are schematically summarised in Fig. 6.1. They can be divided among factors related to mix design (type and content of cementitious material and aggregates, water content, admixtures, etc.), factors related to construction techniques (block shapes and sizes, restraint conditions, speed of placement, artificial cooling systems, curing procedures, heat loss through galleries and shafts, creep, etc.) factors related to the environment conditions (temperature daily fluctuations, heat gain by solar radiation, wind effects, etc.). Also the thermal properties of concrete (conductivity, diffusivity and specific heat) play an important role: they, in turn, mainly depend on the type of aggregate.

Numerous laboratory techniques have been developed to measure the temperature rise in concrete [6.2] [6.3]. They range from sophisticated calorimeters used to monitor the temperature in very small samples of cement to temperature measurements at the centre of a large insulated block of concrete.

The testing methods used to this aim can be divided into the following categories: heat of solution technique, isothermal conduction calorimetry, adiabatic and semi-adiabatic calorimetry. The first two method methods are applied to pure cement or cementitious pastes and make them possible to measure the heat generated by samples kept at constant temperature. Temperature rise in concrete under adiabatic conditions is then calculated, based on the experimental test results. The adiabatic and semi-adiabatic calorimetry can instead be applied to concrete, directly measuring the temperature rise.

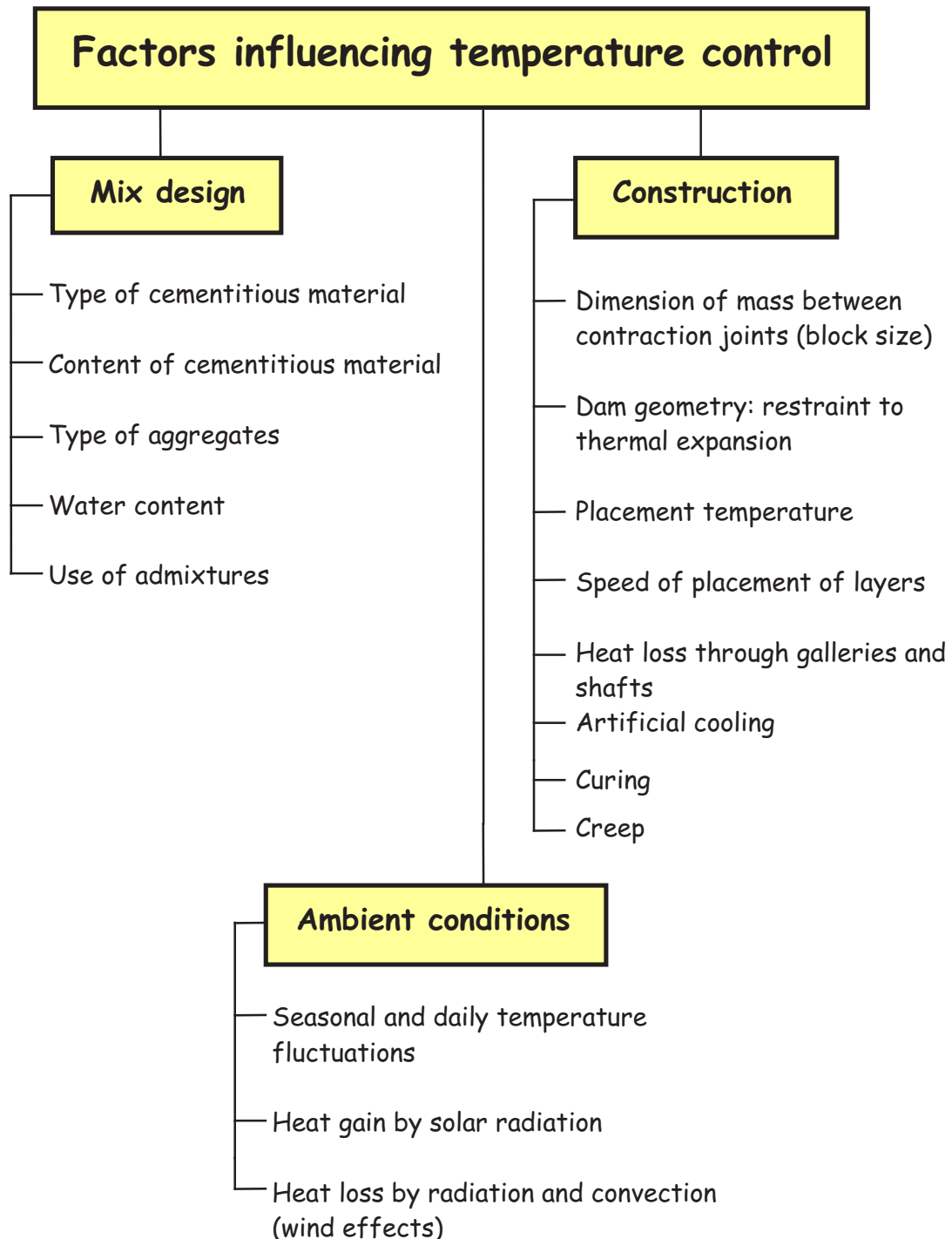


Fig. 6.1 – Lay-out of factors influencing temperature control in concrete

### **6.2.1 Heat of solution technique**

This technique consists of determining the heat of solution of hydrated cement or cementitious material by dissolving the hydrated material in a mixture of acids and recording the temperature rise in an insulated container (calorimeter). By subtracting the equivalent measure for the unhydrated cementitious powder, the heat of hydration can be obtained. Measurements are typically performed after 3, 7 and 28 days of hydration. Standard procedures for determining the heat of hydration of cement by the heat of solution method exist (EN 196/8 and ASTM C186). Low heat cements must not exceed a maximum heat of hydration value of 270 J/g (about 65 cal/g).

The concrete temperature rise under adiabatic conditions  $\Delta T$  is then determined by the following relationship:

$$\Delta T = \frac{Q(t)}{c * \gamma} \quad (6.1)$$

being  $Q(t)$  the total heat of hydration for unit volume of concrete developed at a considered time,  $c$  the concrete specific heat and  $\gamma$  the density of concrete. This methods do not take account of the parameters that affect the temperature rise in real structure, so Equation (6.1) gives rise to large errors.

### **6.2.2 Isothermal conduction calorimetry**

More and more works laboratories refrain from performing the solution method in auto-control procedures, applying an isothermal heat flux calorimeter instead.

With this method [6.4], the heat of hydration of cement paste is directly measured by monitoring the heat flow from the specimen when both the specimen and the surrounding environment are maintained at approximately isothermal conditions (isothermal heat flux calorimeter). Thermopiles are often used to convert the thermal flux into a voltage, which can be continuously monitored. This device measures the release of heat “online” throughout the hydration period, which permits to illustrate the reaction sequences of different cements or cementitious mixes. One difficulty lies in capturing the heat released during the initial mixing (wetting) of the cement and water. Calorimeters have been designed with internal mixing units to attempt to capture the complete heat signature curve.

The heat flux calorimeter further permits to investigate the impact of mineral and chemical admixtures on cement hydration. The chemical admixture can either be input with the water or the cement during the mixing process, or after a time lag. The change in the sequence of heat of hydration release conveys information on the working mechanism of the chemical admixtures.

Again the concrete temperature rise under adiabatic conditions is then determined by the equation 6.1.

The ideal testing method should be able to reproduce the temperature = f(time) curve of each type of concrete during hardening. Since the information obtained though isothermal tests do not reflect the conditions in the real structure, prediction of the temperature rise of concrete from these results can be difficult.

### 6.2.3 Adiabatic or Semi-Adiabatic Calorimetry

Adiabatic and semi-adiabatic methods are much more reliable. They use calorimeters (Fig. 6.2) for measuring directly the temperature rise in a concrete sample being hydrated: the first ones work with no heat exchanges with the external medium, in the second one the heat exchange with the external environment is limited.

Since it is impossible to achieve an adiabatic environment, the calorimeter is considered adiabatic as long as the temperature loss of the sample is not greater than  $0.02\text{ }^{\circ}\text{C/h}$ . Controlling the temperature of the surrounding environment prevents the heat loss. The insulated material could be water, air and heated containers. Water insulation is the most popular way [6.5].

Adiabatic heat measurements are most convenient for producing a continuous heat of hydration curve under curing conditions close to mass curing. And also adiabatic hydration curves are the most suitable starting points for temperature calculation in hardening concrete dams. One of the major drawback of an adiabatic calorimeter is the effect of curing temperature on the rate of hydration is measured implicitly. The activation energy is required to convert the result to the isothermal reference temperature. The result can also be affected by the assumption of the thermal properties of the materials. The advantage is that the heat evolution of an actual concrete mixture can be determined.

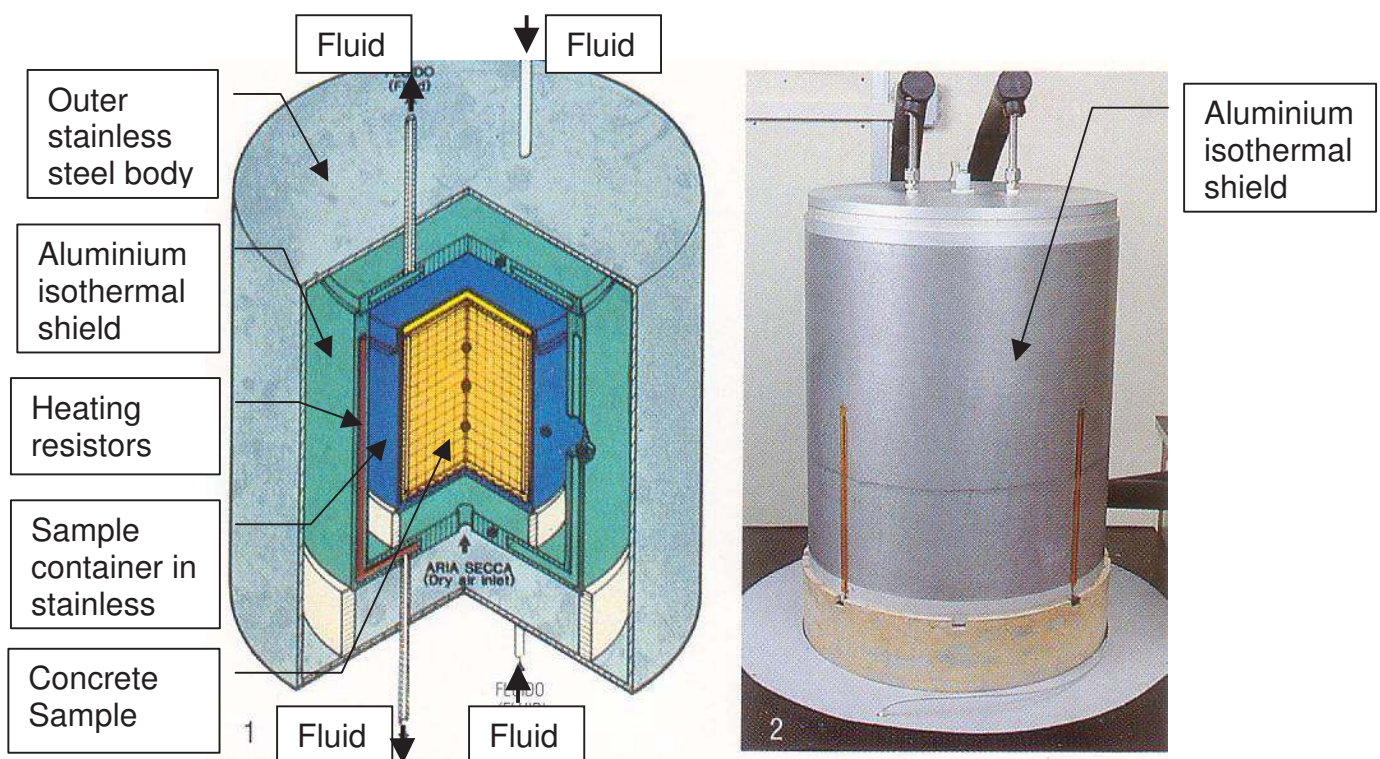


Fig. 6.2 – Adiabatic calorimeter scheme

#### **6.2.4 Comparison among different methods**

True adiabatic conditions are impossible to achieve but they do at least more closely resemble conditions at the centre of a large pour than do the isothermal conditions.

An exhaustive example of experimental data concerns the results given in Fig. 6.3 with respect to a concrete used for an Italian large dam. To prevent a large amount of temperature rise a pozzolanic cementitious mixture has been used.

The mix composition is: cement content 200 kg/m<sup>3</sup>, basalt aggregate 2082 kg/ m<sup>3</sup>, fly ash 50 kg/ m<sup>3</sup>, w/c=0.82. The measurements of heat of hydration of the cementitious mixture performed by the heat of solution method at 3 and 7 days have given 40 cal/g and 49 cal/g respectively.

From the measurement of the specific heat of concrete equal to 0.25 kcal/kg/°C and applying equation 6.1, the corresponding adiabatic temperature rises are 13°C and 16°C, respectively.

The adiabatic temperature rises measured directly at the same time during the hydration of 25 litres of a concrete sample have given 20°C and 24 °C, respectively.

Moreover, the in situ measurement of temperature rise at the centre of a dam block during the construction is only a little lower than the adiabatic temperature rise, as a consequence of an amount of heat losses. In conclusion, the use of the heat of solution technique has given rise to an underestimate of about 35% on the evaluation of the adiabatic temperature rise.

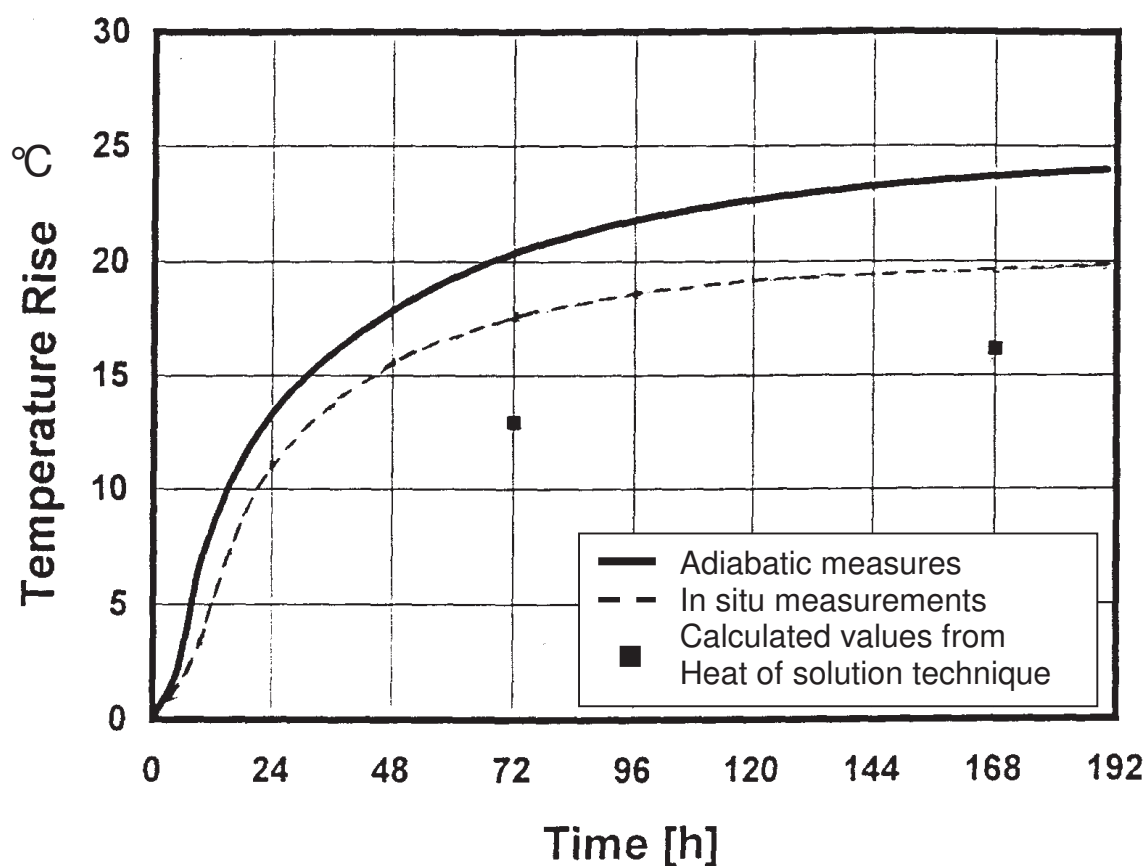


Fig. 6.3 - comparison between heat of solution technique, adiabatic and in situ measurements

This example put also in evidence that a more realistic test would perhaps be to use semi-adiabatic methods where some heat is lost from the calorimeter. It should be realised, however, that even these tests may not truly reflect the conditions in the structure where the rate of heat loss is continually changing. However, also in presence of constant rate of heat losses, it would be very difficult and expensive to accurately reproduce them in the laboratory. So, through a careful calibration, semi-adiabatic calorimeters must be considered as an alternative and less expensive way to reproduce the adiabatic temperature rise with a lower accuracy than adiabatic calorimeters do.

Adiabatic and semi-adiabatic calorimeters have been developed to measure the temperature rise in cement pastes, cement mortars and concrete samples. Although those developed for use with pastes and mortars are often much smaller than those used for concretes, the results obtained do not give a direct measure of the temperature rise in the concrete. The results can only be used to estimate the behaviour of the concrete from a knowledge of the mix proportions and thermal characteristics of the aggregates. Calculations of this kind can be extremely difficult because the kinetics involved are significantly different due to the effects of the aggregate.

For calculations by numerical models, it would be preferable to have an expression describing the heat of hydration of concrete. This is very difficult to obtain since, as it has been mentioned, the number of parameters that affect the heat of hydration of concrete is so high that actually no general expression of the heat of hydration is existing. So, it is common practice to perform a direct measurement of the temperature rise of the concrete by adiabatic or semi-adiabatic methods and use the experimental data in a tabular form as input for numerical methods.

Other examples of adiabatic temperature rise curves from a dam concrete are reported in Fig. 6.4., in Fig. 6.5 and in Fig. 6.6.

In Fig. 6.4 the temperature rise of concretes with constant content of cementitious materials, but different heats of hydration of the cementitious mixes, are reported: they refer to a long period of time, up to 74 days.

Fig. 6.5 shows the temperature rise of concretes with different types of cement (normal Portland, Pozzolanic and Blast Furnace) at different cement contents (from 140 to 300 kg/m<sup>3</sup>). The infinite time temperature rise is obtained by extrapolating the results of the first 7 days.

Finally, for two of the concretes of Fig. 6.5 (Portland cement Ptl 325 at a cement content of 300 kg/m<sup>3</sup> and Pozzolanic cement Pz 225 at a cement content of 200 kg/m<sup>3</sup>), the effect of different initial temperature (over 20 °C and about 15 °C) is shown in Fig. 6.6. Even if the final rise temperature at infinite time is almost the same, the heat evolution with time of the concrete mixtures are quite different, especially at the first week, when the tensile properties of concrete are low. This behaviour underline the importance of the concrete temperature at placement on the crack tendency of a dam.

Thermal cracking in dams is most critical to occur in the core of a lift and at the lift joint. The latter is occasionally forgotten in the thermal analysis (long waiting time at lift joints can create high temperature difference).

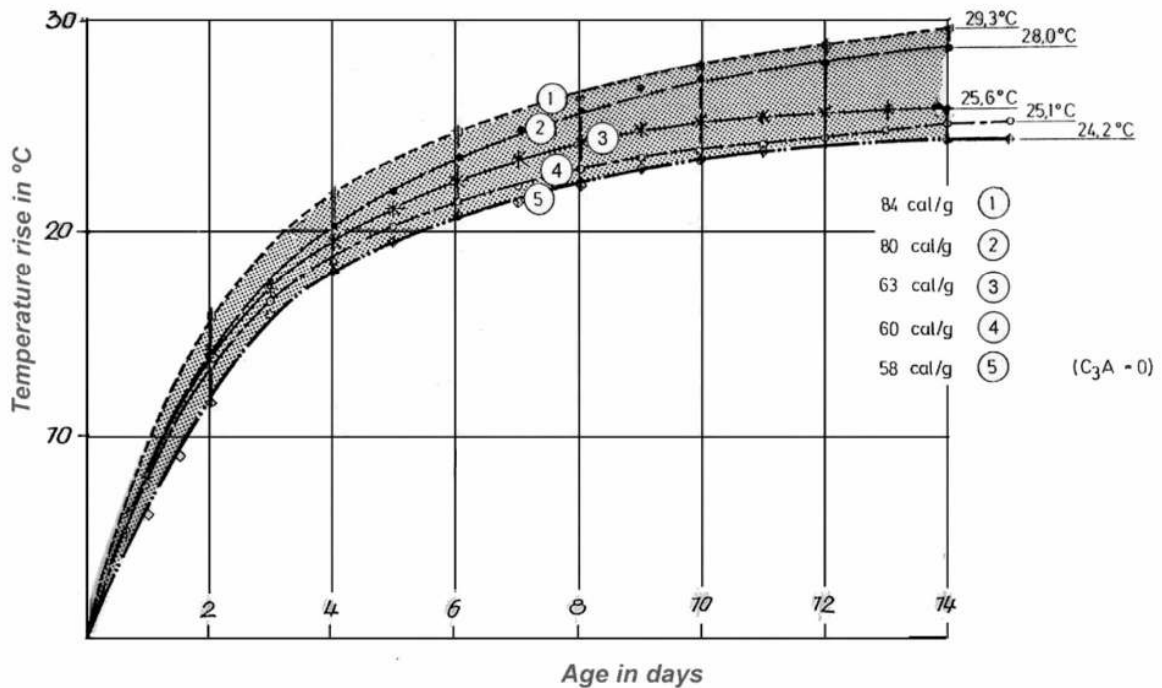


Fig. 6.4 – Example of adiabatic temperature rise with cements of different heat of hydration (content of cementitious material: 180 kg/m<sup>3</sup>) [6.6]

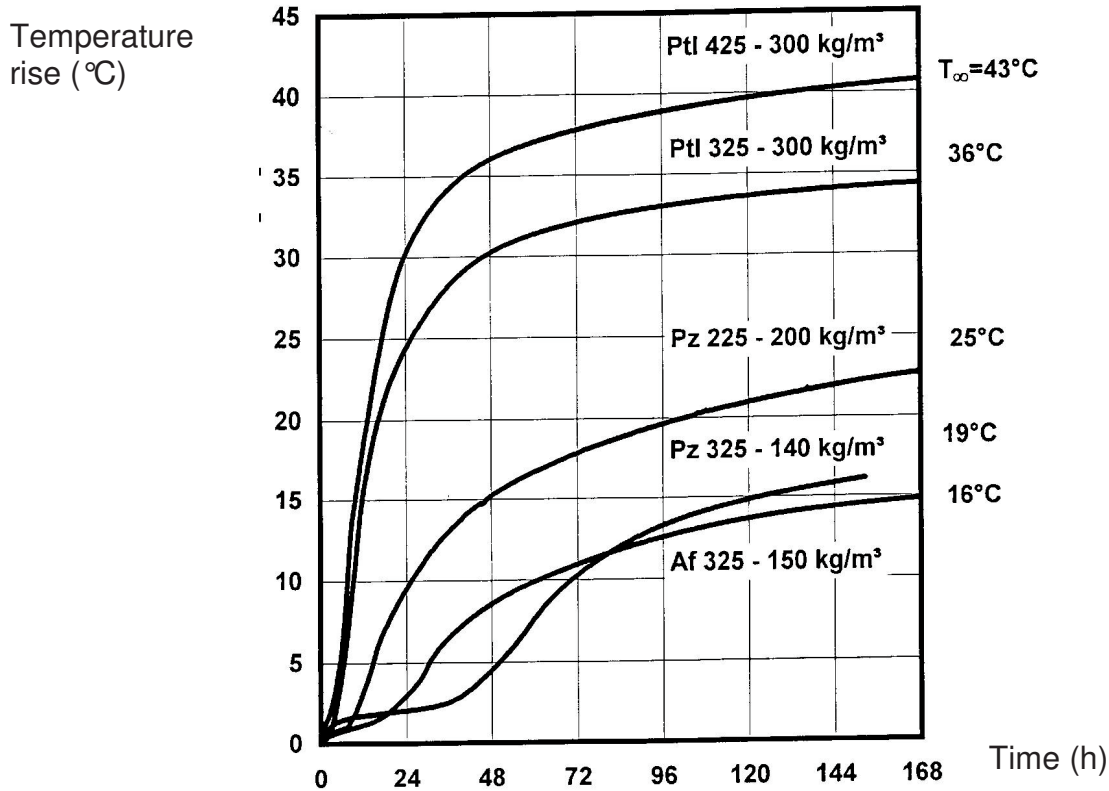


Fig. 6.5 – Examples of adiabatic temperature rise with different cements and cement contents (Ptl = Portland cement; Pz = Pozzolanic cement; Af = Blast Furnace cement) [6.7]



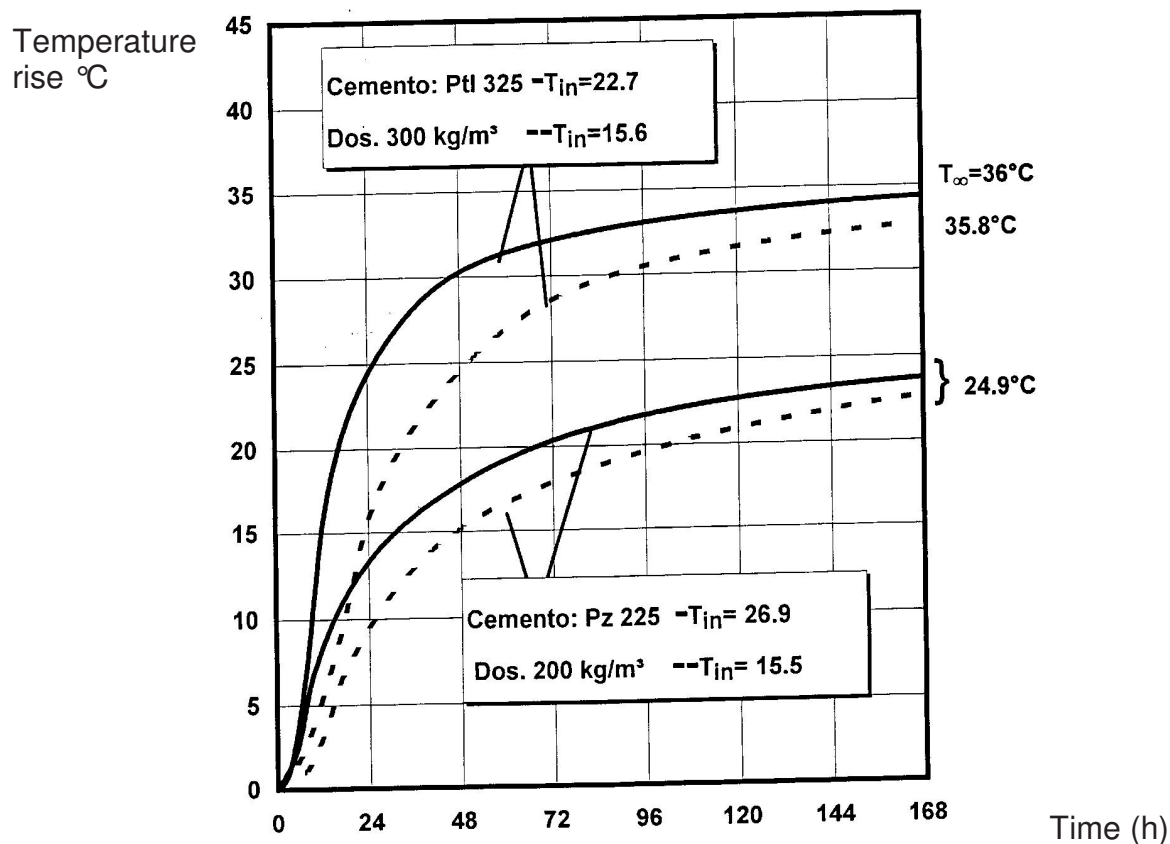


Fig. 6.6 - Examples of adiabatic temperature rise for two concretes with different initial temperature [6.7]

### 6.3 THERMAL CONDUCTIVITY OF HARDENED CONCRETE

The thermal conductivity of a concrete is the rate at which it transmit heat and is defined as the ratio of the flux of heat to the temperature gradient.

Thermal conductivity  $\lambda$  of concrete depends on the moisture content, type of aggregate, porosity, density and temperature. For ordinary hardened concrete in a normal temperature and moisture state, thermal conductivity may vary between 1.2 and 3.0 [W/m<sup>2</sup>/K]. Values beyond 3.0 W/m<sup>2</sup>/K, even up to 3.5 W/m<sup>2</sup>/K, are found as well (Tab. 6.1). Besides a strong dependency on the type of aggregate, the conductivity also depends on the moisture content in the pore system.

Tab. 6.1 – Typical coefficient of thermal conductivity of concrete: typical values (1 W/(m °C) = 0.8598 kcal/(m °C h))

Type of aggregate	Thermal conductivity of concrete	
	[W/(m °C)]	[kcal/(m °C h)]
Quartzite	3.5	3.0
Dolomite	3.2	2.7
Limestone	2.6 - 3.3	2.2 - 2.8
Granite	2.6 - 2.7	2.2 - 2.3
Rhyolite	2.2	1.9
Basalt	1.9 - 2.2	1.6 - 1.9

### 6.3.1 Effect of dry density

The influence of the dry density  $\gamma_0$  is mainly correlated with the content and the type of aggregate. With some exception in concretes with barytes aggregate, the following relationship [6.8] [6.9] between thermal conductivity and dry density can be used:

$$\lambda_0 = 0.072e^{0.00125 \cdot \gamma_0} \quad (6.2)$$

where the thermal conductivity is expressed in W/(m °C) and the dry density in kg/m<sup>3</sup>.

### 6.3.2 Effect of temperature

Data concerning the effect of temperature on thermal conductivity are rather scarce. However, they agree in indicating a decrease in thermal conductivity with the increasing temperature. As order of magnitude, it can be assumed a decrease of about 0.04 W/(m °C) for a rise in temperature of 10 °C [6.8].

### 6.3.3 Effect of moisture content

The thermal conductivity of concrete increases with increasing of the moisture content. For the determination of the effect of the water content on the thermal conductivity of moist concrete the ACI recommends the use of the following formula [6.8] [6.9]:

$$\lambda = \lambda_0 \left( 1 + k_w \cdot \frac{w}{\gamma_0} \right) \quad (6.3)$$

with:  $\lambda_0$  = thermal conductivity of oven-dried concrete

$\gamma_0$  = density of oven-dried concrete [kg/m<sup>3</sup>]

$k_w$  = factor equal to 6 for light weight concrete and to 9 for normal concrete

$w$  = water content [kg/m<sup>3</sup>]

#### 6.3.4 Measurement method

No standard testing method exists to measure the thermal conductivity of concrete. The main reason is that concrete is a complex system constituted from a solid skeleton and pore space, partially filled with water, which can be closed or interconnected. As far as a thermal gradient is applied migration of the water through the interconnected pore spaces takes place. This alters the hygrometric conditions of the sample to be tested, the higher the thermal gradient and the longer the duration of the test, the higher the degree of disturbance is. For this reason the standard testing methods for insulating and dry materials, such as the hot guarded plate method, cannot be applied to concrete samples unless they are in oven-dried conditions. The alternative way is to use transient methods. The most popular is the linear heat source method [6.9], which consists in inserting in the material a thermal probe, heated at constant power, and in measuring the temperature rise during the transient time. Data reduction according to the linear heat source theory allows to determine the thermal conductivity.

### 6.4 SPECIFIC HEAT OF HARDENED CONCRETE

The specific heat  $c$  of concrete is the heat required to rise a unit weight of concrete 1 degree. It can be determined from the values of the component parts of the mix:

$$C = \sum c_i \cdot g_i \quad (6.4)$$

with:  $g_i$  = fraction of content by mass of the mix components  
 $c_i$  = specific heat of the mix components:

The range of specific heats of the constituents are:

aggregate:  $c_a = 0.7 - 0.9 \text{ k J/kg } ^\circ\text{C}^1 = 700 - 900 \text{ J/kg, } ^\circ\text{C}$

cement:  $c_e = 0.84 \text{ kJ/kg } ^\circ\text{C}$

water:  $c_w = 4.186 \text{ kJ/kg } ^\circ\text{C}$

Typical values of the specific heat for ordinary concrete vary between 0.850 and 1.15 kJ/kg °C [6.10].

Because of the high specific heat of water there is a strong correlation between the specific heat of a mix and the amount of water content. The specific heat of concrete increases with increasing moisture content. For water saturated concrete the higher values apply while the lower values can be referred to dry concrete.

---

<sup>1</sup> 1 J/kg, C<sup>0</sup> = 0.24x10<sup>-3</sup> kcal/kg, C<sup>0</sup> = 2.38x10<sup>-4</sup> Btu/lb<sup>0</sup>F

The specific heat also increases with the increasing temperature: an increase of about 10% for an increase in temperature from 10 °C to 66 °C has been reported by ACI [6.8].

## 6.5 THERMAL DIFFUSIVITY OF HARDENED CONCRETE

Diffusivity is described as an index of the ease or difficulty with which concrete undergoes temperature change.

Thermal diffusivity  $a$  is defined as the quotient of the coefficient of thermal conductivity and the specific heat per unit volume:

$$a = \frac{\lambda}{\gamma \cdot c} \quad (6.5)$$

The main factor of influence on the thermal diffusivity is the type of aggregate. Tab. 6.2 gives typical values of thermal diffusivity of concrete for different types of aggregate [6.9].

Tab. 6.2 – Typical thermal diffusivity of concrete for different types of aggregate.

Coarse aggregate	Diffusivity [m <sup>2</sup> /h]
Quartzite	0.0054
Limestone	0.0045 – 0.0055
Dolomite	0.0046
Granite	0.0040
Rhyolite	0.0033
Gneiss	0.00354 – 0.004
Basalt	0.0030

Thermal diffusivity of cement varies between 0.002 and 0.004 m<sup>2</sup>/h.

As for thermal conductivity, also diffusivity depends on dry density, moisture content and temperature. The dependency on the moisture content and temperature follows from the dependency in the coefficient of thermal conductivity and the specific heat from these parameters.

### 6.5.1 Effect of dry density

Very little data are reported about the influence of the dry density on the thermal diffusivity. They however indicate a linear increase of diffusivity with the dry density of the order of  $0.00012 \text{ m}^2/\text{h}$  for an increase in dry density of  $100 \text{ kg/m}^3$ , in the range of  $1500\text{-}2500 \text{ kg/m}^3$  [6.9].

### 6.5.2 Effect of moisture content

As both conductivity and the specific heat increase with increasing moisture content, the net effect on the coefficient of thermal diffusivity is only marginal. Data reported in literature do not indicate a dependence of diffusivity from moisture content.

### 6.5.3 Effect of temperature

The influence of temperature on the thermal diffusivity depends upon the corresponding influence on both the thermal conductivity and the specific heat. Since with increasing temperature the conductivity decreases and the specific heat increases, the thermal diffusivity decreases stronger with increasing temperature (up to about 15% in the temperature range from  $10 \text{ }^\circ\text{C}$  to  $66 \text{ }^\circ\text{C}$ ) than the thermal conductivity [6.11]. This effect has been observed through accurate laboratory measurements (Fig. 6.7).

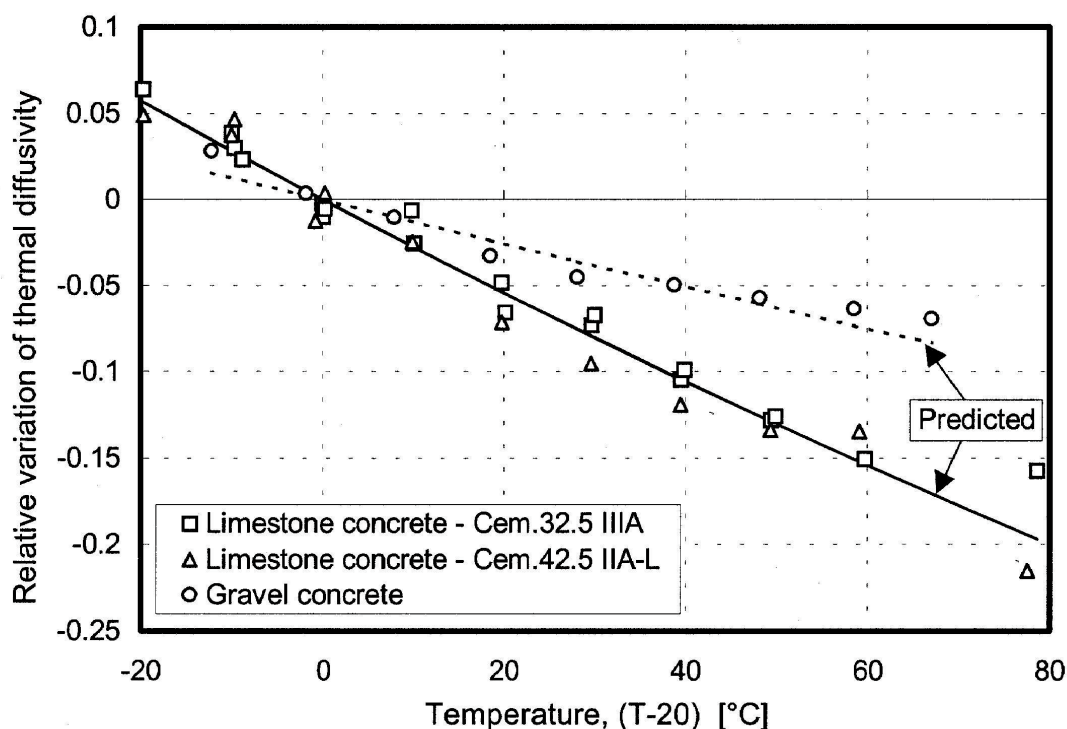


Fig. 6.7 – Relative variation of thermal diffusivity against temperature variation [6.6]

However a measurement campaign of the thermal diffusivity on Brazilian dams in the thermal ranges between 20 and 60°C showed practically no temperature dependence [6.6]. This could be probably due to the difficulties of these types of measurements (paragraph 6.5.4).

#### **6.5.4 Measurement method**

Even more difficult than for conductivity is the problem to measure the thermal diffusivity of concrete. The main reason relies upon the fact that, being the concrete an heterogeneous material, large samples are necessary. Since the testing methods used for metals, such as the laser flash method, work on very little samples, they cannot be applied. In the laser flash method, a short pulse (less than 1 millisecond) of heat is applied to the front face of a specimen using a laser flash, and the temperature change of the rear face is measured with an infrared (IR) detector.

So thermal diffusivity is usually evaluated by measuring the temperature variations in different points of a huge concrete sample, or directly in a concrete dam, under a dynamic temperature field suitably generated inside the concrete. Through a careful data reduction, which takes into account the phase shift of the thermal wave at the different points, thermal diffusivity can be estimated.

Recently a new testing method has been developed [6.9] [6.12]; it can be applied both in laboratory samples as well on site. The method is based on the linear heat source method in the double probe version, namely the two linear parallel probe method (TLPP method). It consists in inserting two probes inside the sample: one is used as heating source, the other as temperature sensor positioned at a known distance from the heating probe.

By applying the linear source theory to the temperature measurements detected by the second probe during the heating time the thermal diffusivity is also determined.

Such method has the advantage that during a single test both thermal conductivity and thermal diffusivity can be measured simultaneously; through the measurement of the density the specific heat can also be determined and, thus, a complete thermal characterisation of the material is obtained. It can be carried out both in laboratory and at the dam site.



Fig. 6.8 – Needle probes for thermal tests on concrete specimens in laboratory

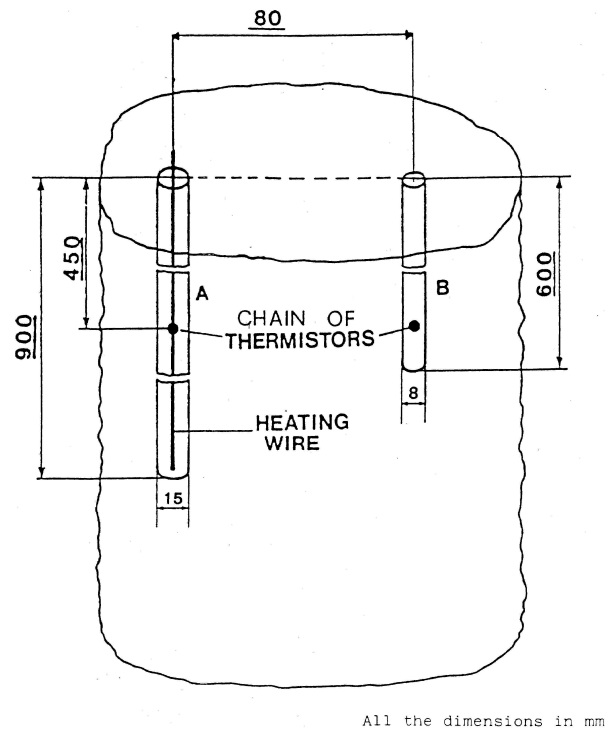


Fig. 6.9 – Lay-out of the two linear parallel probe method for thermal measures in field (all dimensions in mm).



Fig. 6.10 – Thermal measurements on concrete at a dam

## 6.6 COEFFICIENT OF THERMAL EXPANSION OF HARDENED CONCRETE

The coefficient of concrete thermal linear expansion is defined as the change in linear dimension per unit length divided by the temperature change expressed in millionth per °C. It is affected to a large degree by the thermal expansion coefficient of the aggregate, since the latter generally occupies 65-80% of the volume of concrete. The coefficient of thermal expansion of concrete ranges from 4  $\mu\text{m/m } ^\circ\text{C}$  up to 14  $\mu\text{m/m } ^\circ\text{C}$  (Tab. 6.3), usually in the range 8 to 12  $\mu\text{m/m } ^\circ\text{C}$ . The thermal expansion coefficient of pure cement paste is of the order of 20  $\mu\text{m/m } ^\circ\text{C}$ , but as the cement content for unit volume of concrete is very low in respect to the content of aggregate, its influence on the thermal expansion of concrete is only marginal. No influence of the temperature seems to exist in the temperature range going from 10° to 80°C.

There are no data concerning the influence of the moisture content: The reason can be due to the fact that, since it is necessary to reach two different thermal equilibrium conditions of the sample for the measurement of the thermal expansion, it is very difficult to maintain the same water content in the sample during the test.

Tab. 6.3 – Typical coefficient of thermal linear expansion of concrete for different types of aggregate.

Coarse aggregate	Coefficient of linear expansion [ $10^{-6} \text{ } ^\circ\text{C}$ ]
Sandstone	4 to 14
Dolomite	7 to 10
Limestone	4 to 12
Basalt	6 to 8
Granite	7 to 9

Other references on thermal properties of concrete are reported from [6.13] to [6.25].

Finally in Tab. 6.4 and Tab. 6.5 a list of thermal properties of dam concretes, mainly from Bureau of Reclamation, is reported [6.23] [6.26]. Other data of thermal properties of concrete with mica sand are reported in [6.27].



ICOLD Bulletin: The Physical Properties of Hardened Conventional Concrete in Dams  
Section 6 (Thermal properties)

Tab. 6.4 – Thermal properties of mass concrete dams (I) [6.23] [6.26]

Dam/ aggregate	°C	Coeff. linear expansion $\mu\text{m}/\text{m } ^\circ\text{C}$	Thermal conductivity $\text{kcal}/\text{mh } ^\circ\text{C}$	Thermal diffusivity $\text{m}^2/\text{h} * 10^{-3}$	Specific heat $\text{k J}/\text{kg } ^\circ\text{C}$
Hoover/ Limestone- Granite	10	8.6	2.53	4.7	0.887
	38		2.48	4.4	0.941
	66		2.46	3.9	1.050
Grand Coollee/ Basalt	10	8.3	1.61	2.9	0.916
	38		1.61	2.7	0.967
	66		1.62	2.5	1.075
Friant/ Quartzite, Granite, Rhyolite	10	-	1.83	3.4	0.904
	38		1.83	3.2	0.962
	66		1.84	3.1	1.017
Shasta/ Andesite, Slate	10	8.6	1.96	3.6	0.916
	38		1.96	3.6	0.975
	66		1.95	3.2	1.033
Angostura/ Limestone	10	7.2	2.22	4.2	0.925
	38		2.20	3.8	0.992
	66		2.17	3.5	1.054
Kortes/ Granite, Gabbros, Quatz	10	8.1	2.39	4.6	0.870
	38		2.38	4.4	0.925
	66		2.36	4.1	0.979
Hungry Horse/ Sandstone	10	10.3	2.56	4.9	0.908
	38		2.53	4.6	0.971
	66		2.51	4.3	1.033
Canyon Ferry/ Sandstone, Metasiltstone, Quartzite, Rhyol.	10	9.4	2.41	4.6	0.895
	38		2.39	4.4	0.937
	66		2.36	4.2	0.983
Monticello/ Sandstone, Graywacke, Quartz	10	9.4	2.34	4.3	0.941
	38		2.31	4.0	0.992
	66		2.28	3.7	1.046
Anchor/ Andesite, Latite, Limestone	10	8.1	1.70	3.2	0.950
	38		1.70	3.0	1.013
	66		1.71	2.8	1.079

*ICOLD Bulletin: The Physical Properties of Hardened Conventional Concrete in Dams*  
 Section 6 (Thermal properties)

Tab. 6.5 – Thermal properties of mass concrete dams (II) [6.23] [6.26]

<b>Dam/ aggregate</b>	<b>°C</b>	<b>Coeff. linear expansion</b> μm/m °C	<b>Thermal conductivity</b> kcal/mh °C	<b>Thermal diffusivity</b> m <sup>2</sup> /h * 10 <sup>-3</sup>	<b>Specific heat</b> k J/kg °C
Glen Canyon/ Limestone, Chert, Sandstone	10	-	3.19	6.0	0.908
	38		3.06	5.5	0.971
	66		2.94	4.9	1.033
Flaming Gorge/ Limestone, Sandstone	10	-	2.65	5.0	0.925
	38		2.60	4.6	0.979
	66		2.58	4.3	1.038
Yellowtail/ Limestone, Andesite	10	7.7	2.31	4.2	0.946
	38		2.26	3.9	1.000
	66		2.20	3.6	1.054
Libby/ Natural quartz Gravel	36	10.8	3.32	6.2	0.920
Dworshak/ Granite, Gneiss	36	9.9	2.01	3.9	0.920
Ihla Solteira/ Quartzite, Basalt	36	12.5	2.58	4.6	0.920
Itaipu/ Basalt	36	7.8	1.58	2.7	0.975

## 6.7 IN SITU MEASUREMENTS OF CONCRETE TEMPERATURES

In situ temperature measurements in concrete dams are important both in the construction phase and during the normal service life of the structure.

The knowledge of the spatial distribution and the temporal development of internal temperature rise, due to the concrete hydration, is essential to control the induced thermal stresses and to prevent the consequent cracks. The concrete temperature value, which causes a stage of no-stress (Fig. 6.11) is called zero-stress temperature [6.28] [6.29]. The higher the zero-stress temperature of the concrete and the temperature decrease to an average ambient temperature is, the higher is the resulting potential of thermal induced cracking [6.30]. In situ temperature measurements are also used to control the cooling process during the grouting operations.

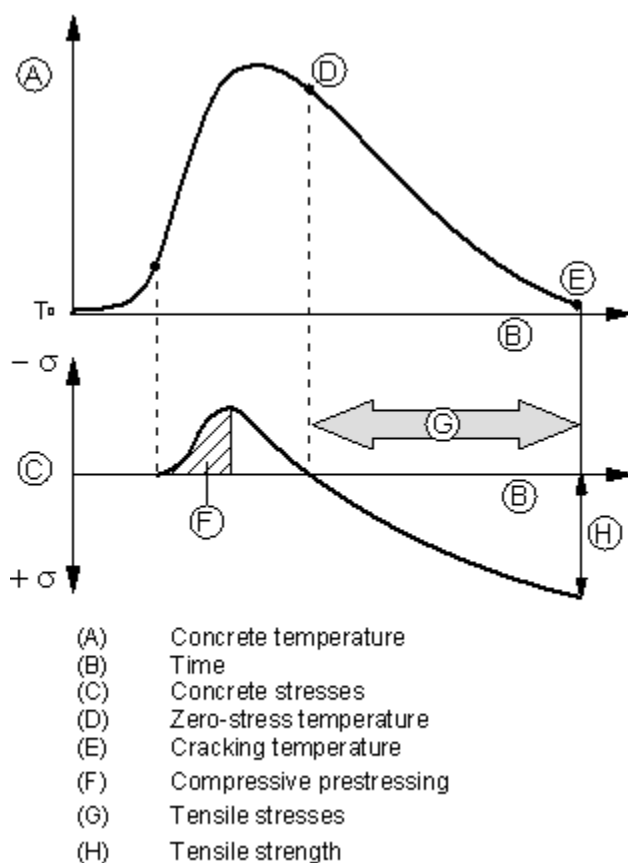


Fig. 6.11 – Stress in young concrete under restrained deformation [6.30]

During the normal service life, the temperature inside of the dam body varies according to the water and air temperature and significant temperature differentials depend on the reservoir and seasonal fluctuation (Fig. 6.12), and are a significant loading for thin dams only.

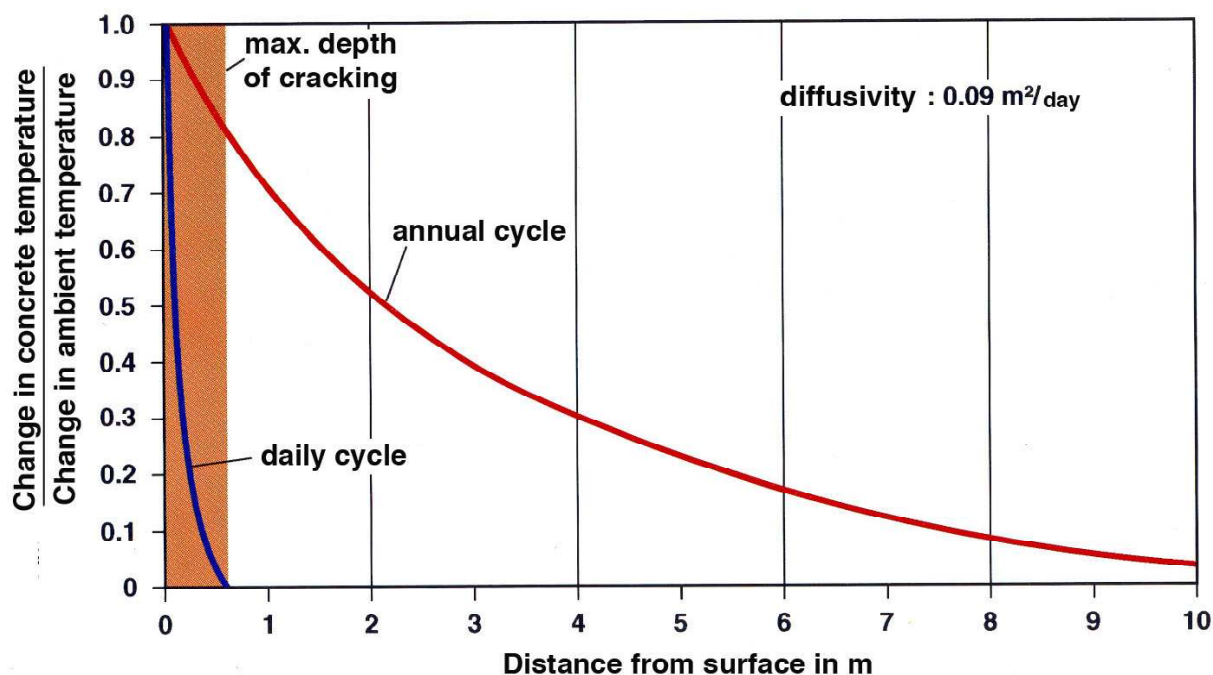


Fig. 6.12 - Influence of ambient temperature cycles on concrete depth

The temperature measurements are important for some dams to determine the causes of dam deformation due to expansion or contraction and to compute actual movements [6.31]. They are very important particularly in thin arch dams since volume change caused by temperature fluctuation is a significant contributor to the loading on such dams.

The temperature in concrete dams may be measured using any of several different kinds of embedded thermometers or by simultaneous temperature readings on devices. The most commonly ones are resistance temperature detectors (RTD's) and vibrating wire sensors. Both provide long-term stability and accuracy. They are to be placed non uniformly along the width of the dam in order to respect the higher temperature gradient towards the faces, Fig. 6.13.

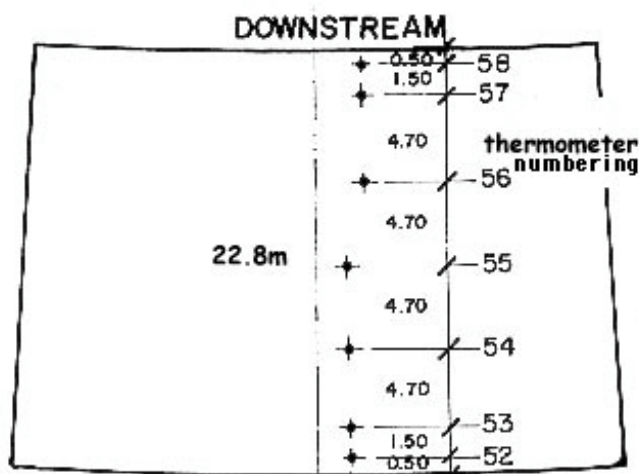


Fig. 6.13 – Typical arrangement of thermometers along the width of an arch dam.

According to the US Army Corps of Engineers [6.32], “thermometers are preferred over thermocouples because they have been more dependable, have greater precision, and are less complicated in their operation. Standpipes filled with water have also been used as a substitute for temperature measurement during construction. In using a standpipe, a thermometer is lowered into the standpipe to the desired elevation and held there until the reading stabilises. Standpipes can be an effective way to obtain vertical temperature gradients but are not practical for measuring temperature variation between the upstream and downstream faces of the dam. The addition of several standpipes through the thickness of the dam will add extra complications to the overall construction process. Standpipes also tend to indicate higher temperatures than thermometers”.

A typical location of thermometers in an arch dam is reported in Fig. 6.14 [6.33].

Usually, concrete temperatures are monitored only through spot measurements. However, recently the technology of fibre optic cables provide the possibility of continuous inline temperature measurements along the fibre cable integrated into the dam structure. This technology allows very accurate and economic measurements of temperature distributions in mass concrete. Examples of applications of the technique of Distributed Fibre optic Temperature Measurements (DFTM) on concrete dams are reported in [6.30] and [6.34] and illustrated in Fig. 6.15.

The thermal history of concrete obtained from the in situ-measurements of temperature are to be used for comparison with thermal numerical studies in a back analysis, where

- (a) the analytical model can be calibrated with the measured temperatures in the concrete, and
- (b) the evolution of temperature and control of cracking can be foreseen by adequate calculations, using adequate “thermal models”.

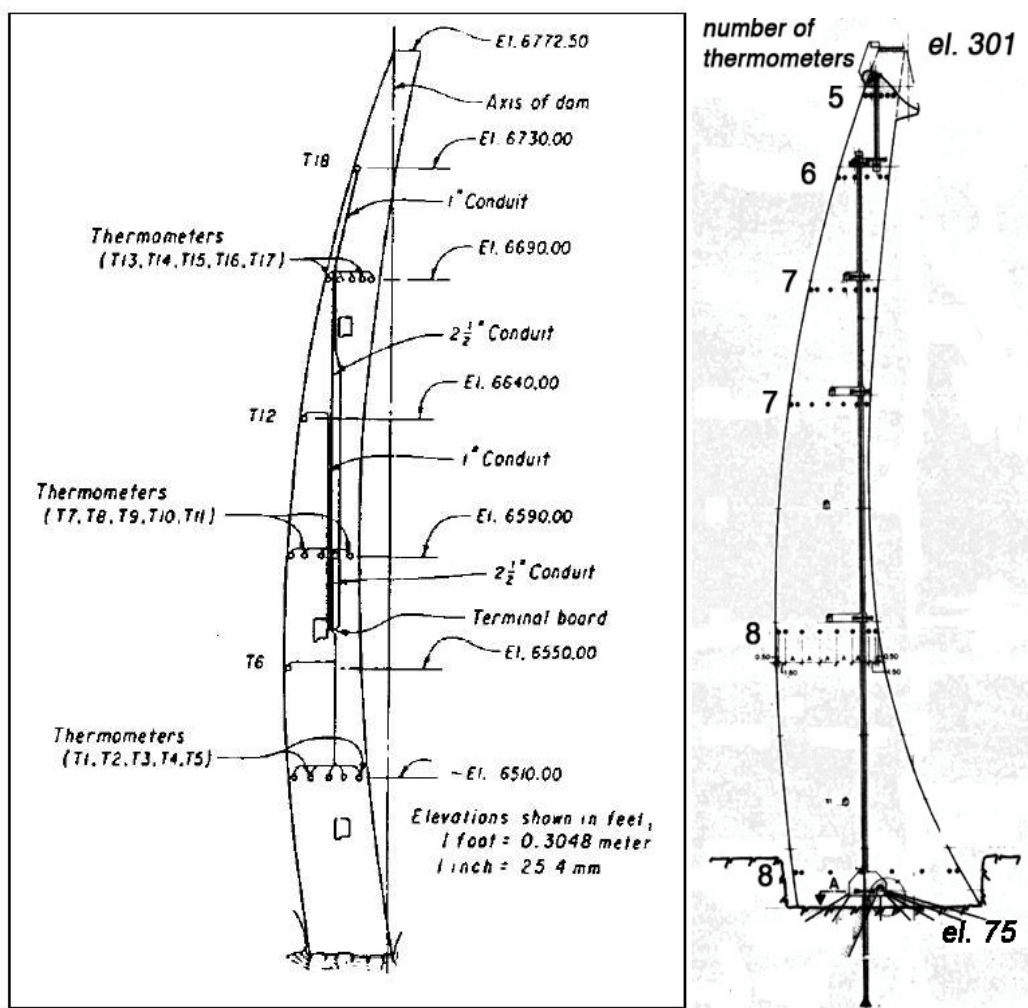


Fig. 6.14 – Layout for thermometer installation from [6.33] (on the left) and from Francisco Morazán Dam – Honduras (on the right) – note the ununiform arrangement of thermometers across thickness

ICOLD Bulletin: The Physical Properties of Hardened Conventional Concrete in Dams  
 Section 6 (Thermal properties)

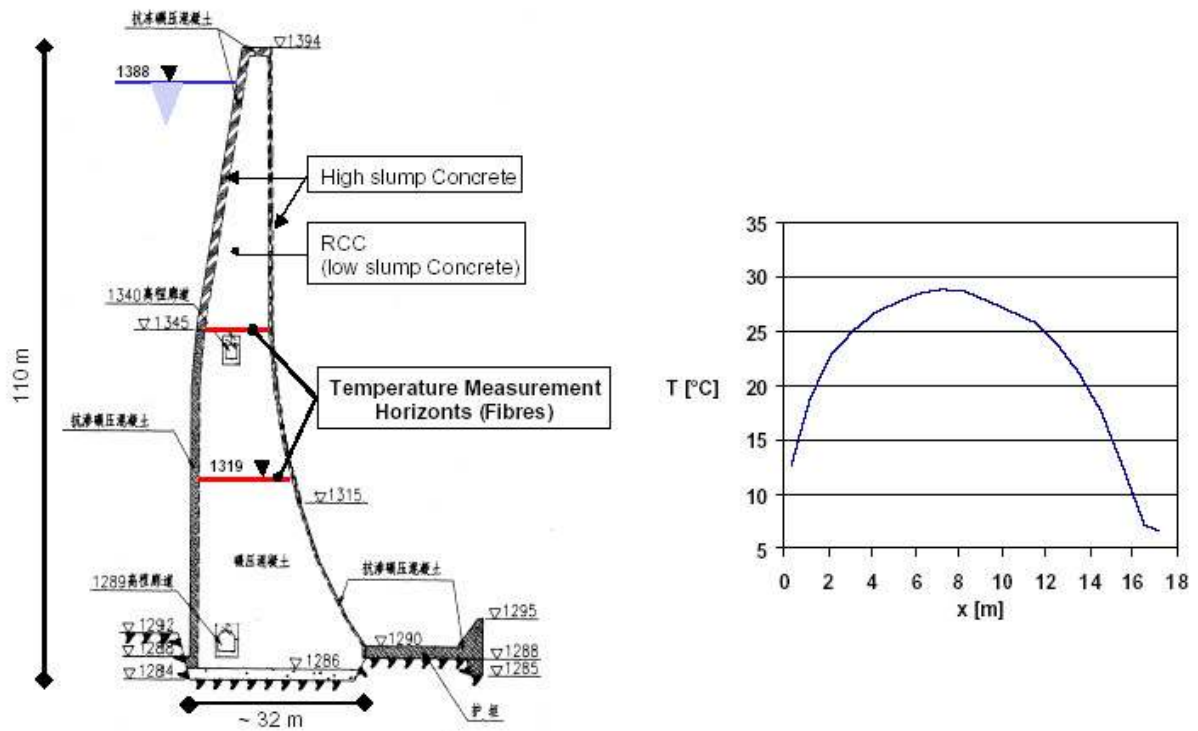


Fig. 6.15 – Cross section of the Shimenzhi arch dam and temperature distribution over the section 1319 (obtained through the horizontal fibres), 170 days after concreting (ambient temperature ~0 °C) [6.34]

## 6.8 REFERENCES

- [6.1] Guerra, E.A., Fontoura, J.T.F., Bittencourt R.M. and Pacelli, W.A., "Mass Concrete Properties for Large Hydropower Constructions", FURNAS CENTRAIS ELETRICAS SA.
- [6.2] Penwarden, A. D., "Measurement of the heat of hydration of concrete using an insulated cube", Building Research Establishment. England, Internal Report N95/86, September 1986.
- [6.3] Tse, F.S., Morse I.E., "Measurement and Instrumentation in Engineering", m. Dekker, New York, 1989.
- [6.4] Forrester, J.A., "A conduction calorimeter for the study of cement hydration", Cement Technology, Vol. 1, No. 3, p. 95-99, 1970,
- [6.5] National Concrete Pavement Technology Center "Developing a simple rapid test for monitoring the heat evolution of concrete mixture for both laboratory and field application", Centre for Transportation Research and Education, Iowa State University (USA), Final report, January 2006.
- [6.6] Kreuzer. H., Personal Communication
- [6.7] Morabito, P. "Thermal Properties of Concrete", IPACS – Improved Production of Advanced Concrete Structures, Report BE96-3843/2001:18-4, 2001.
- [6.8] Costa, U., "A simplified model of adiabatic calorimeter", Il Cemento, Vol. 76, No.2, pp. 75-92, April 1979.
- [6.9] Morabito, P., "Measurement of the thermal properties of different concretes", High temperatures High Pressures, Vol.21, p. 51-59. 1989.
- [6.10] Neville, A. M., "Properties of concrete", Pitman Publishing Ltd. London, 1975.
- [6.11] Beugel, K., Van "Artificial cooling of hardening concrete", *Research Report No. 5-80-9*, 1980.
- [6.12] Morabito, P., "An in-situ method for thermal conductivity and diffusivity measurements", Proceedings of In-situ Heat Measurements in Buildings, Hanover 1990.
- [6.13] British Standards Institution BS 4550, "Methods of testing cement. Part. 3. Physical Tests", 1978.
- [6.14] American Society for Testing Materials ASTM. C 186 86, "Standard test method for heat of hydration of hydraulic cement", 1986.
- [6.15] DIN, 1164, Pt.8.
- [6.16] Association Francaise de Normalisation, "Blinders measurement of hydration heat of cements by means of semi adiabatic calorimetry (Langavant Method)", AFNOR NF P 15 436, 1983.
- [6.17] Suzuki, Y. et al., "Method for evaluating performance of testing apparatus for adiabatic temperature rise of concrete", Concrete library of JSCE, No. 14, March 1990.
- [6.18] Suzuki Y. et al., "Evaluation of adiabatic temperature rise of concrete measured with the new testing apparatus", Concrete Library of JSCE, No 13, June 1989.



*ICOLD Bulletin: The Physical Properties of Hardened Conventional Concrete in Dams*  
Section 6 (Thermal properties)

- [6.19] Yokota, N., "Testing apparatus for measuring temperature rise", The Cement Association of Japan, Review 1985.
- [6.20] Morabito P. et al., "Measurement of adiabatic temperature rise in concrete", CONCRETE 20000. Proceedings of the International Conference, Vol. 1, p. 749-759, 1993.
- [6.21] Wainwright, P. J. and Tolloczko, J. J. A., "A temperature Matched curing system controlled by microcomputer", Magazine Concrete Research. Vol. 35, No. 124, p. 164 169, September 1983
- [6.22] Alegre, R., Cement Calorimetry at the French Hydraulic Binders Research Institute (CERILH), Report No. 333-hc/62 Pt I Adiabatic Calorimeters.
- [6.23] American concrete Institute, "Manual of concrete practice", Part I. ACI 213R-79, ACI 207.1R-70, ACI 207.2R-73, ACI 207.4R-80, 1978.
- [6.24] Equipe de FURNACES, Laboratorio de Concreto, "Concretos, massa, estrutural, projetado e compactado com rolo", Walton Pacelli de Andrade Edition, Pini, Sao Paulo, Brazil, 1997.
- [6.25] Scanduzzi L., Andriolo F.R., "Concreto e seus Materiais: propriedades e ensaios", Pini, Sao Paulo, Brazil, 1986.
- [6.26] Bureau of Reclamation, "Properties of mass concrete in Bureau of Reclamation dams", Concrete Laboratory report n° C-1009, Denver, Colorado (USA), 1961.
- [6.27] Sudhindra, C., Suri, S.B., Ravinder Singh, Varshney J.P., "Role of mica in sand on the strength and thermal characteristics of concrete", 16<sup>th</sup> Int. Conf. On Large Dams, San Francisco (USA), Q. 62, R. 29, 1988
- [6.28] Mangold, M., "Die Entwicklung von Zwang- und Eigenspannungen in Betonbauteilen während der Hydratation", Berichte aus dem Baustoffinstitut der Technischen Universität München. München, Heft 1/1994.
- [6.29] Plannerer, M. "Temperaturspannungen in Betonteilen während der Erhärtung" Dissertation, Technische Universität München, München, 1998.
- [6.30] Aufleger, M., Conrad, M., Strobl, Th., Malkawi, A.I., Duan, Y., "Distributed fibre optic temperature measurements in RCC-Dams in Jordan and China", In: Roller Compacted Concrete Dams, Proc. of the 4<sup>th</sup> Int. Symp. on Roller Compacted Concrete (RCC) Dams, Madrid, 17.-19.11.2003. Ed.: Berga, L.. Lisse: Balkema, 2003, p. 401 - 407.
- [6.31] Stucky, A., Derron, M.H., "Problèmes thermiques posés par la construction des barrages - réservoirs", Lausanne, Sciences et Technique, 1957, Publication EPUL n° 38.
- [6.32] US Army Corps of Engineers, "Engineer Manual EM 1100-2-2201", Chapter 12: Instrumentation, <http://www.usace.army.mil/publications/eng-manuals/em1100-2-2201/c-12.pdf>, 1994.
- [6.33] USBR, "Concrete Dam Instrumentation Manual," October 1987.
- [6.34] Aufleger, M., Conrad, M., "Fibreoptical Temperature Measurements in Hydraulic Engineering", Institute and Laboratory for Hydraulic and Water Resources Engineering Technische Universität München (D), 2000, [http://www.wb.bv.tum.de/forschung/aufleger/glasfaser\\_e.pdf](http://www.wb.bv.tum.de/forschung/aufleger/glasfaser_e.pdf).

## 7 WATER PERMEABILITY

<b>7.1 INTRODUCTION .....</b>	<b>2</b>
7.1.1 <i>Influence of permeability on the dam behaviour .....</i>	2
7.1.2 <i>Permeability in porous media and concrete .....</i>	3
7.1.3 <i>Water in concrete .....</i>	4
7.1.4 <i>Permeability of cement paste .....</i>	5
7.1.5 <i>Permeability of aggregate .....</i>	6
7.1.6 <i>The permeability of concrete .....</i>	7
<b>7.2 FACTORS INFLUENCING THE CONCRETE WATER PERMEABILITY .....</b>	<b>10</b>
7.2.1 <i>General .....</i>	10
7.2.2 <i>Cracks or cavities .....</i>	10
7.2.3 <i>Internal humidity .....</i>	11
7.2.4 <i>Curing conditions .....</i>	12
7.2.5 <i>Degree of hydration .....</i>	14
7.2.6 <i>Water cement ratio .....</i>	15
7.2.7 <i>Large air- or water-filled pores .....</i>	15
7.2.8 <i>Porosity and pore size distribution .....</i>	16
7.2.9 <i>Type, size and amount of aggregate .....</i>	18
7.2.10 <i>Type of cement .....</i>	18
7.2.11 <i>Leaching, self sealing or deposit of material inside a dam .....</i>	18
7.2.12 <i>Workability and placing .....</i>	20
7.2.13 <i>The viscosity of water .....</i>	21
7.2.14 <i>State of stress .....</i>	21
<b>7.3 TEST METHODS FOR WATER PERMEABILITY .....</b>	<b>22</b>
7.3.1 <i>General .....</i>	22
7.3.2 <i>Preparation of specimens .....</i>	24
7.3.3 <i>The test cell .....</i>	25
7.3.4 <i>The pressure side .....</i>	27
7.3.5 <i>Water flow measuring .....</i>	27
7.3.6 <i>Expression of results .....</i>	28
<b>7.4 MODELING WATER PERMEABILITY IN SATURATED CONCRETE .....</b>	<b>30</b>
7.4.1 <i>Introduction .....</i>	30
7.4.2 <i>Macroscopic (non-pore space) models for mass concrete .....</i>	30
7.4.3 <i>Microscopic (-pore space) models for more detailed studies .....</i>	32
7.4.4 <i>Combined water flow in a "real dam" .....</i>	34
<b>7.5 REFERENCES .....</b>	<b>35</b>

## 7.1 INTRODUCTION

### 7.1.1 *Influence of permeability on the dam behaviour*

The permeability of concrete, or how readily water penetrates it, is usually regarded as the single most important property determining the durability of concrete in dams. The permeability has also other influences on the dam behaviour such as on the uplift forces. Some of the influences are mentioned below and also shown in Fig. 7.1

**Leaching:** Highly permeable concrete is more vulnerable to leaching, i.e. water dissolving hydration products making the concrete even more permeable, softer, weaker and vulnerable to other attacks such as freeze-thawing. etc. Leaching phenomena are specifically dealt in the ICOLD Bulletin n° 71 of 1989 (“Exposure of dam concrete to special aggressive waters – Guidelines”).

**Aggressive constituents** (e.g. sulphates, chlorides, carbon acid) can be conveyed more easily in concrete with higher permeability, and the effect of soft reservoir water is intensified.

**Freeze-thawing:** Freeze-thawing attacks are highly dependent on the content of moisture in the concrete. Higher permeability means more concrete parts with higher moisture content and a higher risk for freeze-thawing damages. Sometimes “curtains” of calcite are formed due to leaching on the downstream surface of dams and behind these curtains water are accumulated, which often lead to freeze-thawing damages. The frost resistance of concrete in dams is examined in this Bulletin, in the following Section 8.

**Pore-pressure:** In a concrete with high permeability, water is easier sucked or pressed into the concrete whereby the pore pressure more easily is built up, with increasing uplift pressure. If a dam has sections with different permeability, the pore pressure will also differ between the sections. A special case is when leaking water meets CO<sub>2</sub> at the downstream end and rather tight CaCO<sub>3</sub>-curtains is formed, making pore pressure increase in the concrete.

**Alkali-Aggregate Reaction (AAR):** The alkali-aggregate reaction (AAR) is a reaction between alkali in the pore solution and aggregate reactive for alkali. A gel is formed. In concrete with high content of alkali, reactive aggregate and with an external source of humidity the formation of the gel may be sufficient to cause internal expansion and severe cracking. The permeability is one of the governing properties influencing the supply of water. References could be found in the ICOLD Bulletin n°79 of 1991 (“Alkali-aggregate reactions in concrete dams: review and recommendations”).

**Reinforcement corrosion:** As a consequence of leaching the pH-value will drop in the concrete around embedded reinforcement bars, reducing the passiveness and increasing the potential for corrosion.

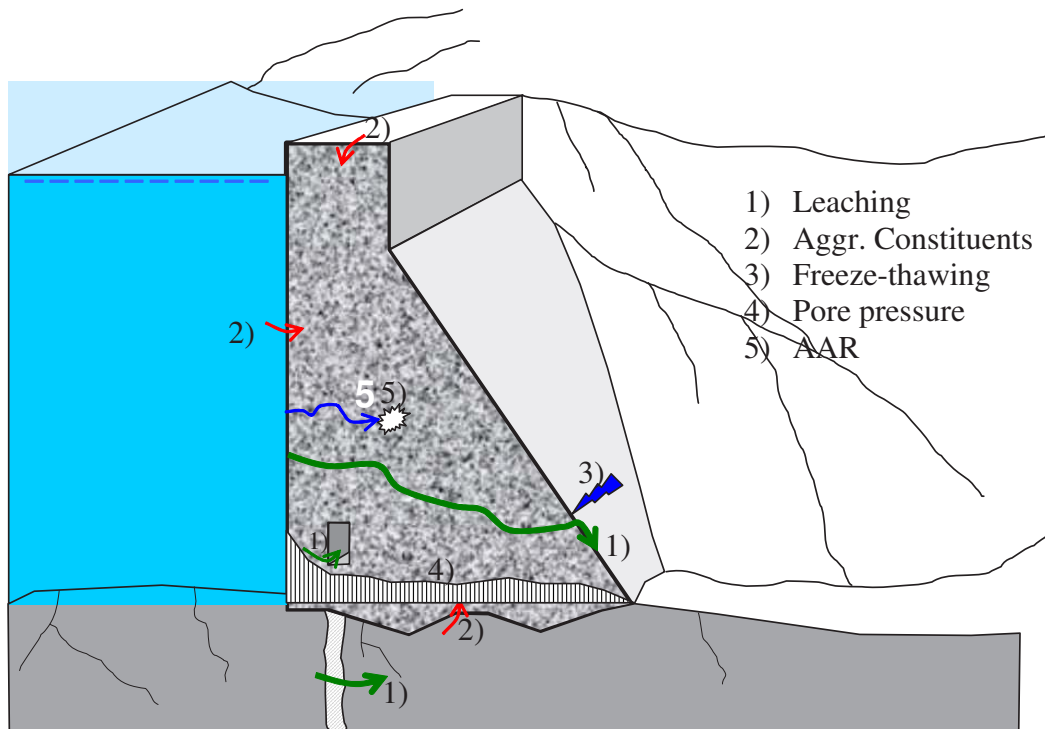


Fig. 7.1 – Different types of environmental attacks on a concrete dam

### 7.1.2 Permeability in porous media and concrete

The permeability of a porous medium is a measure of how readily a fluid penetrates it. Water permeability is often used to denote a number of different mass transfer mechanisms. The diffusion of water moisture, the absorption or desorption of water on the pore walls, liquid flow due to capillary suction, and unsaturated or saturated liquid flow due to external pressure have all been referred to rather loosely in the literature as permeability.

However, permeability mostly refers to homogenous steady-state percolation of water through water-saturated material (Darcian flow). A common mathematical way to describe such permeability is by the well known Darcy's law [7.1]:

$$q_w = k_w \cdot dP/dx \cdot A \quad (7.1)$$

where  $q_w$  = flow of water ( $m^3/s$ );

$k_w$  = permeability coefficient (m/s);

$dP/dx$  = pressure gradient (m/m);

$A$  = cross section area ( $m^2$ ).

Although it would be desirable to be able to find a geometric quantity for characterising the geometry of pores generally, they unfortunately diverge and converge as well as differing markedly in scale, making them very difficult both to measure and to model. The smaller the pores, the greater the effect of the pore walls on the hydrodynamic phenomena. The flux of a fluid tends to occur where it can flow most easily, i.e. in the larger connected pores or cracks.

The flow channels involved can differ very much in shape and origin. During the lifetime of concrete, flow channels can be formed, changed and closed again. The greater the number of flow channels there are in the concrete and the broader, less tortuous, smoother and more connected the flow channels are, the less the resistance is against water mobility and the greater amount of water can be transported.

The flow of water in a porous material can be characterised by a potential that forces water through the pores, and by the resistant forces that slow down the flow. In the case of capillary transport, both the driving force and the transport coefficient are a function of the geometry of the pore space, whereas in permeability the transport coefficient alone is a function of the geometry.

The permeability of concrete depends on the permeability of each phase of the concrete, and thus on

- the permeability of the paste
- the permeability of the aggregate
- the permeability of the interfacial zone

Permeability tests have historically been performed both on paste and concrete. Permeability tests on “mass” concrete as for thick concrete dams are found in the technical literature since the years 1920. Classical investigations are: McMillan & Lyse, 1930 [7.2]; Ruettgers, 1935 [7.3]; Mary, 1936 [7.4]; Mather & Callan, 1950 [7.5], Nycander, 1954 [7.6], Sällström, 1968 [7.7].

### **7.1.3 Water in concrete**

Concrete is a porous material with a strong ability to bind water hygroscopically. The gel pores in concrete have a size of  $\approx 10^{-9}$  m, about 4 to 5 times that of a water molecule. Capillary pores have a size of less than  $10^{-6}$  m [7.8]. They can be filled with water by capillary condensation.

The water contained in concrete is often classified into non-evaporable water ( $W_n$ ) (also denoted as chemically bound water), and evaporable water ( $W_e$ ). The evaporable water is often classified into water adsorbed on pore walls ( $W_{gel}$ ) and mobile water ( $W_m$ ). As can be understood by its name, mobile water is mainly involved in the mass transfer of water. How the water is fixed within the concrete depends on the geometry of the pore system, the type of solid material in the matrix, the humidity, and the thermodynamic balance between the pore system and the surroundings.

The water contained in concrete stems from different phases of construction and curing. For example,

$$W_{\text{tot}} = W_0 + W_{\text{curing}} - W_{\text{hydr}} + W_{\text{forced}} \quad (7.2)$$

where  $W_{\text{tot}}$  = total water;  $W_0$  = mixing water;  $W_{\text{curing}}$  = water added during curing;  $W_{\text{hydr}}$  = chemically bounded water present during hydration; and  $W_{\text{forced}}$  = water forced into the concrete during its life cycle, e.g. by capillary suction or as a result of external water pressure being imposed.

The water bound in concrete during the hydration,  $W_{\text{hydr}}$ , is usually estimated on the assumption that 1kg cement in average binds 0.25 kg water at complete hydration. That is

$$W_{\text{hydr}} = C \cdot \alpha / 4 \quad (7.3)$$

Where C = total amount of cement (kg); and  $\alpha$  = hydration ratio (-). See also 7.2.5.

#### **7.1.4 Permeability of cement paste**

In cement paste, which is free of defects, the degree of permeability depends on the number, size, shape and connectivity, as well as the relative humidity (RH) of the pores. The greater the amount of mixing water available, the greater the extent to which pores are formed during hydration. During the hydration process, the pores are filled to varying degrees with hydration products which lead to a decrease in porosity and connectivity and thus to a drop in permeability.

Fig. 7.2 presents results of a study by Powers et al. [7.9] concerning Darcian permeability in cement paste that was very well hydrated ( $\approx 93\%$ ). The permeability increases very rapidly when certain levels of the w/c ratio or of capillary porosity are reached. The fact that the relation appears to be about the same in both figures is not surprising, since in the Powers structural model capillary porosity is proportional to the w/c ratio. The very rapid increase in permeability at a capillary porosity of about 30% is partly due to larger capillaries and an increasing interconnection between the capillaries. The flow of water in a flow channel is proportional to the fourth power of the radius, which results in a very rapid increase of flow if the capillary radius is enlarged. It seems clear that the permeability of cement paste is controlled by its capillary porosity.

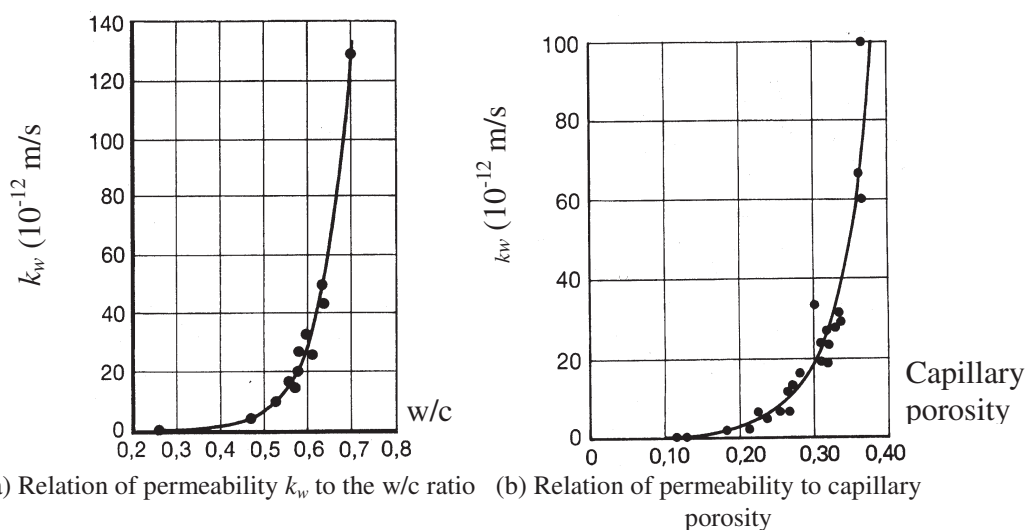


Fig. 7.2 - Water permeability of well hydrated cement paste in relation to (a) the w/c ratio and (b) capillary porosity (Powers et al. 1954 [7.9], presented by Fagerlund in [7.10]).

### 7.1.5 Permeability of aggregate

Despite its generally low porosity (below 3%), aggregate tends to have about the same level of permeability as cement paste [7.11] [7.12] (Tab. 7.1). This can be explained by the difference in typical size between the capillary pores in the paste (10 to 100 nm) and in aggregate (larger than 10  $\mu\text{m}$  in average) [7.12].

Tab. 7.1 - Comparison of the permeability of rocks and of cement paste [7.11].

Type of rock	Permeability (m/s)	W/c ratio of mature cement paste of the same permeability
Quartz diorite	$8.24 \cdot 10^{-14}$	0.42
Marble	$2.39-57.7 \cdot 10^{-13}$	0.48-0.66
Granite	$5.35-15.6 \cdot 10^{-11}$	0.70-0.71
Sandstone	$1.23 \cdot 10^{-10}$	0.71

### **7.1.6 The permeability of concrete**

This discussion about concrete permeability is mainly valid for mass concrete material and not always valid for mass concrete structures as a whole, e.g. dams. Mass concrete materials can be thought of as “defect-free” whereas mass concrete structures, such as dams, often have manmade discontinuities, as for example construction joints, or cavities, for example cracks due to different causes.

Although the reduction in flow area (when the porosity is lower for the aggregate than for the cement paste), segmenting of the flow channels and lengthening of the effective flow channels, suggests that the permeability of concrete should be less than that of cement paste, the permeability of concrete is in fact about 100 times as high as that of the corresponding cement paste [7.13]. The major explanation for this is that the addition of aggregate produces a porous interfacial zone between the aggregate and the paste and that micro-cracks are formed there during hydration [7.12].

The permeability of the interfacial zone is governed mainly by the pore size distribution within the zone, the crystals within the zone (mainly  $\text{Ca}(\text{OH})_2$ ) and micro-cracks within the zone. The interfacial zones are weak and relatively porous and are vulnerable to differential strains between the cement paste and the aggregate induced by drying shrinkage, thermal shrinkage and externally applied loads, such strains resulting in micro-crack. No direct measurements of the permeability of the interfacial zone can be found in the literature.

The flow of water through concrete is the sum of all leakage of water through it, ranging from large-scale flow in large connected and water-filled cracks and cavities (e.g. honey combing, beneath aggregate, along rebar, etc) to very low levels of vapour diffusion through the capillary pores. In defect-free concrete, such as mass-concrete, flow occurs in capillary pores and the porous transition layer around the aggregate. Defects in concrete, such as cracks, can have permeability many orders as high as that of the concrete itself, its level depending on the size of the cracks and on how connected they are within the concrete.

The amount of pores present in the cement paste phase is typical in the order of 35-50% of the volume. In for example ordinary aggregate of granite the pores represent approximately 0.5-1% of the volume. Within the whole concrete, i.e. including both cement paste and aggregate, the porosity is on the order of 10-20 %.

The driving potentials for water flow in a concrete dam exposed to water at the one side and either air or water at the other side is schematically shown in Fig. 7.3. In the figure the conditions are presented at a relative short time after impounding Fig. 7.3 a) and after long time after the reservoir has been filled (Fig. 7.3 b). Water transport is due to a combined flow of different mechanisms such as vapour diffusion and capillary suction in not water saturated concrete and external over-pressure in saturated concrete.



*ICOLD Bulletin: The Physical Properties of Hardened Conventional Concrete in Dams*  
 Section 7 (Water permeability)

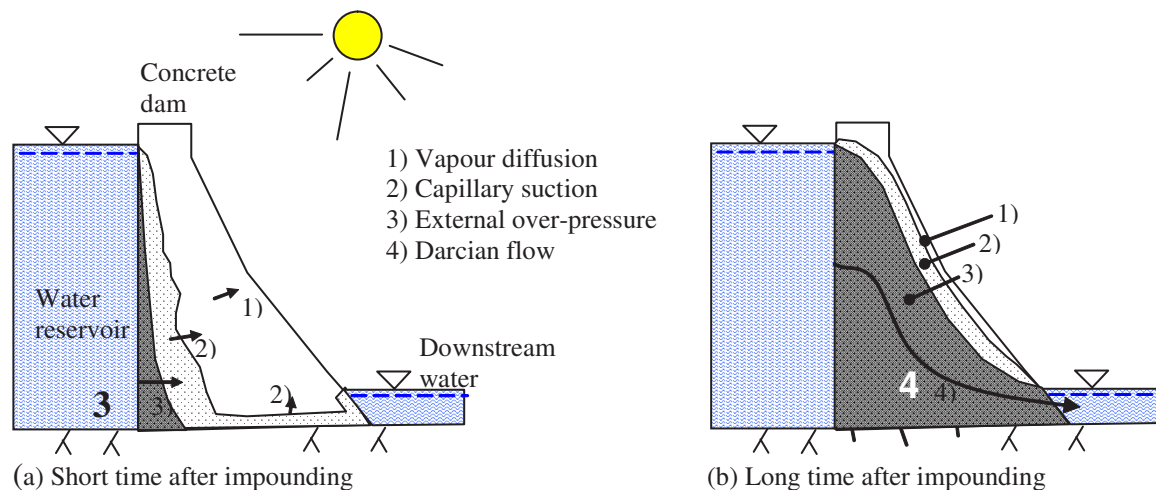


Fig. 7.3 - Scheme of the driving potentials for the flow of water in a concrete dam exposed to water at the one side and either air or water at the other, where (a) shows the conditions found a relative short time after the reservoir has been filled and (b) the conditions long after the reservoir has been filled.

The permeability of i) plain cement paste, ii) the paste phase in concrete and iii) of concrete is shown in Fig. 7.4, on the basis of different studies. The figure indicates that permeability decreases as the hydration ratio increases, the permeability increases as higher w/c-ratios are used, and the permeability increases for concrete compared to plain cement paste. It is also shown that the permeability increases if bigger aggregate particles are used, which also other studies show [7.10]. In reality there is a large scatter in permeability measurements depending on type of curing, type of aggregate, size of the concrete, etc, which can be seen in Fig. 7.5, showing different studies of the permeability of cement paste and concrete.

According to Hearn [7.14], the results of individual studies have shown a direct proportionality between permeability and the w/c ratio, although the data for different studies show a high degree of scatter in relation to each other (Fig. 7.5). This is probably due to differences in specimen treatment and in test procedures, which is important to bear in mind when comparing different permeability studies.

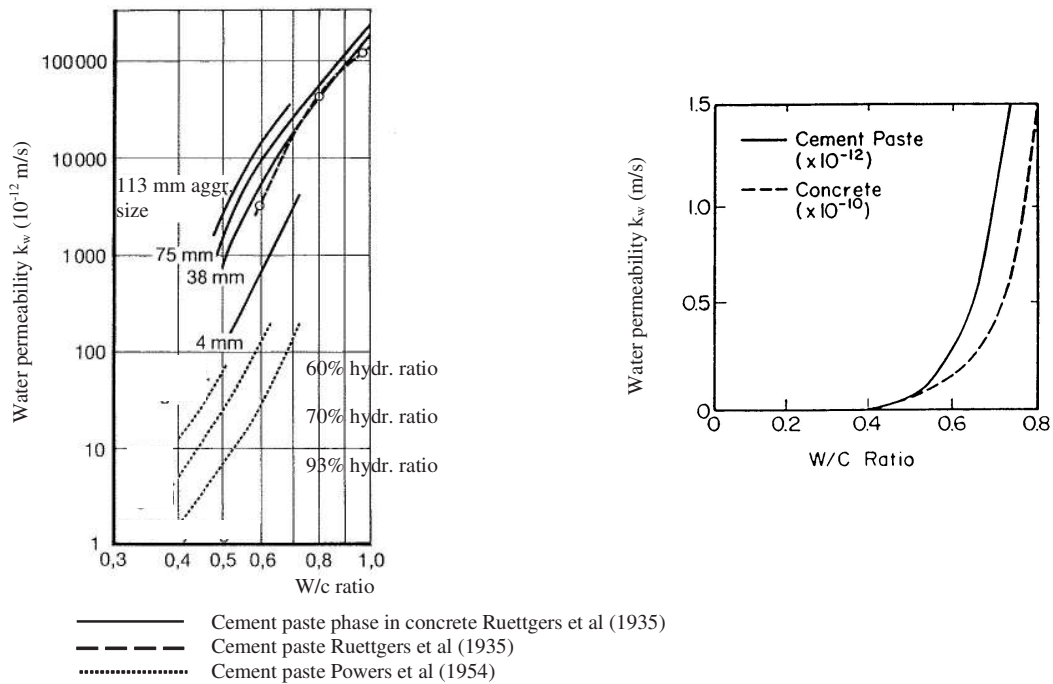


Fig. 7.4 - (a) Permeability to water for various cement pastes and for the cement paste phase in various concretes [7.10]. Observe that the permeability shown for the “paste phase in concrete” (solid line) is for the paste phase in the concrete only, which means that for having the permeability for concrete the values should be multiplied with the share of cement paste. b) Water permeability for cement paste and for concrete [7.13].

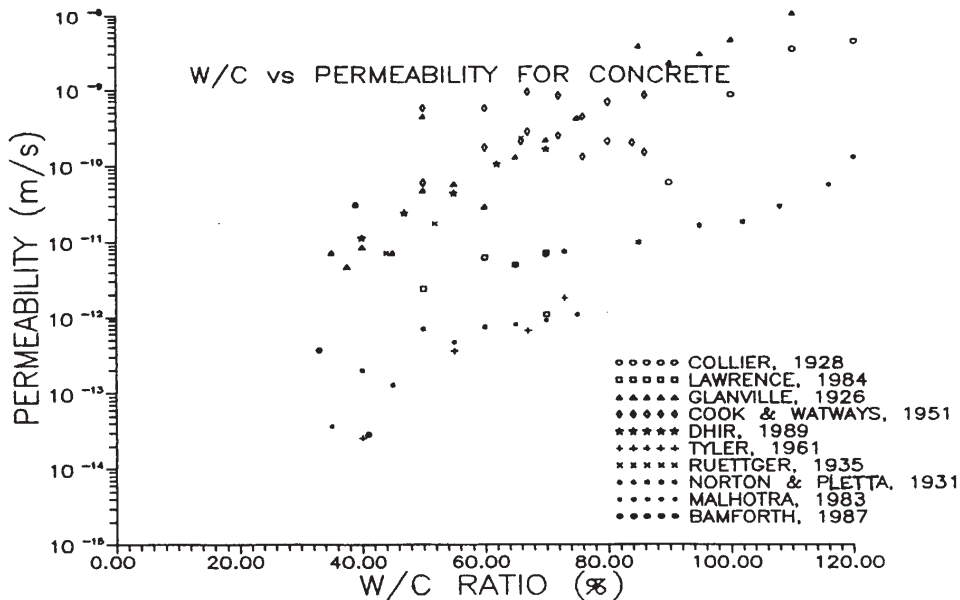


Fig. 7.5 - Correlation between the w/c-ratio and the permeability of concrete on the basis of data from different studies [7.14]. Note the high degree of scatter, probably due to differences in specimen treatment and in test procedures,

## **7.2 FACTORS INFLUENCING THE CONCRETE WATER PERMEABILITY**

### **7.2.1 General**

Permeability of concrete may be divided in:

- \* Laboratory tested permeability
- \* Permeability of mass concrete in a dam
- \* Permeability of the overall dam structure(including joints and interfaces)

It can be said generally that all factors that enlarge, connect or straighten existing flow channels or create new flow channels increase the permeability of the concrete. Since the flow of water in tube-like pores can be said to be proportional to the pore diameter raised approximately to the power of 4 and in a crack the thickness raised approximately to the power of 3, the flow obviously increases rapidly as pores and cracks become wider and more connected.

### **7.2.2 Cracks or cavities**

Cracks or other cavities can be formed due to various factors: man-made joints, imperfect compaction, thermal shrinkage during the cooling period after casting, shrinkage due to drying, flow channels along the reinforcement bars due to water separation and to settlement of the concrete mass, due deflection, due to seasonal changes in temperature, elastic strain and creep and due to externally applied loads. The cracks are found mainly in the interfacial zone between paste and aggregate, but are found in the paste as well. Micro-cracks are always larger than capillary pores. They propagate from one discontinuity to another, creating more or less continuous flow channels throughout the cement matrix. The curing period is particularly important, since drying and cooling produce large variations in stress in the concrete when it has not yet obtained any large degree of strength. The sooner the water curing of concrete starts, the more quickly the concrete gains in strength and the smaller the stresses due to differences in temperature and moisture are. In the massive concrete of dams, cracks are easily formed due to large temperature differences during hardening and along construction joints, unless suitable actions (such as cooling) are undertaken to prevent cracks from being formed. Around water-stopping bands in joints, around embedded steel for gate abutment or in other parts in dams where imperfect compaction may occur, the permeability is often higher than in the mass concrete.

Leakage through cracked concrete can be approximated by using Poiseuille's law and introducing a correcting roughness coefficient for irregularities and crack tortuosity. Fig. 7.6 shows an example for potential leakage assuming a continuous crack (or leaking lift joint). It indicates the importance of high quality (facing) upstream concrete in order to avoid excessive leakage into dam galleries.

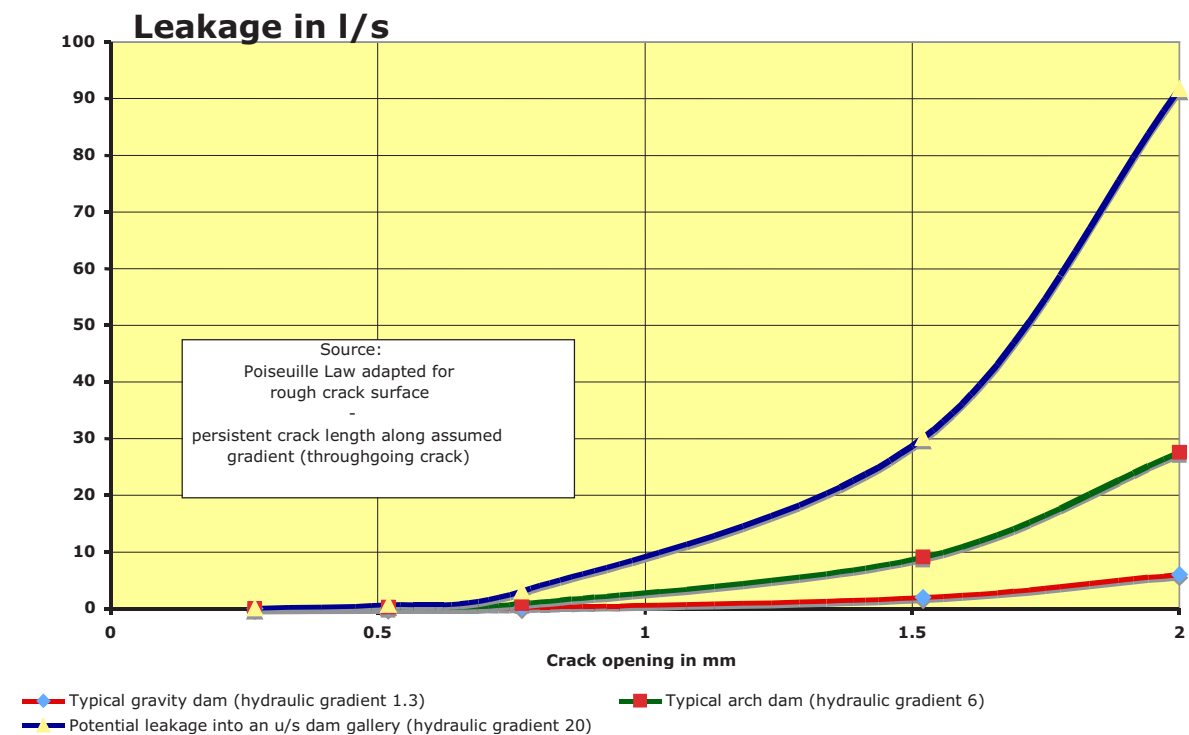


Fig. 7.6 – Leakage along cracked concrete or defect lift joints.

### 7.2.3 Internal humidity

The humidity of the concrete has an important influence on the water permeability. The solid phase changes due to shrinkage or swelling or to chemical reactions, leading to changes in the geometry of the pore system. The moisture content itself influences the extent to which water can flow through the pore system.

In a dam there may be many combinations of moisture conditions throughout the structure, the flow of water being a function of many different types of transport mechanisms. Fig. 7.3 and Fig. 7.7 show in principle how water can be transported through concrete subjected to water on one side and air on the other, e.g. as in a real dam. In the upstream end and as long as the flow channel is filled with water the flow is of a Darcian type. By flow channel is meant any capillary pore, micro-crack, joint, etc, where water is transported in. However, coming closer to the downstream end the channel becomes dryer and not completely filled with water. At RH above about 45 % curved water menisci are formed in narrow passages, leading to capillary condensation. In air-filled parts the water is transported as vapour diffusion along the channel. Some of the water/vapour may also be adsorbed on the walls of the channel, are stuck in very narrow pores or react chemically with compounds in the pore walls. Some pores are so isolated and difficult to reach by the water that they are filled with water first after a long period of water suction.

In thick concrete structures with a low w/c ratio there may be parts located in the interior, which have a humidity of less than 100 %, even if the concrete is always

covered with water. The reason is that much water is used in these parts during the hydration and external water has difficulties to reach these parts.

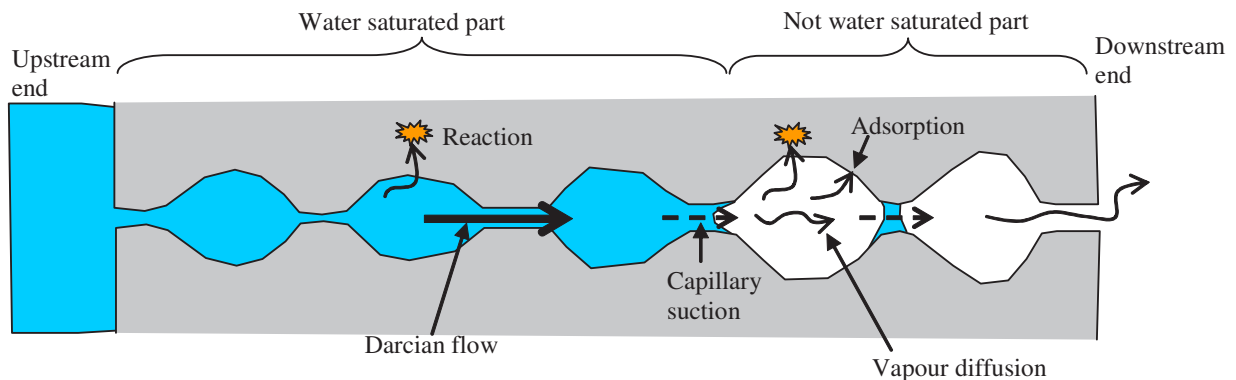


Fig. 7.7 - Movements or fixation of water molecules in saturated or dry pores of cement

#### 7.2.4 Curing conditions

The same type of curing in laboratory and in field are of course different. Adequate laboratory permeability is confirming a good pore structure (mix design) but it does not take into account the influence of work execution and early-age cracking (field curing).

Both the curing of concrete at an early degree of hydration, and the treatment conditions, present at later stages, influence the permeability of the concrete as a result of the formation of micro-cracks. The access to water, and use of an appropriate curing temperature, are of great importance for the tightness of concrete.

Fig. 7.8, Fig. 7.9 and Fig. 7.10 and show laboratory results of the influence of different curing conditions on the water permeability of concrete. The maximum size of the aggregate was 32 mm. The water pressure was applied to a surface of the specimens with a diameter of 170 mm (see paragraph 7.3.3). Fig. 7.8 shows the influence of different water curing times on the 28 day permeability, if curing is started one day after casting. If the curing last 1-5 days the permeability is highly reduced while the permeability is almost not affected by longer curing times. Fig. 7.9 shows the importance of that curing with water begins as soon as possible after casting. Fig. 7.10 shows the influence of different methods of curing on the permeability.

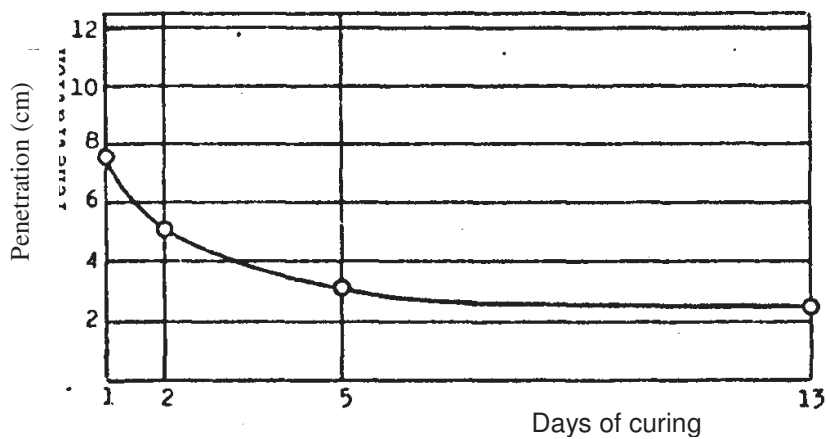


Fig. 7.8 - The influence of the duration of water curing on the permeability, if curing has started day after casting. Concrete w/c ratio = 0.7. Age of specimens at time of test = 28 days [7.6].

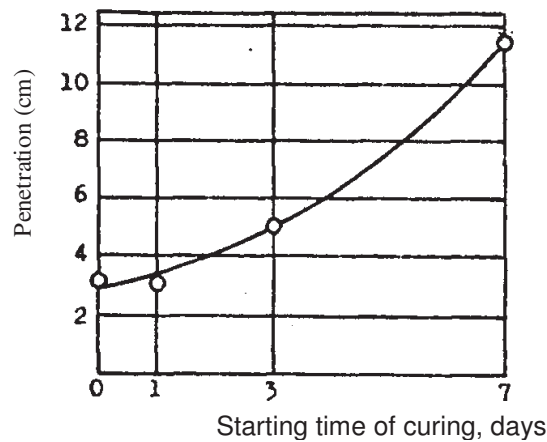


Fig. 7.9 – The influence of the starting time for water curing of five day. Concrete w/c ratio = 0.7 . Age of specimens at time of test = 28 days [7.6].

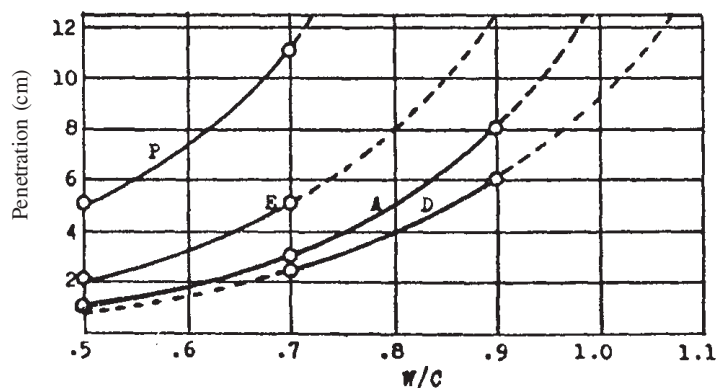


Fig. 7.10 - The influence of different w/c ratios and curing conditions on the penetration of water in concrete tested at 28 days. P = concrete for 14 days in watertight moulds and afterwards in laboratory air; E, A and D = concrete for 2, 5 and 13 days respectively in water prior to its being in laboratory air [7.6].

Powers and Copeland [7.9] showed by laboratory experiments that even in the case of a very slow drying to 79 % RH and re-saturation the coefficient of permeability increased 70-fold. Vuorinen [7.16] found the permeability to increase 100 times in initially fog-cured laboratory specimens if they were first dried at +105°C and then re-saturated. Even a short period of drying after demoulding can “destroy” the tightness of concrete, due to the formation of micro-cracks.

The pore size distribution of the paste phase in concrete is strongly influenced by the curing temperature. High temperatures increase the volume of large pores [7.13] and also lead to micro-cracking, which both lead to higher permeabilities. Ekström [7.17] found that if concrete specimens were heated at an early hydration age but not dried, the initial permeability was about 100 times as high as for virgin specimens, although it later decreased by a factor of about 100, probably due to continued hydration.

### 7.2.5 Degree of hydration

The permeability of concrete, mortar and cement paste is sensitive to the degree of hydration or age at which a permeability test is started. The permeability is much larger when testing is started at a young age [7.2], [7.3] and [7.9] (Fig. 7.11). Concrete exposed to penetrating water at an early age may seal due to continuous hydration. The degree of hydration (hydration rate) is typically around 0.9-0.95 for well hydrated concrete in dams after long time. However, the hydration ratio depends much on the availability of water. The lower the relative humidity (RH) the lower the hydration rate becomes and beneath RH 80% the hydration stops [7.18]. That means that in concrete structures where there might be somewhat dryer parts, as in parts with low w/c ratio or inside thick dams, the hydration ratio will be lower than 0.9 even after long time.

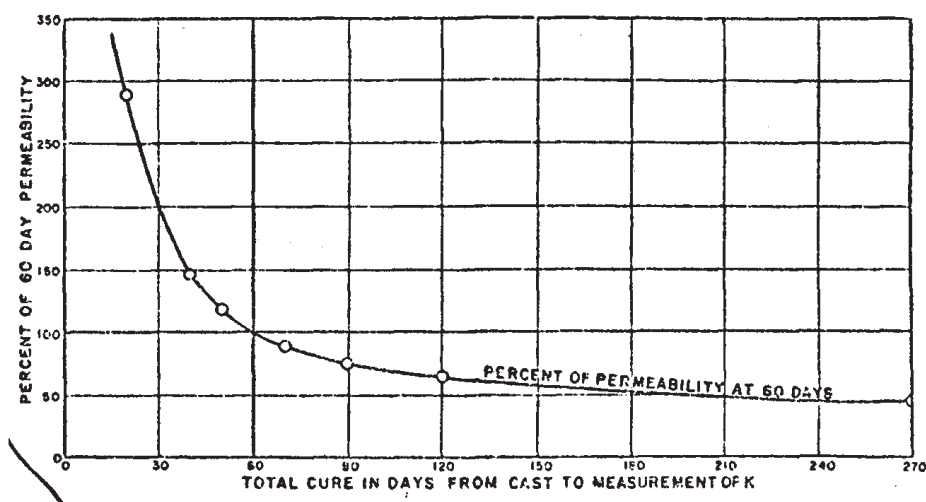


Fig. 7.11 - Effects of length of cure on permeability of concrete [7.3]

### **7.2.6 Water cement ratio**

The higher the w/c ratio, the higher the permeability of both the cement paste and the concrete is. Fig. 7.5 presents results of several investigations concerning the dependency of w/c on the permeability of concrete. The data in the figure include only specimens that were cured for at least 28 days and were tested without any pre-conditioning.

If superplasticizers are used a lower w/c ratio can be used for the same workability as a higher w/c ratio. A lower w/c ratio means a reduction of the permeability.

### **7.2.7 Large air- or water-filled pores**

In hardened concrete there exist air-voids “naturally” made in the compaction process. To improve the freeze-thawing resistance even more air-voids can be made if air-entraining agents are mixed into the fresh concrete. Air-voids prevent water from penetrating the concrete, leading to a lower permeability, as long as they are filled with air.

However, as the water pressure increases, the air is compressed, possibly allowing the water to pass. Also, the air bubble will gradually be filled by water. The higher the pressure, the easier it is for the air in voids to be dissolved in water. However, a long time is required before the air voids are completely filled with water, permitting the permeability to increase. Many authors [7.3] [7.19] [7.20] emphasize the long period of time, possibly hundreds of years that may be required before the water pressure becomes steady across a wide concrete section, such as the gravity dam shown in Fig. 7.12. Water is also sucked into the dam by capillary suction, increasing the saturation rate. A long time is required, nevertheless, before saturation is completed. In reality, water will penetrate more quickly if there are cracks or other cavities in the dam.



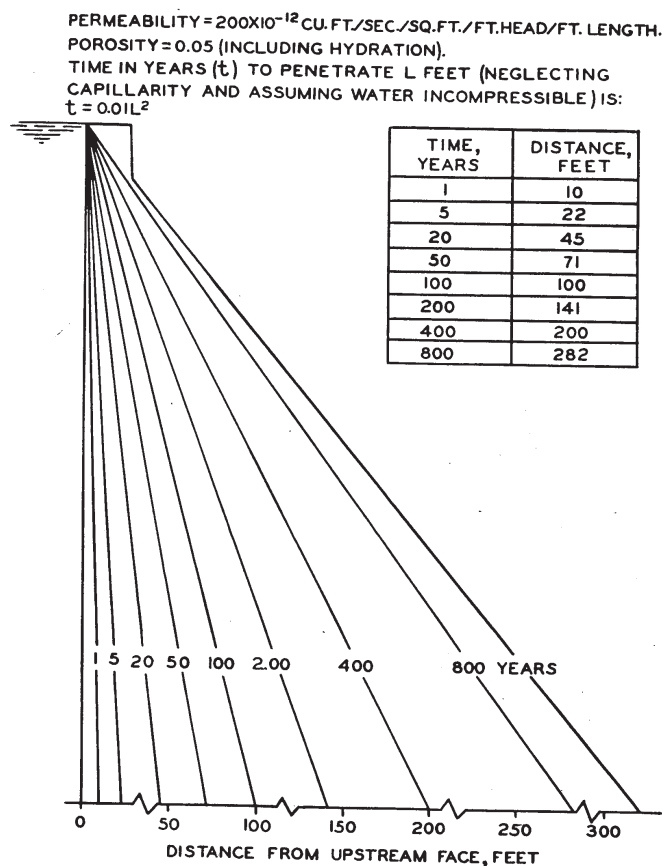


Fig. 7.12 - Calculated penetration of water into a 400-ft (122m) wide concrete dam for various durations of hydraulic head [7.19]. Permeability in figure =  $200 \cdot 10^{-12}$  (ft/s)  $\cdot 0.305$  (m/ft) =  $6.1 \cdot 10^{-11}$  m/s.

### 7.2.8 Porosity and pore size distribution

The hydration of cement results in cement paste in the concrete with two forms of pores: gel pores and capillary pores. The main flow of water goes in the capillary pores (or cracks if these are present), which are much larger than the gel pores, ranging from 10 nm up to 1  $\mu$ m in size. According to Hearn [7.14], Peer [7.21] has shown that pores smaller than  $10^{-7}$  m in diameter and with a length/diameter ratio of 2 or less do not contribute significantly to the water permeability of cement paste for water. With increasing degree of hydration, the capillary pore system becomes less connected, becoming filled with hydration products. Below a w/c ratio of approximately 0.7, the connections within the capillary pore system become largely blocked, whereas above w/c 0.7 no total blocking occurs [7.10].

Due to the highly complex pattern of the pore system in a porous material, no simple relation between porosity and permeability can be found [7.22]. Nyame and Illston [7.23] [7.24] conducted a study of the relationship between the permeability of hardened cement paste and its porosity and pore size distributions with the aim of gaining a better understanding of the significance of a threshold diameter in connection with permeability. The authors concluded that the hydraulic radius of the

pore system describes the measured permeability rather well (Fig. 7.13), except for pore sizes of close to molecular dimensions. They found permeability not to be a unique function of porosity, but to be dependent upon the w/c ratio as well, as can be seen in Fig. 7.14. The authors assumed continued hydration to subdivide the pore system into many unconnected pores. They suggested water flow to occur in distinct flow channels.

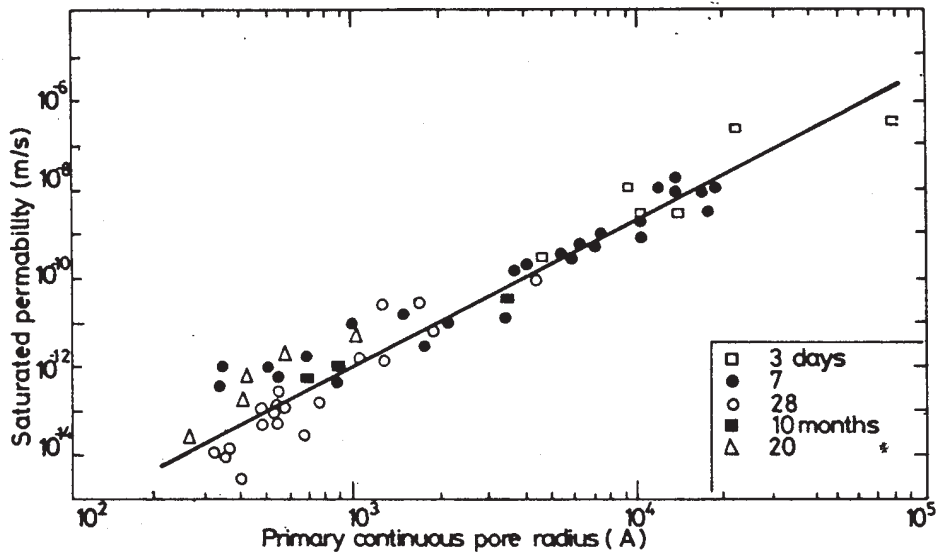


Fig. 7.13 - The relationship between the “continuous pore radius” and the saturated permeability of hardened cement paste [7.23].

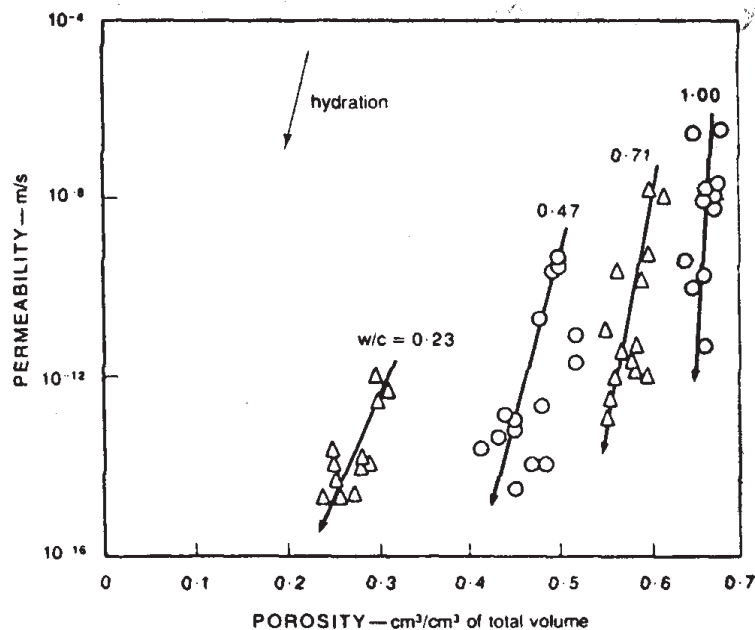


Fig. 7.14 - Permeability of cement paste as a function of the total porosity [7.24] and the w/c ratio

### **7.2.9      *Type, size and amount of aggregate***

For a given water-to-cement ratio, the tightest concrete can be achieved by use of such an aggregate, which has a shape and a size distribution that require a minimum of mixing water. The aggregate should have a grading curve with as much of the space between the larger particles as possible is filled with smaller particles, thus reducing the amount of cement paste. Unstable mixes leading to bleeding might produce channels in the concrete and cavities under big aggregate particles. This will increase the permeability. The grading curve of aggregate shall be such that stable mixes are produced. Use of larger and more porous aggregate makes the concrete more permeable.

The larger the aggregate, the greater the risk of microcracks and the permeability increasing [7.6]. The work of Ruetters et al. [7.3] indicated that with the use of a larger aggregate the concrete was more permeable (Fig. 7.4). Other researchers, however, have not found there to be any strong relationship between the gradation of the aggregate and permeability [7.4] [7.25]. Probably, the permeability is not increased if larger aggregate is used if the concrete is well compacted and well cured. However, if this is not fulfilled, concrete with larger aggregate is probably of higher permeability because micro-cracks and cavities may be formed around the aggregate.

### **7.2.10     *Type of cement***

Ingredients in the cement that consume calcium hydroxide and forms calcium-silica hydrates gels, such as pozzolanic material (fly ash, silica fume, blast furnace slag), usually decrease the permeability of concrete in the micro-scale level. On the other hand, if cracks are formed, the sealing of them (paragraph 7.2.11) may be reduced.

The more finely the cement is ground, the tighter the concrete becomes [7.6]. On the other hand, Powers et al [7.9] maintain that after some time pastes made from coarsely ground cement are just as impermeable as pastes made of finer cement. Any impact of cement fineness on permeability is tied up with the corresponding w/c ratios (required for adequate workability), i.e. finer cement calls for higher w/c ratios, which, in turn may increase water permeability. However, this reasoning is not correct if the workability of fine cement concrete is improved by chemical admixtures (superplasticizers, air entraining agents, etc.).

### **7.2.11     *Leaching, self sealing or deposit of material inside a dam***

The permeability of concrete may change due to the removal or the formation of compounds inside the concrete or on the surfaces. For an example, the dissolution and precipitation of calcium hydroxide may lead to a change in the permeability.

If solid material is leached away, the permeability in the area in question increases. In [7.26] the permeability of concrete specimens made and tested in laboratory often

rose sharply after their being percolated for some time. When the flow of water rose rapidly, it appeared that the increase in flow took place in only a rather few individual flow channels that had been broadened through material being leached away from the channel walls. In such cases the flux could not be described in terms of a steady-state Darcian flow but rather by a number of flow tubes described by Hagen-Poiseuille's law (paragraph 7.4.2).

If leached material comes in contact with carbon dioxide, or bicarbonate comes in contact with calcium hydroxide, the resulting precipitation of  $\text{CaCO}_3$  may decrease the permeability in the area, the concrete is self-sealed. The cement paste in concrete may also seal due to continued hydration, which is discussed in the paragraph 7.2.4. The backing of leaching by carbon dioxide is the reason why siphons are occasionally used at the exit of drains, hindering carbon dioxide to enter the drain hole (Fig. 7.15).



Fig. 7.15 – Siphon in a dam foundation gallery in order to avoid that the leaking water from a limestone formation is exposed to carbon dioxide of the air.

In high dams, the head of water may cause pore rupture and thus increase the length of continuous leakage paths. However, also the opposite may occur, namely that high pressure may block pores by its silting up with material from the reservoir. Permeability rates after first impounding may therefore not be representative for the dam's later life cycle.

Pozzolonic material (fly ash, silica fume, blast furnace slag) decrease the amount of free calcium hydroxide in the pore solution and thus also influence the permeability (see 7.2.10).

According to Meyers [7.27], material can readily deposit inside a thick concrete dam. Both  $\text{Ca}(\text{OH})_2$  and  $\text{CaCO}_3$  are more soluble at lower than at higher temperatures and some of this material will be precipitated in the central portion of the concrete mass or in dam galleries (Fig. 7.16). However, in the majority of cases  $\text{CaCO}_3$  precipitations reduce permeability due to blockage and/or long-term self-colmatation.



Fig. 7.16 – Excessive deposit of  $\text{CaCO}_3$  - leaching from cement grout - in a dam foundation gallery.

### **7.2.12 Workability and placing**

The workability of concrete is important for tightness. The concrete needs to fill out the mould and enclose the reinforcement. The grading of aggregate is decisive for the workability, consistency and stability of the concrete. Experience shows that, at equal w/c ratio, a stiff consistency results in concrete that is less tight than if the concrete has a more plastic consistency [7.6]. In old concrete dams made of stamped concrete, there is a considerable risk of the concrete not being tight, especially at joints between different batches of concrete.

Potentially, entrapped air or honeycombing (large irregular voids due to poor compaction) are damaging, even if they are isolated and do not form continuous flow paths in the cement matrix.

A frequently observed detrimental effect on permeability is honeycombing along lift joints. The reason is mainly incomplete compaction because vibrators are easily damaged when touching the hardened concrete of the lift surface. In order to avoid such damages the workers tend to pull back the vibrators before they touch the lift surface.

Bleeding has equally serious effects; the formation of bleeding channels creates continuous flow paths and the deposition of water pockets underneath coarse aggregate particles” [7.14].

### 7.2.13 The viscosity of water

The flow resistance of a liquid is highly dependent on its viscosity. In large flowing channels, the viscosity of the water depends on the temperature. In very small channels, such as in many of the pores in concrete, large intermolecular forces develop between different ions in the water and between ions in the water and ions bounded in compounds in the pore walls. When strong intermolecular forces need to be exceeded, the viscosity becomes greater. Although all the evaporable water in cement materials is mobile when subjected to hydrostatic pressure, some of it has a high degree of viscosity. Powers [7.28] calculated the effect of w/c-ratio on the viscosity (Tab. 7.2).

Tab. 7.2 - Computed relative viscosity of the fluid in saturated cement pastes, as based on eq. 62 in Powers [7.28].

W/c	Porosity $\epsilon$	Hydraulic radius (Å)	Factor for the increase in viscosity
0.38	0.280	7.8	47 600
0.45	0.346	10	2 700
0.50	0.395	12	600
0.60	0.461	16	134
0.70	0.489	18	78

Powers noted that the permeability is 5-6 times as great when pure water permeates a cement paste than when salts, particularly NaOH and KOH, are dissolved in the water. Powers and Copeland [7.9] also observed that the permeability increased when alkali were removed from the pore solution. Some reports mean that the roughness of the walls of the channels may extend through the laminar layer, causing turbulent flow. The true viscosity also includes the turbulent viscosity [7.29].

### 7.2.14 State of stress

Experiments conducted by Wisnicki et al. [7.30] indicated there to be no significant reduction in permeability due to 2-dimensional compressive stress being applied. A stress of maximally 75% of their compressive strength was applied in the experiment. It appeared that the main effect of stress upon the permeability of concrete was that of closing major cracks.

### **7.3 TEST METHODS FOR WATER PERMEABILITY**

#### **7.3.1 General**

Measuring water mobility in concrete is generally a very difficult task. Unsaturated concrete can be penetrated by water by means of a number of different mechanisms such as adsorption, diffusion, chemical reactions, capillary suction and viscous flow caused by over-pressure. The pore system may change its geometry due to the formation or leaching of compounds or to swelling or shrinking. However concrete permeability serves as a quality indicator of the dam concrete and it needs to be tested, permeability tests being selected very carefully. Permeability through joints or cracks, not here referred, is related to the whole structure more than to the mass concrete materials (paragraph 7.1.6).

Testing samples taken out from real dams is especially difficult because such samples are often not completely water saturated. If they are water saturated in the test this saturation may more or less destroy the pore system, which changes the permeability.

The variation of permeability in concrete is considerably higher than other properties, for example strength. Alterations in preparation of the specimen, or in testing procedures, and different ages of the specimens when tested, can lead to large differences in the measured permeability. The degree of saturation of the concrete is probably the major cause of discrepancies when results from different laboratories are compared.

There are various advantages to use saturated concrete in permeability tests:

- there is only viscous laminar flow of water under such conditions. No absorption, moisture diffusion or capillary suction take place;
- the flow can be calculated with the simple use of Darcy's law, assuming viscous flow;
- the flow is steady over time. Both in-flow and out-flow need to be measured in order to ensure the presence of the equilibrium conditions;
- There is no shrinkage or swelling.

The disadvantage in only studying Darcian flow in saturated concrete is that such concrete is not very frequent in real structures. In dams of reasonable good concrete quality, saturated concrete is limited to a rather narrow portion near the upstream face. The downstream face, exposed to air, has relative humidity below 100%.

Permeability measurements suffer from a lack of standardization. It is usually very difficult to compare the results of different permeability tests due to differences in test setups and procedures. The causes for these different results can be the following:

- Different concrete mix designs (including the maximum size of aggregate);
- Different curing methods (drying, heating, in air, in vapour, in water);
- Different quality of the penetrating water;
- Different concrete ages or different duration time of the test;
- Different applied water pressures;
- Different sizes of test specimens or made on different ways, e.g. cast or drilled out from a larger block of concrete.

One standard method for measuring the permeability in saturated concrete is described in [7.31]. In a comprehensive study made of Scherer et al [7.32] several methods are reviewed such as beam-bending tests, pressure decay test, thermopermeametry test and dynamic pressurization test.

There are also a number of standard methods in which the water is forced into a concrete that are not completely water saturated. After a certain time and under a certain pressure, depending on the considered standard, the specimen is split in two halves and the penetration of the water front is measured. One method is SS 13 72 14 [7.33], shown later on in Fig. 7.20 (paragraph 7.3.3). Other methods are BS1881[7.34], ACI-SP 108 [7.35], DIN 1048 [7.36], ONORM B 3303 [7.37] and ISO 7031 [7.38]. Because the concrete is not completely saturated the test is in reality a test of the combination of capillary suction and water tightness. However, based on other investigations (see paragraph 7.3.6), the penetration depths are transformed to a permeability coefficient comparable to the permeability coefficient in Darcy's law.

The test equipment for measuring water permeability consists usually of (e.g. Fig. 7.17):

- A pressure side applying a pressure on the test specimen;
- A test cell in which the specimen is placed;
- A measuring device at the outlet that measure the flow of water penetrating the specimen.

All parts must be made of materials resistant to both high and low pH-values

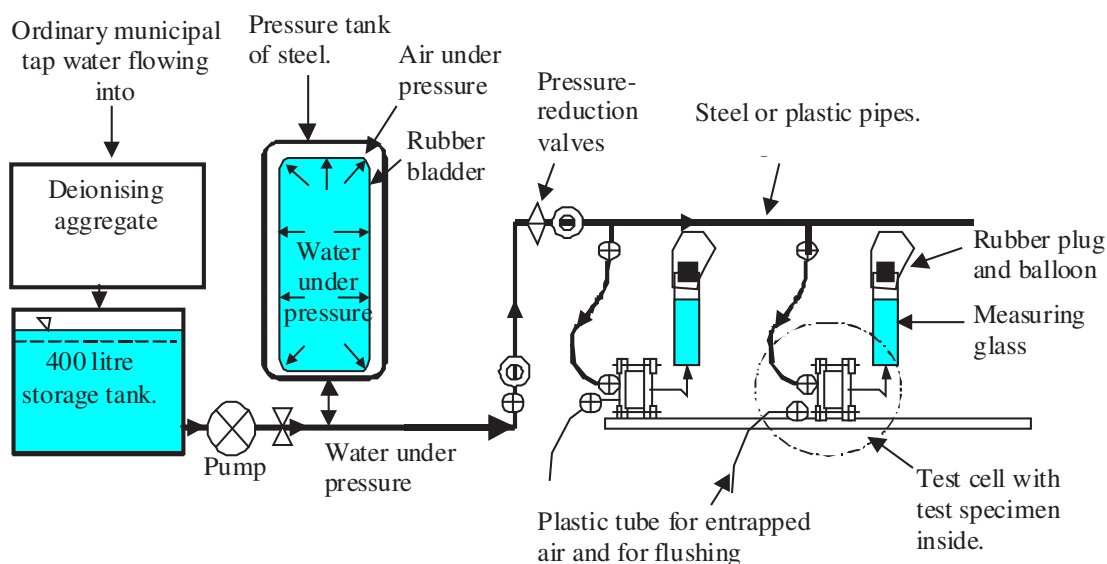


Fig. 7.17 - Permeability equipment, consisting of a deionising aggregate, a storage tank, a pump, a pressure tank, pressure reduction valves and a number of test cells containing concrete specimens [7.26].



### **7.3.2 Preparation of specimens**

The most important task is to decide what the relevant permeability is for the test, for example:

- Permeability of virgin (never dried, never heated) specimens made in laboratory.
- Permeability of not virgin, e.g. dried and/or heated, specimens made in laboratory.
- Permeability of specimens taken out from a real structure.

For dams the first testing is most common and it is used as an indicator of the durability of the concrete mix. Permeability testing should therefore be a standard test in a pre-construction test program (see Table 2.1 in Section 2).

To achieve true Darcian permeability the test specimens preferably must be water saturated before the test starts. If the specimens already are saturated before the test, such as virgin specimens, they can be directly put into the test equipment. If the specimens are not fully saturated, for example laboratory made not-virgin specimens or cores drilled out from dams, the air inside the specimen must be forced or sucked out of the specimen before a steady-state water flow appears. This can take different long time depended mainly on the moisture content in the pore system, the pore size distribution of the specimen, the history of treatment of the specimen, continued hydration reactions, swelling, etc.

To saturate concrete without destroying the pore structure and changing the permeability is difficult. Two main principles are commonly used: Forcing water into the specimen or sucking water into the specimen.

If the specimen is exposed to external water pressure such a long time that the flow becomes steady state, the specimen can be assumed to be water-saturated. In such a case a test method like that described in Fig. 7.17 can be used. The possibilities of continuous hydration or leaching must however be regarded if it takes a long time reaching steady-state flow.

A faster method to water-saturate a specimen is to vacuum saturate the specimen. A suitable method is described in NT Build 492 [7.39], point 6.3.2 . In another method, specimens are dried in oven before the vacuum treatment. This is a quicker method for withdrawing all air inside the specimens. On the other hand, this method will much more alter the pore size distribution and porosity and thereby also increase the short term permeability of the specimen. In long lasting tests the permeability often decrease again due to continued hydration.

Given these difficulties, permeability testing from cores of existing dams is only meaningful if serious defects in material-permeability are found to be prone for investigations.

### 7.3.3 The test cell

A test cell consists usually of a steel cylinder in which the test specimen is placed. Between the specimen and the cylinder there must be some sort of sealing to avoid water leakage. Different types of uniaxial test cells are shown in Fig. 7.18 and in Fig. 7.19.

A passive sealing is made, for example, of bitumen or epoxy that is let to stiff in the gap between the cell and the specimen (Fig. 7.18). An active sealing can for example be a rubber tube in the gap between the cell and the specimen and which is filled with high-pressure air (Fig. 7.19a). Another example is when the specimen is made conical with a membrane around it. The specimen is pressed down by the applied pressure and becomes sealed (Fig. 7.19b). Fig. 7.20 shows a test cell used in the standard method SS 13 72 14 [7.33] that gives the permeability indirectly via the depth of the penetrated water front.

The test cell shown in Fig. 7.19b was used in an experiment described in [7.17] for concrete specimens with a thickness of 50 mm and a diameter of 150 mm. For concrete used in many dams, with aggregate of perhaps 120 mm or more, bigger specimens and larger devices are needed. A rule-of-thumb is a diameter three times as big as the biggest aggregate used in the concrete. Example of the permeability apparatus suitable for testing mass concrete from dams are shown in Fig. 7.21.

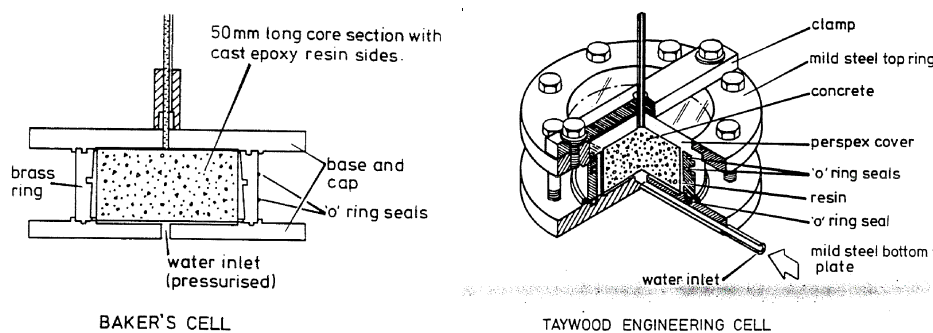


Fig. 7.18 - Examples of uniaxial cells with passive sealing [7.14].

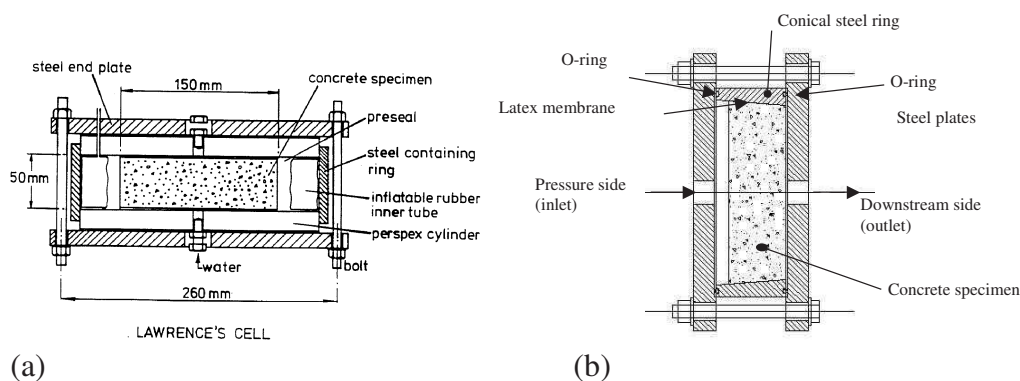
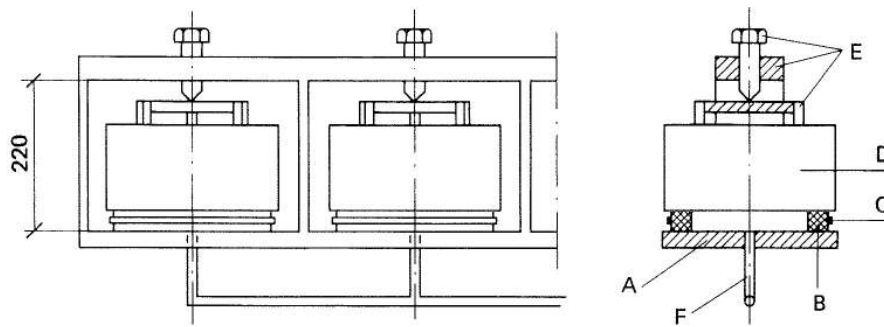


Fig. 7.19 - Examples of uniaxial cells with active sealing from (a) [7.14] and (b) [7.17].

*ICOLD Bulletin: The Physical Properties of Hardened Conventional Concrete in Dams*  
 Section 7 (Water permeability)



- A Flat support, e.g. a table.
- B Tightening ring of rubber with a diameter of 170 mm.
- C Supporting ring of steel outside the rubber ring.
- D Concrete specimen.
- E Supporting and locking frame
- F Pressurized water inlet.

Fig. 7.20 - Text set-up with uniaxial cells described in the standard method SS 13 72 14 [7.33]. In the test a water pressure of 0.8 +/- 0.03 MPa is applied for 24 +/- 2 hours whereupon the specimen is immediately split in two halves and the penetration front is measured.

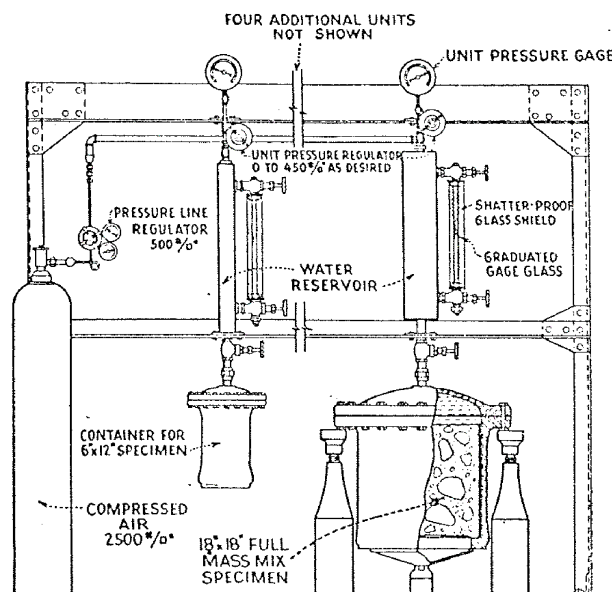


Fig. 7.21 – Permeability apparatus used for testing mass concrete [7.3].

Generally permeability testing at dam sites need to use a simple test set-up.

Fig. 7.22 shows a device used for dams to test permeability at site. The pressure vessel is used for both cylinders and cubes. The pressure is increased stepwise from 0.5 to 30 atm. (or less for small dams). Each pressure range is kept constant for 24 hours and a protocol records any leakage. Generally, good concrete will not leak at all after the 10 cycles reaching 30 atm. Then the specimen is crushed and the water penetration depth is measured and a corresponding Darcy value calculated.

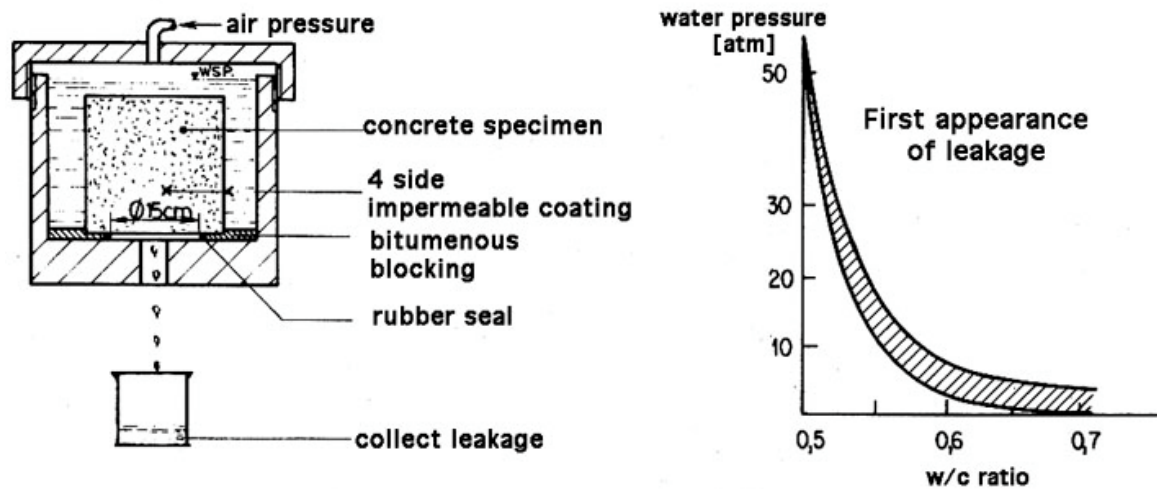


Fig. 7.22 – Device for permeability testing of large concrete dams.

### 7.3.4 The pressure side

Gravity dams have a pressure gradient as low as 1.3 to 1.4 meter water head per meter of width of the structure (m/m), a 100 m high dam being traditionally 75 m wide at the base.

Arch dams can have pressure gradients of up to 12 (m/m). Buttress dams can have gradients of about 30 to 40 (m/m) over their front slabs. The buttress itself may have a more complex pattern of gradients, the complexity depending on the geometry, the possible cracks that leak water and the moisture conditions close to the pillar.

Of particular interest for controlling permeability is the pressure head between reservoir pressure and dam galleries close to the upstream face. Some designers stipulate a gradient not exceeding 25.

The most common ways to achieve a water pressure on the specimen is:

- Place the test cells inside a hydropower station and subjected to the headwater;
- The water is pressurised by a container with high pressure gas;
- A pump pressurises water inside a container (Fig. 7.17)

### 7.3.5 Water flow measuring

The method for measuring the flow of water coming out from the specimens must fulfil the following requirements.

The out-flow end of the specimen must be filled with water, in order to avoid any contact with air before water have percolated out from the specimen.

The measuring exactness must be suitable to the amount of water that comes out from the specimens. Some concrete has very low and some very high permeability. It should be possible to read the amount of water in an exact way, but on the other hand, the water shall not spill over the measuring vessel.

The measuring vessels shall not let air in or moisture out. If air is let in, the CO<sub>2</sub> in it will form CaCO<sub>3</sub> with the percolated solution coming from the specimen. If moisture is let out, the correctness of measured volume of water will be wrong.

There should be careful investigations regarding possible leakage through the sealing. If there is any flow channel in the sealing, the flow of water may be very much higher than through the specimen only.

### **7.3.6 Expression of results**

When steady state flow of water is reached, the permeability coefficient is calculated as (see equation in 7.1.2):

$$k_w = q_w \cdot L / dP_w / A \quad (7.4)$$

where:

$k_w$  = permeability coefficient (m/s)

$q_w$  = water flow (m<sup>3</sup>/s)

$dP_w$  = difference in pressure (m) between upstream and downstream end of the specimen;

$L$  = length of specimen (m);

$A$  = cross section area (m<sup>2</sup>).

For penetration tests, i.e. for not completely saturated specimens, the penetration depths may be transformed to Darcian permeability. Sällström [7.7] studied relations between the standard method SS 13 72 14 [7.33] for testing the water penetration (Fig. 7.20) and one method for testing water permeability. A relation is shown in Fig. 7.23.

Conventional dam concrete has generally a inherently low water permeability [7.40]. Good proportioned concrete mixes placed with good vibration and subjected to a suitable curing, usually show permeability values in the range of 10<sup>-10</sup> to 10<sup>-13</sup> m/s.

In Tab. 7.3 the permeability coefficients  $k_w$  are reported for some Bureau of Reclamation dams. Specimens for Dworshak and Lower Granite dams were 150 x 150 cm (6 x 6 in.) cylinders while specimens for the other dams listed in Tab. 7.3 were 460 x 460 mm (18 x 18 in.). The tests were carried out under a pressure of 2.8 MPa (400 psi).

ICOLD Bulletin: The Physical Properties of Hardened Conventional Concrete in Dams  
 Section 7 (Water permeability)

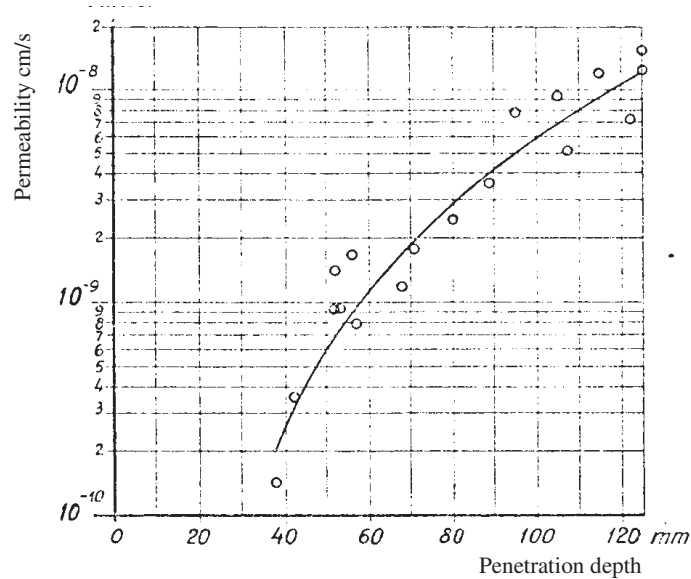


Fig. 7.23 - Relation between permeability and penetration depth for concrete composed of low-heat cement and 4 to 6 percent air, 32 mm maximum aggregate size and various w/c-ratios (0.55 to 0.82) [7.7].

Tab. 7.3 – Mass concrete water permeability [7.41]

Dam	Water permeability coefficient $k_w$ (m/s)
Hoover	$5.99 \times 10^{-13}$
Hungry Horse	$1.79 \times 10^{-12}$
Canyon Ferry	$1.87 \times 10^{-12}$
Monticello	$7.93 \times 10^{-12}$
Glen Canyon	$1.75 \times 10^{-12}$
Flaming Gorge	$1.07 \times 10^{-11}$
Yellowtail	$1.90 \times 10^{-12}$
Dworshak	$1.84 \times 10^{-12}$
Lower Granite	$4.54 \times 10^{-12}$
Anchor	$4.37 \times 10^{-11}$

## **7.4 MODELING WATER PERMEABILITY IN SATURATED CONCRETE**

### **7.4.1 Introduction**

Many models describing the mobility of water in a porous material such as concrete have been developed through the years. It should be emphasized that the complexity of the microstructure of cement paste, mortar and concrete is so great that it is not possible to derive their macroscopic properties from simple flow rules on a micro-scale without efforts being made to model the structure itself [7.42]. It is above all the enormous scale differences in the material, ranging from a 2 nm to approximately 100 nm pore diameter size and to the atomic size of the elements that are difficult to include in a model.

Methods for modelling fluid motion are usually classified into two groups, the one being microscopic models and the other macroscopic models.

Microscopic models describe the motion involved in terms of each of the small tubular conduits in the porous medium, using a statistical approach. By these models more detailed studies can be made regarding transport of water and other constituents as air, ions, etc in concrete at different properties and geometry. On the other hand the verification with experiments is often very complex and difficult, not suitable for any standard tests of mass concrete from dams. Often a microscopic model can be used for macroscopic calculations, if estimations are made of how to “smear out” the microscopic model on a larger volume and in more than one directions.

Macroscopic models describe the fluid as a unit moving at a macroscopic-average velocity, which can be given, for example, by Darcy’s law. Macroscopic models are more useful for estimating the permeability for mass concrete in real structures and they can be used for 2- and 3 dimensional dam structures directly in analytical or numerical models and can be verified in tests in a relatively easily way.

Van Brakel [7.44] divided the modelling of porous media into two other main types: pore space and non-pore space models. Pore space models can involve the conception of connected tubes or discrete particles in one, two or three dimensions. These are often suitable for examining microscopic behaviour. Non-pore space models can be empirical correlations (such as Darcy’s equation), discrete particle models, continuum models or statistical models, often suitable for analysing macroscopic behaviour. Van Brakel is of the opinion that even non-pore space models need always to some extent to be attached to a pore space model. With respect to capillary liquid transport in particular, he regards the sensibility of using the continuum approach as being disputable.

### **7.4.2 Macroscopic (non-pore space) models for mass concrete**

Macroscopic, or non-pore space, models are often used to calculate homogenous percolation of water in a continuous body of concrete, e.g. a dam. A commonly used model is Darcy’s law for saturated concrete, but also other models are used for

example when the concrete is not saturated (e.g. Richard's equation) or if the water velocity through the concrete is rather high (e.g. Brinkman equation).

Darcy [7.1], in filtrating water through sand in a circular tube, found the following empirical relationship (Darcy's law) concerning homogenous flow in saturated, porous media:

$$q_w = -k_w \cdot A_{tot} \cdot \frac{(h_2 - h_1)}{L} \quad (7.5)$$

where  $q_w$  = the amount of the percolating fluid ( $m^3/s$ );  $k_w$  = the bulk permeability coefficient, which depended on both the porous media and the fluid ( $m/s$ );  $A_{tot}$  = the cross sectional area of the filter bed ( $m^2$ );  $h_1, h_2$  = liquid that rises above an arbitrary level at the inlet or outlet end of the filter bed ( $m$ ); and  $L$  = the length of the filter bed ( $m$ ) (Fig. 7.26).

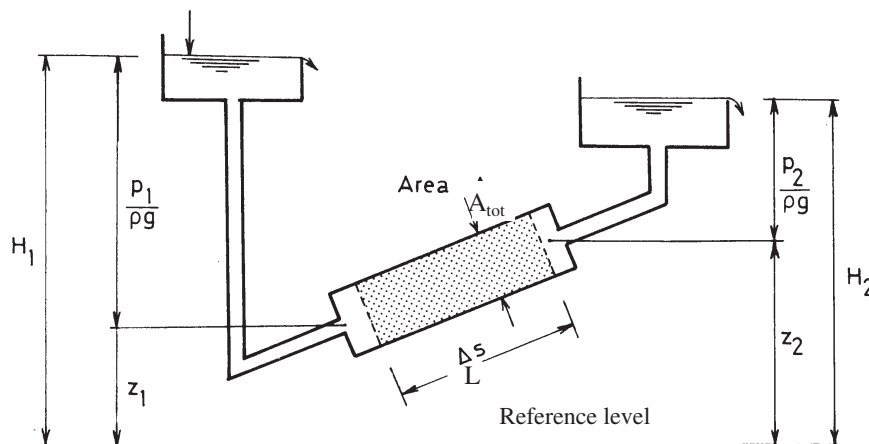


Fig. 7.26 - A principal figure in Darcy's experiment [7.45].

In its original form, Darcy's law overlooked hydrodynamic microscopic flow in a complicated system of pores. The law is an averaging macroscopic one. The macroscopic approach is commonly used in modelling work and is the perhaps the only approach that can be verified experimentally. In practice, it is the value  $k_w$  that is usually measured and reported. According to Collins et al. [7.46], there is evidence, however, that the flow of water through saturated concrete, mortar and hardened cement paste very closely approximates Darcy's law [7.3] [7.11]. Darcy's law is limited in some aspects. It is essentially valid for the following [7.47]:

- Homogenous, steady-state flux in saturated, porous media
- The permeability coefficient  $k_w$ , which is fluid-dependent (it depends on the viscosity)
- Incompressible fluids
- Isothermal conditions
- Creeping, laminar flow (very low velocity)
- Newtonian fluid
- Flow through a relatively long, uniform and isotropic porous medium
- A low level of hydraulic conductivity in the medium



Darcy's equation can be restated in terms of the pressure  $p$  and the density  $\rho$  of the liquid. The pressure at the two ends (see Fig. 7.26) can be written as [7.22]:

$$h_1 = p_1/(\rho \cdot g) + z_1; \quad h_2 = p_2/(\rho \cdot g) + z_2 \quad (7.6)$$

where  $p/(\rho g)$  = pressure head (m); and  $z$  = height above an arbitrary reference level.

Darcy's equation is then reformulated to

$$q_w = -k_w \cdot A \cdot \frac{(p_2 - p_1) + \rho \cdot g (z_2 - z_1)}{L} = -k_w \cdot A \cdot \frac{(\Delta p + \Delta z) \rho g}{L} \quad (7.7)$$

Trying to write the equation for infinite filter lengths  $\Delta l$  and at the same time simplify by introducing a hydraulic potential (sometimes called a piezometric head),  $P_w = p/\rho g + z$ , and assuming no variation of  $k_w$  or  $\rho$ , Darcy's equation becomes:

$$v_w = -k_w \cdot \nabla P_w \quad (7.8)$$

where  $v_w$  = seepage velocity (m/s). Note that the velocity  $v_w$  is to be understood as the bulk velocity and not as the velocity  $u$  in an individual flow channel. For an isotropic porous medium, permeability becomes a tensor:

$$v_w = -\mathbf{k}_w \cdot \nabla P_w \quad (7.9)$$

A balance of the water volume can be written as

$$D \frac{\partial P_w}{\partial t} = \hat{c}_w - \nabla \cdot (v_w) \quad (7.10)$$

where  $D$  = damping; and  $\hat{c}_w$  = source or sink (e.g. hydration) of water (m<sup>3</sup>/s). Under steady-state conditions, the partial time derivatives and source term  $\hat{c}_w$  vanish. Equation (7.10) suits well to be calculated using the Finite Element Method.

### 7.4.3 Microscopic (-pore space) models for more detailed studies

Microscopic, or pore space, models can be used directly for calculations of water flow in distinct flow channels as for example in cracks or they can be transformed to a homogenous percolation of water in a continuous body of concrete.

According to Scheidegger [7.22], flow through porous media appears to take place along flow channels at the local (pore) velocity,  $u$ . The macro scale filter velocity  $v$  of the fluid is smaller than the local velocity, as often described by the Dupuit-Forchheimer equation:

$$v = \Phi \cdot u \quad (7.13)$$

where  $v$  = filter (bulk) velocity of the fluid (m/s);  $\Phi$  = porosity (m<sup>3</sup>/m<sup>3</sup>); and  $u$  = local velocity of the fluid in the flow channels (m/s). The local velocity is assumed to

fluctuate both between channels and along channels. In the Fochheimer equation,  $v$  is an average velocity.

A pore space model of the flow of a fluid through a porous medium is often based in some way on the Navier-Stokes equations for incompressible fluids.

$$\nabla \cdot \mathbf{u} = 0 \quad (7.14)$$

$$\rho_w \frac{\partial \mathbf{u}}{\partial t} + \rho_w \mathbf{u} \cdot \nabla \mathbf{u} + \nabla p - \mu \nabla \cdot (\nabla \mathbf{u} + \nabla \mathbf{u}^T) + \rho_w \mathbf{g} = \mathbf{0} \quad (7.15)$$

where  $\rho_w$  = density of water (kg/m<sup>3</sup>);  $u$  = local velocity of water (m/s);  $p$  = hydrostatic pressure (Pa);  $\mu$  = dynamic viscosity (Pa·s); and  $g$  = acceleration due to gravity (m/s<sup>2</sup>). Note that the velocity  $u$  is the velocity within each small flow channel and not the bulk velocity of the material.

Assuming steady-state flow, a straight, smooth and horizontal circular tube, laminar flow and the velocity of the fluid being zero on the walls of the tube allows Navier-Stoke flow to be integrated with the Hagen-Poiseuille equation:

$$u_{mean} = \frac{\phi^2}{32\mu} \cdot \frac{\Delta p}{L} \quad (7.16)$$

where  $u_{mean}$  = mean velocity in the tube (m/s);  $\Delta p$  = pressure gradient (Pa);  $L$  = length of the tube (m);  $d$  = diameter of the tube (m). Observer that in small tubes/pores the water at the walls is hard bounded to the wall and not involved in the transport, so the diameter should be reduced to the diameter in which the flow take place. The total flow of water through a tortuous, rough tube in concrete may be estimated by

$$q_{w,tube} = r_w \cdot u_{mean} \cdot \frac{\Delta p}{L} \cdot A_{tube} = r_w \cdot \frac{d^2}{32\mu} \cdot \frac{\Delta p}{L} \cdot \frac{\pi \cdot d^2}{4} = r_w \cdot \frac{\pi \cdot d^4}{128 \cdot \mu} \cdot \frac{\Delta p}{L} \quad (7.17)$$

where  $q_{w,tube}$  = flow through the tube (m<sup>3</sup>/s); and  $r_w$  = reduction factor (-) taking account reductions for real flow tubes in cement materials due to deviation from a large, strait and smooth cylinder (that the Hagen-Poiseuille equation assumes). Fluxes caused by gradients in hydraulic head  $P_w$  (m) are written in terms of the same equations as above but are multiplied by the fluid density  $\rho_w$  and the gravity coefficient  $g$ .

Under these same conditions the integration of Navier-Stoke for the flow of fluids through parallel slits, for example for a real crack in a dam, gives

$$q_w = r_w \cdot \frac{b \cdot w^3}{12 \cdot \mu} \cdot \frac{\Delta p}{L} \quad (7.18)$$

where  $L$  = flow channel length of the slit (m);  $w$  = slit width (m); and  $b$  = slit length perpendicular to the flow direction (m);  $r_w$  = "surface roughness factor", generally about 0.01-0.2 .

A very simple capillary model of flow in one direction in concrete is that of a bundle of straight parallel capillaries of uniform diameter together with the Hagen-Poiseuille equation.

$$q_a = -r_w \cdot \frac{n_a \phi_a^2}{32\mu} \cdot A_a \cdot \frac{\partial p}{\partial x} = -\frac{k_a}{\mu} \cdot A_a \cdot \frac{\partial p}{\partial x} \quad (7.19)$$

$$k_a = r_w \cdot \frac{n_a \phi_a^2}{32} \quad (7.20)$$

$$A_a = \frac{\pi \cdot \phi^2}{4} \quad (7.21)$$

where  $q_a$  = water flow in all capillaries with a particular size  $a$  ( $\text{m}^3/\text{s}$ );  $k_a$  = specific permeability of all capillaries with a particular size  $a$  ( $\text{m}^2$ );  $\delta p/\delta x$  = the pressure gradient ( $\text{Pa}/\text{m}$ );  $n_a$  = the number of capillaries of diameter  $\phi_a$  per square meter cross section ( $\text{nos.}/\text{m}^2$ ); and  $\mu$  = the dynamic viscosity ( $\text{Ns}/\text{m}^2$ );  $r_w$  = reduction factor, see equation (7.17); and  $A_a$  = the cross-sectional area of one capillary of size  $a$  ( $\text{m}^2$ ).

#### 7.4.4 Combined water flow in a “real dam”

In a real structure exposed to one side water pressure, the water flow is a combination of true Darcian flow (in saturated media) and moisture flow in not saturated media [7.48]. Fig. 7.25 shows a thick concrete dam where there is a hydrostatic pressure against the upstream face of the dam and the downstream face is exposed to air. The concrete is saturated and the internal water pressure is hydrostatic down into a point near the downstream face, where the humidity reaches 100 % RH. Further downstream, the internal relative humidity decreases down to the current climatic condition at the downstream face. A sunny summer day, the relative humidity at the downstream face can reach as low as about 30-40 % RH. The water transport is caused by a combination of over-pressure, suction and diffusion. Finally, at the downstream face, evaporation to the surrounding air occurs.

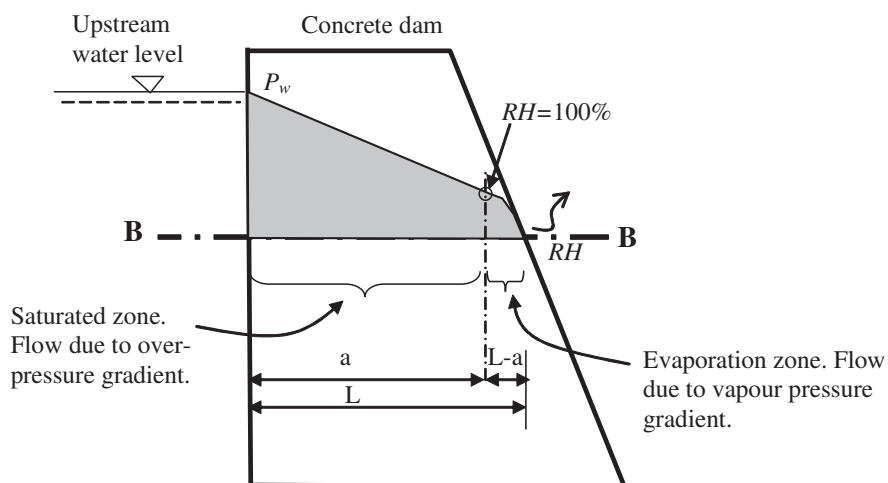


Fig. 7.25 - A schematic of a thick concrete dam with a combined water flow in a section B-B. In this section the upstream face is in water and the downstream face is in air. The section has one saturated zone and one evaporation zone

In a combined transport of water, the flow of water in the over-pressure part is the same as the moisture flow in the not saturated part. Assuming Darcy's law to be valid the flow of water in the saturated part is:

$$v_w = B \frac{dp}{a} \quad (7.22)$$

where  $v_w$  = water flow (kg/(m<sup>2</sup>s));  $B$  = permeability coefficient (s);  $dp$  = pressure difference (Pa); and  $a$  = distance to the saturation level (m) (Fig.7.25). This distance  $a$  to where the concrete is not longer water saturated can be written as [7.49]:

$$a = \frac{k_w \cdot dp \cdot L}{v_{w < 100\%RH} \cdot H_{< 100\%RH} + k_w \cdot dp} \quad (7.23)$$

where  $v_{w < 100\%RH}$  = measured flux of water below 100 % RH in laboratory (kg/(m<sup>2</sup>s));  $H_{< 100\%RH}$  = the thickness of the specimen tested in laboratory (m); and  $L$  = the total thickness of the dam (m). Downstream this saturation level where RH goes below 100 % the flow of water is driven by a vapour pressure gradient. Data of some types of concrete considering equation (7.23) can be found in Hedenblad [7.48].

Another case of combined water flow in a concrete dam with an inspection tunnel is from the upstream surface to the tunnel. The saturation point RH=100% lays a little bit into the upstream wall of the tunnel. Upstream this point there is saturated Darcian water flow and downstream this point, and out in the air inside the tunnel, there is a diffusion flow.

If there is water at the downstream face, water flow will of course be depended only on hydrostatic pressure all the way from the upstream to the downstream face.

## 7.5 REFERENCES

- [7.1] Darcy H. (1856), "Les fontaines publiques de la ville de Dijon", Dalmont, Paris.
- [7.2] McMillan F.R., Lyse I. (1930), "Some permeability studies of concrete", Journal of the American Concrete Institute Nov. 1929 – June 1930.
- [7.3] Ruettgers, A., Vidal, E. N., Wing, S. P. (1935), "An investigation of the permeability of mass concrete with particular reference to Boulder Dam", ACI Journal, Proceedings 1935(31):4, pp. 382-416.
- [7.4] Mary, M. (1936), contribution to the discussion with Ruettgers, Proceedings of the ACI, vol. 32, pp. 125-129.
- [7.5] Mather B., Callan E.J. (1950), "Permeability and Triaxial Tests of Lean Mass Concrete", Corps of Engineer.
- [7.6] Nycander P. (1954), "The permeability of concrete", From the journal Concrete 1954 n° 2 (in Swedish), Swedish concrete association, Stockholm.

*ICOLD Bulletin: The Physical Properties of Hardened Conventional Concrete in Dams*  
Section 7 (Water permeability)

[7.7] Sällström S. (1968), "Watertightness of Dam concrete" (in Swedish), Nordisk Betong 1968:1, Stockholm.

[7.8] Powers T. C., Brownyard T. L. (1948), "Studies of the physical properties of hardened Portland cement paste. Chicago, Illinois. PCA Research Laboratories, Bulletin 22.

[7.9] Powers T.C., Copeland L.E. (1954), Hayes J.C., Mann H.M., (1958), J. ACI, Proc., Vol. 5, pp. 285-98.

[7.10] Fagerlund, G. (1980b), "Moisture-mechanical properties", (in Swedish), The concrete Handbook Material, Svensk Byggtjänst, Stockholm.

[7.11] Powers T.C. (1958), J. Am. Ceram. Soc., Vol. 4, No. 1, pp. 1-5.

[7.12] Mehta P.Kk. (1986), "Concrete – structure, properties and materials", Prentice-Hall, U.S.A.

[7.13] Young J.F. (1988), "A review of the Pore Structure of Cement Paste and Concrete and its Influence on Permeability", Conference proc. Permeability of concrete, ACI.

[7.14] Hearn N. (1992), "Saturated permeability of concrete as influenced by cracking and self-healing", Dissertation submitted to the University of Cambridge.

[7.16] Vuorinen J. (1985), "Applications of diffusion theory to permeability tests on concrete Part I: Depth of water penetration into concrete and coefficient of permeability", Imatran Voima OY, Finland.

[7.17] Ekström T. (2003), "Leaching of concrete – The leaching process and its effects", Doctoral thesis TVBM-1020, Div. of Building Materials, Lund Institute of Technology, Sweden.

[7.18] Fagerlund, G. (1994), "Structure and development of structure", (in Swedish), The concrete Handbook Material, Svensk Byggtjänst, Stockholm.

[7.19] Carlson R.W. (1950), "Permeability, pore pressure, and uplift in gravity dams", Appendix to "Permeability and Triaxial Tests of Lean Mass Concrete", Corps of Engineer.

[7.20] Bažant Z.P. (1975), "Pore pressure, uplift and failure analysis of concrete dams", Proc. of the Int. Symp. of "criteria and assumptions for numerical analysis of dams", 8-11 Sept., 1975, Swansea.

[7.21] Peer L. B. B. (1990), "Water flow into unsaturated concrete", Ph. D., U. Of Cambridge.

[7.22] Scheidegger, A. E., (1960), "The physics of flow through porous media", 2nd ed., University of Toronto Press.

[7.23] Nyame B.K., Illston J.M. (1980), "Capillary pore structure and permeability of hardened cement paste", 7th Int. Symp. on the Chemistry of Cement paste", Paris, 1980, vol. III.

[7.24] Nyame, B. K., Illston, J. M. (1981), "Relationships between permeability and pore structure of hardened cement paste", Magazine of Concrete Research, Vol. 33, No. 116.

*ICOLD Bulletin: The Physical Properties of Hardened Conventional Concrete in Dams*  
Section 7 (Water permeability)

- [7.25] Markestad A. (1977), "An investigation of concrete in regard to permeability problems and factors influencing the results of permeability tests", Norwegian Institute of Technology, STF 65 A 77027.
- [7.26] Ekström T. (2003), "Leaching of concrete – The leaching process and its effects", Doctoral thesis TVBM-1020, Div. of Building Materials, Lund Institute of Technology, Sweden.
- [7.27] Meyers S.L. (1935), "Discussion of a paper by Messrs. Ruettgers, Vidal and Wing" (see Ruettgers et al 1935), ACI Journal, Proceedings Nov. – Dec. 1935.
- [7.28] Powers T.C. (1969), "Physical properties of cement paste", Proc. 4th Int. Symp. on the Chemistry of Cement, Washington D.C.
- [7.29] Kou S. (1996), "Transport phenomena and material processing", University of Wisconsin, John Wiley & Sons, U.S.A.
- [7.30] Wisnicki B.P., Balbi R., Hula J., Matsuba D., Gutstein D., Lachnit F. (1969), "State of stress and permeability in concrete", University of British Columbia, Vancouver.
- [7.31] Ekström T., Jonsson G. (2006), "Water permeability of water saturated concrete", Nordic Innovation Centre, Oslo.
- [7.32] Scherer G.W., Valenza J.J., Simmons G. (2006), "New methods to measure liquid permeability in porous materials", Cement and Concrete Research 37 p. 386-397.
- [7.33] Swedish Standards Institution, SS 13 72 14, Concrete testing – Hardened Concrete – Impermeability.
- [7.34] British Standard Institution (1996), BS 1881, part 208, Initial surface absorption Test.
- [7.35] American Concrete Institute, ACI SP-108: Permeability of Concrete
- [7.36] DIN 1048 (1972), Test Methods for Concrete – Impermeability to Water, pp. 10.
- [7.37] Österreichisches Normungsinstitut (Austria) - ONORM B-3303 Testing of Concrete
- [7.38] ISO/DIS 7031, (1983). Concrete hardened - Determination of the depth of penetration of water under pressure.
- [7.39] North Test Methods (1999), NT Build 492, Concrete, mortar and cement-based repair materials, Chloride migration coefficient from non-steady-state migration experiments.
- [7.40] ACI Manual of Concrete Practice, (1994) « Mass Concrete », ACI 207.1R
- [7.41] Bureau of Reclamation, (1961) « Properties of mass concrete in Bureau of Reclamation dams », Concrete Laboratory report n° C-1009.
- [7.42] Breyse & Gérard (1997), "Modelling of permeability in cement-based materials ; Part 1 uncracked medium "

*ICOLD Bulletin: The Physical Properties of Hardened Conventional Concrete in Dams*  
Section 7 (Water permeability)

[7.44] Van Brakel J. (1975), "Pore space models for transport phenomena in porous media – Review and evaluation with special emphasis on capillary liquid transport", *Powder Technology*, 11, 205-236, Elsevier Sequoia S.A., Lausanne.

[7.45] Cederwall K., Larsen (1979), "Hydraulics for civil engineers" (in Swedish), Liber läromedel, Malmö.

[7.46] Collins et al (1986), "Permeability of concrete mixtures", *Civil Engineering for practicing and design engineers*, vol. 5, USA.

[7.47] Lage J.L. (1998), "The fundamental theory of flow through permeable media from Darcy to turbulence", Presented in "Transport phenomena in porous media", edited by Ingham & Pop, Elsevier Science Ltd, U.K.

[7.48] Hedenblad, G. (1993), *Moisture Permeability of Mature Concrete, Cement Mortar and Cement Paste*, report TVBM-1014, Div. of Building Materials, Lund Institute of Technology.

[7.49] Fagerlund G. (1996), *Service life prediction of concrete structures*, (in Swedish), report TVBM-3070, Lund.

## 8 FROST RESISTANCE

<b>8 FROST RESISTANCE</b> .....	<b>1</b>
<b>8.1 GENERAL</b> .....	<b>1</b>
<b>8.2 FROST RESISTANCE, MECHANISMS AND EFFECTS</b> .....	<b>2</b>
<b>8.3 FACTORS AFFECTING THE FROST RESISTANCE</b> .....	<b>5</b>
<i>8.3.1 Conditions of external exposure</i> .....	<i>5</i>
8.3.1.1 The humidity content inside the concrete during freezing.....	5
8.3.1.2 The number of cycles of freezing-thawing cycles, the lowest temperature and the freezing rate.....	5
<i>8.3.2 Quality of concrete</i> .....	<i>6</i>
8.3.2.1 Pore structure in the concrete.....	6
8.3.2.2 Concrete permeability.....	6
8.3.2.3 Concrete mix design.....	7
8.3.2.4 Casting technique.....	11
<b>8.4 METHODS FOR EXPERIMENTAL DETERMINATION OF THE CONCRETE FROST RESISTANCE</b> .....	<b>11</b>
<b>8.5 LABORATORY DIAGNOSTIC INVESTIGATIONS</b> .....	<b>13</b>
<i>8.5.1 Diagnostic investigations</i> .....	<i>14</i>
<b>8.6 FREEZING AND THAWING ON CONCRETE DAMS</b> .....	<b>15</b>
<b>8.7 REFERENCES</b> .....	<b>18</b>

### 8.1 GENERAL

The deterioration of the concrete in a dam can be ascribed to a series of chemical and physical causes (both internal and external). Almost all of them are related to the permeability of concrete which represents the most important engineering parameter for evaluating the concrete durability. From this point of view an important influence is also played by the presence of cracks and defects on the surface of construction joints and on vertical block joints.

The aggressive waters in the reservoirs are the most common cause of external chemical deterioration while the alkali-aggregate attack can be considered a chemical attack from within the concrete. They have been specifically dealt with in “ad hoc” ICOLD Bulletins such as Bulletin n° 71 (“Exposure of dam concrete to special aggressive waters”) and Bulletin n° 79 (“Alkali-Aggregate Reaction in concrete dams”).

Freezing and thawing is the most common external physical attack in moderate climates and it is specifically treated in this Section. A frequent internal physical cause for concrete deterioration, such as the rise in concrete temperature due to the cement hydration, has already been examined and discussed in the previous Section 6 – Thermal Properties.



## 8.2 FROST RESISTANCE, MECHANISMS AND EFFECTS

The deterioration by frost action (freezing and thawing cycles) on a saturated concrete is related to the transition phase from water to ice, inside the concrete, and to the correspondent increase of volume (around 9%). If the degree of saturation (% of water filled pores) is less than 80 to 90% this increase of volume could be sustained by the concrete without any damage. On the contrary if the degree of saturation reaches these threshold percentages, the ice formation is able to induce an internal tensile stress state that can lead to concrete deterioration, with cracking and spalling (Fig. 8.1 and Fig. 8.2).

According some authors a value less than 90% should be considered as threshold value for the degree of saturation [8.1].

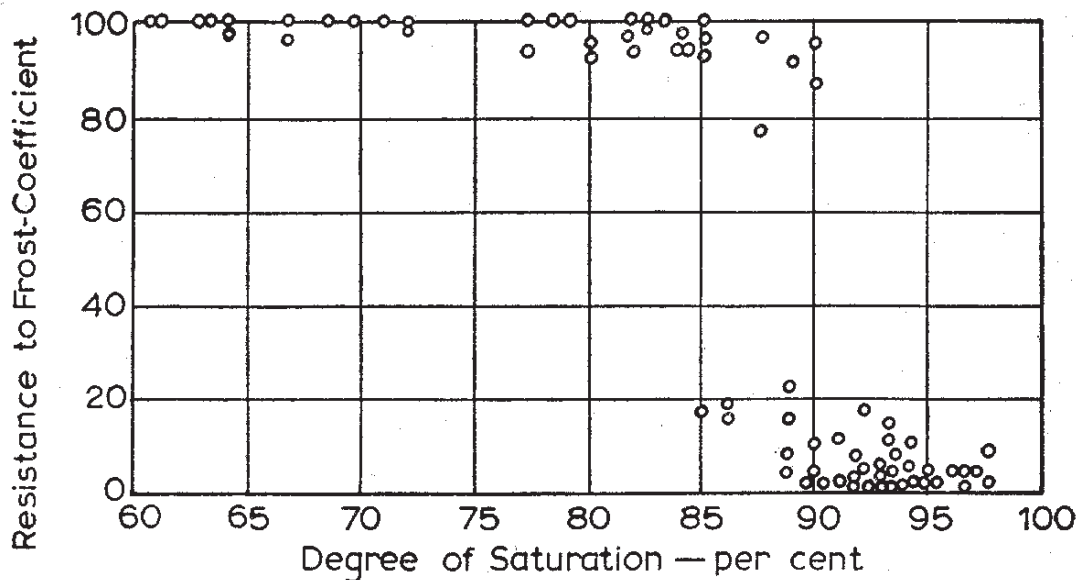


Fig. 8.1 - Influence of the degree of saturation on the frost resistance of concrete [8.2]



Fig. 8.2 - Concrete spalling on a spillway pier [8.3]

Freezing starts in the largest capillary pores and, as soon as the temperature decreases, gradually extends to the smaller ones. Due to the wide range of pore radii in the cement paste, it is only about 1/3 of pore water, which will be frozen at a temperature of  $-30^{\circ}\text{C}$ , and only 2/3 will be frozen at  $-60^{\circ}\text{C}$  [8.3]. Water in gel pores does not freeze above  $-78^{\circ}\text{C}$ . This explains why at lower temperatures more ice is formed and a greater damage is induced. Repeated cycles of freezing and thawing naturally involve a more severe deterioration through a cumulative effect.

During freezing a diffusion process is also developed: not yet frozen water in the smallest pores tends to move towards the larger ones, where freezing is already possible (Fig. 8.3). This favours the filling of larger pores with ice. Any subsequent water flow causes an internal hydraulic pressure whose magnitude depends on several factors as the possibility of water to find “an escape way” (for example nearby air bubbles, suitably provided by air entraining agent), the water permeability of the cement paste and the rate at which ice is formed [8.4] [8.5].

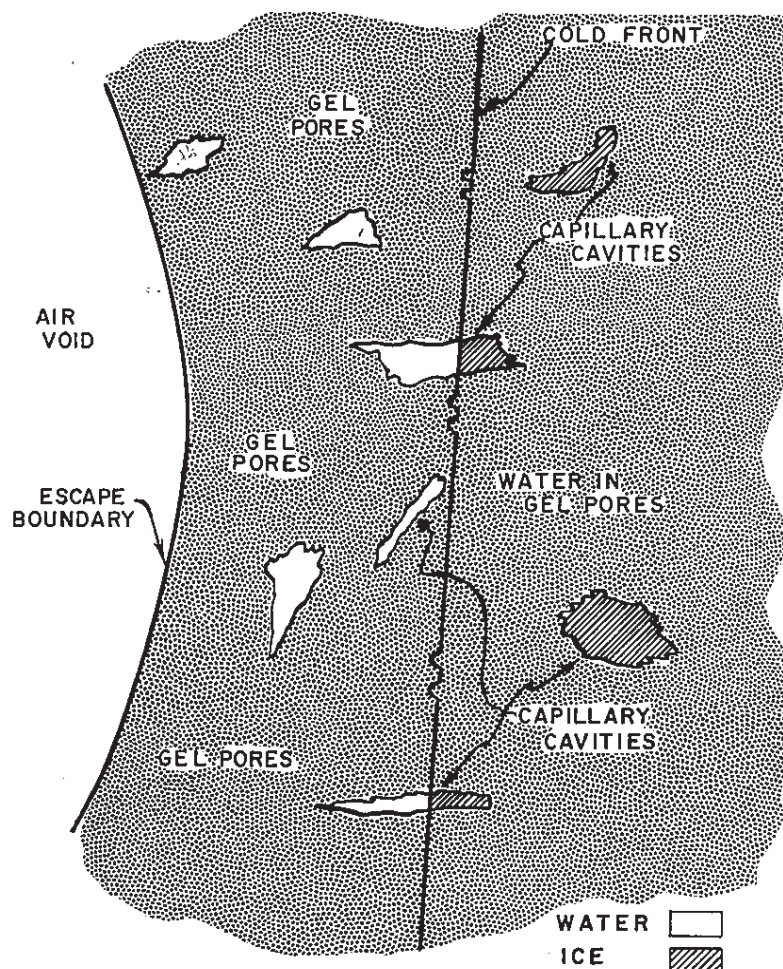


Fig. 8.3 – Scheme of the cement paste and air void in a concrete with capillary pores where the water is freezing and the cold front running to the escape boundary represented by the surface of the air void system [8.4].

If the expansion of the system exposed to freezing and to the consequent internal hydraulic pressure, is such as to generate tensile stresses higher than the concrete tensile strength, then deterioration takes place. It can appear in several forms.

The most common is cracking that can be so widely extended as to cause part of the concrete be detached (“spalling” - Fig. 8.2 - and “pop-outs”).

In concrete slabs or blocks cracks can sometimes appear with a course parallel to the joints or to the boundaries, assuming a D-like shape called “D-cracking”. If the aggregate is non-frost resistant pop-outs can appear, starting from the pebble itself.

In the presence of de-icing salts, as in the case of roads running on the top of a dam, where salts are used to lower the water freezing point and therefore to reduce the risk of ice formation, the deterioration mechanism and freezing pattern is further complicated [8.6] [8.7]. (see Fig. 8.8 and Fig. 8.9 in paragraph 8.3.2)

### **8.3 FACTORS AFFECTING THE FROST RESISTANCE**

Freezing and thawing deterioration of concrete is affected by several factors, some of which can be related to the external exposure conditions and some other to the quality of concrete (cement paste and aggregates).

#### ***8.3.1 Conditions of external exposure***

The main factors related to the external environment are:

- the humidity content inside the concrete during freezing
- the number of freezing-thawing cycles, the lowest temperature and the freezing rate
- the eventual de-icing salt presence.

This last is a typical condition for roads and relative concrete structures but not for dams. Therefore it will not be treated in this Section.

##### *8.3.1.1 The humidity content inside the concrete during freezing*

The humidity content inside the concrete (degree of saturation) depends on the intrinsic water content and on the exposure conditions of the concrete elements. The most critical zones are those that favour the preservation of the saturation conditions during freezing as parts of the hydraulic structures in contact with water and the horizontal surfaces exposed to the external environment.

Among the more susceptible elements in the hydraulic structures the upstream faces can be quoted (in the zone of reservoir fluctuations), the spillways, the inlets and the exits of galleries. Typical horizontal surfaces of concrete elements exposed to the external environment are the dam crest and parts of appurtenant structures (spillway piers, valve chamber roofs), all not a part of the dam's proper mass concrete. The vertical surfaces of concrete simply exposed to the rain are hardly affected by freezing, unless subject to a water load.

Concrete at low temperatures can easily reach the saturation conditions if exposed to flows of damp and warm air.

##### *8.3.1.2 The number of cycles of freezing-thawing cycles, the lowest temperature and the freezing rate*

The number of freezing and thawing cycles is usually higher at the beginning and at the end of the winter and the total number depends on the geographical location of the structure, its altitude above the sea level and the exposure conditions to the sun. Besides, as already mentioned, the lower the temperature reached during the frost cycles, the larger the freezing effects - reaching even water in smallest pores. Furthermore the freezing rate has a significant influence on the frost resistance. Some authors [8.8] have reported that the rate of freezing inside concrete exposed to natural cycles rarely exceeds 4 to 6 °C/h but on the concrete surface it can be much higher.

### **8.3.2 Quality of concrete**

Among the concrete characteristics, the pore structure in the cement matrix and the permeability are of particular importance in relation to the frost resistance. They are strictly related to the concrete mix design and to the casting technique.

#### *8.3.2.1 Pore structure in the concrete*

The pore structure is characterised by the type of pore and its dimensional distribution inside the cement paste. As for the type of pore, isolated or interconnected pores can be found: the interconnected porosity is naturally of main interest as it allows the water transport inside the concrete.

The dimensional range of the pores in the hydrated cement paste embraces different orders of greatness: from  $10^{+4}$  to  $10^{-4}$  microns as radius. A possible classification is as follows:

- macro-pores (and cavities)
- capillary pores
- micro-pores (the gel's pores).

The macro-pores have a size larger than 10 to  $10^{+2}$  microns. In this range falls the air bubbles artificially produced for withstanding the freezing and thawing cycles. The capillary pore embrace the range that goes from  $10/10^{+2}$  microns down to a  $10^{-1}/10^{-2}$  microns. Finally the micro-pores are those smaller than  $10^{-1}/10^{-2}$  microns. Only the macro-pores and the interconnected capillary pores are of interest in relation to the concrete frost resistance. The lower is the presence of macro and capillary pores in the cement pastes and the higher is the concrete frost resistance.

Tests by the US Portland cement Association indicate that vibration frequency generally has a detrimental effect on the stability of the air-entrained void system, particularly at higher water/cement ratios [8.9].

#### *8.3.2.2 Concrete permeability*

The permeability represents the main engineering parameter affecting the concrete frost resistance. It depends not only on the macro- and capillary interconnected porosity (intrinsic permeability of cement paste) but also on the porosity of the interface between cement and aggregate [8.10].

Furthermore, the presence of cracks and discontinuities (like lift joints) can produce important changes in the water flow conditions inside the mass concrete, affecting considerably its permeability. The reduction of the permeability is to be considered as the first provision to adopt for the protection of the concrete from frost damages. The test methods for its evaluation have been presented and discussed in the previous Section 7.

### 8.3.2.3 Concrete mix design

Provision of escape boundaries in the cement paste and refinement of its pore structure are the two parameters that should be assured through a proper concrete mix design [8.4] [8.5].

It is generally accepted that for withstanding the frost action a minimum volume of air bubbles (A), suitably sized and homogeneously distributed in the cement paste, is to be present in the concrete. This air volume is related to the maximum size aggregates (MSA) and, for mass concrete, the values suggested by the American Concrete Institute [8.11] are those reported in Tab. 8.1. Because this amount of air is usually not formed inside the concrete, a suitable air bubble system is to be induced and entrapped through the use of special air-entraining admixtures, during mixing.

Tab. 8.1 – Volume of air required versus the maximum size of aggregate (MSA)

Maximum Size Aggregates (mm)	Volume of required air (%)
150	3.0
70	3.5
50	4.0
40	4.5

If the value of air formed in the concrete is less than prescribed in Tab. 8.1, the concrete is not to be considered frost resistant. If, on the contrary, the air value is satisfactory, then the other parameters of the air bubble system are to be evaluated: micro-bubbles average diameters (D) and their mutual distance (L). The average diameter of the air micro-bubbles has to be in the range of approximately 20 and 100  $\mu$  while their mutual distance should not be larger than 100 – 200  $\mu$ . This last value defines in practice the sphere of action of every micro-bubble, acting as escaping way for the internal hydraulic pressure. The influence of the “spacing factor” L on the concrete frost resistance, quantified through the durability factor (D.F.), as defined by the ASTM C666 (paragraph 8.4) is shown in Fig. 8.4. The influence of air-entraining agents on the frost resistance is clearly documented in Fig. 8.5, where the freezing and thawing performance of different concretes, with and without air-entraining agents, is reported and compared [8.12].

As for the pore structure of a hardened concrete is concerned, the water/cement ratio and the degree of cement hydration are the main factors involved [8.4] [8.5]. For a given degree of cement hydration, the higher the water/cement ratio the higher will be the volume of the pore system and then the amount of freezable water that resides in the large pores (Fig. 8.3 and Fig. 8.6).

ICOLD Bulletin: The Physical Properties of Hardened Conventional Concrete in Dams  
 Section 8 (Frost resistance)

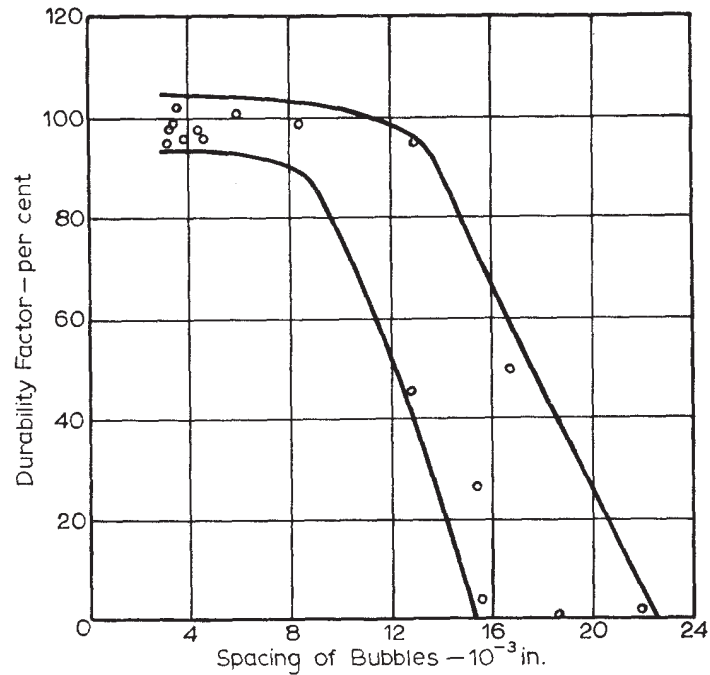


Fig. 8.4 - Influence of the spacing factor on the frost resistance evaluated through the durability factor [8.2]. 1 inch = 24.5 mm)

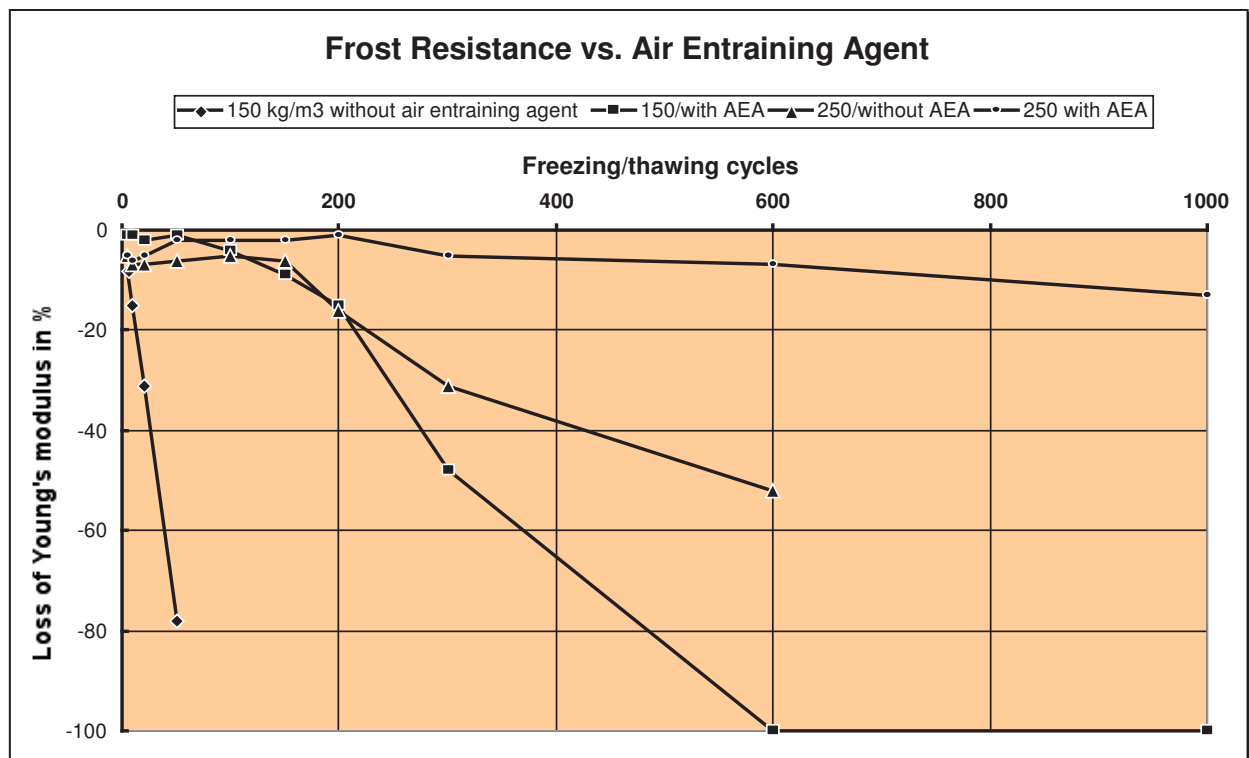


Fig. 8.5 - Concrete frost resistance related to the presence of air-entraining agents [8.12]

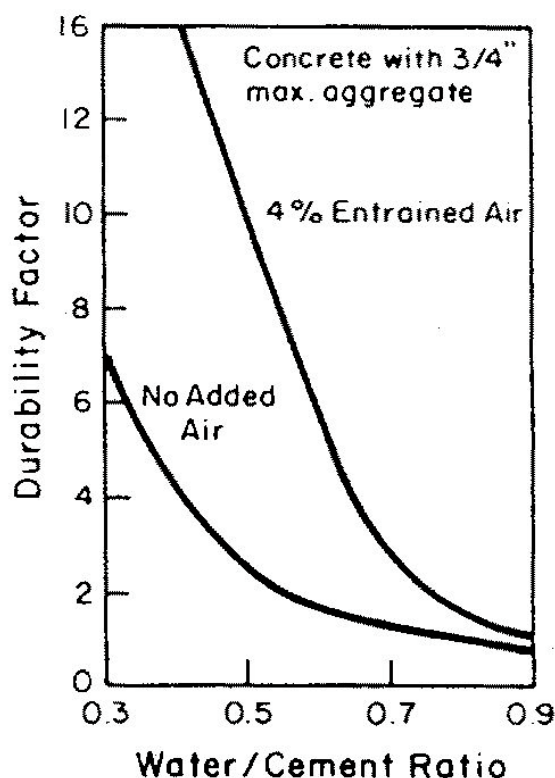


Fig. 8.6 – Example of the water/cement effect on the concrete frost resistance [8.13]

The importance of the water/cement ratio on the freezing and thawing resistance is recognised by the standard. For example, for concrete subjected high saturation without deicers as in exposure classes XF3 (High saturation without deicers) of EN 206 [8.14] (that is the most common case for dam concrete) the Standards requires a maximum water/cement ratio of 0.5, together with a minimum cement content and entrapped air.

High water/cement ratio means large capillary pores and voids that could act as “escape way” for the water under pressure due to the cold front. However this high non-uniformly distributed porosity is the cause of high permeability and high degree of saturation that are predominant factors in concrete decay.

Fig. 8.7 is showing the influence of maximum size of aggregate (MSA) to frost resistance [8.12]: at equal cement content, the Young modulus of concrete specimens with lower MSA is subjected to a more fast freezing and thawing deterioration. The behaviour of concrete with 250 kg/m<sup>3</sup> cement content is better than the other (175 kg/m<sup>3</sup>) because of the better quality mix and lower permeability. Contradictory results are however reported by other authors [8.15]. However, numerous test results confirm that larger MSA-concrete needs less air content than concrete with smaller MSA to achieve frost resistance, the difference being approximately 1% of air content between MSA=150 mm as compared to MSA=30 mm [8.12].



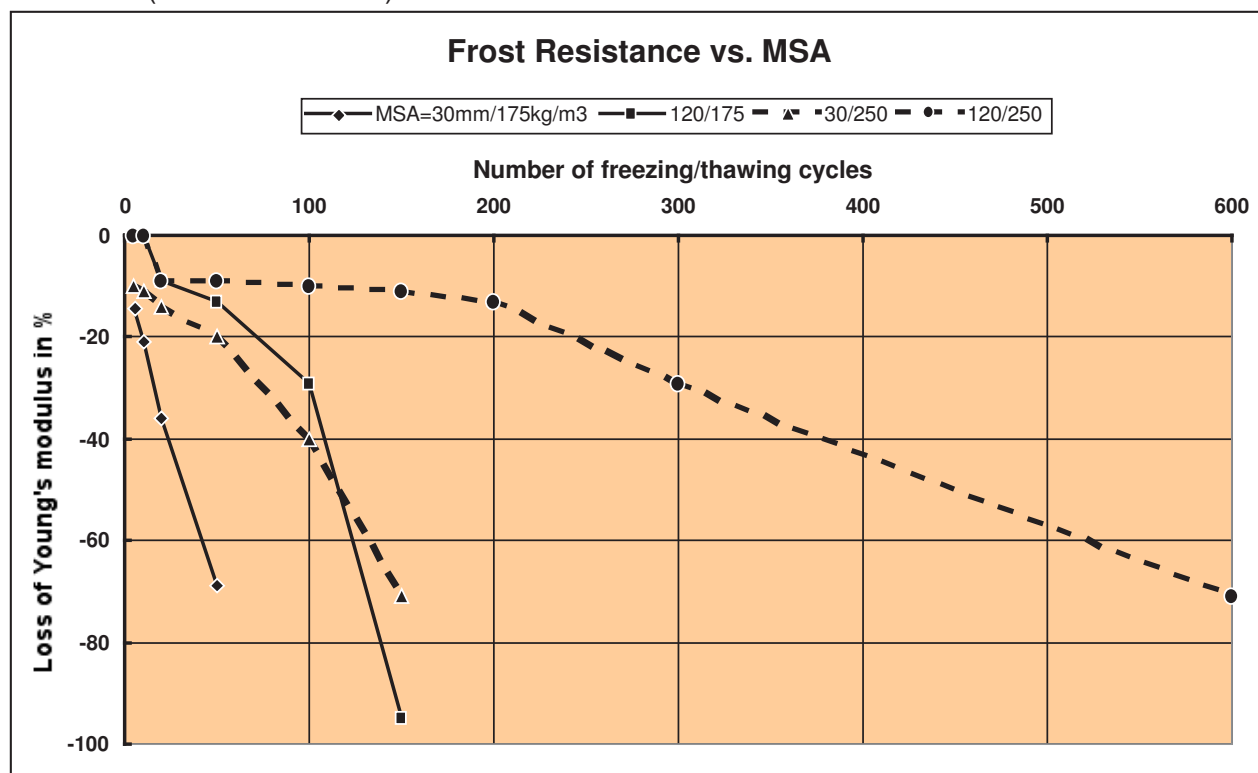


Fig. 8.7 – Concrete frost resistance related to the maximum size of aggregate (MSA) [8.12]

Porous and permeable aggregate are not suitable for concrete to be used in frost sensitive structures. The mechanism of the aggregate deterioration by freezing and thawing is similar to that of cement paste, already described in this Section (paragraph 8.2). The stress on aggregates depend, among other factors, on the degree of water saturation, as well as the rate of cooling. Suitable test methods for assessing the aggregate resistance to this form of weathering are reported in national standards for concrete aggregates.

For example in the European Standard (EN1367-1) the aggregates, having been soaked in water at atmospheric pressure, are subjected to 10 freezing-thawing cycles. This involves cooling to  $-17.5\text{ }^{\circ}\text{C}$  under water and then thawing in a water bath at about  $+20\text{ }^{\circ}\text{C}$ . After completion of cycles, the aggregates are examined for any changes (crack formation, loss in mass and changes in strength).

Well documented is also the influence on frost resistance when blending Portland cements with mineral admixtures (pozzolans, slag, fly ash). This can be concluded from a changed decline of the modulus of elasticity during frost-thaw cycles when replacing part of ordinary Portland cement by the above admixtures [8.12], [8.13],[8.16]. However, whatever composite is used, the beneficial influence very much depends on the adequacy of the air-void system within the concrete (use of an air-entraining agent) and the curing conditions. Some investigations also showed that pozzolans seem to enhance frost resistance more than fly ash and slag [8.17], [8.18], [8.19], [8.20].

#### *8.3.2.4 Casting technique*

The concrete pore system is related not only to the concrete mix design but also to the casting technique and in particular to the type of vibration. Low vibration can induce large pores and cavities that are detrimental, as above explained, for the concrete frost resistance. But also excessive vibration of concrete during placing, with the consequence of reducing air bubbles generated through the use of air-entrainment admixtures, has a detrimental influence on the frost resistance.

Measurements on concretes from some Swiss dams [8.21] showed that the air content, as measured in the laboratory, decreased considerable when measured much later (after 20 years) from cores. For example, at their Moiry and Sambuco dams the initial laboratory air content value of 3.6% decreased down to 1.1% and 1.5% respectively in the concrete cores. An evaluation of frost resistance by the method of "critical degree of saturation" (paragraph 8.4) of the 20 year old dams concrete showed then also insufficient frost resistance because of a low percentage of "not fillable" pores (1.2 to 2.3%).

### **8.4 METHODS FOR EXPERIMENTAL DETERMINATION OF THE CONCRETE FROST RESISTANCE**

Different test methods have been proposed by National or International Standards for the experimental determination of the frost resistance of concrete, both with and without de-icing salts. Some of them are here presented, with reference to the case without de-icing salts, more frequent for the concrete dams.

Most of the tests include placing the concrete specimen, after an initial curing period, in a freezing chamber where nominal freezing-thawing cycles are applied. They consist in alternatively lowering the temperature of the specimens from about +5°C to about – 20/25 °C, in a period of time sufficient to freeze to centre of the specimens, and then rising it from – 20/25 °C to + 5 °C. The rate of temperature changes varies between 5 and 15 °C/h. The specimens are repeatedly subjected to these cycles until visual observed or objective damages are assessed. For example the length change and the weight loss of the specimen is measured and the static or dynamic modulus of elasticity of the concrete is calculated. The frost resistance is quantified by the number of cycles at which the concrete properties show an appreciable variation. A concrete expansion of 0.1% or a reduction of the modulus of elasticity to about 50-60% of the value of the start of the freezing-thawing test are usually considered to represent concrete failure as this degree of disintegration is associated to loss of structural usefulness and concrete integrity [8.22]. Examples of results of this test are reported in Fig. 8.5 and in Fig. 8.7

Usually this test is not intended to provide a quantitative measure of the length of service that may be expected from a specific type of concrete; satisfactory freeze-thaw resistance is considered as a indicator for durable concrete. Therefore freeze-thaw testing is also meaningful for climates without sub-zero temperatures.

Section 8 (Frost resistance)

In fact the freezing process in the real structures is different and affected by a large number of factors and local conditions not represented in the test. For example in the real structures the cold front normally proceeds in a unique direction from outside to inside, while in the test the cold front proceeds from all the surfaces of concrete at the same time [8.23].

In the ASTM C666 Standard test method (“Resistance of concrete to rapid freezing and thawing”) two different procedures are proposed: Procedure A, rapid freezing and thawing in water and Procedure B, rapid freezing in air and thawing in water”. Procedure B is considered less severe and less like nature as it acts on hydraulic structures than Procedure A [8.24].

According to the ASTM C666, a Durability Factor (DF) can be calculated as follows:

$$DF = P \cdot N / M$$

Where:

- P = relative dynamic modulus of elasticity at N cycles, %
- N = number of cycles at which P reaches the specified minimum value for discontinuing the test or the specified number of cycles at which the exposure is to be terminated
- M = Specified number of cycles at which the exposure is to be terminated (300)

Among the other types of test methods proposed for assessing the frost resistance of concrete, the critical degree of saturation method [8.25] is worth while to be quoted. The test is based upon the existence of critical degrees of saturation at freezing, where degree of saturation is defined as:

$$S = V_w / V_p$$

Where  $V_w$  is the total water volume evaporable at 105 °C and  $V_p$  is the total open volume before freezing. In  $V_p$  are also included the air entraining air bubbles, the compaction pores and the aggregate pores. Hence  $S = 1$  corresponds to a complete waterfilling of all pore space in the concrete.

The frost resistance is defined as

$$F = S_{CR} - S_{ACT}$$

Where  $S_{CR}$  is the critical and  $S_{ACT}$  is the actual degree of saturation.  $S_{CR}$  is supposed to be independent of outer climatic conditions. It can, therefore, be regarded as a material characteristic analogous to the “compressive strength”. At moisture contents higher than  $S_{CR}$ , the concrete will be seriously damaged by freezing and thawing. Below  $S_{CR}$  no damage occurs even after a large number of freezing and thawing cycles.

$S_{ACT}$  is the moisture content prevailing in the concrete at the actual instant.  $S_{ACT}$ , for a certain concrete, will be a function of the way the concrete is used, of the environment and of time. Hence  $S_{ACT}$  is dependent on environmental and construction factors only and is therefore analogous to the “actual stress”.

The test is divided into two parts:

- part 1: a freezing and thawing test for determining  $S_{CR}$
- part 2: a moisture absorption test for determining  $S_{ACT}$ .

Section 8 (Frost resistance)

Even if this last test method appear as a promising test, it still remains in the research field [8.26].

Some guidance criteria for the test methods to be highly accurate and reliable are reported in reference [8.27].

### 8.5 LABORATORY DIAGNOSTIC INVESTIGATIONS

The best method to avoid frost damage to concrete is to prevent it from absorbing water and this is most effectively achieved with low water permeability. To this aim the good practice for concrete designing, mixing, transporting and placing is to be followed [8.28]. Fore example, overvibration reduces the content of air voids and is therefore detrimental to frost resistance.

Among the suggested actions to be taken, the use of air-entraining admixtures able to produce air micro-bubbles is strongly suggested [8.29]. Some investigations show that best frost resistance is obtained when the pore diameter is within a range of 20 to 100 microns. Is the pore structure coarser, frost resistance declines, is it finer initial frost resistant concrete might loose it with time [8.12].

However, the only presence in the cement paste of these air bubbles cannot guarantee the concrete frost resistance. In fact if the volume of the entrapped air is insufficient or if the mutual distance among the air bubbles (“spacing factor”) is leaving non protective zones, because too much distant, then the concrete can be at risk of damage.

Other investigations on cores from air-entrained facing concrete of three Swiss dams showed that a criterion for frost resistance is the % of all pores, which cannot be filled with water. It was found that a critical degree of saturation lies between 70 and 80% [8.30]. Among the dam concrete, found to have insufficient frost resistance, the most likeable reason given is over-vibration.

Fig. 8.8 and Fig. 8.9 show thin sections of frost resistance and frost damaged concrete.

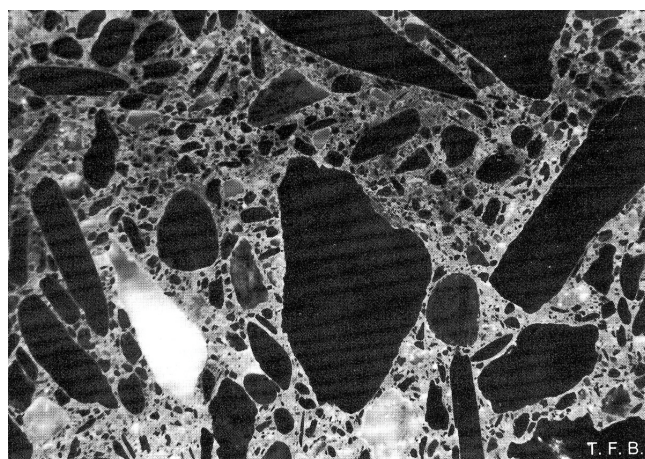


Fig. 8.8 – Specimen after 10 frost/thawing cycles (test without salt) without any micro-structural damage, hence frost resistant.

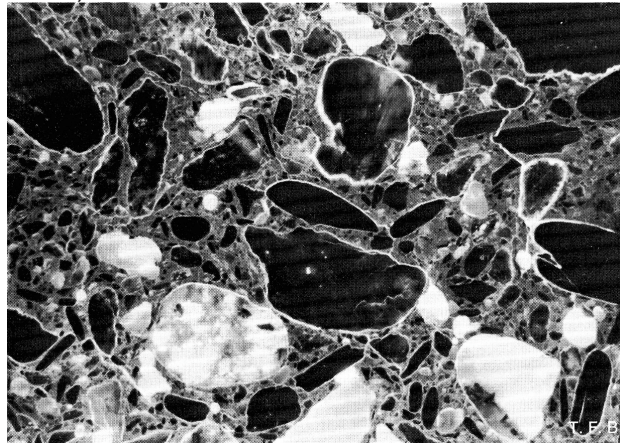


Fig. 8.9 – Specimen from the same mix as above after 10 frost/thawing cycles (test with salt) showing damaged contact between paste and aggregates indicating insufficient frost resistance.

### **8.5.1 Diagnostic investigations**

Diagnostic investigations are therefore advisable to ascertain the microstructure of the air bubbles system inside the cement paste and in particular the total air volume and the spacing factor (average distance between bubbles) [8.31]. These diagnostic investigations are suitable for both laboratory poured specimen or cores drilled from the structure.

The method generally adopted for the characterisation of the air system is that proposed by the ASTM Standard C457 (“Microscopical Determination of Air-Void Content and Parameters of the Air-Void System in Hardened Concrete”). It is based upon measurements of the air void system by prescribed microscopical procedures on sawed and ground sections intersecting portions of the interior of samples or specimens of concrete. Voids of 10  $\mu$  diameters should be well distinguished at 50 times magnification. However a good laboratory experience is necessary for distinguishing the air bubbles of air entrapped through the air-entraining admixtures by the voids of air accidentally entrapped during the mixing and still by the voids of water.

From the data collected during observations the following parameters of the air-system can be calculated:

- A = air content
- D = average diameter of the air micro-bubbles
- L = spacing factor
- A/p = ratio between air and cement paste

Automatic Image Analysis [8.32] can also be usefully adopted for air void determination on samples of hardened concrete.

## 8.6 FREEZING AND THAWING ON CONCRETE DAMS

Dams in moderate climates are structures extremely exposed to frost cycles and also in contact with water on one side over long periods of time. Therefore freezing and thawing is a frequent cause of deterioration of concrete dams, depending both on the quality of the materials and on the exposure conditions. Some dams that were constructed at the beginning of the XX<sup>th</sup> century, with the technology in use at that time (fluid chuted concrete), were characterised by low quality concrete and then showed significant frost damage already after a short period. With the progress in concrete technology, the use of air-entraining admixtures in the concrete mixes of dams built after World War II has reduced the freezing and thawing effects, by introducing artificial pores into concrete. Nonetheless, the phenomenon also concerns the more recent dams.

Usually the most affected zone is on the upstream face, along the water line, for a thickness which may reach up to about 40 cm but also spillways and appurtenant works are often involved. Fig. 8.10 shows the temperature variations registered during some winter days at Upper Glendevon concrete dam in Scotland (U.K.), at an altitude of 335 m above sea level, in three different positions: 1) air; 2) concrete surface; 3) 45 cm below surface [8.33].

The fastest rates of surface temperature changes measured were 10 °C/h in the cooling phase and 8 °C/h in the heating phase. It was observed that the most rapid rates of temperature change at the concrete surface occur with clear skies on faces exposed to the sun when warming in direct sunlight is followed by rapid radiation loss at night (and vice versa).

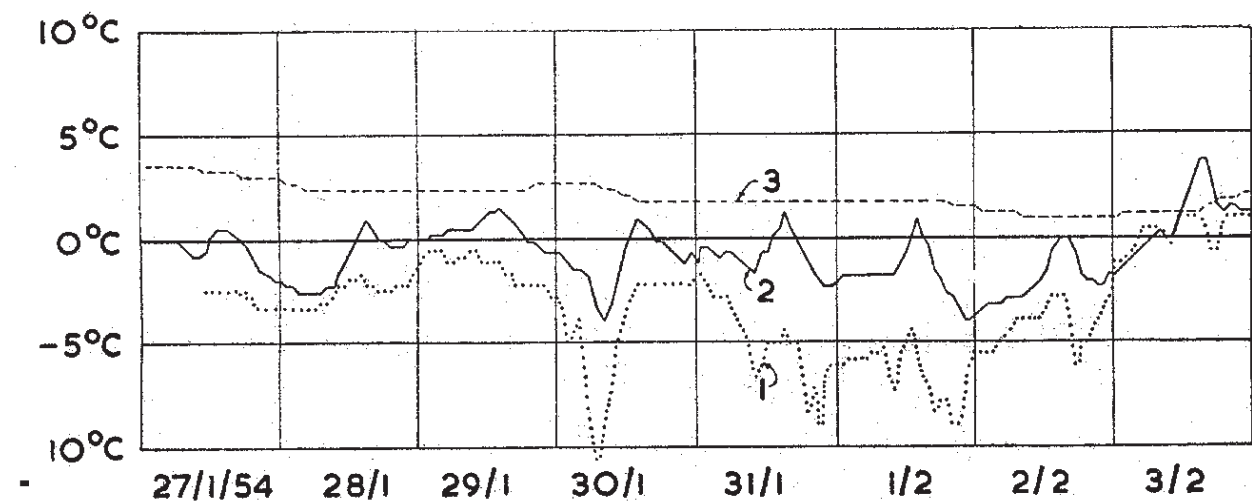


Fig. 8.10 - Temperatures at Glendevon dam, Scotland, upstream face facing west [8.33].

- (1) Air temperature -
- (2) Concrete surface temperature
- (3) Concrete temperature 45 cm below surface

*ICOLD Bulletin: The Physical Properties of Hardened Conventional Concrete in Dams*  
Section 8 (Frost resistance)

An extensive research have been carried out in Japan with the aim to find a correlation between frost resistance on the real dam concrete in field environment and frost resistance on small concrete specimens in laboratory testing conditions [8.34].

1.0 x 1.0 x 1.0 m concrete blocks were placed at six different dam locations scattered throughout Japan and exposed to severe natural weather conditions for some decades, starting from 1964. In Fig. 8.11 the Okuniikappu dam is shown, with the concrete blocks on upstream right bank. They were alternately submerged in water and exposed in air for a long term [8.34].

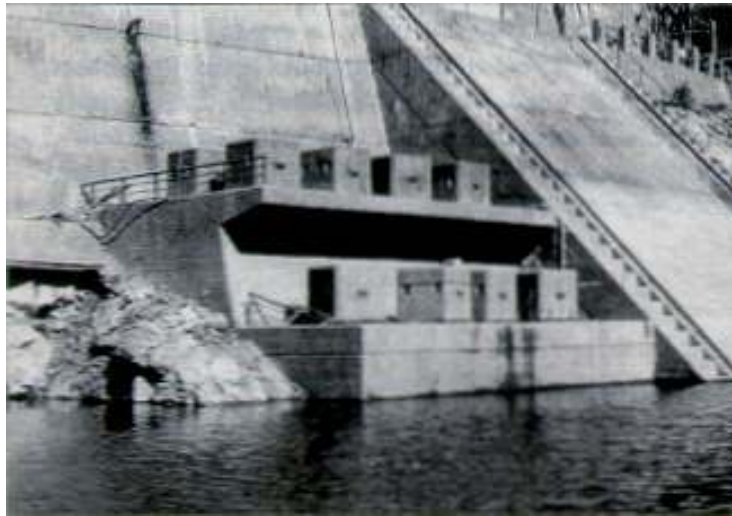


Fig. 8.11 – Location of concrete blocks on upstream right bank of Okuniikappu [8.34]

Small size specimens (for example 15 x 30 cm cylinders) were also prepared, with the same concrete proportions as those used for larger blocks, by wet-screened at 25 mm, and tested through laboratory freezing and thawing (300 cycles at +5° to –18°C). parameters as water/cementitious ratio, fly ash and air entrainment content were considered.

Variations in dynamic modulus of elasticity were monitored and compared with field measurements. These last included modulus of elasticity increase due to hydration process, as the observations started at one year age.

It was generally noticed that any deterioration of concrete occurs provided that water/cementitious ratio is kept below 0.60 and carefully placed and consolidated. The effectiveness of air entrainment was verified also in large concrete blocks and fly ash cement substitutions up to 25% by weight were found highly effective. Note that this is not consistent with a lot of literature results quoted in the paragraph on mix design (8.3.2.3).

The Durability Factor Indexes from laboratory accelerating testing on small specimens, after 300 cycles as defined in paragraph 8.4, were compared with almost 40 years of natural testing on large blocks. Even if a further confirmations of results are needed, because of data scattering, dynamic modulus changes of these blocks can be related to DFI if the total number of natural freezing and thawing cycles (temperature falling below freezing point) are 2500 or more [8.34]. In Fig. 8.12 the comparison for the concrete blocks at some dam locations is illustrated. At the stage of about 250 cycles or less (left part of the figure) the dynamic modulus of elasticity are higher than 100% in all considered concrete blocks and concrete is not deteriorated. A similar trend has been found at 2000 cycles. However at 2500 cycles (right part of figure) for the concrete blocks at on dam location, the elasticity modulus begin to decrease, if the DFI are lower than a certain value.

Finally, based on these data of natural exposure conditions for decades, a prediction method of dam concrete deterioration from cycling freezing and thawing has also been proposed. Details can be found in the reference [8.35]

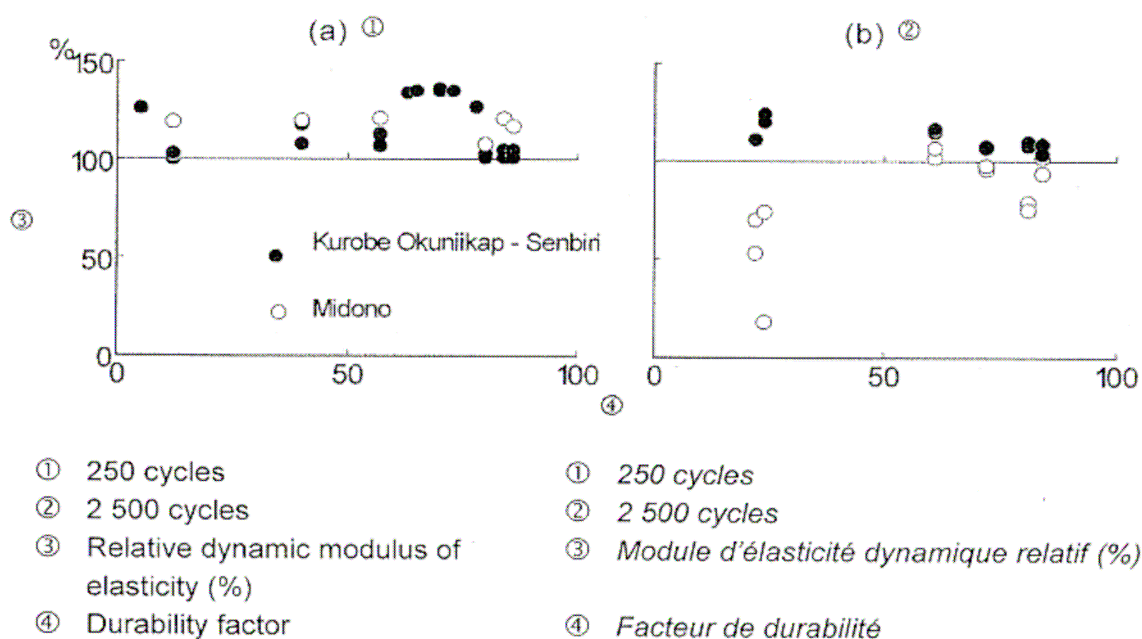


Fig. 8.12 – Relations between durability factor of small specimens subjected to laboratory testing and relative dynamic modulus of elasticity in dam concrete in natural environment [8.34]



## 8.7 REFERENCES

- [8.1] Fagerlund, G., RILEM, "The critical degree of saturation method of assessing the freeze/thaw resistance of concrete", *Materials and constructions*, p. 217-229, July-August 1977.
- [8.2] Neville, A.M., "Properties of Concrete", Sir Isaac Pitman & Sons LTD., p. 350, 1963.
- [8.3] Berra M., "Manuale – Diagnosi e scelta dei materiali da ripristino per le strutture in calcestruzzo degradate dall'azione dei cicli di gelo e disgelo", Enel – Polo Idraulico e Strutturale, Internal Report n° 5944, 1999. (in Italian).
- [8.4] Cordon, W. A. "Freezing and Thawing of Concrete Mechanisms and Control ", ACI Monograph n° 3, pag. 28, 1966.
- [8.5] Metha, P. K. "Concrete structure, properties and materials", Prentice-Hall, Inc., Englewood Cliffs, New Jersey 070632, 1986.
- [8.6] CEB (Comité Euro-International du Béton), "Draft CEB-Guide to durable concrete structures", Bulletin d'information n° 166, 1985.
- [8.7] CEB (Comité Euro-International du Béton), "Durability of concrete structures-State-of-the-art report", Bulletin d'information n° 148, 1982.
- [8.8] Pigeon, M., Prévost, J. And Simard, J.M., "Freeze-Thaw durability versus freezing rate", *Aci Journal*, p. 684-690, September-October 1985.
- [8.9] Stark D.C., "Effect of Vibration on the Air-Void System and Freeze-Thaw Durability of Concrete", Portland Cement Association (RD092.01T) 1886.
- [8.10] Tognon, G. and Cangiano, S., "Sulla gelività del calcestruzzo", *Manutenzione, riparazione e durabilità delle strutture in cemento armato – Collana di Ingegneria Strutturale n°6 – International Centre for Mechanical Sciences CISM, Udine*, p.66-80, 1986. (In Italian).
- [8.11] American Concrete Institute, ACI Building Code 318,
- [8.12] Hess R. E., "Künstliche Luftporen im Beton" [Artificial air entrained in Concrete], *Gazettenverlag Zurich* (Switzerland).
- [8.13] U.S. Bureau of Reclamation, "Concrete Manual », 8<sup>th</sup> edition, 1975
- [8.14] European Standard EN 206, "Concrete, Performance, Production, Placing and Compacting Criteria", 2002.
- [8.15] Macinis, C., Lau, e.C., « Maximum Aggregate Size effect on frost resistance of concrete, *ACI Journal*, p. 144-149, 1968.
- [8.16] Kennedy T.B., "Investigations of pozzolanic and other materials to replace part of the Portland cement in mass concrete dams", *ICOLD Proc. 6<sup>th</sup> Congress, New York*, 1958, Q.23, R120.
- [8.17] Ammann A., "Research on the influence of pozzolan and other admixtures on the frost-resistance of concrete", *ICOLD Proc. 6<sup>th</sup> Congress, New York*, 1958, Q.23, R105.
- [8.18] Gebler S.H., Klieger P., "Effect of Fly Ash on the Durability of Air-Entrained Concrete", Portland Cement Association (RD090.01T), ACI Publication SP-91, 1986.

*ICOLD Bulletin: The Physical Properties of Hardened Conventional Concrete in Dams*  
Section 8 (Frost resistance)

- [8.19] ACI 232-1R-94, "Use of Natural Pozzolans in Concrete".
- [8.20]. ACI 233R-03, "Slag Cement in Concrete and Mortar".
- [8.21] Kreuzer, H. Personal communication, 2001
- [8.22] Verbeck, G., "Non destructive tests for deterioration of concrete specimens subjected to frost action", Fifth Congress on Large Dams, Q.19, R.70, paper n°3, 1955.
- [8.23] Roulet, C.A., "Effet du gel", Durabilité du béton armé – Origine des dégats, Prévention, Assainissement – SIA Documentation n°89, Lausanne, p.23-27, 1985.
- [8.24] Malhotra, V.M., "Mechanical properties and freezing and thawing resistance of non-air-entrained, air entrained, and air-entrained superplasticized concrete using ASTM test C 666, Procedures A and B", Cement, Concrete and Aggregates, p. 3-23, Summer 1982.
- [8.25] Setzer, M.J., RILEM, "RILEM 117-FDC: Freeze-Thaw and deicing resistance of concrete – Report", Materials and constructions, p. 3-6, Supplement March 1997.
- [8.26] Giuliotti, P., Tognon, G.P. "Il metodo del grado di saturazione critico per la prova della resistenza al gelo del calcestruzzo, a confronto con il metodo UNI 7087-72: prime considerazioni sulla base di risultati sperimentali", AITEC Conference – La durabilità delle opere in calcestruzzo, Padova, p. 231-238, 8-9 October 1987 (in Italian).
- [8.27] Fagerlund, G., RILEM, "The critical degree of saturation method of assessing the freeze/thaw resistance of concrete", Materials and constructions, p. 217-229, July-August 1977.
- [8.28] Orchard, D.F., "Concrete Technology Vol.1 Properties of Materials", Applied Science, London , 1979.
- [8.29] American Concrete Institute, "Guide to Durable Concrete – ACI 201.2R-77", ACI Manual of Concrete Practice, Part 1, Detroit, MI, USA, 1991.
- [8.30] Bitterli K. et al., "Zusammenhänge zwischen Betonporosität und Frostbeständigkeit" (Relation between concrete porosity and frost resistance), Schweizer Ingeieur & Architekt, 25/85, 628-636.
- [8.31] Hulshizer, A.J., "Air-Entraining Control or Consequences", Concrete International, p. 38-40, July 1997.
- [8.32] Concrete Society, "Analysis of Hardened concrete", Concrete Society Technical Report n° 32, London, 1989.
- [8.33] Lee, C.R., "Surface temperatures in concrete dams subjected to frost", Fifth ICOLD Congress on Large Dams, Q.19, R.70, paper n°6, 1955.
- [8.34] Kokubu, M., Kobayashi, M., "Long term observations on frost damage to concrete using large test blocks", 20<sup>th</sup> ICOLD Congress on Large Dams, Q.78, R.61, Beijing, 2000.
- [8.35] Ihii, K., Egawa, K., Tsutsumi. T., Noguchi, H., "Prediction of concrete deterioration by cyclic freezing and thawing", Concrete library of JSCE, n° 31, June 1998.